Université Lumière Lyon 2

Ecole Doctorale 483
Sciences Sociales

Università di Firenze

Dipartimento di
Scienze della Terra

HISTORY OF THE EVOLUTION OF LANDSCAPES OF THE ETRUSCAN MARITIME FACADE (TUSCANY, ITALY) THROUGH THE USE OF PALYNOLOGY

Matteo Pili

Under the Supervision of Dr. Jean-Philippe Goiran and Prof. Adele Bertini

Presented and publicly defended on 18 December 2025

Doctoral Examination Committee (Jury):

Éric Fouache, Professor, Sorbonne University (Paris) — President of the Jury
Federica Badino, Research Fellow, Università di Firenze
Marta Dal Corso, Postdoctoral Researcher, Università di Padova
Gonzalo Jiménez-Moreno, Professor, Universidad de Granada
Adele Bertini, Professor, Università di Firenze
Jean-Philippe Goiran, Researcher, CNRS

Invited members:

Yann Callot, Professor Emeritus, Université Lumière Lyon 2

Reviewers (Rapporteurs):

Éric Fouache, Professor, Sorbonne University (Paris)
Andrea De Giorgi, Professor, Florida State University

Résumé

Cette étude présente une reconstitution paléoenvironnementale multiproxy de trois zones humides côtières de la Toscane méridionale – Orbetello, Burano et Orti-Bottagone – visant à documenter l'évolution écologique récente des lagunes tyrrhéniennes sous l'influence combinée des processus naturels et de l'impact anthropique. Des analyses palynologiques à haute résolution ont été réalisées sur des carottes sédimentaires prélevées dans chaque site, en les intégrant aux non-pollen palynomorphs (NPP), aux données granulométriques et microplastiques, ainsi qu'à des échantillons de surface et de mousses. L'ensemble de ces approches apporte de nouvelles informations sur la dynamique de la végétation, l'histoire de l'eutrophisation et les transformations anthropiques du paysage côtier au cours des derniers siècles à millénaires.

Les résultats mettent en évidence des tendances communes et des particularités locales. Les trois séquences témoignent d'une persistance des taxons forestiers méditerranéens et sub-méditerranéens (types *Quercus ilex-coccifera* et *Q. pubescens*), indiquant une stabilité boisée à long terme, mais diffèrent quant à l'intensité des perturbations anthropiques et trophiques. Orbetello montre les épisodes d'eutrophisation et de crises dystrophiques les plus marqués, bien corrélés aux données de gestion du XXe siècle, tandis que Burano présente une réponse écologique plus atténuée, ponctuée de brèves proliférations algales et de déclins de macrophytes. Le site d'Orti-Bottagone, localisé dans une plaine alluviale remaniée et industrialisée, conserve un signal distinct d'instabilité hydrologique et de régression des zones humides.

Les incertitudes chronologiques, principalement liées aux datations radiocarbone sur sédiment en vrac et aux remaniements, limitent la précision temporelle, mais sont partiellement compensées par l'intégration de traceurs radiométriques (^{210}Pb, ^{137}Cs) et d'indicateurs écologiques indépendants. Malgré ces limites, l'approche multiproxy démontre que les lagunes tyrrhéniennes réagissent rapidement, mais de manière hétérogène, aux forçages anthropiques et climatiques. Cette recherche souligne l'importance d'une intégration de multiples indicateurs – microplastiques, marqueurs géochimiques et biologiques – pour reconstituer les changements environnementaux récents dans les systèmes côtiers. Au-delà de ses implications paléoécologiques, le travail contribue à l'archéologie du paysage en reliant les processus écologiques actuels à la longue histoire de l'exploitation et de la gestion humaine du littoral toscan.

Mots-clés : Palynologie ; Lagunes côtières ; Changements environnementaux ; Impact anthropique.

Abstract

This study presents a multiproxy palaeoenvironmental reconstruction of three coastal wetlands of southern Tuscany – Orbetello, Burano, and Orti-Bottagone – aimed at documenting the recent ecological evolution of Tyrrhenian lagoons under the combined influence of natural processes and human impact. High-resolution palynological analyses were conducted on sediment cores from each site, integrated with non-pollen palynomorphs (NPPs), granulometric and microplastic data, and supported by complementary evidence from surface and moss samples. The research provides new insights into vegetation dynamics, eutrophication history, and anthropogenic transformations of the coastal landscape over the last centuries to millennia.

The results reveal both shared and site-specific patterns. All three sequences record persistent Mediterranean and Sub-Mediterranean forest taxa (*Quercus ilex-coccifera* and *Q. pubescens* types), reflecting long-term woodland stability, but differ in the degree of anthropogenic and trophic disturbance. Orbetello exhibits the most pronounced eutrophication and dystrophic episodes, well correlated with twentieth-century management records, while Burano displays a relatively buffered ecological response, punctuated by short-term algal blooms and macrophyte collapses. Orti-Bottagone, located in a reclaimed and industrially modified alluvial basin, preserves a distinct signal of hydrological instability and wetland regression.

Chronological uncertainties, largely related to bulk radiocarbon dating and sediment reworking, limit temporal precision but are mitigated through integration of radiometric markers (^{210}Pb, ^{137}Cs) and independent ecological indicators. Despite these constraints, the combined proxy approach demonstrates that Tyrrhenian lagoons respond rapidly yet heterogeneously to anthropogenic and climatic forcing. The study underscores the importance of multiproxy frameworks – including microplastics, geochemical, and biological markers – for reconstructing recent environmental change in coastal systems. Beyond its palaeoecological implications, the research contributes to landscape archaeology by linking modern ecological processes to the long history of human exploitation and management along the Tuscan coast.

Keywords: Palynology; Coastal lagoons; Environmental change; Anthropogenic impact.

.

Acknowledgements

I would like to express my sincere thanks to Adele Bertini and Jean-Philippe Goiran for their attentive and demanding supervision throughout my doctoral research, conducted as a joint PhD between Université Lumière Lyon 2 and the University of Florence. I also wish to thank the IDEX Breakthrough scientific project, directed by Jean-Philippe Goiran and entitled "*Thalassocracies without ports: fact or fiction*?", for funding my doctoral fellowship through Université Lumière Lyon 2, as well as for supporting the fieldwork missions and scientific analyses.

At the University of Florence, I would like to thank Federica Badino for her careful support and valuable assistance during the revision of the manuscript. Gabriele Niccolini and Niccolò Degl'Innocenti provided early-stage guidance, laboratory training, and support for pollen and non-pollen palynomorph identification.

At Université Lumière Lyon 2, Cécile Vittori (ostracod analysis), Gilles Brocard (sedimentology), Pierre Sabatier (^{210}Pb–^{137}Cs chronology), Christine Oberlin (radiocarbon dating), Amber Goyon (sedimentology and archaeology), and Camille Gonçalves (malacology) contributed complementary data sets within the broader project. I especially thank Cécile Vittori for the many discussions and exchanges on paleoenvironmental and chronostratigraphic issues. I am also grateful to Philippe Sorrel for welcoming me into his laboratory at Université Lyon 1 and for enabling me to complete my pollen analyses under excellent conditions. Many thanks also to Gwenaëlle Pequay (laboratory manager at Archéorient) and Serena Cartei (secretariat of the University of Florence) for their help and patience.

I would like to thank Yanni Gunnell and Adele Bertini for funding the sediment core and for carrying out the coring operation at the Orti-Bottagone site. I am also grateful to the Franco-Italian University and the VINCI program for funding travel expenses. My sincere thanks go to the Italian archaeological superintendencies for the permits granted, as well as to the Tuscany Region, the WWF (Orbetello, Burano, Orti-Bottagone), Natura 2000, the municipality of Orbetello, the *Carabinieri Forestali* station of the Duna Feniglia Natural Park, the Canottieri association, and the fishermen's society of Orbetello for their authorizations and valuable assistance during fieldwork. I also warmly thank the OMEAA laboratory platform at Université Lumière Lyon 2 for providing access to facilities and technical support.

I would like to express my sincere gratitude to the two reviewers of this thesis, Éric Fouache and Andrea De Giorgi, for their careful reading and constructive feedback. I also warmly thank the members of my PhD committee: Éric Fouache (President of the Jury), Federica Badino, Marta Dal Corso, Gonzalo Jiménez-Moreno, Adele Bertini, and Jean-Philippe Goiran. I also thank the invited member Yann Callot for his participation.

Table of Contents

Acknowledgements 4

Chapter 1 – General introduction 11

1. Scientific framework 11

1.1 Coastal wetlands as archives of climate and culture: a palynological approach 11

1.2 State of the art of palynological and paleoenvironmental research in the Mediterra-nean basin 13

1.2.1 Lacustrine and volcanic records of central Italy 13

1.2.2 Coastal and lagoonal records of Tuscany and Latium 14

1.2.3 Central Mediterranean comparative evidence 14

1.2.4 Paleoclimatic and geomorphological perspectives 15

1.3 Knowledge gap 15

2. Geological and geomorphological background at the regional scale 17

2.1 Brief geological history of southern Tuscany 17

2.2 Holocene evolution of coastal plains and lagoons 17

2.3 Shared features of Burano, Orbetello and Orti-Bottagone 19

3. Historical and archaeological overview 19

3.1 Neolithic and Chalcolithic beginnings 19

3.2 The Etruscan world 20

3.3 Roman colonisation 20

3.4 The Middle Ages 21

3.5 Early modern and contemporary transformations 21

3.6 Environmental and cultural significance 22

4. Final synthesis and research objectives 23

4.1 Linking the macroregional framework and the palynological archives 23

4.2 Research questions 23

4.3 Original contribution of the thesis 24

Chapter 2 – Materials and methods 26

1. Materials 27

1.1 Sediment cores 27

1.2 Surface sediments 30

1.3 Moss samples and pollen trap 31

2. Methods 33

2.1 Chemical-physical treatment of sediment cores and surface sediment samples for palynological analyses 33
2.2 Treatment of mosses and pollen trap 35
2.3 Microscopic analysis and data processing 36
2.4 CONISS Analysis 38
2.5 Microplastics extraction and analysis 39
2.6 Laser granulometric analysis 43
Chapter 3 – Lake Burano 44
Introduction 44
1. Environmental and cultural context 44
1.1 Geography and climate 44
1.2 Hydrology and overview of the submerged and emergent vegetation (Fig. 4) 47
1.3 Geological and environmental history 51
1.4 Human influence and conservation: history and current situation 52
2. Chronological framework of the core LB5B 54
2.1 Radiocarbon dating 54
2.2 Lead-210, Caesium-137, and Americium-241 content analysis 55
Results 58
3. Palynological analysis of the sediment core 58
3.1 Palynomorph concentrations 58
3.2 Flora (Tab. 1 of Appendix I. Figs. 8, 9) 60
3.3 Vegetation (Figs. 8–11) 63
3.4 Pollen zones description (Figs. 12, 13) 66
3.5 NPP (Figs. 14, 15) 70
4. Surface samples 75
4.1 Results of laser granulometric analysis 75
4.2 Palynological analysis of surface samples (Figs. 18, 19) 77
4.3 Analysis of moss samples (Figs. 20, 22) 81
4.4 Analysis of the pollen trap (Figs. 21, 22) 83
5. Preliminary microplastics analysis on selected samples 86
Discussion 89
6. Strengths and weaknesses of the study 89
7. Interpretation of the chronological framework 90
8. Interpretation of the fossil palynological record 92
8.1 Pollen assemblages and vegetation changes 92
8.2 NPPs and associated lagoonal trophic shifts 93
8.3 Vegetation and NPPs trends in the climatic and historical context of the site 95

9. Surface samples 97
9.1 Granulometry and hydrodynamic implications (Figs. 16, 17) 97
9.2 Surface samples comparison (Figs. 18, 19, 25) 98
9.3 Moss samples and pollen trap (Figs. 20–22, 26, 27) 99
10. Microplastic evidence and anthropogenic pressure 101
11. Synthesis and interpretive cautions 104
Chapter 4 – Orbetello Lagoon 105
Introduction 105
1. Environmental and cultural context 105
1.1. Geography and climate 105
1.2. Geological and environmental history 107
1.3. Modern environmental changes and management strategies 109
2. Chronological framework of the core OLP-11B 112
2.1. Radiocarbon dating 112
2.2. Lead-210, Caesium-137, and Americium-241 content analysis 113
Results 115
3. Palynological analysis of the sediment core 115
3.1. Palynomorph concentrations 115
3.2. Flora (Tab. 2 of Appendix I. Figs. 6, 7) 117
3.3. Vegetation (Figs. 6–9) 121
3.4. Pollen zones description (Figs. 10, 11) 124
3.5. NPP (Figs. 12, 13) 127
4. Surface samples 131
4.1. Results of laser granulometric analysis (Figs. 14–16) 131
4.2. Palynological analysis of surface samples (Figs. 17, 18) 135
4.3. Analysis of moss samples (Figs. 19, 20) 139
5. Microplastics analysis on selected samples 142
6. Prospective application of Amino Acid Racemization 144
Discussion 145
7. Strengths and weaknesses of the study 145
8. Interpretation of the chronological framework 147
9. Interpretation of the fossil palynological record 150
9.1. Pollen assemblages and vegetation changes 150
9.2. NPPs and associated lagoonal trophic shifts 151
9.3. Vegetation and NPPs trends in the climatic and historical context of the site 153
10. Surface samples 155

10.1. Granulometry and hydrodynamic implications (Figs. 14–16) 155
10.2. Surface samples comparison (Figs. 17, 18, 23) 156
10.3. Moss samples (Figs. 19, 20, 24) 158
10.4. Integrated comparison of core, surface, and moss records 159
11. Microplastics evidence and anthropogenic pressure 160
12. Synthesis and interpretive cautions 161
Chapter 5 – Orti-Bottagone Marshes 163
Introduction 163
1. Environmental and cultural context 163
1.1 Geography, geological context and climate 163
1.2 Overview of the current vegetation 165
1.3 Geological and environmental history during Holocene 166
1.4 Archaeological history and human impact in the area 168
1.5 Recent anthropogenic impact and conservation challenges 170
2. Chronological framework of the core POP22-01 171
2.1 Radiocarbon dating 171
Results 173
3. Palynological analysis of the sediment core 173
3.1 Preservation and concentration of pollen and NPP 173
3.2 Flora (Tab. 3 of Appendix I. Figs. 5, 6) 175
3.3 Vegetation (Figs. 5–8) 179
3.4 Pollen zones description (Figs. 9, 10) 183
3.5 NPP (Fig. 11, 12) 188
4. Surface samples 192
4.1 Palynological analysis of moss samples (Figs. 13–16) 192
Discussion 197
5. Strengths and weaknesses of the study 197
6. Interpretation of the chronological framework 198
6.1 Challenges in establishing a reliable chronology 198
6.2 Assessment of the radiocarbon chronology 199
7. Interpretation of the fossil palynological record 201
7.1 Pollen assemblages and vegetation changes 201
7.2 NPPs and associated lagoonal trophic shifts 202
7.3 Vegetation and NPPs trends in the climatic and historical context of the site 203
8. Surface samples (mosses) (Figs. 13–16, 18, 19) 207
9. Synthesis and interpretive cautions 209

Chapter 6 – Regional synthesis and conclusions 210
1. Objectives and regional framework 210
2. Chronological challenges and multiproxy constraints 211
3. Synthesis of site records 212
3.1. Shared trends 215
3.2. Site-specific differences 215
3.3. Comparative value 216
4. Regional and comparative perspectives 217
5. Methodological conclusions and future perspectives 218
References 220
Appendix I – Floristic lists 233
Appendix II – Photos 243
Appendix III – Photos of microplastics 246

Chapter 1

General introduction

The southern coast of Tuscany (central Italy), stretching from the promontory of Piombino in the north to the border with Latium in the south, is characterised by a long cultural history and by the presence of diverse habitats supporting a remarkable richness of flora and fauna. This coastline hosts several lagoons and marshes whose geomorphological and hydrological configuration is virtually unique within the Italian peninsula. These environments are significant not only from a historical and archaeological perspective, having been continuously inhabited for millennia, but also from an ecological standpoint, as they are today protected areas due to their biodiversity and the ecological value of their ecosystems.

The aim of this thesis is to reconstruct the vegetation and climate history of this region from prehistory to the present, with particular attention to the role of human impact in shaping the environment over time. To this end, three sediment cores have been analysed from the sites of Burano, Orbetello, and Orti-Bottagone, providing new palaeoecological insights into the environmental history of southern Tuscany.

1. Scientific framework

1.1 Coastal wetlands as archives of climate and culture: a palynological approach

Coastal wetlands represent highly valuable archives for reconstructing past environmental dynamics and the long-term interactions between climate, ecosystems, and human societies. They are transitional ecosystems, located at the interface between terrestrial and marine systems, and their evolution is closely linked to hydrological, geomorphological, and climatic factors, as well as to human interventions. Because of their marginal position along the shoreline, wetlands are particularly sensitive to sea-level fluctuations and climatic variability. These changes are often recorded in their sedimentary sequences with a resolution that is higher than in other depositional environments (Benjamin *et al.*, 2017).

Palynology, defined as the study of pollen grains and other non-pollen palynomorphs (NPPs), provides a powerful tool to unlock the information preserved in lagoonal deposits. Pollen grains and spores consist of sporopollenin, a highly resistant biopolymer that ensures their preservation over thousands to millions of years, while their distinct morphological features (e.g., apertures and sculpturing) allow identification at different taxonomic levels, in many cases down to species (e.g. Moore *et al.*, 1991).
This makes pollen an exceptionally reliable proxy for reconstructing past vegetation and, by extension, climate variability and human impact. NPPs, including algal remains and coprophilous fungi, provide complementary evidence on aquatic ecosystem functioning and land-use dynamics, especially regarding grazing pressure and eutrophication (Cugny *et al.*, 2010). The combined analysis of pollen and NPPs thus enables an integrated reading of natural and cultural processes that have shaped Mediterranean coastal landscapes.

The study area of this thesis, the southern Tuscan coast between Piombino and the border with Latium, is of particular interest for several reasons. On the one hand, it hosts well-preserved lagoonal and marsh environments such as Burano, Orbetello, and Orti-Bottagone, which preserve valuable sedimentary archives for palaeoecological research.
On the other hand, this region has been intensively inhabited and exploited since the Neolithic, with evidence of Villanovan settlements, flourishing Etruscan centres such as Populonia, and later Roman colonisation (Sadori *et al.*, 2016).
Subsequent transformations during the medieval period, Renaissance, and modern age – ranging from land reclamation and canal construction to industrialization and conservation policies – further modified these landscapes. Today, these wetlands are recognized as protected areas under the Ramsar Convention, reflecting both their ecological importance and their long-term cultural value.

The chronological framework of this research extends from the onset of the Northgrippian stage (8,200 years ago) through the entire Meghalayan stage (4,200 years ago to the present) (Walker *et al.*, 2018). These two official subdivisions of the Holocene encompass some of the most relevant episodes in Mediterranean environmental and cultural history. The Northgrippian includes, among others, the 8.2 ka event, one of the most significant rapid cooling and aridification episodes of the Holocene, with marked impacts on ecosystems and human societies (Magny *et al.*, 2006). The Meghalayan, by contrast, is characterized by the increasing anthropogenic pressure on landscapes, the intensification of agricultural practices, and the expansion of key Mediterranean cultivars such as olive

and vine (Langgut *et al.*, 2019), culminating in the major environmental transformations of the modern and contemporary ages.

Within this framework, palynological studies on the coastal wetlands of southern Tuscany pursue a dual objective: on the one hand, documenting vegetation responses and coastal ecosystem dynamics to major climatic events of the mid-to-late Holocene; and on the other, reconstructing how successive societies inhabiting the region modified and reshaped the landscape, leaving tangible imprints in the pollen record. This integrated perspective, bringing together natural and cultural dimensions, constitutes the foundation of the present research.

1.2 State of the art of palynological and paleoenvironmental research in the Mediterranean basin

Over the last decades, numerous palynological and multiproxy studies have been carried out in the central Mediterranean region, providing an increasingly detailed picture of late Quaternary vegetation dynamics, climate variability, and human impact. These records, however, are unevenly distributed, with a strong concentration on volcanic crater lakes and inland basins of central Italy, while coastal and lagoonal environments remain comparatively less investigated.

1.2.1 Lacustrine and volcanic records of central Italy

The most continuous and detailed palynological records for the Holocene come from volcanic lakes of Latium and Tuscany. Lago dell'Accesa has been the focus of extensive multiproxy studies (e.g. Colombaroli *et al.*, 2008; Drescher-Schneider *et al.*, 2007; Finsinger *et al.*, 2010; Magny *et al.*, 2006, 2007b; Vannière *et al.*, 2008). These investigations have documented vegetation changes over the last 15,000 years, disentangling climatic signals from anthropogenic activities, and highlighting the role of fire regimes in shaping the landscape. The Mezzano sequence (Ramrath *et al.*, 2000; Sadori, 2018) offers another well-dated and high-resolution record spanning the Lateglacial and Holocene, with clear evidence of both rapid climatic oscillations and early human impact. Additional important records derive from Lago di Vico (Magri & Sadori, 1999) and Lagaccione near Bolsena (Magri, 1999), which document the persistence of deciduous oak forests and subsequent phases of anthropogenic modification. Lake

Albano has also been investigated through organic geochemistry and pollen analysis (Ariztegui *et al.*, 2001), providing insights into Holocene environmental evolution in Latium.

1.2.2 Coastal and lagoonal records of Tuscany and Latium

Despite the richness of lacustrine data, coastal environments have been less extensively explored. Important exceptions include the pollen and ostracod study from ancient Ostia (Sadori *et al.*, 2016), which integrated paleoenvironmental evidence with the archaeological record of the Roman harbour, and the Holocene pollen sequence of Lake Massaciuccoli in northern Tuscany (Colombaroli *et al.*, 2007; Mariotti Lippi *et al.*, 2007), which traced vegetation dynamics and fire activity along the Ligurian and Tuscan coastal plains. Further south, the Vendicio coastal plain in Latium has been studied through geomorphological and paleoenvironmental analyses (Aiello *et al.*, 2007).

1.2.3 Central Mediterranean comparative evidence

Beyond central Italy, numerous records contribute to a broader understanding of Holocene vegetation and climate in the central Mediterranean. In Sicily, the Lago di Pergusa sequence has yielded detailed palynological reconstructions from the Late Glacial to the Holocene (Sadori & Narcisi, 2001; Sadori *et al.*, 2008), while comparative studies have examined the Balearic Islands and Sicilian records (Pérez-Obiol & Sadori, 2007). More recently, Langgut *et al.* (2019) synthesised fossil pollen evidence for the origin and spread of olive cultivation across the Mediterranean, highlighting the interplay of climatic and cultural drivers, with important case studies from southern Italy. Other examples include Mljet Island in Croatia (Bakrač *et al.*, 2024; Jahns & van den Bogaard, 1998), the Gargano coast (Caroli & Caldara, 2007), and the Lago Alimini Piccolo (Di Rita & Magri, 2009) in Apulia, which together illustrate the diversity of vegetation trajectories and the regional variability of anthropogenic impact in the central Mediterranean.

Given the very large number of studies available across the entire basin, this discussion is deliberately limited to the central Mediterranean; however, excellent syntheses covering the whole Mediterranean are provided by Benjamin *et al.* (2017) and Langgut *et al.* (2019).

1.2.4 Paleoclimatic and geomorphological perspectives

Palynological research has been complemented by independent paleoclimatic and geomorphological studies. Lake-level reconstructions at Accesa and other European sites (Magny *et al.*, 2006, 2007a, 2007b) revealed millennial- and centennial-scale oscillations during the early and mid-Holocene, including the Preboreal oscillation and the 8.2 ka event.

Investigations in the Tyrrhenian Sea (Ermolli & Di Pasquale, 2002) confirmed large-scale vegetation responses to climatic variability. A major synthesis of sea-level changes and their socio-environmental consequences was provided by Benjamin *et al.* (2017), while geomorphological work in the northern Tyrrhenian sector (D'Orefice *et al.*, 2020b) documented postglacial environmental transitions in coastal Tuscany and Elba Island.

Additional insights into long-term landscape transformations are provided by paleoenvironmental reconstructions from the Po Plain (Ravazzi *et al.*, 2013), which highlight parallel dynamics of hydrological change and human impact in northern Italy, offering a useful comparative perspective with central Mediterranean records.

1.3 Knowledge gap

Despite the significant advances achieved by palynological and multiproxy research in central Italy and across the Mediterranean, important gaps remain in our understanding of coastal environments and their long-term evolution. Most of the available high-resolution pollen sequences for the Holocene derive from volcanic lakes or inland basins (e.g., Accesa, Mezzano, Vico, Albano, Lagaccione), while lagoonal and coastal systems have received comparatively little attention. The few available studies from coastal Tuscany and Latium, such as Massaciuccoli (Colombaroli *et al.*, 2007; Mariotti Lippi *et al.*, 2007), Ostia (Sadori *et al.*, 2016), and Vendicio (Aiello *et al.*, 2007), provide valuable insights but are geographically limited and often do not extend back to the early or mid-Holocene.

Another important limitation concerns the discontinuity and heterogeneity of available records. Some archives provide high chronological resolution and allow robust multiproxy correlations, whereas others are affected by poor dating control, sediment reworking, or incomplete stratigraphies. Such variability hampers regional comparisons,

particularly when evaluating the respective roles of climatic oscillations and human activities in shaping coastal vegetation and landscapes.

In addition, comparative studies that integrate multiple sites within the same coastal sector remain scarce. Although the value of combining pollen evidence with other proxies - such as ostracods, charcoal, and geochemical indicators - has been repeatedly emphasised (Finsinger *et al.*, 2010; Sadori *et al.*, 2016), comprehensive multiproxy investigations of Tuscan lagoonal archives are still lacking. This absence makes it difficult to establish regional synchronicity, to distinguish local dynamics from broader-scale drivers, and to assess the complex feedbacks between natural and anthropogenic processes.

In conclusion, the southern Tuscan coast remains underrepresented in palynological research. Despite its strategic position between northern Tuscany and Latium, and its well-documented archaeological significance from the Neolithic to the Roman period and beyond, the area has not yet been the focus of continuous, multi-millennial pollen studies from lagoonal environments. Therefore, the interplay between climatic variability, sea-level changes, and anthropogenic impact in this sector of the Tyrrhenian coast is still poorly understood.

The present thesis aims to address these shortcomings by analysing three sedimentary sequences from coastal wetlands of southern Tuscany (Burano, Orbetello, and Orti-Bottagone). These records together cover the last ca. 8,000 years, spanning the Northgrippian and Meghalayan stages of the Holocene. By combining pollen analysis with non-pollen palynomorphs and complementary proxies, they provide an unprecedented opportunity to: (I) reconstruct long-term vegetation and ecosystem dynamics in lagoonal contexts; (II) evaluate the responses of coastal environments to major Holocene climatic events; and (III) assess the scale and timing of anthropogenic impact on the landscape. In doing so, this research not only fills a geographic and chronological gap in Mediterranean palynology, but also contributes to a broader understanding of human-environment interactions along the Tyrrhenian coast.

2. Geological and geomorphological background at the regional scale

2.1 Brief geological history of southern Tuscany

The southern Tuscan coast is situated within the broader geodynamic context of the Tyrrhenian margin, whose evolution has been controlled by complex interactions between tectonics, volcanism, and eustatic sea-level change during the Quaternary. The Tyrrhenian Sea represents a back-arc basin generated during the Neogene as a result of the eastward retreat of the Apennine subduction system, which led to progressive extension, crustal thinning, and magmatic activity across central Italy. This tectonic setting produced both the volcanic complexes of Latium and Tuscany (e.g., Vulsini, Vico, Amiata) and the subsiding coastal plains that today host major lagoonal and wetland systems.

The stratigraphic subdivision of the Quaternary, recently formalised by the International Commission on Stratigraphy (Head, 2019), provides the framework within which the evolution of these landscapes can be understood. Following the Last Glacial Maximum, the Tyrrhenian margin experienced rapid responses to deglacial sea-level rise, accompanied by significant geomorphological reorganisation. Subsidence processes along the coastal troughs of southern Tuscany favoured the accumulation of thick Holocene sequences, while tectonic uplift in nearby sectors shaped the alternating promontories and embayments that define the present coastline.

2.2 Holocene evolution of coastal plains and lagoons

Climate variability has played a major role in shaping the Holocene evolution of the Tuscan coastal plains. Mediterranean-type climates are characterised by strong interannual to millennial variability, linked to the North Atlantic Oscillation and orbital-scale forcing (Seager *et al.*, 2019). In Tuscany, these fluctuations influenced hydrology, sediment supply, and vegetation, leaving distinct signatures in both terrestrial and coastal records.

The present-day morphology of the southern Tuscan coast is largely the product of postglacial sea-level rise and subsequent coastal dynamics. During the late Pleistocene, much of the coastal plain was subaerially exposed; the subsequent eustatic rise drowned

river valleys, created embayments, and promoted the formation of lagoons and wetlands behind coastal barriers. Local subsidence enhanced accommodation space, allowing the preservation of thick sedimentary sequences.

Sea-level reconstructions along the Tyrrhenian coast show that postglacial transgression during the early Holocene rapidly inundated coastal depressions, while the relative stabilization of sea level in the mid-to-late Holocene promoted delta progradation and the formation of lagoonal systems (Mazzini, 1999). Comparable processes have been recognised elsewhere in the central Mediterranean, for example in Sicily (Calò *et al.*, 2012), where the interplay of marine transgression, fluvial input, and climatic oscillations generated a mosaic of wetlands, lagoons, and coastal lakes.

The Holocene evolution of Tuscan lagoons has also been shaped by climatic events. The mid-Holocene climatic optimum favoured forest expansion and stabilisation of catchments (Magri, 1997; Sadori *et al.*, 2011). By contrast, later intervals were marked by pronounced instability, such as the 4.2 ka event, which brought increased aridity and vegetation changes in the central Mediterranean (Di Rita & Magri, 2019). At shorter timescales, hydro-sedimentary responses to climatic oscillations are evident in the infilling history of the Burano paleo-lagoon (D'Orefice *et al.*, 2020a), where alternations of marsh expansion, brackish phases, and terrestrialisation mirror broader environmental trends.

From the Neolithic onwards, human activity became a major driver of landscape transformation. Paleoenvironmental records document deforestation, grazing, and the spread of cultivars such as olive and vine (Di Rita & Magri, 2012; Langgut *et al.*, 2019). These anthropogenic imprints are particularly visible during the Bronze and Iron Ages, when land-use intensification combined with natural processes to reshape coastal plains (Zanon *et al.*, 2019). In the historical and recent past, canalisation, reclamation, and drainage profoundly modified the original morphology, as shown by sedimentary and historical analyses of the central Tyrrhenian coast (D'Orefice *et al.*, 2022; Mensing *et al.*, 2015).

Overall, the Holocene trajectory of the southern Tuscan coastline reflects the combined effects of postglacial transgression, local subsidence, sediment supply, climatic oscillations, and long-term anthropogenic pressure.

2.3 Shared features of Burano, Orbetello and Orti-Bottagone

Within this regional framework, the three sites investigated in this thesis – Burano, Orbetello, and Orti-Bottagone – share several geomorphological and ecological characteristics that make them highly suitable as paleoenvironmental archives. They are all located in low-lying coastal plains formed by the interplay of marine transgression and fluvial-deltaic input during the Holocene, and they are transitional environments positioned at the interface between marine and terrestrial domains, sensitive to both climatic oscillations and human interventions.

Sedimentary sequences from these wetlands typically consist of alternations of silts, clays, peats, and organic-rich layers, reflecting shifts between open lagoonal, marshy, and terrestrialised conditions. This stratigraphic variability captures both natural drivers, such as changes in hydrological balance and sediment supply, and cultural imprints, including land clearance, reclamation works, and agricultural expansion.

Despite differences in size and hydrological setting, Burano, Orbetello, and Orti-Bottagone thus share a set of regional controls, including Holocene sea-level dynamics, episodes of subsidence, and long-standing human occupation. These factors underpin their value as complementary palaeoecological archives. Together, they allow an integrated reconstruction of environmental change in southern Tuscany, bridging natural and cultural perspectives within a coherent geomorphological context (D'Orefice *et al.*, 2022; Mensing *et al.*, 2015; Perkins, 2017).

3. Historical and archaeological overview

3.1 Neolithic and Chalcolithic beginnings

The earliest evidence of human settlement in southern Tuscany dates back to the Neolithic, when communities established themselves along river valleys and coastal margins. Archaeological findings, including lithic tools and pottery, indicate subsistence economies based on hunting, gathering, and early cultivation (Mercuri *et al.*, 2011). Paleoenvironmental records suggest that climatic amelioration during the early Holocene favoured the expansion of deciduous forests, which provided both resources and challenges for these groups. Fire management may already have been a tool for opening

landscapes and promoting certain plant communities, a pattern consistent with wider Mediterranean trends (Buonincontri *et al.*, 2020).

The transition to the Chalcolithic and Bronze Age marked the emergence of metal use and more complex social structures. In coastal Tuscany, burial mounds and fortified sites testify to growing territorial control, while palaeobotanical evidence points to the cultivation of cereals and pulses, alongside continued reliance on wild resources (Mercuri *et al.*, 2011; Zanon *et al.*, 2019). This period saw the first systematic transformations of the environment, highlighting regional patterns of deforestation and land use intensification linked to expanding agriculture (Dallai *et al.*, 2024; Zanon *et al.*, 2019).

3.2 The Etruscan world

Southern Tuscany formed part of ancient Etruria, one of the most dynamic regions of pre-Roman Italy. Between the 9th and 4th centuries BCE, the Etruscans developed a highly organised urban system, centred on cities such as Populonia and Vetulonia, closely connected with coastal lagoons and mineral-rich hinterlands (Corretti & Benvenuti, 2001; Prayon, 2010). Mining and metallurgical activities, particularly for copper and iron, profoundly altered the landscape, leaving archaeometallurgical evidence that can be traced in soil and sediment geochemistry (Chiarantini *et al.*, 2018).

Agriculture was also central to Etruscan society. Archaeobotanical studies from farmhouses and wells in Tuscany provide direct evidence of agricultural practices combining cereals, legumes, vine, and olive, reflecting both subsistence and market-oriented production (Mariotti Lippi *et al.*, 2003, 2020). The integration of agriculture, metallurgy, and maritime trade turned the Tuscan coast into a nexus of economic and cultural exchange. From an environmental perspective, Etruscan land use reshaped forest composition, promoted extensive grazing, and intensified soil exploitation (Dallai *et al.*, 2024).

3.3 Roman colonisation

Roman expansion from the 3rd century BCE introduced new dynamics of territorial organisation. The establishment of colonies, road networks, and centuriation reshaped the coastal plains and hinterlands (Giroldini, 2010). The lagoons of Burano and Orbetello

were strategically important for fisheries and salt production, while nearby forests were harvested for shipbuilding and fuel. Written sources, combined with archaeobotanical evidence, attest to the spread of olives, vines, and fruit trees, integrated into mixed farming systems (Nijboer, 2021).

Hydraulic works under Roman rule also transformed landscapes through canals, drainage systems, and harbour infrastructures, facilitating both agriculture and commerce while contributing to sediment redistribution and transformations in lagoonal hydrology (Calastri, 2019; Di Pasquale *et al.*, 2014).

3.4 The Middle Ages

After the decline of Roman political structures, the coastal territory underwent fragmentation and reorganisation under Lombard, Carolingian, and later feudal dominions. Archaeological and paleoenvironmental data suggest partial woodland regeneration in some areas, but also intensification of agro-pastoral exploitation in others, reflecting the mosaic character of medieval land use (Di Pasquale *et al.*, 2014).

Fire played a significant role during the medieval period, as indicated by charcoal and pollen records, pointing to cycles of deforestation and regrowth linked to both subsistence and pastoral needs (Buonincontri *et al*., 2020). Settlement patterns shifted between coastal strongholds and inland fortified sites, balancing exposure to maritime trade with vulnerability to incursions. The lagoons retained their economic role, especially for salt and fisheries, while their ecological condition was increasingly shaped by human regulation.

3.5 Early modern and contemporary transformations

From the Renaissance onwards, the Tuscan coast became an arena of renewed territorial control, first under regional states such as Siena and Florence, and later under Spanish rule in the Stato dei Presidi. These centuries saw significant hydraulic interventions, including embankments and drainage works aimed at reclaiming marshlands for agriculture (Calastri, 2019).

The interventions escalated under the Lorena dynasty (18th and 19th centuries), with large-scale reclamation projects altering lagoonal dynamics and reducing wetland extension (Dallai *et al.*, 2025). The drainage of the swamp of the former Prile Lake,

located between Grosseto and Castiglione della Pescaia, represents a notable case. It was carried out through the San Leopoldo Drainage Canal, commissioned in 1828 by Grand Duke Leopoldo II, which stands as a well-documented instance of large-scale reclamation (De Silva *et al.*, 2018; Guarducci *et al.*, 2021; Salvagnoli-Marchetti, 1859).

The industrial age added new layers of transformation. Mining activities, particularly for mercury and other metals, left chemical imprints in soils and sediments (Pasquetti *et al.*, 2020). Urban expansion and industrialisation during the 19th and 20th centuries further reconfigured the coastal environment, bringing both economic growth and ecological stress. Pollution, eutrophication, and biodiversity loss became pressing issues, while at the same time the recognition of ecological value led to the creation of protected areas and WWF reserves in the late 20th century (Dallai *et al.*, 2024).

3.6 Environmental and cultural significance

Across these long-term processes, southern Tuscany offers a clear example of the interplay between natural and cultural forces in shaping Mediterranean landscapes. From Neolithic clearings to Etruscan mining, Roman hydraulics, medieval fire regimes, and modern reclamations, each phase has left tangible signatures in soils, sediments, and vegetation. These cumulative transformations underline the importance of viewing archaeological and historical evidence not only as records of human societies but also as integral components of environmental history (Guideri & Matteini, 2021; Pieruccini *et al.*, 2021).

For this reason, the region provides an ideal case study for palaeoecological research. By linking archaeological data with palynological and sedimentary archives, it is possible to reconstruct how human communities adapted to climatic variability, exploited natural resources, and redefined coastal ecologies over the last eight millennia. This integrated perspective is essential for understanding both the resilience and vulnerability of Mediterranean landscapes, offering insights of relevance well beyond Tuscany itself.

4. Final synthesis and research objectives

4.1 Linking the macroregional framework and the palynological archives

The preceding sections have outlined three key perspectives of the southern Tuscan coast: (I) the scientific relevance of palynology and lagoonal archives for reconstructing Holocene environmental history; (II) the geological and geomorphological evolution of the Tyrrhenian coastal plain, shaped by tectonics, postglacial sea-level rise, and lagoonal sedimentation; and (III) the historical and archaeological record of continuous human settlement, from prehistoric communities to Etruscan urbanisation, Roman colonisation, medieval transformations, and modern reclamation.

Within this framework, the three records analysed in this thesis are not treated as isolated case studies, but as complementary archives embedded in a shared regional history. Together, they cover a temporal range that encompasses major Holocene climatic events such as the 8.2 ka and 4.2 ka episodes, as well as the long-term ecological consequences of human activities ranging from Etruscan and Roman land use to medieval and modern reclamation. While chronological gaps limit continuous coverage, their combined evidence still allows us to test synchronicity across lagoonal systems, separate local responses from regional drivers, and highlight the interplay between natural and cultural dynamics.

4.2 Research questions

On this basis, the thesis addresses the following questions:

1. Climatic drivers – How did major Holocene climatic oscillations, including the 8.2 ka and 4.2 ka events, affect vegetation and lagoonal dynamics along the southern Tuscan coast?
2. Anthropogenic impacts – What were the main phases of human-induced landscape transformation, from prehistoric clearings to Etruscan metallurgy, Roman colonisation, medieval land use, and modern reclamation?
3. Human-environment interactions – To what extent can changes in vegetation and lagoonal ecosystems be attributed to climate variability versus anthropogenic activity, and how did these drivers interact?

4. Comparative dimension – How do the Burano, Orbetello, and Orti-Bottagone archives differ in recording these processes, and what does their comparison reveal about coherence and diversity in coastal responses across central Tyrrhenian Italy?
5. Methodological contribution – What insights can be gained from the integration of multiple proxies (pollen, NPPs, sedimentary and archaeological evidence) for improving the reconstruction of environmental change in Mediterranean lagoonal settings?

These questions deliberately bridge natural and cultural history, integrating paleoecological, archaeological, and geomorphological evidence.

4.3 Original contribution of the thesis

This thesis provides a novel contribution to the environmental history of the central Mediterranean by generating and comparing three palynological records from the coastal lagoons and wetlands of southern Tuscany. These sites – Burano, Orbetello, and Orti-Bottagone – represent distinct geomorphological contexts but share a common regional background, making them highly complementary for reconstructing Holocene vegetation and landscape change.

The first contribution lies in offering a comparative palaeoecological perspective on a coastal sector of the Tyrrhenian Sea that has been central to Mediterranean cultural history yet underrepresented in long-term palynological studies. By placing the three records side by side, the thesis refines our understanding of both synchronicity and divergence in coastal responses to climatic variability and human pressure.

The second contribution is the integration of climatic and cultural perspectives. The analysis demonstrates how the major global-scale climatic events of the Holocene and local human activities (deforestation, cultivation, reclamation, and industrialisation) are both inscribed in lagoonal sediments, sometimes as overlapping or interacting signals.

The third contribution concerns the methodological dimension. By combining pollen and non-pollen palynomorphs with sedimentological and archaeological evidence, the thesis illustrates the advantages and challenges of a multi-proxy approach in lagoonal environments. This perspective not only strengthens the interpretation of local sequences but also provides guidance for future palaeoecological research on Mediterranean

wetlands, where discontinuous stratigraphies and strong anthropogenic overprints often complicate reconstructions.

Overall, the thesis highlights the dual role of lagoonal systems as sensitive observatories of climatic variability and as archives of human-environment interaction. In doing so, it situates the southern Tuscan records within broader debates on Holocene landscape history in the Mediterranean, while also offering methodological insights applicable to other coastal regions.

Chapter 2

Materials and methods

The materials analysed in this study include sediment cores, surface sediments, mosses, and pollen trap samples, all subjected to palynological analysis. These were collected from three sites located along the southern Tuscan coast in central Italy (Fig. 1):

I. Lake Burano,

II. Orbetello Lagoon,

III. Orti-Bottagone marshes.

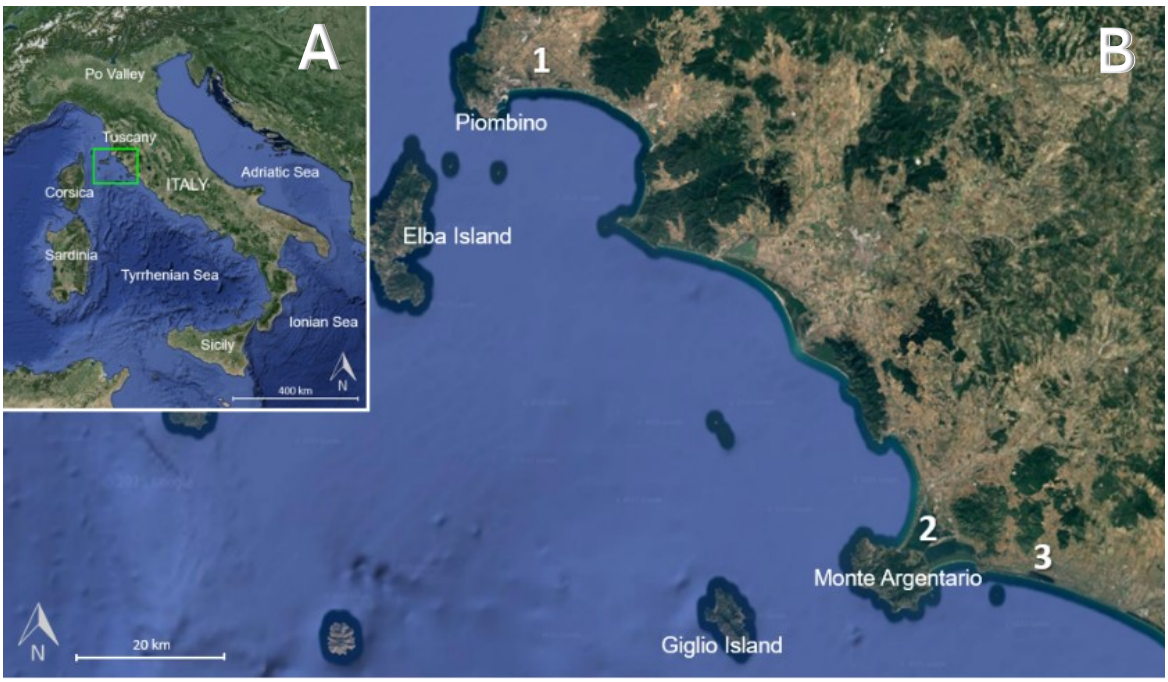

Fig. 1: A. Satellite image of the Italian peninsula. The green rectangle (enlargement in B) includes the studied territory. B. Studied sites 1: Orti-Bottagone; 2: Orbetello; 3: Burano. (modified from Google Earth 2023).

1. Materials

1.1 Sediment cores

Lake Burano

At the site of Lake Burano, the sediment core LB5B (lithology shown in Fig. 2) was extracted in 2020 from the centre of the lagoon (coordinates: 42º24'1.213" N; 11º22'47.647" E) (Fig. 3). The extraction was carried out using an Uwitec gravity core barrel.

Core LB5B is 151 cm long and consists entirely of clayey silt and silty clay for the entire length of the core, with colour ranging from black to dark grey and dark brown. Shell fragments are generally sparse, while some layers contain abundant vegetal fibers (Fig. 2). The core was sampled at approximately 2 cm intervals, yielding a total of 75 samples analysed for palynology.

Orbetello Lagoon

At the nearby site of Orbetello, located approximately 10 km west of Lake Burano, the sediment core OLP-11B (lithology shown in Fig. 2) was extracted in autumn 2020 from the central part of the Ponente Lagoon (coordinates: 42º27'8.888" N; 11º11'47.353" E) (Fig. 4). The extraction was performed using an Uwitec gravity core barrel, transported to the lagoon by boat. The recovery of this core was carried out within the framework of the LabEx-IMU-Urbo project financed by the University of Lyon, which involved the extraction of 26 sedimentary cores over the course of several years at various locations within the lagoon (both on the "Ponente" (West) and "Levante" (East) sides), as well as 16 cores on the Feniglia tombolo and 6 on the Giannella tombolo (Fig. 4; Appendix II, Figs. 1–3). Palynological analyses were conducted on the OLP-11B core. The general objectives and preliminary results of this multidisciplinary research have been presented in Jouve *et al.* (2022).

The OLP-11B core is 222 cm long and consists mainly of grey to dark grey clayey silt. The sediment includes scattered shell fragments and occasional layers of shell concentrations, though shells with connected valves are rare. Some intervals contain variable amounts of macroscopic vegetal fibers (Fig. 2). The sedimentary core was sampled at

approximately 2 cm intervals and fully processed for palynological analyses, for a total of 109 samples.

Orti-Bottagone marshes

The Orti-Bottagone site is located approximately 75 km north of the Orbetello Lagoon. The sediment core POP22-01 (42º57'56" N; 10º35'39" E) was extracted (2022) at the WWF Oasis Padule Orti-Bottagone in the framework of the LabEx-IMU-Urbo project funded by the University of Lyon (Fig. 5).

Core POP22-01 is 1487 cm long. The lowermost section, below 1440 cm, contains heterometric sediments with coarse to fine sands. Between 1440 and 178 cm depth, silty clays predominate, with lesser occurrences of clayey silts, alongside the presence of several peat layers at 1277-1279 cm and at 1088-1096 cm. The uppermost section comprises clayey and peaty silts between 178 and 110 cm, transitioning to slightly sandy silts from 110 cm up to the top. Shell fragments and plant micro- and macroremains, both fibers and roots or rootlets, are frequently founded. In some layers carbonate concretions and rounded or angular gravels are present. Some layers also contain a variable content of microcarbons (Fig. 2). It was sampled approximately every 2 cm (Appendix II, Fig. 4). In the section between 188 cm and 405 cm depth, approximately one sample every 50 cm was selected for palynological analysis. In the section between 405 cm and 984 cm, one sample every 16 cm was selected for palynological analysis. The sparser sampling in the section of the core above 188 cm is due to the aim of focusing on the central portion of the core, to target the chronological interval of greatest relevance for this study. A total of 42 samples were analysed.

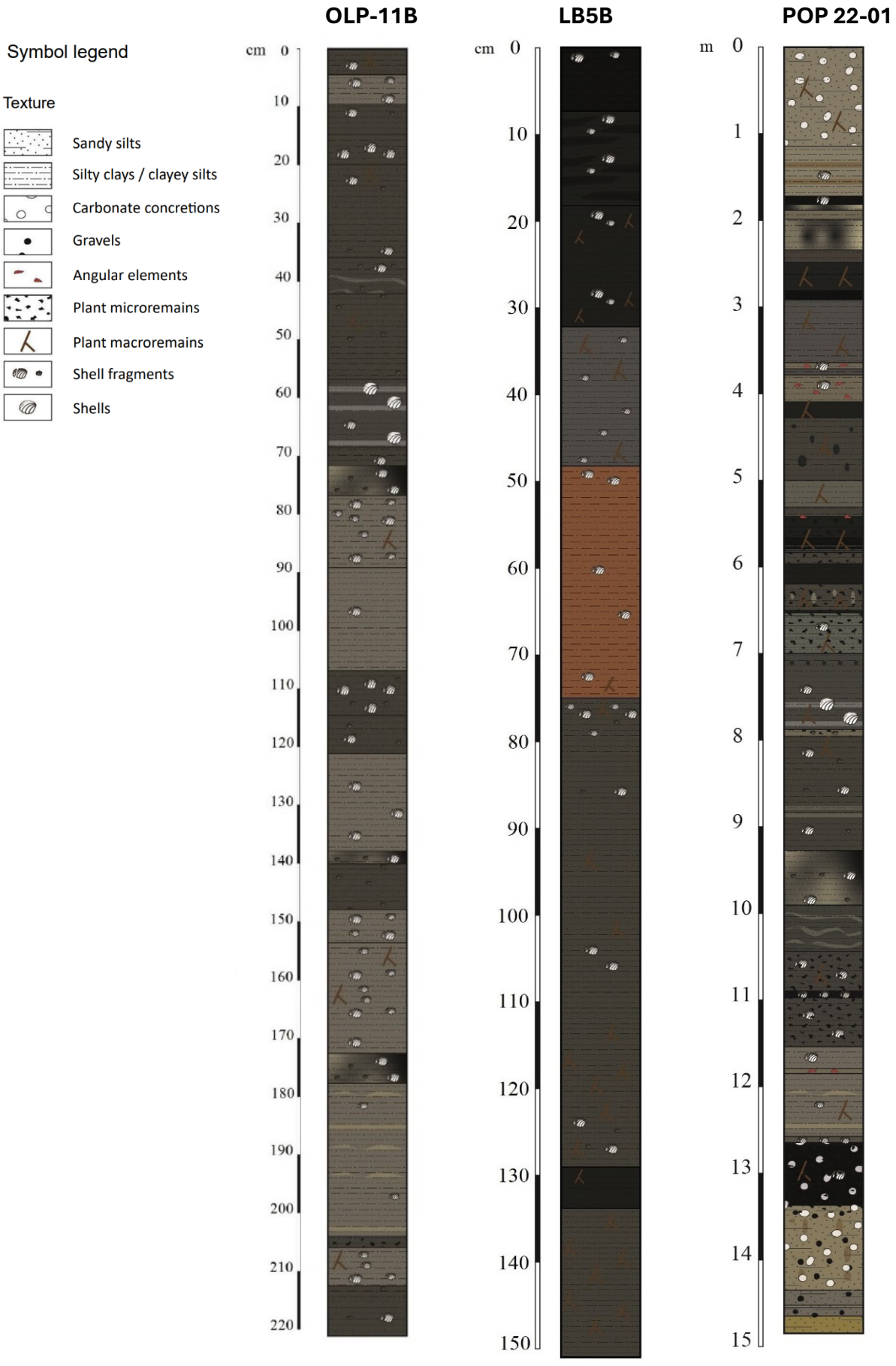

Fig. 2: Stratigraphic logs of the studied cores. Scale bars of OLP-11B and LB5B are expressed in cm, scale bar of POP22-01 is expressed in m. The log of POP 22-01 is modified from Goyon, 2024.

1.2 Surface sediments

In summer 2022, 7 surface sediment samples were collected across the Lake Burano (coordinates in Tab. 1) (Fig. 3), and 15 surface sediment samples were collected across the Orbetello Lagoon (coordinates in Tab. 1) (Fig. 4), and. All these samples were retrieved using a Van Veen grab sampler, and include surface sediments of the basin approximately between 2 and 10 cm depth. Although technically corresponding to sub-surface material, they are hereafter referred to as "surface samples" for simplicity.

Site	Reference sample	Latitude	Longitude
Burano	PS-POL-BUR 01	42º24'18.27"N	11º21'48.29"E
Burano	PS-POL-BUR 02	42º24'9.349"N	11º22'21.194"E
Burano	PS-POL-BUR 03	42º24'2.074"N	11º22'50.012"E
Burano	PS-POL-BUR 04	42º24'8.305"N	11º22'54.239"E
Burano	PS-POL-BUR 05	42º23'54.136"N	11º22'45.106"E
Burano	PS-POL-BUR 06	42º23'54.305"N	11º23'18.614"E
Burano	PS-POL-BUR 07	42º23'46.817"N	11º23'47.072"E
Orbetello	PS-POL-ORB 01	42º26'53.963"N	11º11'38.54"E
Orbetello	PS-POL-ORB 02	42º27'42.034"N	11º11'58.319"E
Orbetello	PS-POL-ORB 03	42º28'31.066"N	11º12'0.95"E
Orbetello	PS-POL-ORB 04	42º26'30.793"N	11º11'10.237"E
Orbetello	PS-POL-ORB 05	42º26'8.318"N	11º10'37.988"E
Orbetello	PS-POL-ORB 06	42º25'57.407"N	11º10'18.062"E
Orbetello	PS-POL-ORB 07	42º26'1.68"N	11º12'9.454"E
Orbetello	PS-POL-ORB 08	42º26'50.856"N	11º13'42.87"E
Orbetello	PS-POL-ORB 09	42º26'32.69"N	11º12'40.756"E
Orbetello	PS-POL-ORB 10	42º25'13.771"N	11º12'11.189"E
Orbetello	PS-POL-ORB 11	42º25'49.188"N	11º12'54.371"E
Orbetello	PS-POL-ORB 12	42º26'10.568"N	11º14'2.465"E
Orbetello	PS-POL-ORB 13	42º26'10.421"N	11º15'28.804"E
Orbetello	PS-POL-ORB 14	42º25'41.56"N	11º16'12.677"E
Orbetello	PS-POL-ORB 15	42º26'35.855"N	11º14'44.052"E

Tab. 1: coordinates of surface samples collected at the Burano and Orbetello sites.

1.3 Moss samples and pollen trap

3 moss samples were collected (December 2022) near the Burano site, specifically within the WWF Oasis Lago di Burano, and 1 annual pollen trap (2022) were installed in the same area (Tabs. 2, 3; Fig. 3).

2 moss samples were collected (December 2022) near the site of Orbetello, precisely in the WWF Oasis of the "Laguna di Ponente" (Tab. 2; Fig. 4).

5 moss samples (collected in January 2022 and January 2023) were collected in the Orti-Bottagone marshes (Tab. 2; Fig. 5).

Site	Reference sample
Burano	MOSS1 BUR1-23
Burano	MOSS2 BUR1-23
Burano	MOSS3 BUR1-23
Orbetello	MOSS1 ORB1-23
Orbetello	MOSS2 ORB1-23
Orti-Bottagone	MOSS1 OBS1-22
Orti-Bottagone	MOSS2 OBS1-22
Orti-Bottagone	MOSS3 OBS1-22
Orti-Bottagone	MOSS1 OBS1-23
Orti-Bottagone	MOSS2 OBS1-23

Tab. 2: moss samples collected at the Burano, Orbetello, and Orti-Bottagone sites.

Site	Reference sample
Burano	TRAPY1 BUR1-22

Tab. 3: coordinates of pollinic trap installed at the Burano site.

Fig. 3: Satellite image of the Lake Burano with sampling locations. Red circle: location of the LB5B core; blue squares: location of the surface samples (PS-POL-BUR 01 to 07); green triangles: moss sampling sites; orange rhombus: location of the pollen trap.

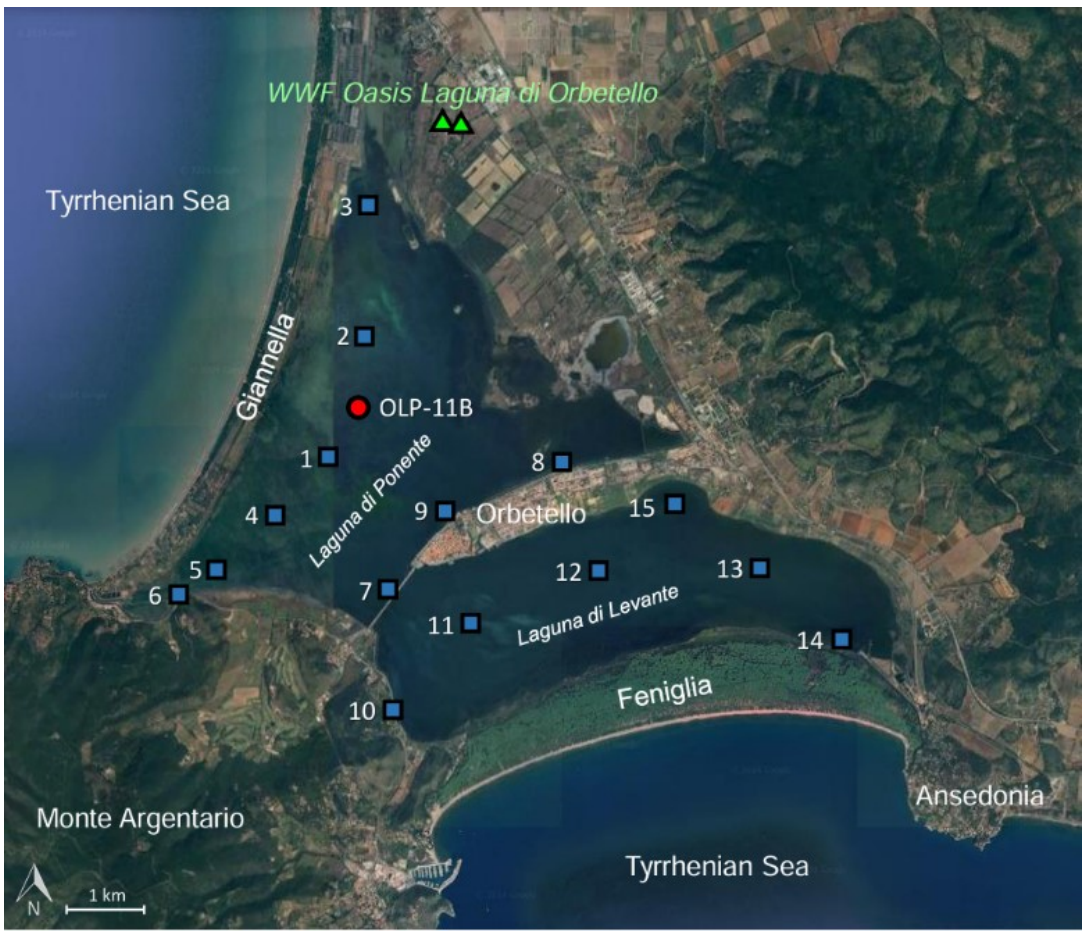

Fig. 4: Satellite image of the Orbetello Lagoon with sampling locations. Red circle: location of the OLP-11B core; blue squares: location of the surface samples (PS-POL-ORB 01 to 15); green triangles: moss sampling sites.

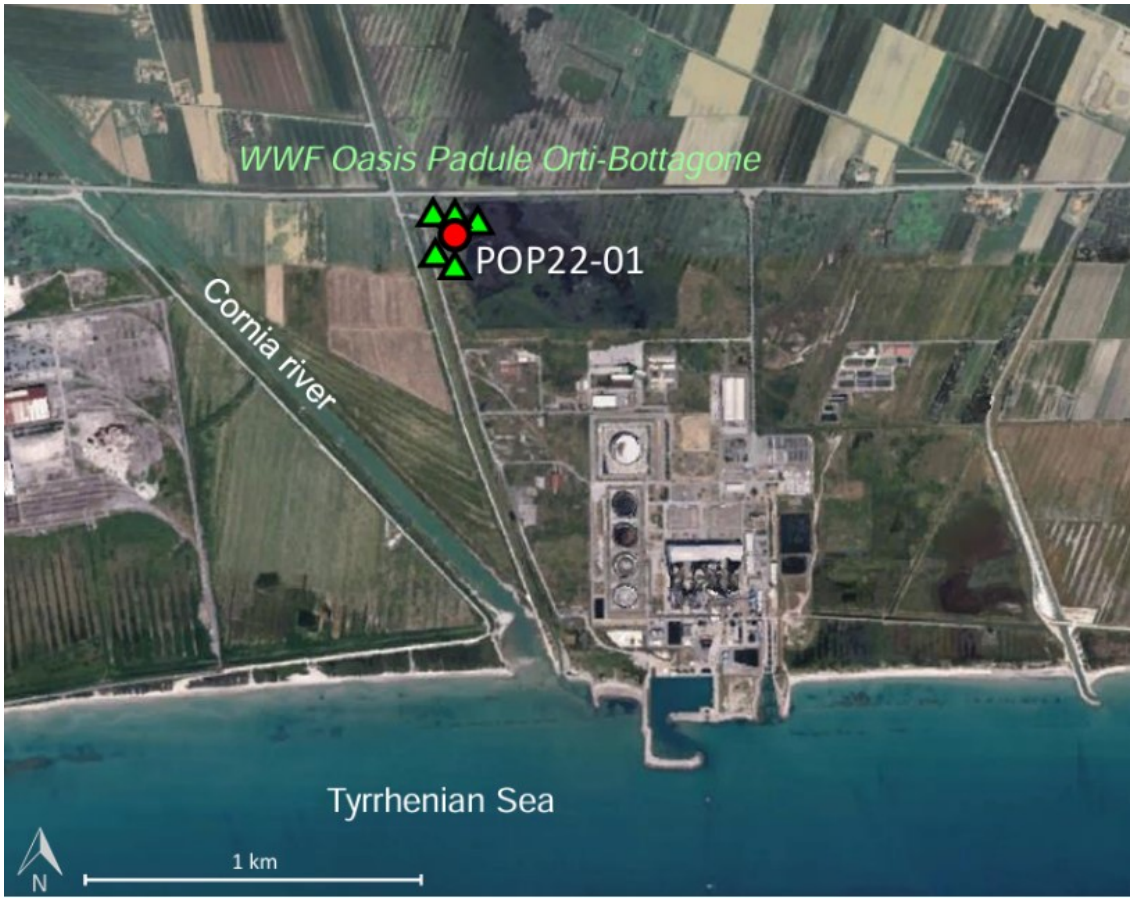

Fig. 5: Satellite image of Orti-Bottagone marshes with sampling locations. Red circle: location of the POP22-01 core; green triangles: moss sampling sites.

2. Methods

2.1 Chemical-physical treatment of sediment cores and surface sediment samples for palynological analyses

Sub-samples for palynological analysis of the sediment cores LB5B (Lake Burano), OLP-11B (Orbetello Lagoon), and POP22-01 (Orti-Bottagone) underwent chemical-physical treatment in the laboratory (Appendix II, Fig. 5), with the aim of breaking down and eliminating the mineral fraction and recovering the organic fraction.

For each sample of the core OLP-11B, a dry sediment quantity of approximately 2 g (min. 1.5 g, max. 2.4 g) was prepared. The samples were initially ground using a manual pestle, and a tablet of an exogenous marker (*Lycopodium*) was then added (tablet supplied by the

University of Lund, batch no. 100320201; 14285 ± ca. 501 spores per tablet) to allow the pollen grains concentration to be calculated according to the marker grains method (Matthews, 1969).

For each sample of the core LB5B, a quantity of dry sediment of approximately 1.5 g (min. 1.4 g, max. 1.8 g) was prepared. The exogenous marker tablets (*Lycopodium*) were supplied by Lund University, batch no. 100320201 (14285 ± ca. 501 spores per tablet).

For each sample of the core POP22-01, an amount of dry sediment of approximately 2 g (min. 2.0 g, max. 2.2 g) was prepared. The laboratory preparation of the samples is the same as described for the OLP-11B and LB5B cores samples, with the difference that the treatment with sodium hexametaphosphate was skipped because not necessary given the lithology of the core. The exogenous marker tablets (*Lycopodium*) were supplied by Lund University, batch no. 140119321 (19855 ± ca. 521 spores per tablet).

For each surface sediment sample (both from Burano and Orbetello), an amount of dry sediment of approx. 2-3 g (min. 1.4 g, max. 2.9 g) was prepared. The exogenous marker tablets (*Lycopodium*) were added (Lund University, batch no. 100320201; 14285 ± ca. 501 spores per tablet).

Sediment cores and surface sediment samples were processed as follow.

After grinding with the pestle and adding the exogenous marker, each sediment sample was then placed in a 50 cl test tube, to which hydrochloric acid (HCl) diluted in water (vol. HCl 7% of total vol.) was added to dissolve the carbonate fraction of the sediment. The sediment was stirred periodically. After approximately 2 hours, the samples were centrifuged (3000 rpm for 10 minutes) (with a centrifuge model Thermo Scientific, Heraeus Megafuge 40) and the supernatant hydrochloric acid solution was discarded.

Hydrofluoric acid (HF) diluted in water (HF vol. 38% of total vol.) was then added to remove the silicate fraction of the sediment. The sediment was left in solution for 48 hours, with periodic stirring. Afterwards, small amounts of hydrochloric acid were added to stop the reaction, and then the samples were subjected to centrifugation at 3000 rpm for 10 minutes.

Sodium hexametaphosphate ($(NaPO_3)_6$) was then added to the tube (122.4 g of $(NaPO_3)_6$ in 1000 ml of water). The sodium hexametaphosphate solution, at pH 7, destroys any bonds between the clay particles by removing specific cations, particularly Fe^{2+} and Fe^{3+}. The sediment was first stirred and then left immersed in the solution for at least an hour, and finally centrifuged (3000 rpm for 10 minutes). Subsequent washes with water

(repeated cycles of adding water, mixing, centrifuging, decanting) were then carried out until the water was clear.

Once the residual water was removed, potassium hydroxide (KOH) diluted in water (KOH vol. 10% of total) was added to the samples to dissolve humic and fulvic acids and other unstructured organic material. The sediment was soaked for five minutes while being stirred continuously. The sample was then filtered (200 µm metal-mesh filter), to retain any seeds and other organic macro-rests, and collected in a 250 ml test tube. The fraction passed through the filter was then centrifuged (3000 rpm for 10 minutes) and the supernatant was discarded.

The next treatment was physical in nature and involved passing the sample through a 10 µm mesh filter into an ultrasonic bath (model Branson 2200), following a method introduced by Wolfram (1954). The ultrasound breaks up the residue and allows the elements with a smaller mesh diameter, particularly clays, to pass through, while retaining the elements with a larger diameter, particularly palynomorphs. The residue remaining in the filter (i.e., larger than 10 µm) was then transferred back into 50 cl tubes, immersed in water and centrifuged again at 3000 rpm for 10 minutes. The supernatant was then removed, and the residue was left to stand under a fume hood for a few hours until almost completely dry.

The residue obtained was diluted using micropipettes (Gilson, model PIPETMAN Classic) in a glycerine solution with a dry residue : glycerine ratio of 1 : 10.

Finally, the microscope slide was prepared using 50 µl of sample diluted in glycerine. A thin strip of histolaque was affixed around the perimeter of the coverslip, so that the latter remained slightly separated from the microscope slide. This creates a very thin gap that allows the sediment to move slightly depending on the pressure exerted on the slide. This makes it possible to rotate the pollen grains and observe them from different angles.

2.2 Treatment of mosses and pollen trap

Each moss sample was cleaned of residual terrigenous sediment, as far as possible, before preparation and before weighing. Depending on availability, a variable amount of material (min. 1.0 g, max. 3.5 g) was prepared. The exogenous marker tablets (*Lycopodium*) were supplied by Lund University. Batch nr. 100320201 (14285 ± ca. 501

spores per tablet) for samples MOSS 1 OBS1-22, MOSS 2 OBS1-22, and MOSS 3 OBS1-22. Batch no. 140119321 (19855 ± ca. 521 spores per tablet) for all other moss samples.
Treatment of the moss samples (from whichever site they came from) initially consisted of immersion in hot 10% potassium hydroxide (KOH) for one hour. The residue was then filtered (200 µm mesh), and then treated with 7% hydrochloric acid (HCl), followed by 38% hydrofluoric acid (HF) for 48 hours, hydrochloric acid again, and finally filtration (10 µm mesh) in an ultrasonic bath. The resulting residue was then diluted in glycerine and used for slide preparation as described above.
The treatment of the annual pollen trap consisted of the following steps, carried out in the manner described above: numerous successive washes and centrifugations; addition of 7% hydrochloric acid (HCl); addition of 38% hydrofluoric acid (HF); new addition of hydrochloric acid; immersion in hot 10% potassium hydroxide (KOH) for 10 minutes; filtration (10 µm mesh) in an ultrasonic bath; new immersion in hot 10% potassium hydroxide for 10 minutes; new filtration (10 µm mesh) in ultrasonic bath. The exogenous marker tablets (*Lycopodium*) were supplied by Lund University, batch no. 140119321 (19855 ± ca. 521 spores per tablet).

2.3 Microscopic analysis and data processing

Microscopic analysis of all samples was carried out under an optical microscope (Leica ICC50 W (Appendix II, Fig. 6), NIKON Eclipse 50i (Appendix II, Fig. 7) and Nachet microscopes were used) at 400x, 500x and 1000x magnification (the latter with oil immersion). For the identification of palynomorphs, LO analysis was applied when necessary (Erdtman, 1952, 1954, 1969).
For the identification of pollen grains, mainly the atlas *Pollen et spores d'Europe et d'Afrique du Nord* by Maurice Reille (1992) and subsequent supplements (Reille, 1995, 1998) were used, as well as some monographs on pollen and other bibliographical sources. The comparison collection of the Department of Earth Sciences of the University of Florence provided further support for identification.
Each sample was analysed through optical counting and identification of pollen grains and other palynomorphs (including pteridophyte spores, algae and fungal remains, dinocysts, foraminiferal organic linings, and other NPPs, i.e. Non-Pollen Palynomorphs) at the species, genus, or family level, although species-level identification was rarely

possible. A minimum count of 150 pollen grains was achieved, excluding the dominant taxon and NPPs.

Using an Excel spreadsheet, the percentages (for pollen: percentage of occurrence of a given taxon out of the total number of pollen grains recorded; for NPPs: percentage of occurrence of a given taxon out of the total number of palynomorphs recorded) were calculated. Pollen concentrations were also calculated, according to the following formula:

$$\frac{\text{(Number of counted pollen grains) x (Number of } \textit{Lycopodium} \text{ spores in pill)}}{\text{(Weight of the treated samples (g)) x (Number of counted } \textit{Lycopodium} \text{ spores)}}$$

The pollen graphs were then obtained with the software Tilia (version 3.0.1; Grimm, 2015) and processed with Adobe Illustrator 2023 version 27.5.

Graphs were produced based on both pollen grain concentrations and percentages (see Results sections in chapters 3–5). Percentage diagrams were created for individual taxa as well as for broader categories such as arboreal and herbaceous types. Additionally, to represent the aggregation of various taxa into ecological or functional groups, taxa were organized according to the subdivisions described below.

I. Anthropogenic: includes allochthonous taxa introduced by humans, as well as autochthonous taxa whose presence at the site is however probably due to human activities such as cultivation or plant nurseries.
II. Mediterranean: includes taxa characteristic of Mediterranean vegetation, typically adapted to hot, dry summers and mild, wet winters. These species are often drought-tolerant and well suited to sclerophyllous shrublands and woodlands.
III. Sub-Mediterranean: includes taxa typically found in temperate deciduous or mixed forests, representing transitional vegetation between Mediterranean and Central European forest types.
IV. *Pinus*: the genus is treated separately due to the ecological variability of its species, some adapted to Mediterranean climates, others to montane or subalpine environments. Its separate classification also reflects its relevance in tracking vegetation change across the three study sites.
V. Mountain taxa: includes plant species generally supporting cooler temperatures under good humidity and are indicators of montane or subalpine vegetation belts.
VI. Riparian: taxa that prefer environments close to streams, ponds, or lakes.

VII. Helophytes: taxa that, despite being rooted to the ground, live mainly with their roots and buds covered by water. They prefer humid soils and are typically found in marshy ground. The Poaceae family has been included in a separated group named Helophytes/NAP, because this family comprehends both taxa of prairie environment and hygrophilous species of a humid environment (in this latter case, the common bulrush (*Typha latifolia*) can be noted). Grains of Poaceae recognized as cereals, which have probable anthropic origin, are instead included in the "Anthropogenic" group.

VIII. Hydrophytes: taxa of aquatic environments, which live totally submerged.

IX. Halophytes/NAP: includes salt-tolerant plants that grow in soils or waters with high salinity.

X. Upland Herbs: includes terrestrial herbaceous taxa typical of open environments.

XI. Xerophytes: includes taxa that have adaptations to survive in environments with water scarcity.

The list of taxa ascribed to each group is in Appendix I, Tabs. 1–3.

2.4 CONISS Analysis

The CONISS (Constrained Incremental Sum of Squares) cluster analysis was conducted using the Tilia program, employing a constrained hierarchical clustering method that is particularly effective for identifying clusters within sequential data. This approach allows for the identification of sample groups within the stratigraphic sequence that share similar characteristics at both individual taxa and informal palynological group levels, thus permitting the identification of pollen zones along the sedimentary record.

The dendrogram's x-axis displays the total sum of squares, representing the variance within the identified clusters, while the square root transformation was applied to the data, using Edwards & Cavalli-Sforza's chord distance as the measure of similarity.

The CONISS dendrogram for individual taxa was generated by including only those taxa that reached 2% of the total pollen in at least one sample. This approach focuses on the more dominant taxa, thereby enhancing the interpretive clarity of the clustering results. The CONISS analysis based on the informal palynological groups was instead conducted with the exclusion of the hydrophyte group, as the evolution of the ecosystem within the

lagoon may not follow the same changes as the terrestrial emergent vegetation surrounding the lagoon. The analysis performed on core OLP-11B excluded, in addition to the group of hydrophytes, the taxon *Quercus* sp., as it does not correspond to a clearly defined ecological group and would have introduced inaccuracies into the dendrogram structure. The analyses conducted on single-taxa data and informal palynological groups data resulted in similar dendrograms.

2.5 Microplastics extraction and analysis

Nine samples, six from the OLP-11B core and three for the LB5B core, were analysed for microplastics (MPs) content using a modified protocol from Gimiliani *et al.* (2020). The advantages of using this protocol for microplastic analysis are the reduction in the number of steps, which limits potential contamination, and the possibility of cleaning microplastics from organic matter and clay agglomerates, which facilitates identification and analysis of physicochemical properties (e.g. Raman spectroscopy). This protocol is especially targeted for the analyses of small microplastics (1 µm–1000 µm; Frias *et al.*, 2018).

The entire procedure and subsequent analysis of the microplastic content were carried out at the Earth Sciences Department of the University of Florence.

Samples (ca. 13-15 g of wet sediment) were placed in glass beakers, dried for 16 h at 75°C in an oven and weighted again. Dried samples masses ranged from 8 to 10 g. They were put for 24 h in a solution of 50% sodium hypochlorite (NaClO) and 50% sodium hexametaphosphate $(NaPO_3)_6$. The sediment was gently wet sieved using distilled water through a nested series of metal sieves with mesh sizes of 0.125 and 0.063 mm. The different size classes (125 µm-5 mm and 63-125 µm) were transferred into a Petri dish and analysed under a ZEISS stereomicroscope at 63x magnifications. Visual identification of microplastics was based on size, type, and colour criteria, and followed mainly Frias *et al.* (2018), Löder & Gerdts (2015), and photos within Abidli *et al.* (2018), Murphy *et al.* (2022), Srihari *et al.* (2022), and Turner *et al.* (2019). Focus was placed on the 125–62 µm fraction, as it is the most abundant in the surface sediments (Badino *et al.*, submitted).

To exclude modern contamination by microplastics originating from materials used for core extraction and storage or during laboratory analyses, 12 fragments of plastic material

from tubes, films, adhesive tape, and wrappings used for the extraction and conservation of sediment cores were taken and examined under the microscope (Fig. 6). Additionally, six procedural blanks were processed in parallel, and MPs counts in sediment samples were corrected accordingly (Frias *et al.*, 2018; Turner *et al.*, 2019). (Tab. 1 of Appendix III).

At the time of counting an estimate of the contaminant was subtracted from the total number of fragments observed, following the method in Turner *et al.*, 2019. Specifically, for each type of plastic identified in the control samples, the observed count of that plastic type in each fossil sample was adjusted by subtracting the highest number of that plastic type found in any control sample, plus one. This adjustment was applied to ensure that potential contamination was accounted for conservatively, reducing the likelihood of overestimating the actual microplastic presence in the fossil samples.

Microplastic analyses were conducted on a limited number of targeted levels as an exploratory screening within the broader multiproxy framework; further high-resolution sampling would be required to refine microplastic occurrence and quantify its stratigraphic variability.

Abbreviation	Core (site)	Depth (cm)	Wet weight (g)
MP-BUR-1	LB5B (Burano)	9-18	12,3
MP-BUR-2	LB5B (Burano)	40-50	13,0
MP-BUR-3	LB5B (Burano)	81-89	13,8
MP-ORB-1	OLP-11B (Orbetello)	7,5-18,5	8,1
MP-ORB-2	OLP-11B (Orbetello)	24-34	12,7
MP-ORB-3	OLP-11B (Orbetello)	52-63	12,5
MP-ORB-4	OLP-11B (Orbetello)	84-95	13,9
MP-ORB-5	OLP-11B (Orbetello)	129-140	14,7
MP-ORB-6	OLP-11B (Orbetello)	193-199	12,9

Tab. 4: Abbreviations, withdrawal cores and wet weight of the samples treated for the analysis on microplastics.

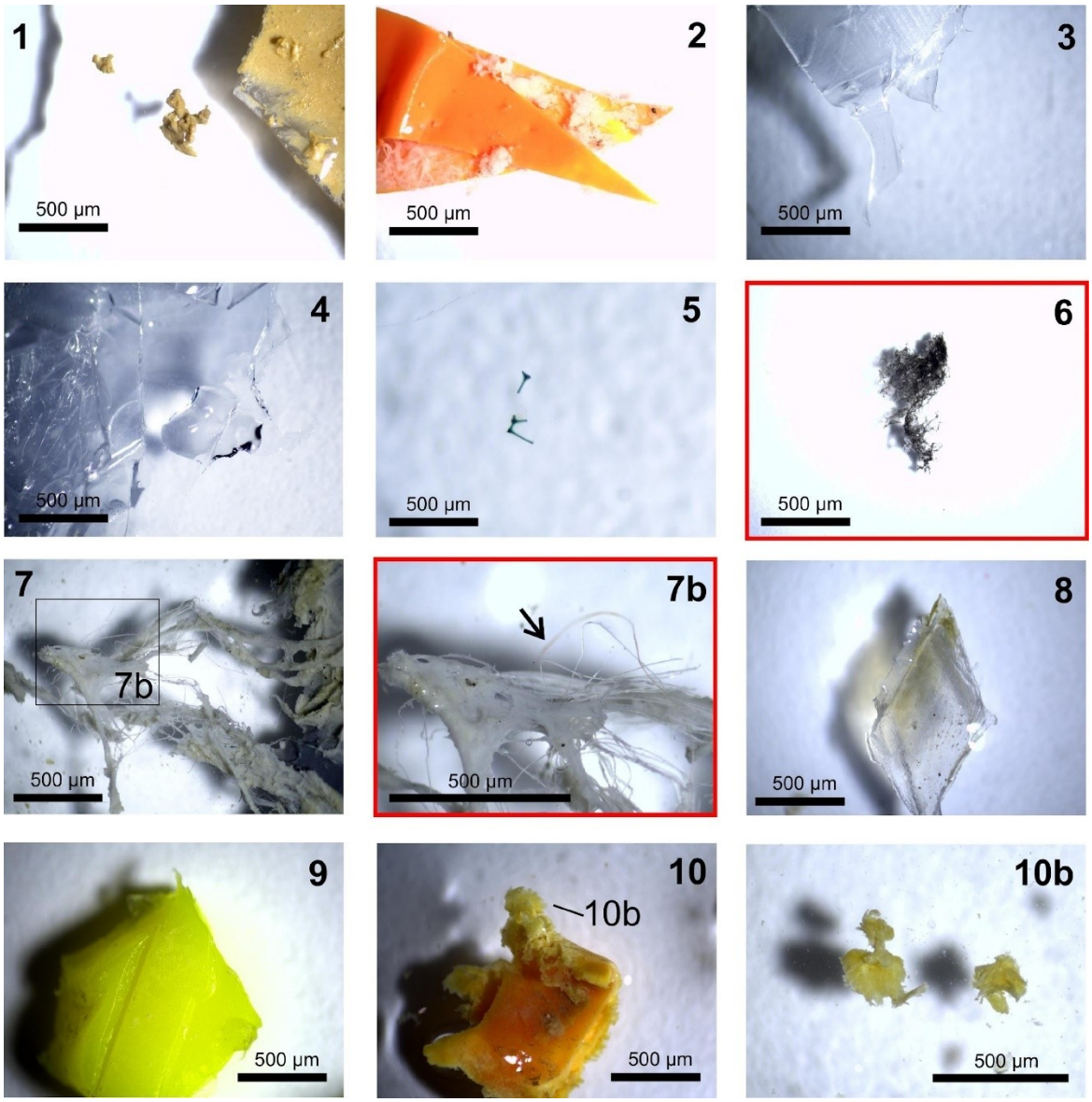

Fig. 6: Plastic samples collected from the casing material of cores and surface samples. 1, 2, 7, 7b: fragments of adhesive tape; 3, 4: fragments of plastic film; 5, 6: fragments of foam rubber; 8, 10, 10b: fragment of plastic tube (gray and orange) for storing the cores; 9: fragment of plastic closure of the tubes.

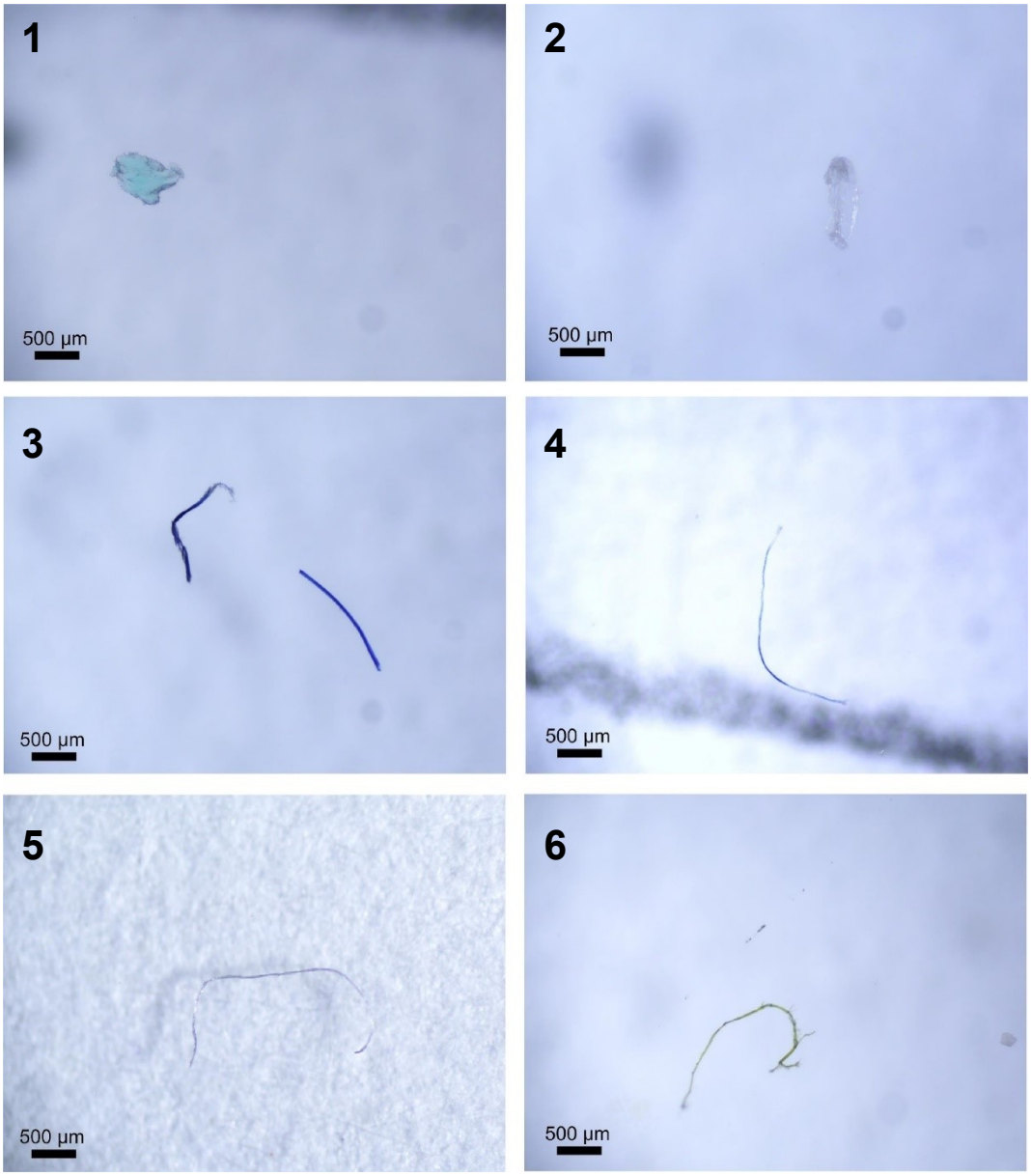

Fig. 7: Fragments and fibers found in the control blanks. 1: blue fragment; 2: transparent fragment; 3, 4: blue fibers; 5: nylon-like transparent wire; 6: red fiber.

2.6 Laser granulometric analysis

A granulometric analysis was carried out on all the surface samples extracted from the lagoons (7 in Lake Burano and 15 in Orbetello Lagoon, see Tab. 1 for the complete list) at the laboratories of the OMEAA complex, University of Lyon.

Approximately 2 g was taken from each surface sediment sample, immersed in ethanol. Pure hydrogen peroxide (H_2O_2) was subsequently added to the samples to cover the sediment, to encourage a dissolution reaction of the organic matter. The sediment was then left to dry after which 20% HCl was added until the reaction ended in order to dissolve the carbonates present in the sediment.

Once the sediment has dried, it is transferred into 50 cl test tubes. KCl is added at 0.1 M (0.75 g/L) and then at 0.02 M (1.5 g/L), in two successive cycles of mixing (defloculation), centrifugation, decantation. Finally, a final similar cycle is carried out with water at 40°. Centrifuge at 3500 rpm for 10 minutes. The sediment is then immersed in sodium hexametaphosphate (5.5 g/L) and mixed for five hours.

The sediment is then subjected to laser grain size analysis using a Fritsch Analysette 22 Next granulometer (Appendix II, Fig. 7). Subsequently, graphs were drawn up from the raw data using Excel.

This analysis was conducted to characterise the present-day hydrodynamic and depositional conditions of the studied basins. Grain-size distributions provide an independent proxy for sediment transport and settling processes, allowing the identification of low-energy, confined settings dominated by fine-grained deposition versus higher-energy zones influenced by marine exchanges or fluvial inputs. This information is essential to interpret modern depositional dynamics, the potential degree of surface mixing and resuspension, and the spatial heterogeneity of sediment sources. Importantly, granulometry also supports the interpretation of palynological surface samples by constraining taphonomic processes (transport, reworking, and differential preservation of pollen and non-pollen palynomorphs), thereby strengthening the linkage between modern assemblages and their depositional environment.

Chapter 3

Lake Burano

Introduction

Lake Burano is a coastal lagoon located along the Tyrrhenian Sea coast, at the southern edge of Tuscany, between the Promontory of Ansedonia and the Mouth of the Chiarone River, near the Lazio border, in the municipality of Capalbio (Province of Grosseto) (Chapter 2, Fig. 3). This area holds high ecological, geological, and environmental value due to its rich biodiversity and unique coastal lagoon ecosystem (e.g. Angiolini *et al.*, 1998, 2002). Lake Burano and its surrounding areas were declared a Ramsar site in 1977, and managed as a nature reserve by the WWF since 1969. It represents one of the most important protected areas in southern Tuscany and is part of the Maremma.

1. Environmental and cultural context

1.1 Geography and climate

The lake stretches parallel to the coastline, separated from the sea by a narrow sandpit, a dune formation typical of coastal lagoons (D'Orefice *et al.*, 2020a, 2022). The sandpit is formed by two parallel dune ridges with an interdunal depression between them: the outer ridge is higher and steeper, while the inner one is lower and more gently sloping. This geomorphological structure shapes the lake's hydrology and vegetation. The lagoon is connected to the sea via a narrow channel located roughly in the middle of the sandspit (Fig. 1). The lake is also connected to two artificial canals that flow into the north-west corner (Fosso del Melone, with its tributary Fosso di S. Floriano) and into the north-east corner (Scaricatore della Bassa), where pumping stations regulate water flow from or to the basin (Lenzi & Angelini, 1985) (Fig. 2).

Fig. 1: Satellite image of Lake Burano, with the indication of the connection to the sea (modified from Google Earth 2023).

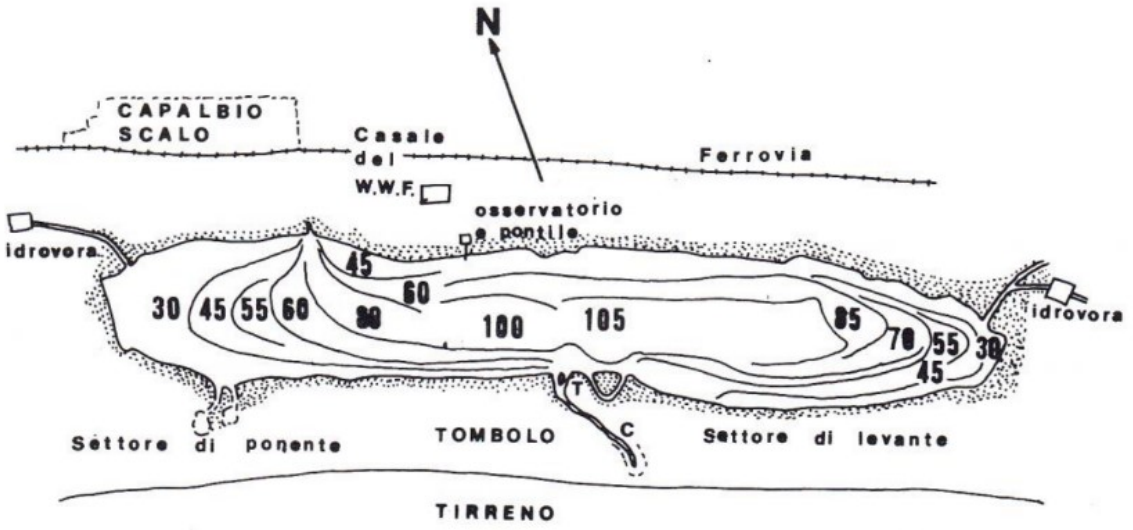

Fig. 2: Drawing of Lake Burano from Lenzi & Angelini (1985). Bathymetric values are indicated (values in cm). The connection with the sea and the two artificial canals at the NE and NW corners of the basin are visible. C = interred canal; T = Spanish tower.

The lake has a rectangular shape, measuring approximately 3.5 km in length and 500 m in width. The water depth averages around 1 meter, with a maximum depth of 2 meters. Its surface area spans 140 ha, although the entire reserve area, including surrounding dunes and wetlands, covers around 360 ha (Angiolini *et al.*, 2002; Lenzi & Angelini, 1985) (Fig. 1). Lake Burano's salinity fluctuates throughout the year, ranging from 15‰

to 32‰ (data from 1970s–1980s, Ardizzone *et al.*, 1983), reflecting the lagoon's limited exchange with the sea and freshwater inputs from local tributaries (D'Orefice *et al.*, 2020a).

Lake Burano lies within the coastal plain of southern Tuscany, shaped by Holocene deposits. The coastal dunes surrounding the lake are composed of quartz-rich sands, mixed with calcium carbonate, chlorides, and iron minerals such as magnetite, which give the dunes a distinctive dark grey colour (Angiolini *et al.*, 2002; D'Orefice *et al.*, 2020a). These sands, shaped by marine and aeolian processes, form the sandspit separating the lake from the sea.

Inland, soil shifts to silty and peaty deposits, typical of lagoon and marsh environments. Peat sediments form through the accumulation of organic material under anaerobic conditions. Such areas act as freshwater reservoirs that supply the lake, helping to maintain the hydrological balance of the lagoon ecosystem. The dunes are currently subjected to erosion due to wave action and other coastal dynamics, altering the lagoon's morphology (Bellotti *et al.*, 2007; Pranzini, 2001). Subsidence from marshland compaction further affects water depth and hydrology (e.g. Lenzi & Angelini, 1985). This geological setting plays a crucial role in shaping the vegetation and ecological processes within the lagoon (Angiolini *et al.*, 1998, 2002).

The region is classified within the meso-Mediterranean bioclimatic zone (Angiolini *et al.*, 2002). In the climatic classification map of Tuscany (Bigi & Rustici, 1984), the Lake Burano area is identified as having a dry sub-humid climate (data from the Orbetello Terra Rossa station), characterized by a marked summer water deficit and a pronounced winter water surplus.

Average annual temperature is around 16°C with extremes from -5°C in winter to 38°C in summer. Surface ice formation has been recorded occasionally, most recently in 1991. Warmer conditions in recent decades are evidenced by extreme values such as 19 °C in January 2016 (Ministero dell'Ambiente - Studio multidisciplinare, 1993). Meteorological data from the Capalbio Station (2006–2022) reveal an average annual precipitation of 541.8 mm, with extremes of 898.6 mm in 2009 and 147.6 mm in 2017. The wettest period of the year occurs between October and November, with a secondary, less intense, rainy season between February and March. The summer months are typically dry (Ministero dell'Ambiente - Studio multidisciplinare, 1993). Thermo-pluviometric analyses from the Burano weather station confirm a mesothermal climate with a Mediterranean rainfall

regime, although relatively recent data show a decrease in both precipitation and minimum temperatures compared to 20th-century records (Angiolini *et al.*, 2002; Ministero dell'Ambiente - Studio multidisciplinare, 1993) (Fig. 3).

Coastal areas are influenced by sea-land breezes, particularly during the summer, which blow from the sea towards the land and vice versa (therefore in a NE-SW direction), and which play a key role in shaping local climatic conditions (Piano antincendio boschivo (PAIB) 2022-2026). At higher elevations (above 600 m) south-easterly winds prevail (Monte Argentario station; Ministero dell'Ambiente - Studio multidisciplinare, 1993).

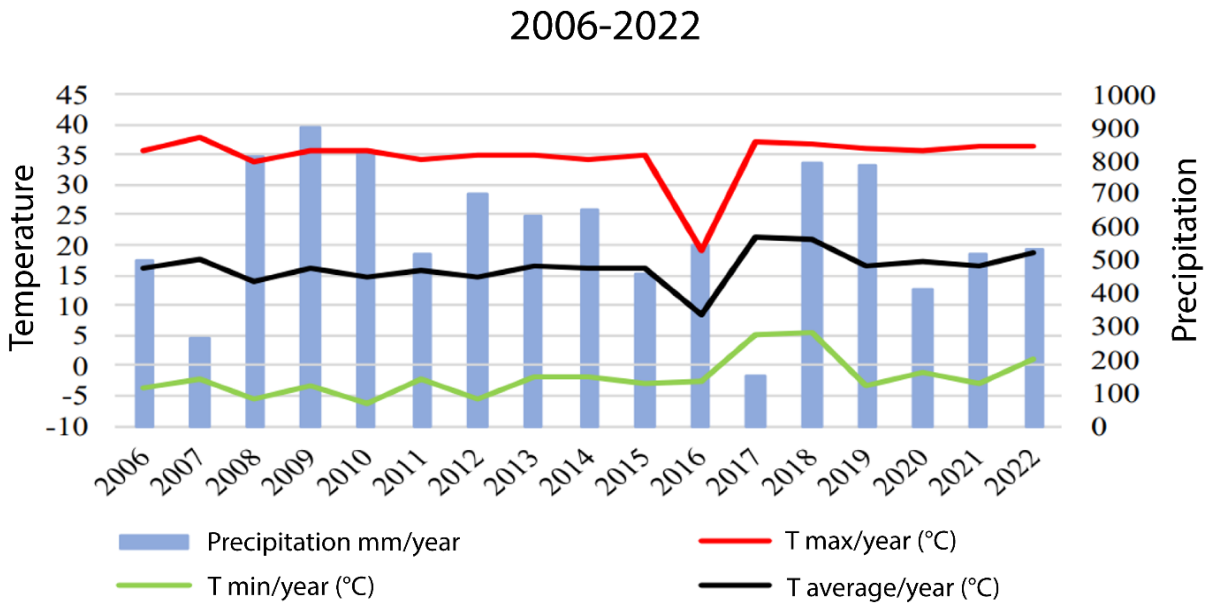

Fig. 3: Graph showing maximum temperatures, minimum temperatures, average temperatures, and precipitation recorded between 2006 and 2022 at the Capalbio Weather Station (modified from agroambiente.info.regione.toscana.it).

1.2 Hydrology and overview of the submerged and emergent vegetation (Fig. 4)

Lake Burano is characterized by brackish waters with a limited and controlled connection to the sea. Periodic dredging is necessary to maintain this connection, as the lagoon mouth naturally fills with sand (Ardizzone *et al.*, 1983). Two small tributaries provide freshwater inputs, but their flow is minimal.

The hydrology of the lagoon is influenced by seasonal rainfall variability, evaporation rates, and wind-driven circulation, which together determine the salinity gradient and water level fluctuations throughout the year. Salinity values are highest during summer, when evaporation exceeds freshwater inflow, and lowest during wetter months, particularly after intense autumnal and winter rains.

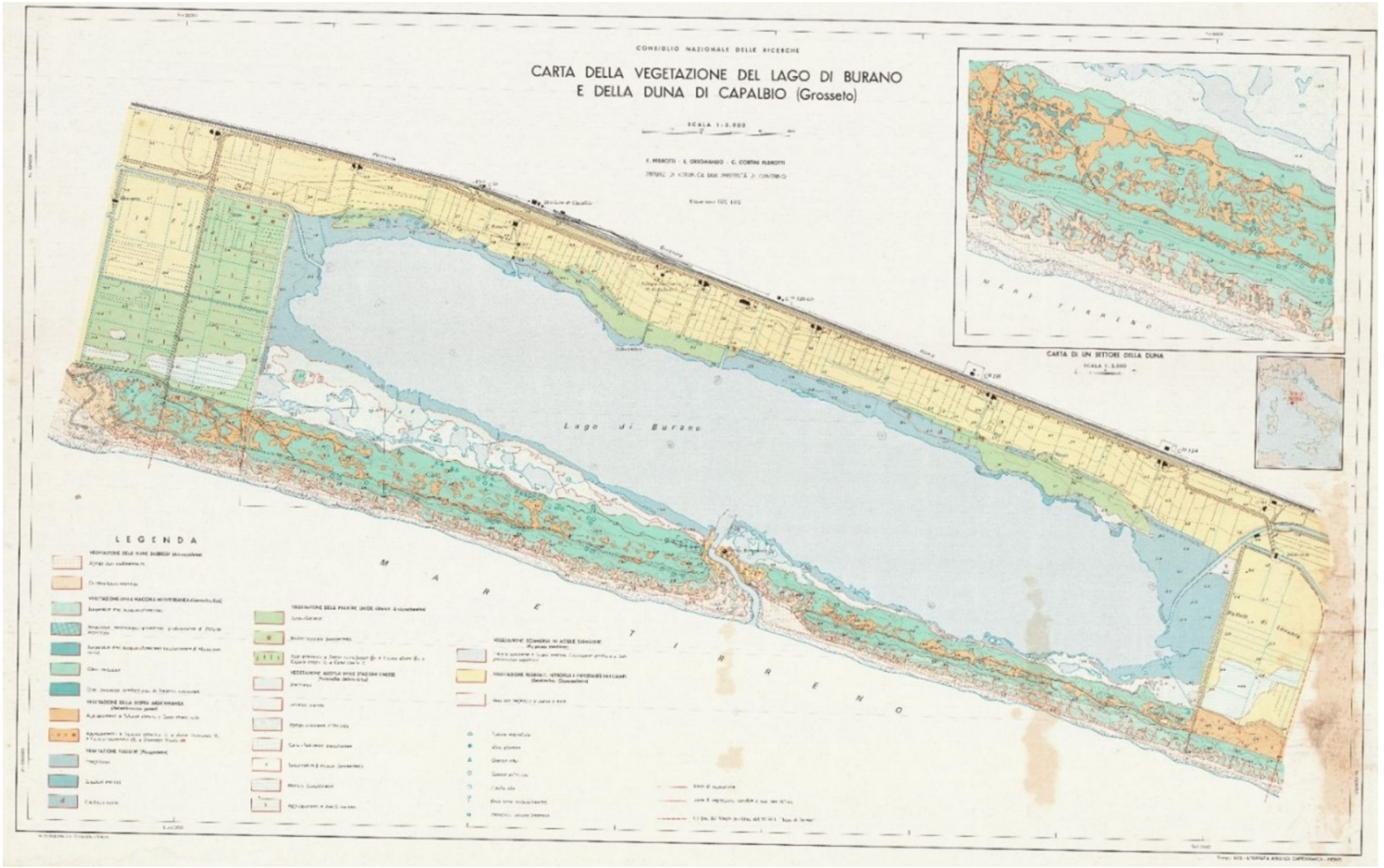

Fig. 4: Map of the phytosociological survey conducted on Lake Burano by Pedrotti *et al.* (1979).

These seasonal dynamics are further modulated by the limited water exchange with the sea, often constrained by the partial closure or silting of the lagoon mouth, which reduces mixing and exacerbates evaporative concentration during the dry season. The restricted connectivity to the open sea leads to salinity peaks and nutrient accumulation during the summer, which in turn promote episodes of eutrophication, algal blooms, and fish kills caused by oxygen depletion (Ardizzone *et al.*, 1983). Studies on the nutrient pathways in the lagoon show significant seasonal variations in nutrient concentrations. For instance, ammonium (NH_4^+) and nitrate (NO_3^-) levels peak in winter, while phosphate (PO_4^{3-}) concentrations are highest during the summer, likely due to the breakdown of organic matter in the warmer months (Ardizzone *et al.*, 1983; Ministero dell'Ambiente - Studio multidisciplinare, 1993). These nutrient dynamics are crucial in shaping the lagoon's vegetation and overall ecology.

The aquatic vegetation of Lake Burano plays a key role in the ecological balance of the lagoon. Submerged macrophytes, including several species of the genus *Ruppia* (*R. maritima*, *R. spiralis*, *R. cirrhosa*, according to three surveys between 1984 and 2021 (Angiolini *et al.*, 2002; Lenzi & Angelini, 1985; Lenzi & Cianchi, 2022), thrive in the shallow brackish waters. However, the composition of the submerged vegetation has been significantly impacted by the increased nutrient load, leading to periodic algal blooms that reduce light penetration and impact plant growth (Lenzi & Angelini, 1985). The study by Lenzi and Angelini (1985) emphasizes how submerged macrophyte communities in this site are shaped by interactions between vegetation and environmental factors, particularly climatic fluctuations, sedimentation, and hydrology. Changes in water level and salinity, driven by shifts in climate, affected species composition: dry periods and increased sediment input raised salinity levels, favouring salt-tolerant species, while wetter phases promoted greater plant diversity. Additionally, the input of organic matter and nutrients during certain climatic events likely stimulated macrophyte growth, leading to changes in biomass and community structure.

Although the emergent vegetation surveys referenced here are not recent, more up-to-date assessments of the site's plant communities are currently unavailable. Emergent vegetation around the lake is highly diverse and includes several distinct communities. The coastal dunes display a rich and well-preserved vegetation thanks to the relatively limited human impact. This ecosystem supports a variety of psammophilous halophytes, i.e. sand-loving plants, well-adapted to the strong winds, intense solar exposure, and to soils with high permeability and high salt concentrations, such as *Ammophila arenaria*,

Crucianella maritima, *Salicornia patula*, and *Arthrocnemum fruticosum*. These plants form dense mats along the shoreline and play an important role in stabilizing sediments and preventing further erosion (Angiolini *et al.*, 2002). Pioneer species, such as *Cakile maritima* (sea rocket), *Eryngium maritimum* (sea holly), and *Pancratium maritimum* (sea daffodil), thrive both in the dune system and in the interdunal zone. The low-growing shrubby vegetation in the back-dune area, which acts as a transition between the herbaceous dune vegetation and juniper shrublands, is dominated by *Helichrysum* and *Crucianella* species.

The marshy area around the lake hosts rare and endangered plant species, such as *Cladium mariscus* and *Ranunculus sceleratus*. Phytosociological research by Lenzi & Angelini (1985) highlights the presence of vegetation associations including *Ruppietum cirrhosae* (which was observed fruiting across 80% of the surveyed area), *Scirpetum maritimi*, and *Cladietum marisci*. These species are indicators of wetland habitats and are often restricted to areas with standing freshwater or seasonally inundated soils (Angiolini *et al.*, 2002; Lenzi & Angelini, 1985).

Further inland, Mediterranean scrub dominates, featuring species such as junipers (*Juniperus oxycedrus*, *J. phoeniceae*), and myrtle (*Myrtus communis*), in addition to arboreal species (*Quercus ilex*, *Q. suber*, *Pistacia lentiscus*) (Angiolini *et al.*, 2002). The nature reserve also contains patches of hygrophilous broad-leaved woodlands, including formations of *Salix cinerea*, as well as native broad-leaved trees like *Populus alba* and *Salix alba*. In the surroundings of the lake a narrow area of agricultural land separates this flat area from the nearby hills where olive groves, vineyards and arable fields predominate (Angiolini *et al.*, 2002; Piano antincendio boschivo (PAIB) 2022-2026).

Several species of high phytogeographical and conservation interest have been recorded in the Lake Burano Nature Reserve. Among them there are species which are endemic or close to the edge of their distribution range, such as *Dorycnium rectum*, *Fumaria bicolor*, *Linaria purpurea* subsp. *cossoni*, *Polygonum romanum*, and *Quercus frainetto*. The reserve also hosts important psammophilous species (such as *Crucianella maritima*, *Euphorbia paralias*, *Medicago marina*, *Matthiola sinuata*, and *Stachys maritima*), most of which are listed as threatened in Tuscany, and species with a fragmented distribution associated with wet habitats (both saline and freshwater) (Angiolini *et al.*, 2002). Other notable species include *Artemisia coerulescens var. palmata* and *Orchis palustris*, both of which are considered vulnerable or rare in the region (Angiolini *et al.*, 1998, 2002).

1.3 Geological and environmental history

The paleo-lagoon that later became Lake Burano, has experienced significant environmental changes over the last 8,000 years. According to D'Orefice *et al.* (2020a), five major phases characterize its transformation. Prior to approximately 7.5 ka BP, an open lagoon, larger than the current lake extended both north-west and south-east of the present basin, along the coastline. Around 6 ka BP, a barrier-lagoon system emerged, transforming the open lagoon into a closed one. Over time, the width of the lagoon increased, developing into a lacustrine environment. By 4 ka BP, discontinuous lacustrine facies appeared, and eventually, the lagoon transitioned into the current wetland area during the last 4,000 years (D'Orefice *et al.*, 2020a).

The Holocene history was driven by regional sea-level rise and sedimentary processes influenced by fluvial and marine inputs. Sea level followed the general Mediterranean trend: a rapid rise between 8000 and 6000 years ago, followed by a much more gradual increase in the late Holocene (about 2 m in the last 6000 years) (Lambeck *et al.*, 2011; Vacchi *et al.*, 2016, 2018). Geochronological data based on radiocarbon and optically stimulated luminescence (OSL) dating techniques allowed to reconstruct the environmental shifts and sediment accumulation rates, particularly in relation to the building of barrier-lagoon systems (D'Orefice *et al.*, 2020a).

Vegetation around Lake Burano has transformed in response to these paleoenvironmental changes over time. The terrestrial vegetation surrounding the lagoon, as evidenced by pollen analyses conducted in D'Orefice *et al.* (2020a), was dominated by thermophilus deciduous forests, with a mixture of Mediterranean and Sub-Mediterranean taxa. The pollen data showed the prevalence of *Quercus cerris*, *Q. pubescens* type, and *Carpinus orientalis*, which are typical of lowland and hilly areas.

Other notable taxa include *Olea*, *Phillyrea*, and *Pistacia*, which thrive in Mediterranean conditions. Additionally, herbaceous taxa such as Amaranthaceae and Cyperaceae expanded during certain periods, possibly linked to fluctuations in the lagoon's size and salinity (D'Orefice *et al.*, 2020a).

The faunal assemblages in these sediments further support the hypothesis of a dynamic paleo-lagoon ecosystem. Ostracods and foraminifera are particularly valuable bio-indicators in these contexts. D'Orefice *et al.* (2020a) report the dominance of *Ammonia tepida*, a euryhaline species commonly found in brackish environments, along with other

benthic foraminifera such as *Haynesina germanica* and *Porosononion granosum*. The high dominance of these species, coupled with low taxonomic diversity, suggests a highly fluctuating lagoon environment with varying degrees of marine influence during the middle Holocene, particularly between approximately 7000 and 4000 years BP, when barrier development and partial isolation of the basin intensified (D'Orefice *et al.*, 2020a; Lenzi & Angelini, 1985).

Ostracod assemblages, dominated by species such as *Cyprideis torosa* and *Loxoconcha elliptica*, also indicate shifts between open and closed lagoon conditions. These organisms thrive in environments with significant salinity gradients, which likely occurred as the barrier-lagoon system evolved, particularly during the transgressive phases of the Holocene. The progressive isolation of the lagoon, followed by the emergence of a more stable lacustrine environment during the late Holocene (from ca. 4000–3000 years BP onwards), is also evident in the transition to freshwater taxa such as *Limnocythere inopinata* and *Candona angulata* (D'Orefice *et al.*, 2020a).

Also, dinoflagellate cysts (dinocysts) found in the sediment cores provide further evidence of changing salinity and nutrient levels within the lagoon. D'Orefice *et al.* (2020a) observed significant peaks in dinocysts abundance (particularly *Lingulodinium machaerophorum*, which is associated with nutrient-rich, brackish waters), during humid episodes around 6800 and 4000 years BP. This suggests that periods of increased fluvial runoff, possibly linked to climatic changes, brought nutrients into the lagoon, supporting algal blooms (D'Orefice *et al.*, 2020a).

1.4 Human influence and conservation: history and current situation

The impact of human activity on Lake Burano and its surroundings became more evident in the latter part of the Holocene, beginning approximately 3000 years BP. During the Roman period, agricultural activities and land reclamation projects likely modified the hydrology of the lagoon (D'Orefice *et al.*, 2020a). Drainage canals and dikes, which continued into the medieval and modern periods, fundamentally altered the natural sedimentation processes (D'Orefice *et al.*, 2020a). Historically, the lake also served as a fish farm, with artificial water control structures installed to prevent the escape of fish to the sea (Ardizzone *et al.*, 1983).

By the 19th century, the reclamation of wetlands for agriculture drastically reduced the size of the lagoon, leaving behind what is now the Lake Burano. The transformation of

the lagoon into a wetland, and eventually a shallow lake, resulted in the loss of much of the original submerged vegetation and faunal diversity (D'Orefice *et al.*, 2020a). Moreover, in the last decades agricultural practices surrounding the lake significantly contribute to the influx of nutrients, particularly nitrogen and phosphorus, due to the use of synthetic and organic fertilizers. An estimate from the early 1990s indicates that in the Tuscan-Lazio Maremma region, agricultural lands release approximately 27 kg of nitrogen and 9 kg of phosphorus per hectare annually (Ministero dell'Ambiente - Studio multidisciplinare, 1993). This nutrient input increases the risk of eutrophication, disrupting the lake's trophic balance, and leading to nutrient accumulation in sediments, which promotes algal proliferation. Tree crops and intensive farming are the primary sources, emitting higher nutrient levels compared to forage crops. Tourism, especially during the summer months, contributes additional nutrients to the basin, with wastewater plants often unable to fully treat peak discharge volumes, adding significant quantities of nitrogen and phosphorus to the lake (Ministero dell'Ambiente - Studio multidisciplinare, 1993).

While these factors influence the lagoon's hydrology and nutrient balance and affect the vegetation, in more recent times the establishment of the WWF-managed nature reserve has provided some protection for the remaining wetland ecosystems (Lenzi & Angelini, 1985). Today, conservation efforts focus on maintaining the delicate balance between the lagoon's saline and freshwater inputs, as well as managing the nutrient load to prevent further episodes of eutrophication.

The important pioneer vegetation of the beach is currently subject to adequate conservation measures. Maintenance activities are performed without the use of mechanical tools, and the deposition of stranded organic material is preserved. This organic matter is essential for the survival of various beetle species and other invertebrates, contributing to the ecological integrity of the coastal habitat. The rich biodiversity, including bird species such as flamingos and herons, relies on the health of the aquatic vegetation and the continued presence of seasonal freshwater inflows (Lenzi & Angelini, 1985).

The area is also subject to seasonal fire risk, particularly in summer when dry conditions make the Mediterranean scrubland highly flammable. A comprehensive fire prevention plan has been implemented to protect the reserve's biodiversity (Piano antincendio boschivo (PAIB) 2022-2026).

Given the close interdependence of the site's geological history, hydrology, and vegetation, Lake Burano represents a dynamic environment that supports a wide range of plant and animal species. Ongoing conservation is essential to maintain this balance, especially in light of persistent threats such as nutrient pollution and coastal erosion.

2. Chronological framework of the core LB5B

2.1 Radiocarbon dating

At the Lake Burano site, the chronological framework was based on radiocarbon dating carried out by Christine Oberlin (Centre de Datation par le RadioCarbone, UMR 5138 "Archéométrie et Archéologie", Lyon, AMS ARTEMIS). Radiocarbon dating was performed on three cores, namely LB6, LB5A, and LB5B (Fig. 5). Two samples of the LB5B core were analysed for radiocarbon dating, as indicated in Table 1.

The first sample analysed for ^{14}C is at 101 cm depth, about halfway down the core, and the second sample is at 147 cm, close to the bottom of the core (Tab. 1). Because chronological control relies on few radiocarbon dates and bulk-sediment samples, the resulting age estimates should be regarded as indicative.

Although the Burano coastal system has a well-documented Holocene evolution spanning several millennia, the 151-cm core LB5B records only the most recent ~250 years of sedimentation when considering the marine-calibrated radiocarbon chronology. The broader geomorphological reconstruction is therefore provided as contextual background.

Reference sample	Depth (cm)	Sample material	Uncalibrated Age (± error)	Calibrated Age (± error)	Calibration
Lyon-19778 (sacA-67925)	101	Bulk	modern	modern	Marine (R ~450 y, ΔR=0, Oxcal V444. Marine data Heaton *et al.*, 2020)
Lyon-19779 (SacA-67926) *	147	Bulk	870 ± 30 ^{14}C yr BP	1764 ± 144,5 CE	Marine (R ~450 y, ΔR=0, Oxcal V444. Marine data Heaton *et al.*, 2020)

Tab. 1: Radiocarbon dating analyses carried out on the LB5B core (Lake Burano). The asterisk indicates the date used for the construction of the age-depth model.

Fig. 5: Location of cores LB6, LB5A, and LB5B within Lake Burano. Cores LB5A and LB5B were extracted a few meters apart in the centre of the lake.

2.2 Lead-210, Caesium-137, and Americium-241 content analysis

Analyses on ^{210}Pb, ^{137}Cs, and ^{241}Am elements were carried out by Pierre Sabatier (EDYTEM Laboratory, Université Savoie Mont Blanc and CNRS, Le Bourget-du-Lac, France) on the LB5B core. The analysis involved 23 samples between 0 and 58 cm (Tab. 2).

N°	Reference sample	Depth (cm)	Weight (g)	Volume (ml)	Density (g/ml)
1	LB5B(A) 0-2	0	4,666	4,8	0,972
2	LB5B(A) 2-4	2	3,402	3,6	0,945
3	LB5B(A) 4-5,5	4	2,669	3,3	0,809
4	LB5B(A) 5,5-7	5,5	4,429	4,8	0,923
5	LB5B(A) 7-9	7	4,788	4,6	1,041
6	LB5B(A) 9-11	9	4,232	4,5	0,940
7	LB5B(A) 11-13	11	4,547	4,7	0,967
8	LB5B(A) 13-15	13	4,481	4,5	0,996

9	LB5B(A) 15-18	15	4,829	4,5	1,073
10	LB5B(A) 18-20	18	3,931	4,4	0,893
11	LB5B(A) 20-22	20	4,080	5,0	0,816
12	LB5B(A) 22-24	22	4,508	4,9	0,920
13	LB5B(A) 24-25,5	24	4,081	4,2	0,972
14	LB5B(A) 25,5-27	25,5	4,059	4,2	0,966
15	LB5B(A) 28-30	28	4,443	4,4	1,010
16	LB5B(A) 30-32	30	4,107	4,5	0,913
17	LB5B(A) 32-34	32	4,204	4,5	0,934
18	LB5B(A) 36-38	36	3,825	4,2	0,911
19	LB5B(A) 40-42	40	3,356	3,7	0,907
20	LB5B(A) 44-46	44	3,339	3,3	1,012
21	LB5B(A) 48-50	48	3,937	4,4	0,895
22	LB5B(A) 52-54	52	4,456	4,6	0,969
23	LB5B(A) 56-58	56	3,316	3,1	1,070

Tab. 2: List of samples selected for the ^{210}Pb, ^{137}Cs, and ^{241}Am analyses on the LB5B core (Lake Burano).

We focused the analyses on the uppermost interval of the core to achieve a stratigraphic resolution sufficient to detect the peaks of ^{137}Cs from the second half of the twentieth century. This isotope is produced by the detonation of nuclear weapons and by the fission process in nuclear power plant reactors. Therefore, its peaks can be correlated with known events, in particular the nuclear test explosions in 1955 and 1963, and the disaster of the Chernobyl nuclear power plant in 1986. The ^{241}Am peak, concurrent with the ^{137}Cs fallout in 1963, provides an independent and more conservative chronostratigraphic marker, corroborating ^{137}Cs-based dating and offering greater reliability in cases of caesium redistribution or post-depositional disturbance (Bruel & Sabatier, 2020).
The peak of ^{137}Cs detected at 29 cm depth has been correlated with 1963. The ^{137}Cs peaks of 1955 and 1986 are not visible, probably because the stratigraphic recording of these peaks did not coincide with the samples selected for the analysis, and therefore were not detected. Moreover, depending on the geographical location, the visibility of the 1986 peak is limited or even absent in some sites (Bruel & Sabatier, 2020).

The ^{210}Pb dating method is commonly used to determine the age of sediment layers, especially in aquatic environments, over the past 100-150 years. This technique relies on

the decay of ^{210}Pb, a naturally occurring radioactive isotope of lead with a half-life of 22.3 years. This isotope is continuously supplied to sediments through atmospheric deposition. By measuring the excess concentration of ^{210}Pb from atmospheric sources relative to the amount naturally present in sediments due to *in situ* decay of ^{226}Ra and applying decay models, the sedimentation rate can be determined.

In this case the data on ^{210}Pb showed a clear and constant decreasing trend of this isotope (Fig. 6). Since the concentration of ^{210}Pb in sediments decreases at a known rate, its vertical distribution in the analysed section, integrated with the results of the ^{137}Cs analysis, has enabled the estimation of a linear mean sedimentation rate of 4.98 mm/year for this section of the core (Fig. 6).

The analysis of the amount of ^{210}Pb did not report significant values beyond 45 cm due to the excessive scarcity of this isotope beyond this depth, and they are therefore not represented in the graph below (Fig. 6).

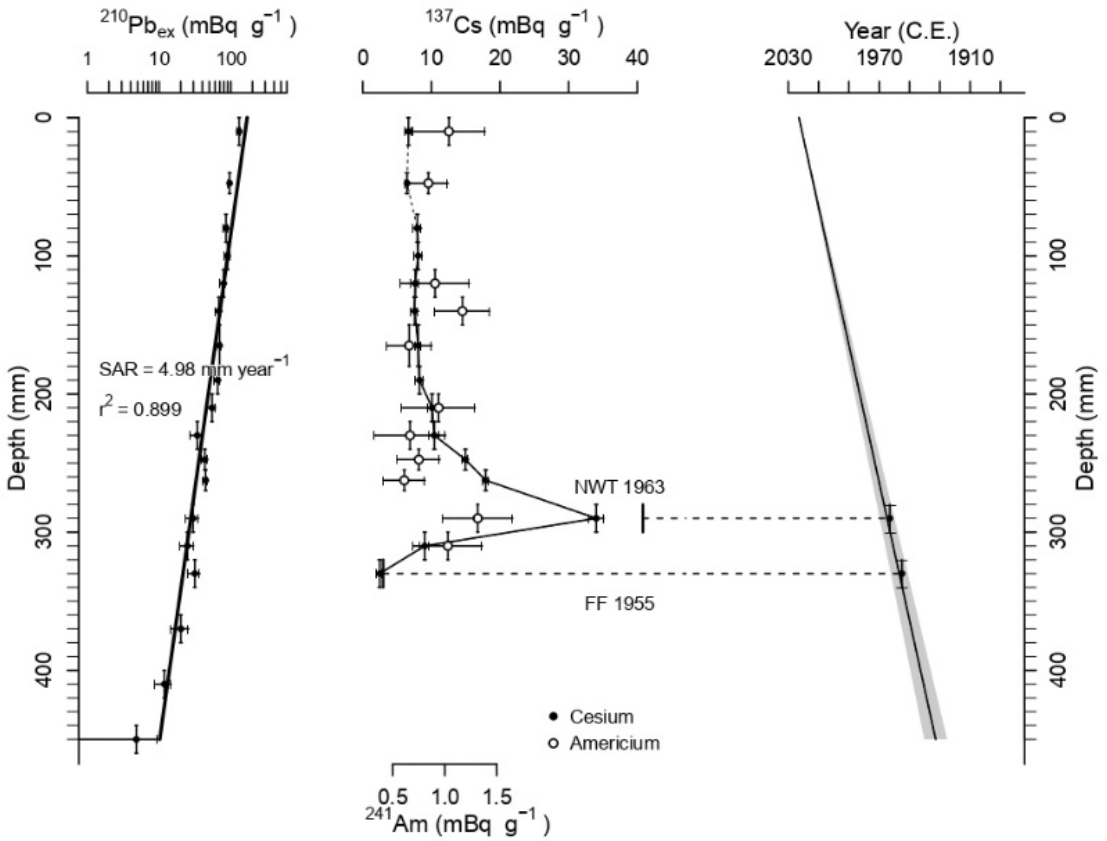

Fig. 6: Trend of ^{210}Pb, ^{137}Cs, and ^{241}Am, with relative model age, on the first 45 cm of the LB5B core (image elaborated by Pierre Sabatier).

Results

3. Palynological analysis of the sediment core

3.1 Palynomorph concentrations

Palynomorphs are abundant in almost all LB5B core samples, and the state of preservation of the grains was generally good. Organic matter was found to be particularly abundant. The concentration of palynomorphs reaches maximum values of 92,172 granules per gram of sediment, minimum values of 11,244 granules per gram of sediment, and average values of 40,247 granules per gram of sediment (Fig. 7).

The concentration of pollen grains (the total of palynomorphs excluding NPP) varies along the core, showing peaks, and in general slightly higher values, in the deeper half than the upper half. The maximum values are 70,744 granules per gram of sediment and the minimum values are 10,498 granules per gram of sediment, with average values at 32,872.

In some samples, concentration peaks depend on the high concentration of specific ecological groups. An example of this is the peak around 64 cm depth, especially due to the high concentrations of *Pinus* (pine), Sub-Mediterranean taxa, Helophytes, Upland Herbs and Xerophytes, whereas the other groups seem to record less significant increases. However, the peak at 81 cm is relevant in the Mediterranean taxa, in the Hydrophytes, Halophytes/NAP, Upland Herbs and Xerophytes, while it is almost absent for example in the *Pinus* concentration. Other similar examples are visible in the graphs in Fig. 7.

The concentration values of NPPs are on average below those of pollen, with maximum values of 21,427 cells per gram of sediment, minimum values of 525 cells per gram of sediment, and average values of 7,375 cells per gram of sediment. The concentration of NPPs reflects the trend of pollen concentration along the entire length of the core (Fig. 7). Only between 36 and 42 cm the concentration of NPPs does appear to present a higher peak than that shown by pollen (Fig. 7). This trend is entirely due to a clear increase in the concentration of the green alga *Botryococcus* (which reaches a peak of almost 12,000 cells per gram at 40 cm, with a trend of increased concentration both lower and higher

than this depth), and, to a much lesser extent, of the green alga *Euastrum*, which presents a significant increase at the same depth (Fig. 14).

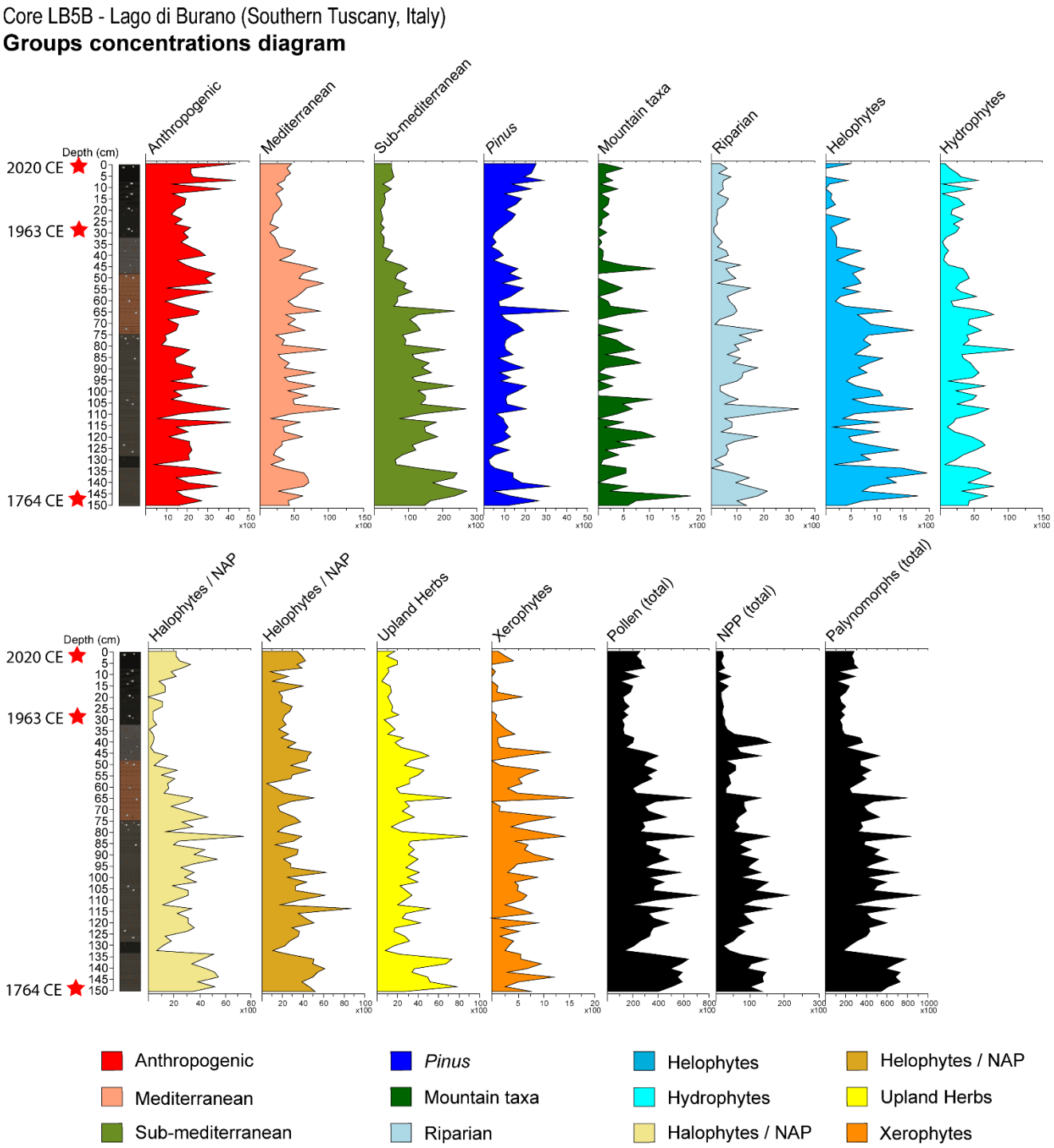

Fig. 7: Concentrations of selected informal palynological groups of the core LB5B. Calibrated marine dates are reported.

3.2 Flora (Tab. 1 of Appendix I. Figs. 8, 9)

The palynological analyses of the LB5B core from Lake Burano reveal a flora composition mainly consisting of Fagaceae and Oleaceae in its arboreal component. The most abundant pollen taxa are the morphological types *Quercus ilex-coccifera* and *Quercus pubescens*, among the Fagaceae, together with *Olea europaea* (olive), *Fraxinus* sp. (ash), and *Phillyrea* sp. (mock privet) among the Oleaceae, with the addition of *Pistacia* sp. (mastic and terebinth, fam. Anacardiaceae) and the occasional occurrence of *Celtis australis* (hackberry, fam. Cannabaceae). Among the trees, *Pinus* sp. (pine) is also abundant, while other Pinaceae such as *Abies* sp. (fir) and *Picea* sp. (spruce) are not attested.

Among the Betulaceae the genera *Alnus* (alder), *Betula* (birch), *Carpinus* (hornbeam), *Ostrya* (hophornbeam), and *Corylus* (hazel) are prevalent, to which are added genera of temperate broad-leaved trees such as *Juglans* sp. (walnut), *Acer* sp. (maple), *Ulmus* sp. (elm), *Sambucus* sp. (elderberry).

Among the shrubs it is documented *Tamarix* sp. (tamarisk), an element of the Mediterranean scrub, in addition to *Juniperus* sp. (juniper), and other taxa such as *Ziziphus* sp. (jujube), *Viburnum* sp. (wayfarer), and to elements of the Myrtaceae (*Myrtus* sp., the myrtle, has also been identified) and Ericaceae families.

The floristic variety of herbaceous pollen is quite rich. The most abundant families are Amaranthaceae, Asteraceae (especially genus *Artemisia*), Plantaginaceae, Rosaceae, Brassicaceae, Cistaceae, and Scrophulariaceae, with the occasional addition of Polygonaceae, Fabaceae, Ranunculaceae, as well as other less represented but still attested families (Euphorbiaceae, Saxifragaceae, Malvaceae, Hypericaceae, Araliaceae, Rutaceae, Geraniaceae, Liliaceae, Iridaceae, Apiaceae, Lamiaceae, Rubiaceae, Crassulaceae, etc.).

Helophytic plants (particularly Cyperaceae) and aquatic plants (hydrophytes) are present, with *Ruppia* (beaked tasselweed or widgeon grass) being especially noteworthy. Subordinate occurrences include the *Sparganium/Typha angustifolia* type (bur-reed/lesser bulrush) and *Lemna* sp. (duckweed), both widely recorded. Poaceae are also well represented. Among introduced and cultivated species, evidence is found for *Castanea* (chestnut), *Vitis* (grapevine), *Eucalyptus* (eucalyptus), cultivated cereals, indeterminate Cupressoideae, and Solanaceae (*Solanum* cf. *nigrum*).

A total of 105 pollen taxa were identified. Specifically, 31 arboreal taxa, 7 shrub taxa, and 67 herbaceous taxa were recorded. The anthropogenic indicators group includes 9 ta-

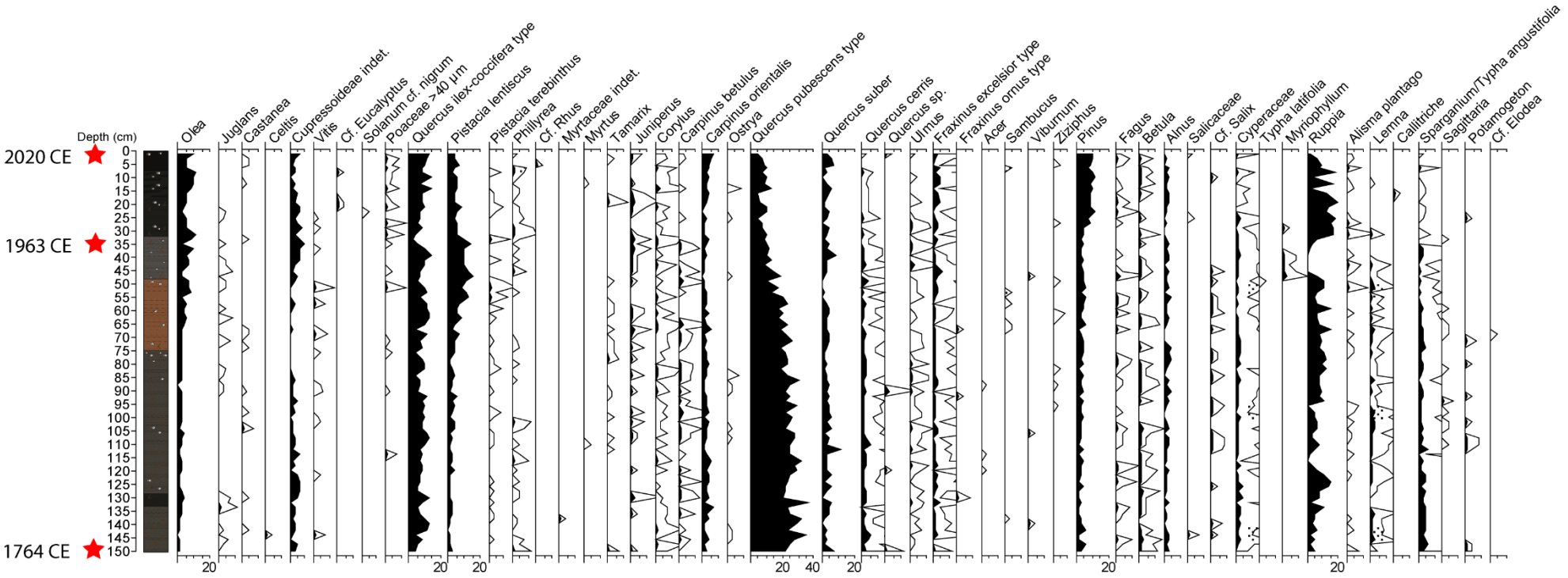

Fig. 8: Detailed palynological diagram of the core LB5B (exaggeration 8x). Calibrated marine dates are reported.

Core LB5B - Lago di Burano (Southern Tuscany, Italy)

Single taxa diagram (exaggeration 8x)

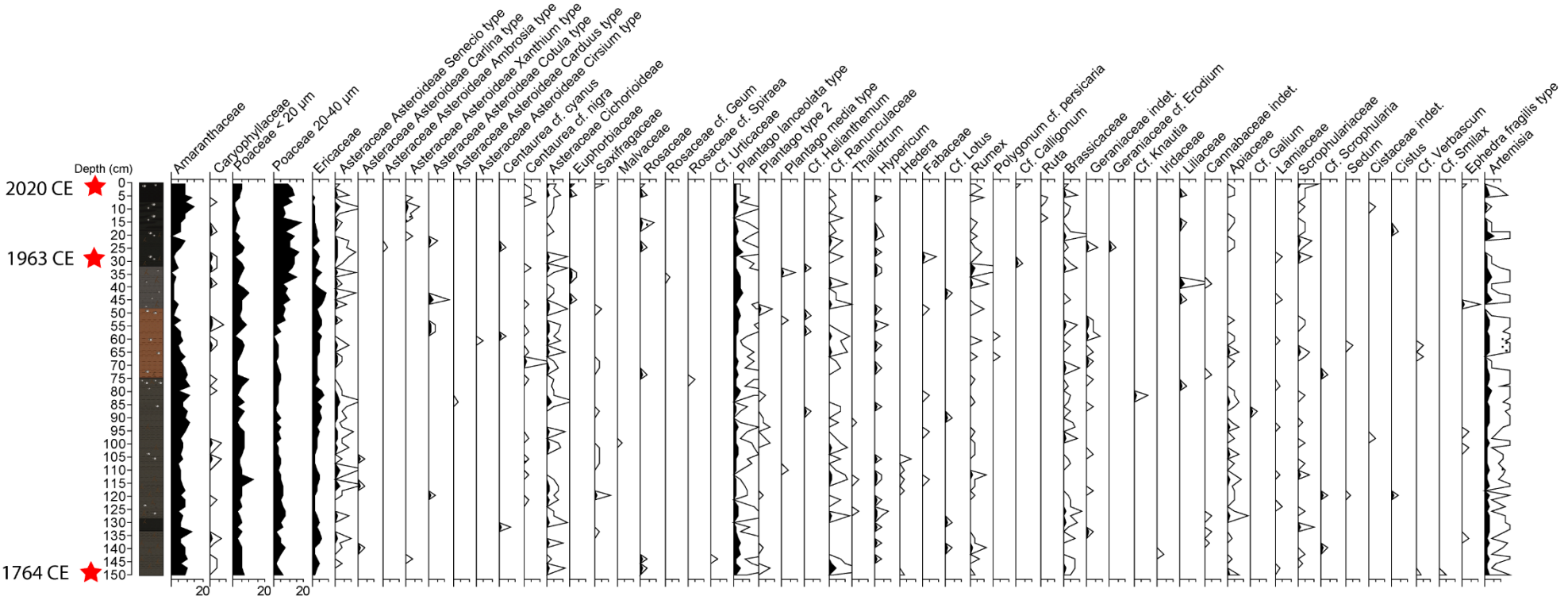

Fig. 9: Detailed palynological diagram of the core LB5B (exaggeration 8x). Calibrated marine dates are reported.

xa, Mediterranean 9 taxa, Sub-Mediterranean 15 taxa, Montane 2 taxa, Riparian 3 taxa, Helophytes 2 taxa, Hydrophytes 9 taxa, Halophytes/NAP 2 taxa, Helophytes/NAP 2 taxa, Upland Herbs 49 taxa, and Xerophytes 2 taxa. *Pinus* was counted separately.

3.3 Vegetation (Figs. 8–11)

The palynological analysis of the LB5B core indicates a predominance of arboreal plants over herbaceous ones, with tree pollen averaging 60% throughout the core. This percentage slightly decreases to around 50-55% from 35 cm depth to the surface, yet remains relatively stable overall (Fig. 10).

In the deepest layers, Sub-Mediterranean taxa are particularly well represented, reaching 30-40%. This group is mainly composed of *Quercus pubescens* (downy oak) type, whose abundance gradually declines upward. This reduction is partly compensated by slight increases in *Quercus suber* (cork oak) and *Fraxinus excelsior* (common ash), particularly in the middle and upper layers. In contrast, the other groups display relatively stable percentages, consistently remaining below 20% during this phase (Fig. 11).

Between 65 and 35 cm depth, a moderate rise in Mediterranean taxa is observed, reaching 20-25%, largely due to an increase in *Pistacia lentiscus* (mastic). In this same interval, halophytic taxa, primarily Amaranthaceae, reach occasional peaks of 15% in the lower-middle segments but show a notable decline between 50 and 30 cm, stabilizing below 5%. Poaceae with grain size of 20-40 μm show a slight but steady increase starting from around 55 cm, culminating in values approaching 20% near the surface. In contrast, Poaceae under 20 μm exhibit no significant trends (Fig. 11).

Anthropogenic indicators, which remain around 5-10% between 149 and 45 cm, begin to rise modestly (up to 15%) in the uppermost 45 cm, primarily due to increased values of *Olea* (olive), which also contributes to the slight uptick in Mediterranean elements alongside *Carpinus orientalis*. *Juniperus* and other Mediterranean taxa remain consistently low throughout. In the upper 30 cm, *Pinus* shows a noticeable increase from values <5% in the lower part of the core to approximately 10% at the top. Riparian and mountain taxa, including *Alnus* (alder), *Fagus* (beech), and *Betula* (birch), remain under 5% throughout the core, with no significant fluctuations. *Abies* and *Picea* are entirely absent. Upland herbs show limited variation, fluctuating between 6% and 15%, with Ericaceae being the most frequent representative. Xerophytes are sparsely represented,

mainly by *Artemisia* (mugwort) and sporadic occurrences of *Ephedra fragilis* (joint pine) (Fig. 11).

Among the aquatic taxa, hydrophytes fluctuate considerably, with *Ruppia* being the most prominent aquatic taxon. *Ruppia* shows marked variability in the deeper layers and eventually disappears around 35-40 cm, whereas *Myriophyllum* (water milfoil), absent from the lower samples, becomes more common during this phase. Simultaneously, *Sparganium/Typha angustifolia* type gradually decreases in representation toward the upper sections of the core. The other helophyte and hydrophyte taxa remain minor and show no significant variation (Fig. 11).

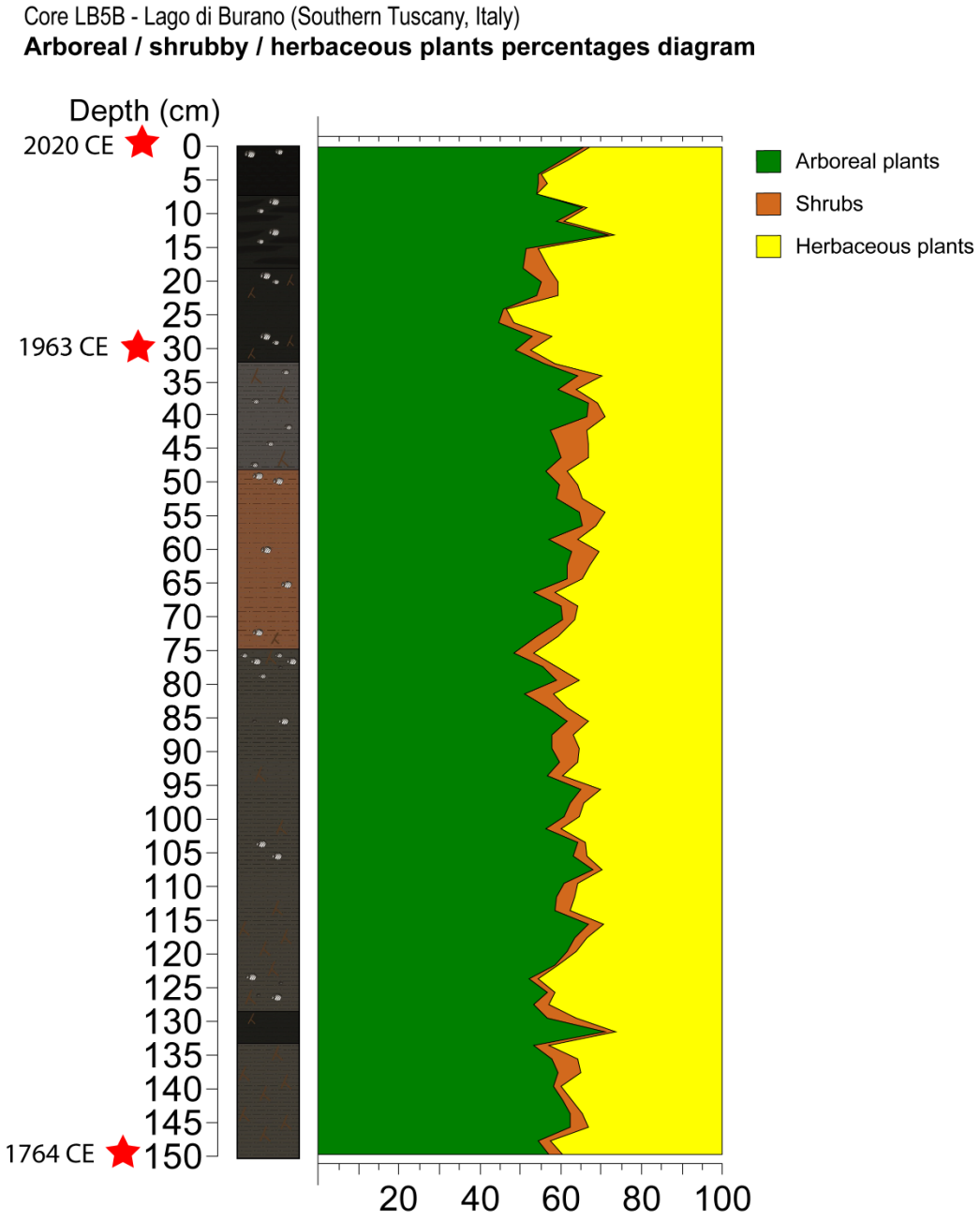

Fig. 10: Summary pollen diagram of arboreal / shrubby / herbaceous percentages of the core LB5B. Calibrated marine dates are reported.

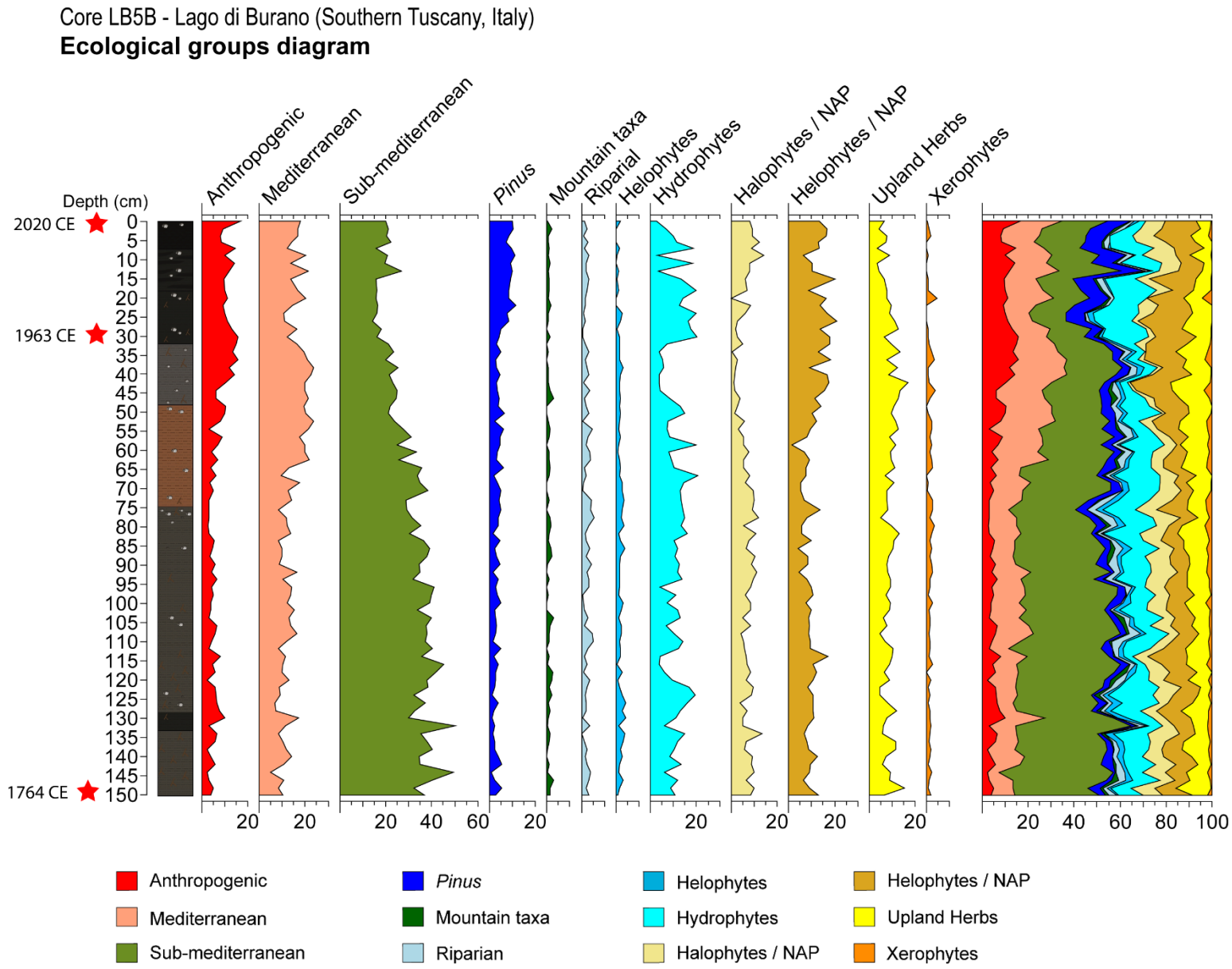

Fig. 11: Informal palynological groups percentages of the core LB5B. Calibrated marine dates are reported.

3.4 Pollen zones description (Figs. 12, 13)

Based on the CONISS analysis results, we identified four main zones, with both the first and fourth zones further subdivided into two sub-zones (as indicated by the dark and light grey bands, Figs. 12 and 13). These zones are labelled, from bottom to top of the core, as BUR-1 (a and b), BUR-2, BUR-3, and BUR-4 (a and b).

1. Zone BUR-1 (149 cm to 64 cm) is marked by relatively stable percentages of the most represented taxa. Among tree taxon *Quercus pubescens* type is the most abundant, followed by *Quercus ilex-coccifera* type. Among herbaceous and shrubby taxa, Amaranthaceae dominate followed by Ericaceae and Poaceae >20 µm. Within BUR-1a subzone (149 cm to 103 cm) Amaranthaceae and Ericaceae occur in slightly lower percentages than in the overlying BUR-1b subzone (103 cm to 64 cm), Poaceae >20 µm also show a gradual decrease from the basal to the upper portions of the subzone (Fig. 12).

   The Anthropogenic group is poorly represented, never exceeding 10%. Mediterranean and Helophytes/NAP taxa are minor components while *Pinus* is recorded at even lower percentages. The Sub-Mediterranean group exhibits high percentages (around 30–40%) throughout this phase, although a decreasing trend toward the less basal portion of the zone is observed. The Halophytes/NAP group remains low but stable, with a modest increase towards BUR-1b, driven by the rise in Amaranthaceae. Upland Herbs maintain relatively low and stable percentages (Fig. 13).

   Overall, this zone reflects an environment dominated by arboreal species, with a clear prevalence of Sub-Mediterranean taxa particularly *Quercus pubescens* type, while Mediterranean and Anthropogenic elements are notably reduced.

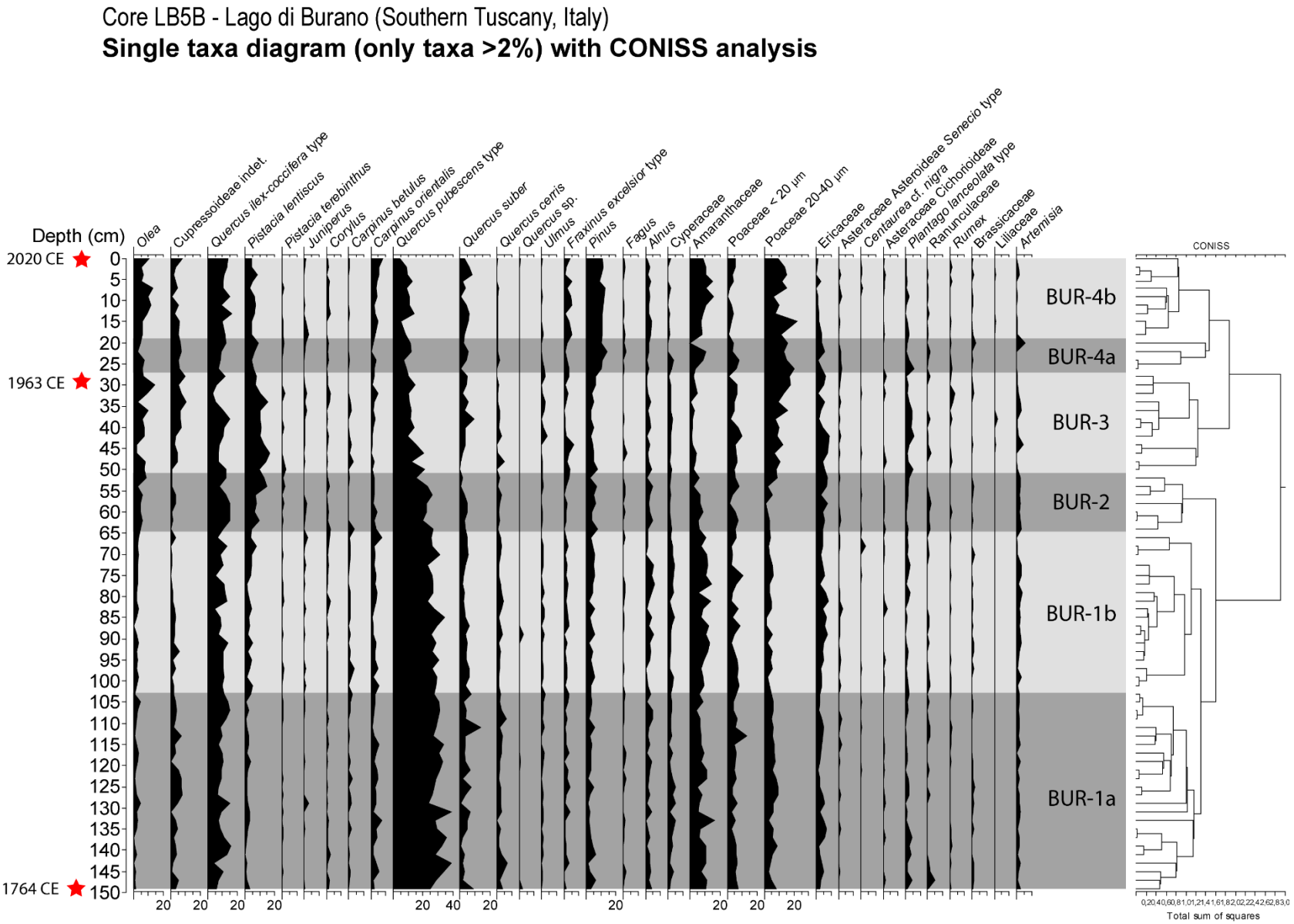

Fig. 12: Single taxa diagram with CONISS analysis and subdivisions of the zones. Only taxa reaching 2% in at least one sample were considered in the analysis. Calibrated marine dates are reported.

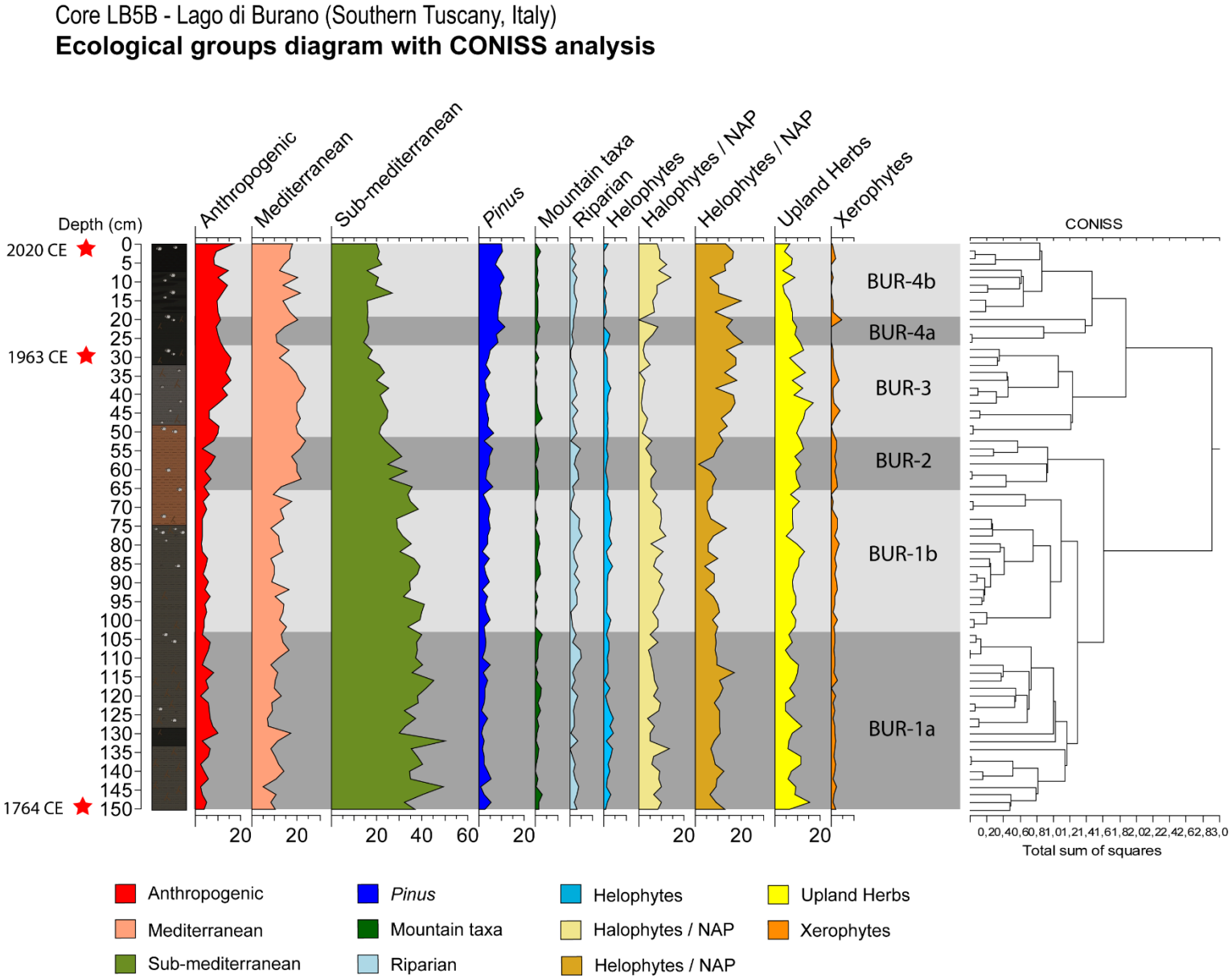

Fig. 13: Informal palynological groups diagram with CONISS analysis and subdivisions of the zones. Hydrophytes have not been considered in the analysis and thus are not represented in the graph. Calibrated marine dates are reported.

2. Zone BUR-2 (64 cm to 52 cm) appears to be for many taxa a transitional zone between the previous and subsequent phases. The increasing percentages of the Mediterranean group are due to the trend of *Pistacia lentiscus* which begins a phase of high values extending in the overlying zones, rather than *Quercus ilex-coccifera* type. *Olea* also shows a slight increase anticipating higher percentages in the upper part of the core (Fig. 12). A similar, though less pronounced, upward trend is observed in the Upland Herbs group. Poaceae >20 μm also show a slightly increasing trend compared to the previous phase. In contrast, the Sub-Mediterranean group display a more pronounced decreasing trend during this phase, continuing the slight decline that began in the final levels of BUR-1. Amaranthaceae, and consequently the Halophytes/NAP group, also decrease compared to their higher values in the BUR-1. The Anthropogenic and Helophytes/NAP groups maintain low and stable values, with a slight tendency to rise toward the upper part of the zone. *Pinus* remains at low values (Fig. 13).

   Overall, BUR-2 marks the transition from an environment dominated by Sub-Mediterranean species, particularly *Quercus pubescens* type, to an environment characterized by higher percentages of Mediterranean, Anthropogenic and Poaceae.
3. Zone BUR-3 (52 cm to 26 cm) represents the full expression of the transitional shift observed in BUR-2, with a clear departure from the two underlying zones. Percentages of *Quercus pubescens* type decrease significantly, while *Olea*, Cupressaceae, *Pistacia lentiscus* and Poaceae >20 μm become more abundant (Fig. 12). As a result, Sub-Mediterranean taxa decline, whereas Anthropogenic and Helophyte/NAP elements show a marked increase, reaching higher percentages that persist up to the top of the core. Zone BUR-3, for these two groups, appears to be a transitional period from lower percentages in deeper layers to higher percentages in the upper layers. The Halophytes/NAP group shows lower values compared to the higher averages found in other sections of the core. Upland Herbs percentages are similar to the BUR-2, thanks to slightly higher values of *Plantago lanceolata* type in this zone compared to all other sections of the core. *Pinus* remains consistently stable and low, as in the two previous zones (Figs. 12, 13).

   In conclusion, BUR-3 marks a consolidation of the transition toward a more open and anthropized environment. This phase is characterized by reduced deciduous oak cover, increases presence of anthropogenic species (notably *Olea* and Cupressaceae) and more open landscapes dominated by Poaceae. *Pinus* coverage, however, remains unchanged.

4. Zone BUR-4 (26 cm to the top) is distinguished primarily by higher percentages of *Pinus* (with values averaging around 10%) compared to the rest of the core. The Mediterranean group shows a slight decline due to reduced *Pistacia lentiscus*, while *Quercus ilex-coccifera* type remains stable (Fig. 12). Anthropogenic species maintain moderately high percentages due to the abundance of *Olea*, and despite a minor decrease in Cupressoideae). Sub-Mediterranean taxa, including *Quercus pubescens* type continue their downward trend, observed since BUR-2. In this zone, deciduous oaks (*Quercus pubescens* type) are reduced to values comparable to, and often lower than, those of evergreen oaks (*Quercus ilex-coccifera* type) (Fig. 12).
   Helophytes/NAP maintain high values, driven by the abundance of Poaceae >20 µm. Halophytes/NAP, primarily Amaranthaceae, show a new increase, especially in BUR-4b (18 cm to the top), compared to the minimum recorded in BUR-3. Differences between subzones BUR-4a (26 cm to 18 cm) and BUR-4b are mainly among herbaceous groups: Amaranthaceae increase trend from the bottom to the top, whereas Upland Herbs, particularly Ericaceae and *Plantago lanceolata* type, exhibit slightly higher values in BUR-4a than in BUR-4b. This reflects a decreasing trend relative to BUR-3 (Figs. 12, 13).
   In conclusion, BUR-4 reflects an environment similar to that of the preceding zone, but with a notably higher presence of *Pinus*. The increase in Amaranthaceae and the slight decrease in *Pistacia lentiscus* represent additional differences compared to BUR-3, indicating subtle shifts in both Mediterranean and herbaceous components.

Montane, Riparian, Helophytes, and Xerophytes groups maintain very low percentages throughout the core, showing no significant variation (Fig. 13).

3.5 NPP (Figs. 14, 15)

The NPPs are relatively low in abundance along the entire length of the core, with average percentages of 17.31% of the total palynomorphs (max. 44.51%; min. 4.08%). Fig. 15 shows the relative percentage of pollen and NPPs on the total of palynomorphs.
From the base of the core up to approximately 45 cm depth, the non-pollen palynomorph (NPP) assemblage is characterized by relative stability in both composition and abundance (Fig. 14). During this interval, NPPs account for around 20% of the total palynomorphs (Fig. 15). *Botryococcus* is the dominant taxon, showing a constant and substantial presence with average percentages of 11% of the total NPPs. *Cosmarium* also

contributes significantly, maintaining stable values from 132 cm to about 32 cm depth, while its presence is negligible below 132 cm. Spores of pteridophytes, dinocysts, and benthic foraminiferal linings are all present throughout this portion, though they remain at low percentages and exhibit no major fluctuations (Fig. 14). The green algae *Spirogyra* (water silk), *Pseudoschizaea* (*incertae sedis*), and less common taxa such as *Closterium*, various indeterminate algae, *Arcella* (a testate amoeba), fungal spores of the genus *Glomus*, and diatoms are also sporadically present across the core.

Between 45 and 30 cm depth, a marked increase in the total NPP percentages is observed, culminating in a distinct peak of 44.51% at 40 cm (Fig. 15). This peak is largely driven by the sharp increase in *Botryococcus*, which alone accounts for 59.36% of the NPPs at 40 cm and shows an increasing trend in the surrounding levels. *Euastrum* also contributes notably, reaching 20.53% at 38 cm and maintaining 9.63% at 40 cm. In contrast, *Cosmarium* remains relatively stable through this section without a marked increase (Fig. 14). Concurrently, a notable presence of pteridophyte spores is observed, particularly of a type resembling *Isoetes* (cf. *Isoetes*), which averages 2.5% between 38 and 30 cm. In general, the relative abundance of pteridophyte spores increases significantly in this phase, with average values rising from 8% to approximately 24% of the total NPPs (Fig. 15). This trend culminates in a major peak at 32 cm, where pteridophyte spores reach 68.75%, driven mainly by a surge in monolete spores. Meanwhile, *Botryococcus*, which previously dominated the assemblage, rapidly declines above 30 cm, becoming only sporadically represented toward the surface. *Euastrum* follows a similar trend, showing negligible percentages above its earlier peak. *Cosmarium* also decreases markedly above 35 cm, appearing only occasionally in the uppermost layers.

In the upper section of the core (above 20 cm), dinocysts become increasingly dominant, with several sharp peaks. Notably, *Spiniferites* shows a dramatic rise, reaching 76.09% of the total NPPs at 11 cm, contributing to a broader increase in dinocysts up to 80.43% at certain points (Fig. 14). This upper-phase expansion of dinocysts contrasts with the deeper part of the core, where the assemblage is primarily composed of *Botryococcus*, and to a lesser extent of *Cosmarium* and *Euastrum*, as discussed above.

Benthic foraminiferal linings remain present in small percentages throughout the core, with a maximum of 5% and an average of 1% of the total NPPs. Pteridophyte spores, dominated by monolete forms (up to 9.24%) and to a lesser extent trilete forms (up to 2.83%), are found consistently throughout the sequence, showing particularly elevated values in the middle and upper sections of the core (Fig. 14).

Among the other NPPs, a fairly ubiquitous presence of dinocysts is attested. The genus *incertae sedis Pseudoschizaea* and the spores of the green alga *Spirogyra* (known as water silk) are also found approximately along the entire core, although not in abundance. Even more sporadic are the findings of the green alga *Closterium* and various other indeterminate algae, of the testate amoeba *Arcella*, of the fungal spore of the genus *Glomus*, of diatoms, and other genera (Fig. 14).

The subdivision of taxa between pteridophyte spores, dinocysts and other NPPs follows the table in Appendix I.

Core LB5B - Lago di Burano (Southern Tuscany, Italy)

Single taxa diagram (NPP) (exaggeration 8x)

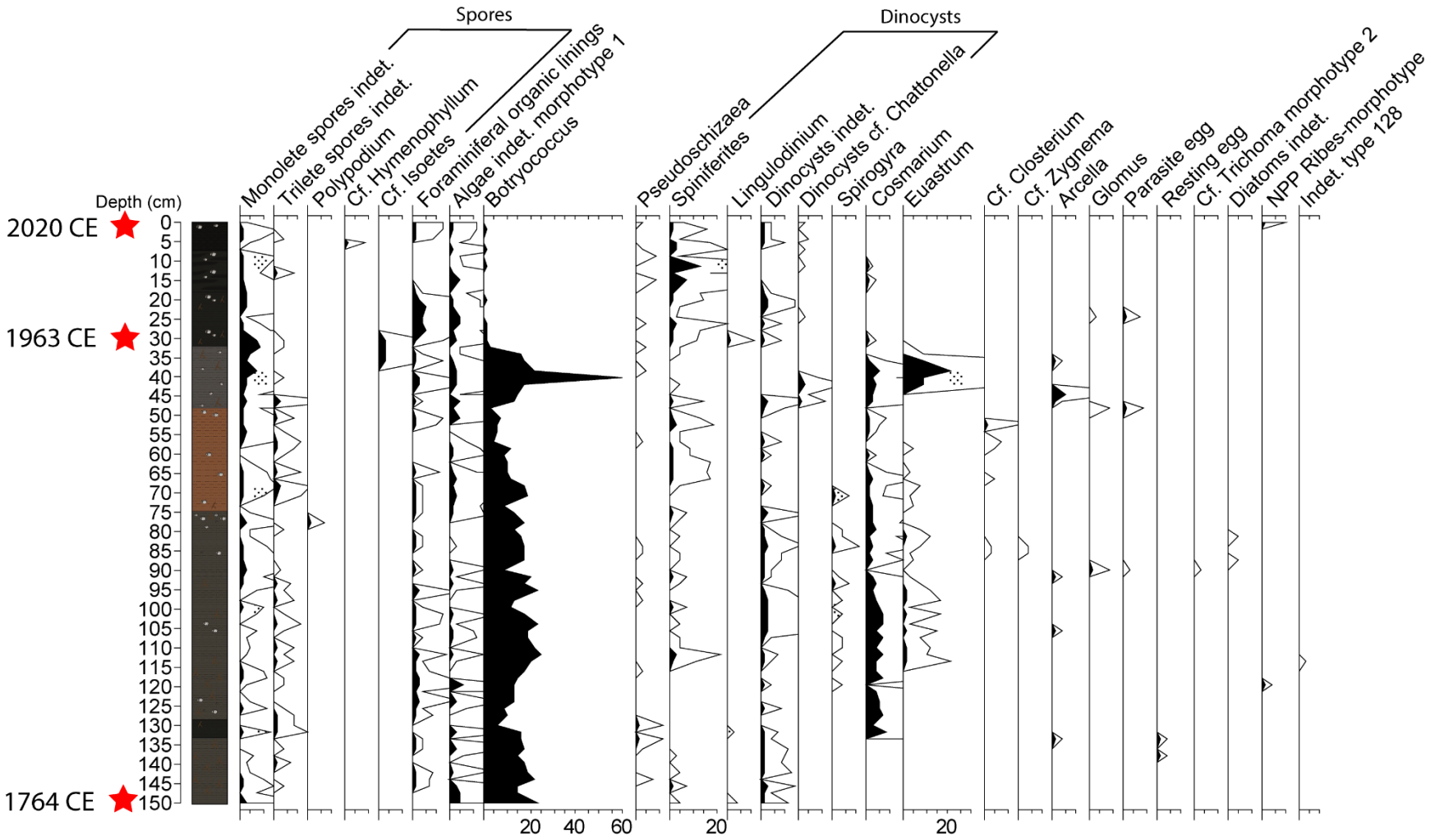

Fig. 14: Detailed palynological diagram of the core LB5B (exaggeration 8x), showing NPP taxa. Calibrated marine dates are reported.

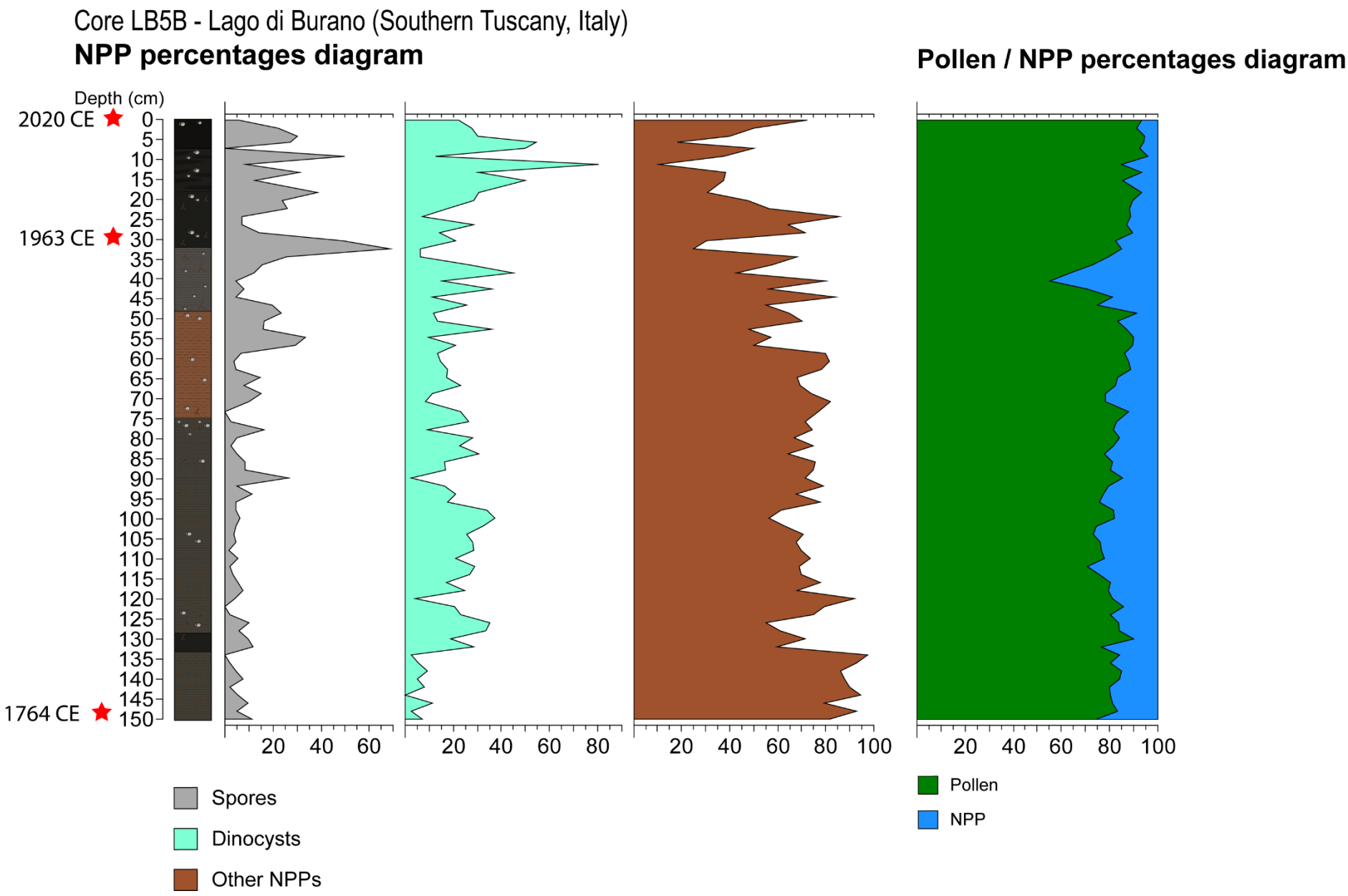

Fig. 15: percentages of various types of NPPs on the total NPPs (left); percentages of pollen and NPPs on the total palynomorphs (right) of the core LB5B. Calibrated marine dates are reported.

4. Surface samples

4.1 Results of laser granulometric analysis

The granulometric composition of the seven surface samples taken from Lake Burano was analysed (see Chapter 2, paragraph 2.6 for methodological details). Each sample was subjected to three successive analyses, the average of which is represented in the following graphs (Fig. 16). The samples were labelled using the code PS-POL-BUR 01 through PS-POL-BUR 07. For brevity, in this and the following paragraphs the prefix PS-POL-BUR is omitted, and only the numerical identifiers are used.

Granulometric analysis revealed that the surface samples collected from Burano are primarily composed of silt, frequently accompanied by a notable amount of fine sand and, in some cases, a subordinate clay component. The samples show a variability in the average size of the sediment grains. Samples 01, 03 and 06 show a smaller average grain size, with most of the grains concentrated between 1.5 and 33 μm, and with maximum peaks of about 3 μm in the case of sample 01 and about 14 μm in the case of the other two samples. Samples 02, 04, 05, and 07 instead show a slightly larger grain size. In particular, sample 02 is the only clearly sandy sample, in which the sand fraction exceeds the silt fraction and in which most of the grains are evidently concentrated between 120 and 500 μm.

All samples show a unimodal distribution, apart from samples 01 and 07, which have a bimodal distribution. We note that samples 01, 04, 05, and 07 are those closest to the shore, while 02, 03 and 06 are those furthest away (Fig. 17; Chapter 2, Fig. 3, Tab. 1). Samples closer to the coasts 04, 05, and 07 are the coarsest, exhibiting a predominantly silty and fine sandy grain size, whereas samples further from the coast 03 and 06 are the finest, characterized by finer silt and a higher clay content. Sample 02, though situated further from the coast than sample 01, is markedly coarser than the latter. Thus, with the exception of samples 01 and 02, there is a tendency for samples to be finer as the distance from the shore increases (Figs. 16, 17). The relatively high sand content in sample 07 may also be related to its proximity to the northeastern tributary inlet (Scaricatore della Bassa). In contrast, sample 01 shows a finer average grain size, with a high percentage of clay, and appears to be less influenced by the proximity of the northwestern tributary inlet (Fosso del Melone).

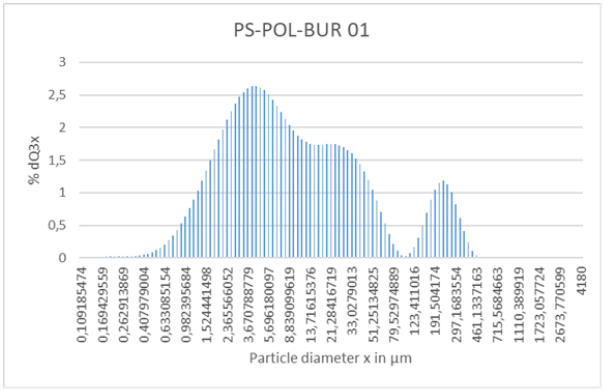

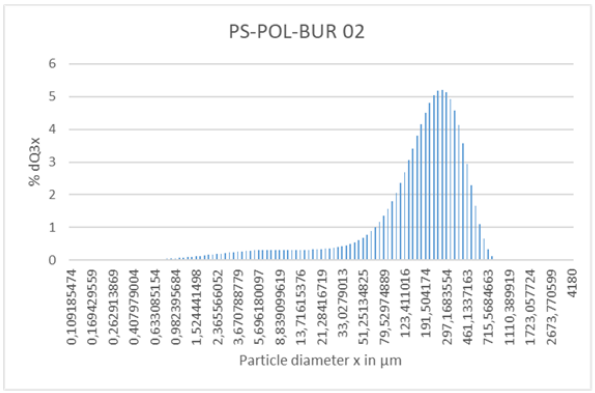

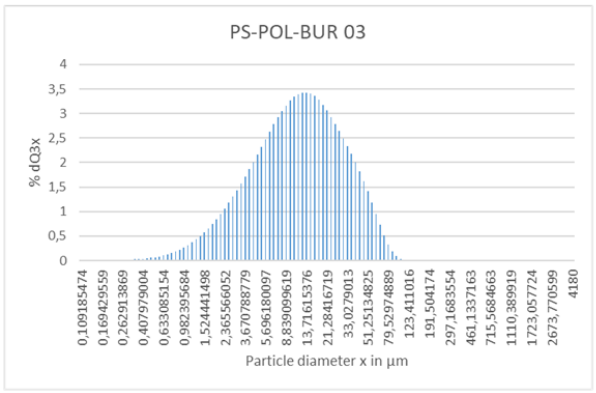

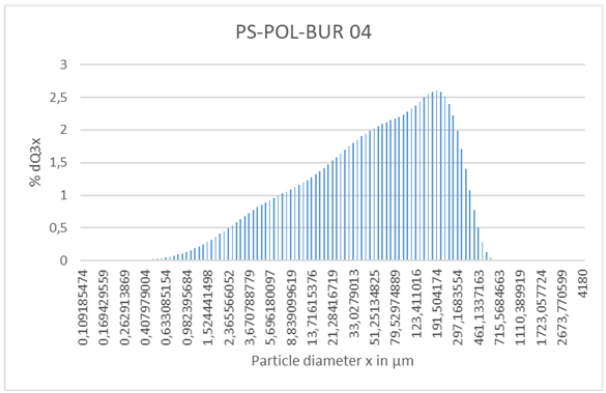

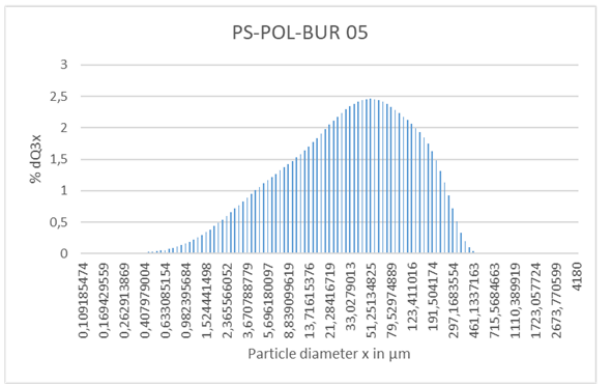

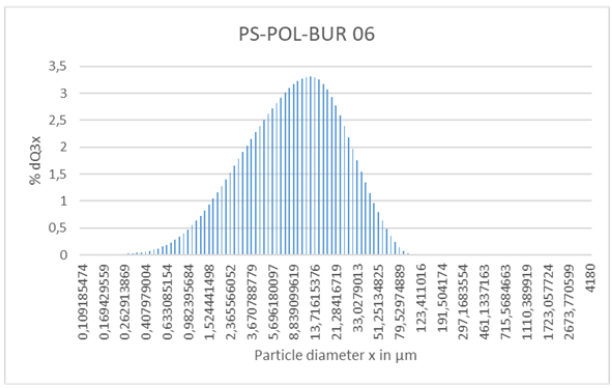

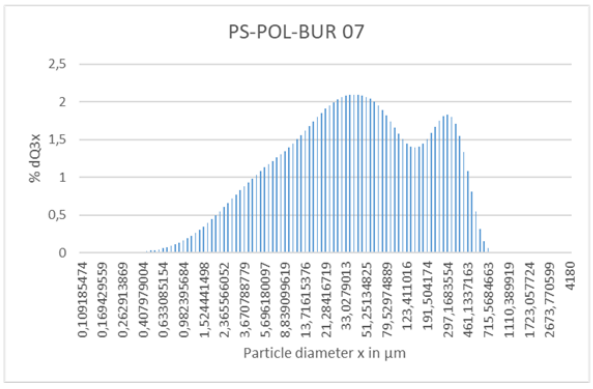

Fig. 16: Grain size profile of the surface sediments collected in the Burano site. Y- axis indicates the percentage of particles per grain size class; X-axis (in logarithmic scale) indicates the diameter of the particles in microns.

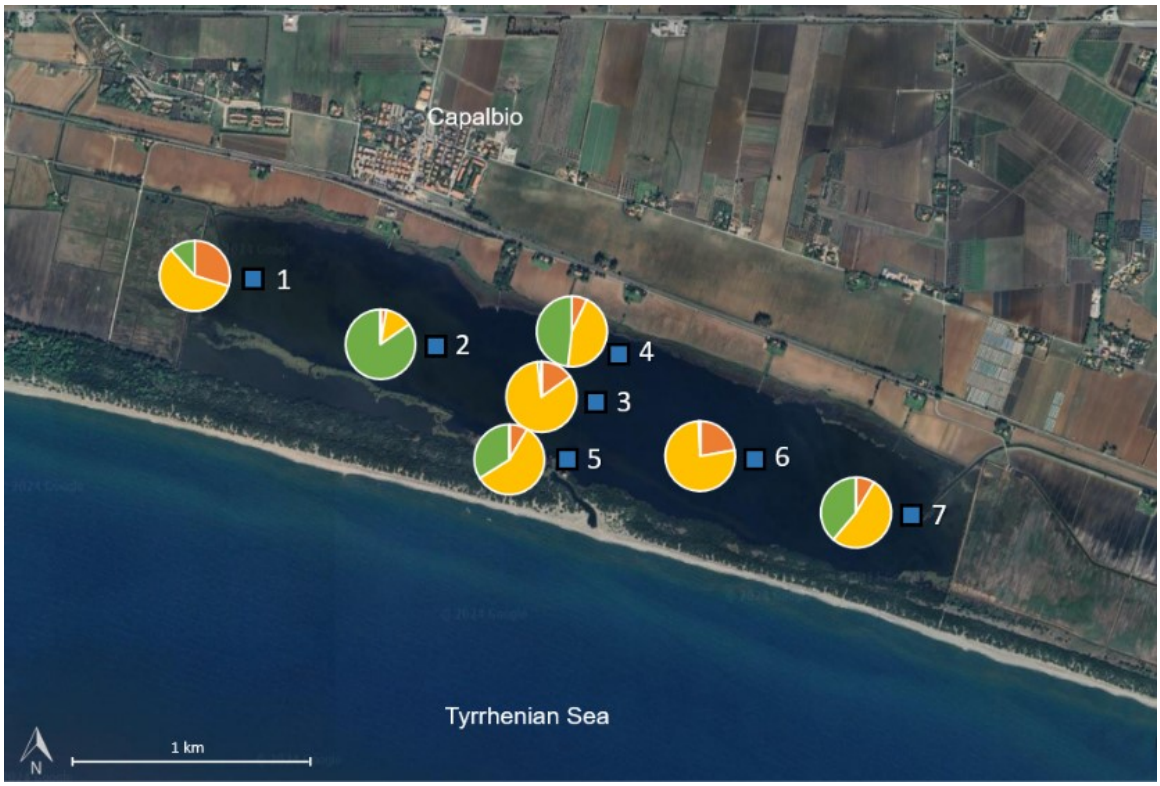

Fig. 17: Pie charts showing grain size profile of the surface sediments of Burano site. Legend: orange: clay (particle size < 3.9 μm); yellow: silt (particle size between 3.9 μm and 62.5 μm); green: fine sand (particle size between 62.5 μm and 2000 μm).

4.2 Palynological analysis of surface samples (Figs. 18, 19)

Palynological analyses on 7 subsurface samples (Chapter 2, Fig. 3, Tab. 1) from Lake Burano were carried out. The surface samples include sediments up to 5 cm depth on average, and considering the sedimentation rate suggested by the above-mentioned analysis of ^{210}Pb and ^{137}Cs, these samples likely represent several years to decades, though resolution may be affected by local variability and dredging.

The surface samples show fairly homogeneous results in the various points of the lagoon. In the group of Anthropogenic taxa, the most represented taxon is *Olea* (with values ranging from 6.30% in sample 01 to 23.70% in sample 07). Also present, though not abundant, are indeterminate Cupressoideae (values between 0.74% in sample 01 and 2.37% in sample 07), and *Vitis* (with a maximum value of 1.33% in sample 06, but absent in some samples). *Eucalyptus*, on the other hand, is present in only two samples, where it records very significant percentages (8.15% in sample 01 and 4.49% in sample 02). The Anthropogenic group represents 16.29%. In particular, in sample 07, it reaches the highest

percentage (27.01%) due to the elevated percentages of *Olea*, making it the most numerous group in the sample (Figs. 18, 19).

In the Mediterranean group, there is a clear predominance of the *Quercus ilex-coccifera* type (minimum 9.48% in sample 07; maximum 19.74% in sample 03), with a constant presence of *Pistacia lentiscus* (maximum 2.37% in sample 07), *Pistacia* sp., and, only in some samples, *Juniperus* and *Phillyrea* (averaging around 1%). The Mediterranean group is generally the most represented across all samples, with an average of 19.30%, and percentages ranging from 16.21% in sample 04 to 25.66% in sample 03 (Figs. 18, 19).

The *Quercus pubescens* type generally prevails in the Sub-Mediterranean group (minimum 2.22% in sample 01; maximum 5.32% in sample 05), along with *Quercus suber*, which is abundant especially in samples 01 (5.56%), 05 (4.30%), and 07 (4.27%). Other significant elements include *Fraxinus excelsior* (with a maximum of 1.77% in sample 05 but absent in others) and *Carpinus orientalis* (minimum 1.26% in sample 04; maximum 3.29% in sample 05). The Sub-Mediterranean group as a whole ranges from minimum percentages of 11.79% in sample 04 to maximum percentages of 22.28% in sample 05 (Figs. 18, 19), with an average of 15.76%.

Pinus is present in all samples, with minimum percentages of 4.17% in sample 06 and maximum percentages of 11.18% in sample 03 (Figs. 18, 19). The average percentage across all samples is 6.37%.

The group of Mountain taxa is generally poorly represented, with an average of 1.15% among all samples, with the partial exception of *Betula* (2.00% in sample 06) and *Fagus* (1.28% in sample 02).

The group of Riparian species is poorly represented (minimum 0.95% in sample 07; maximum 4.07% in sample 01 (Figs. 18, 19)), with an average of 2.04%. The predominant taxon is *Alnus glutinosa* type (minimum 0.95% in sample 07; maximum 3.95% in sample 03). The taxon cf. Eleagnaceae was recorded only in sample 01 (2.59%).

The Helophyte group includes only the family Cyperaceae (minimum 0.00% in samples 03 and 07; maximum 2.22% in sample 01), with an average of 1.06%.

Among the hydrophytes, noteworthy taxa include *Ruppia* (minimum 0.00% in sample 03; maximum 4.42% in sample 04), *Alisma plantago-aquatica* type only in sample 02 (1.92%), and *Sparganium* only in sample 01 (1.48%). Also recorded in minimal percentages are *Lemna*, *Myriophyllum*, and *Thalictrum* cf. *T. flavum*. The group has minimum percentages of 0.47% in sample 07, maximum percentages of 6.74% in sample 04 due to the incidence of *Ruppia* (Figs. 18, 19), and an average of 3.05%.

The Halophytes/NAP show a significant prevalence of Amaranthaceae (minimum 8.61% in sample 05; maximum 31.17% in sample 06). Caryophyllaceae, on the other hand, present reduced percentages, around 1%. The sample with the highest percentages is clearly 06 (32.67%), while the one with the lowest percentages is sample 05 (9.11%) (Figs. 18, 19), with an average of 18.64%.

Among the Helophytes/NAP, Poaceae < 20 µm generally prevail over Poaceae > 20 µm. The group has minimum percentages of 1.97% in sample 03 and maximum percentages of 12.42% in sample 04 (Figs. 18, 19), with an average of 8.54%.

Among the Upland Herbs, the prevalent taxon is Ericaceae, with minimum percentages of 0.50% in sample 06 and maximum percentages of 2.56% in sample 02. Sample 01 stands out for a relatively high percentage of Asteraceae Cichorioideae (3.70%), almost absent in other samples. Also recorded are Asteraceae Asteroideae (minimum 0.64% in

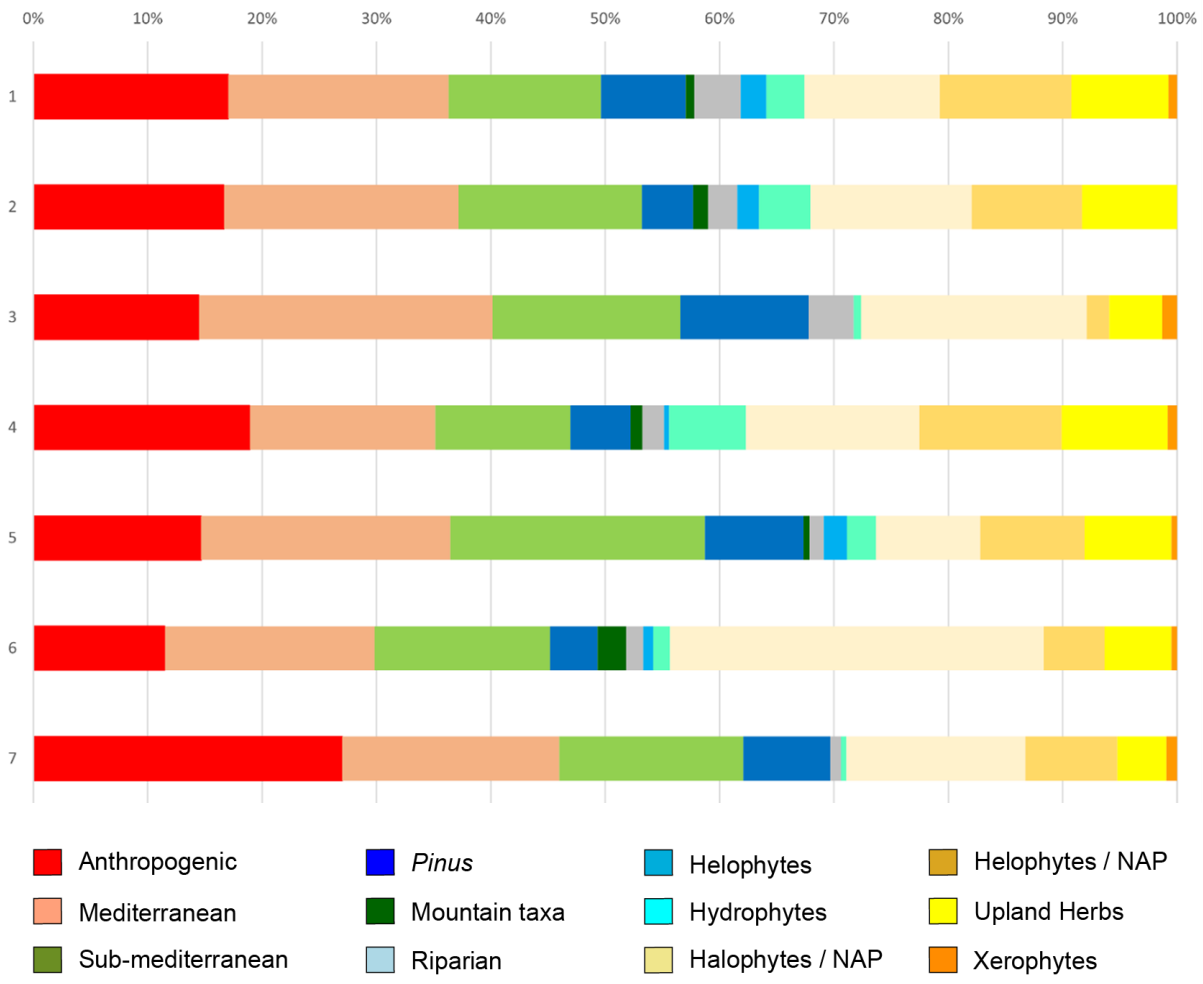

Fig. 18: Percentages of pollen content of surface samples from the Burano site, subdivided by informal palynological group. Y-axis labels: 1 = PS-POL-BUR 01; 2 = PS-POL-BUR 02; 3 = PS-POL-BUR 03; 4 = PS-POL-BUR 04; 5 = PS-POL-BUR 05; 6 = PS-POL-BUR 06; 7 = PS-POL-BUR 07.

sample 02; maximum 1.68% in sample 04), *Plantago lanceolata* (minimum 0.00% in sample 03; maximum 3.29% in sample 05), and, limited to some samples, *Rumex acetosella*, Ranunculaceae, Scrophulariaceae. The sample with the highest percentages of Upland Herbs is 04 (9.26%), and the one with the lowest percentages is sample 07 (4.27%) (Figs. 18, 19), with an average percentage of 7.13%.

Among the Xerophytes, very poorly represented, the prevalent taxon is *Artemisia* (absent in sample 02; maximum 0.95% in sample 07). Also recorded are *Ephedra fragilis* and *Hippophae*. The group shows minimum percentages in sample 02 (0.00%) and maximum in sample 03 (1.32%) (Figs. 18, 19), with an average percentage of 0.66%.

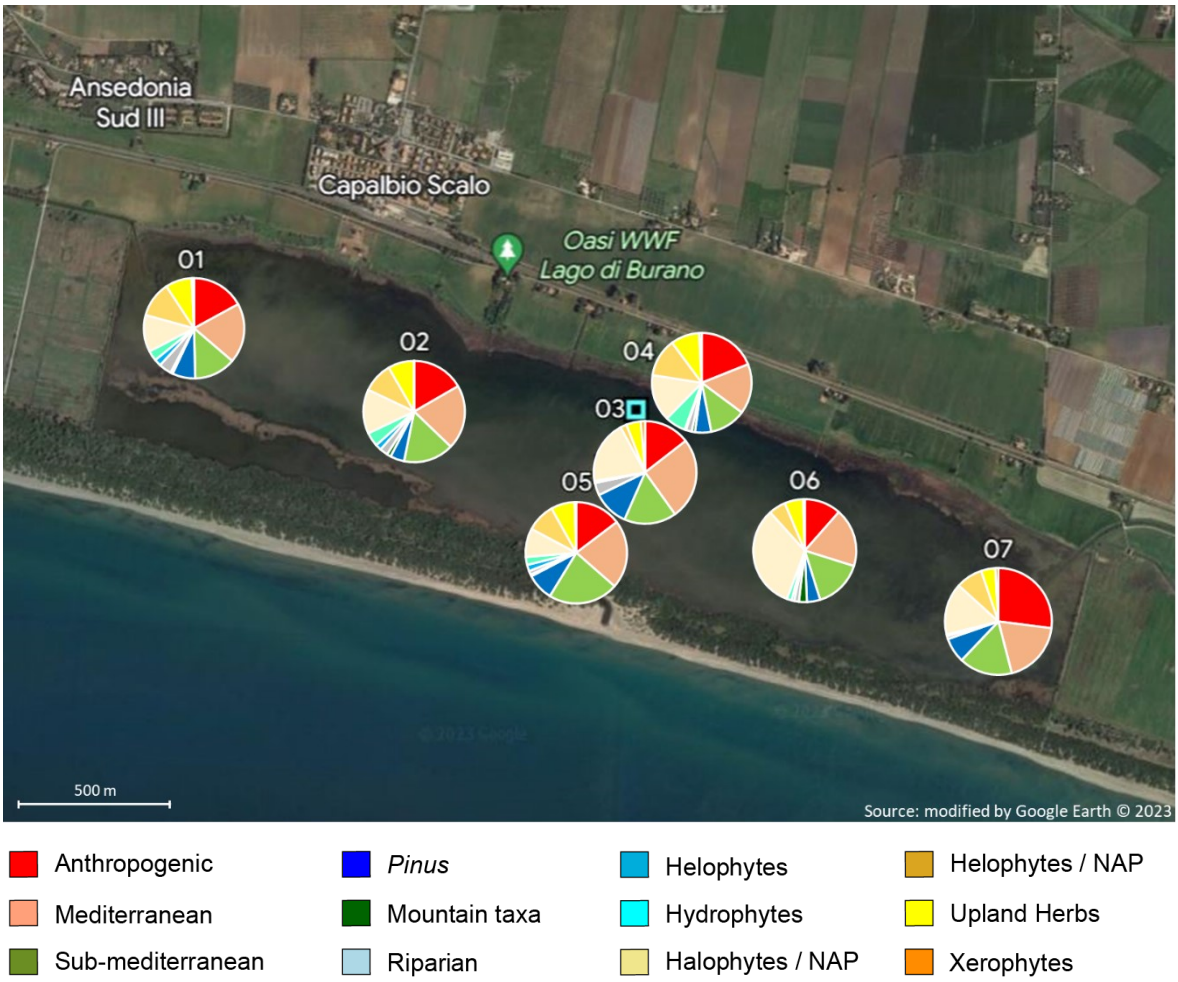

Fig. 19: Pie charts and geographical position of the surface samples extracted at the Burano site. Labels: 01 = PS-POL-BUR 01; 02 = PS-POL-BUR 02; 03 = PS-POL-BUR 03; 04 = PS-POL-BUR 04; 05 = PS-POL-BUR 05; 06 = PS-POL-BUR 06; 07 = PS-POL-BUR 07.

4.3 Analysis of moss samples (Figs. 20, 22)

Palynological analyses on 3 moss samples (MOSS1 BUR1-23, MOSS2 BUR1-23, MOSS3 BUR1-23; Chapter 2., Tab. 2) from Lake Burano were carried out. These were all collected close to the northern shore of the lake (Fig. 22; Chapter 2, Fig. 3). For brevity, the suffix BUR1-23 is omitted in the following sections.

The palynological analyses have highlighted that, in the group of anthropogenic taxa, the principal taxon is *Olea*, with maximum percentages of 19.35% in sample MOSS2 and similar values (min. 11.39%) in the other two samples. *Castanea* is also present in negligible percentages. The group as a whole has minimum percentages of 9.73% (MOSS1), maximum percentages of 14.42% (MOSS2) (Figs. 20, 22), and an average of 11.55%.

Among the Mediterranean elements, the dominant taxon is the *Quercus ilex-coccifera* type, with variable percentages across the three samples (1.94% in sample MOSS2; 10.76% in sample MOSS1; 18.92% in sample MOSS3). *Phillyrea*, *Pistacia lentiscus*, *Ligustrum*, and undetermined Oleaceae are also present. The group has minimum percentages of 2.88% (MOSS2), maximum percentages of 16.22% (MOSS3) (Figs. 20, 22), and an average of 10.00%.

Among the Sub-Mediterranean elements, the predominant taxon is the *Quercus pubescens* type in samples MOSS1 (5.06%) and MOSS3 (3.38%), while it is absent in sample MOSS2, which instead contains *Corylus*, *Quercus suber*, and *Fraxinus* spp. *Carpinus orientalis* is besides found in samples MOSS1 and MOSS3, and *Viburnum* appears only in sample MOSS1. The group shows relatively low percentages (min. 3.37% in sample MOSS2; max. 8.56% in sample MOSS1; average of 6.03% (Figs. 20, 22)).

Pinus has minimum percentages of 7.69% in sample MOSS2 and maximum percentages of 12.97% in sample MOSS3 (Figs. 20, 22). The average across all three samples is 10.52%. No mountain taxa were recorded.

Among riparian taxa, both *Alnus glutinosa* and *Salix* are present at relatively low percentages (<2%), with *Salix* absent from sample MOSS2. The group percentage is lowest in sample MOSS1 (1.07%) and highest in sample MOSS3 (2.70%) (Figs. 20, 22), with an average of 1.72%.

For the Helophytes (all Cyperaceae), minimum percentages are found in sample MOSS2 (0.00%) and maximum in sample MOSS3 (2.03%) (Figs. 20, 22), with an average percentage of 0.69%.

Among the Hydrophytes, both *Myriophyllum* and *Alisma plantago-aquatica* type are recorded, consistently at percentages below 0.70%, except for *Alisma plantago-aquatica* type in sample MOSS1, where it reaches 1.90%. The group's minimum percentage is in sample MOSS2 (0.48%) and maximum in sample MOSS1 (2.14%) (Figs. 20, 22), with an average of 1.03%.

Within the Halophytes/NAP group, Amaranthaceae are dominant (min. 6.08% in sample MOSS3; max. 16.45% in sample MOSS1) over Caryophyllaceae (min. 0.00% in sample MOSS2; max. 1.27% in sample MOSS1). The group has minimum percentages of 5.41% in sample MOSS3, maximum percentages of 14.97% in sample MOSS1 (Figs. 20, 22), and an average of 10.86%.

Among Helophytes/NAP, Poaceae >20 μm clearly dominate over Poaceae <20 μm in sample MOSS2, whereas the opposite is true in sample MOSS3, while sample MOSS1 shows similar percentages for both. The group has minimum percentages of 4.81% in sample MOSS2, maximum percentages of 10.81% in sample MOSS3 (Figs. 20, 22), and an average of 7.76%.

Among Upland Herbs, Asteraceae Cichorioideae are distinctly dominant across all samples (15.19% in sample MOSS1; 20.95% in sample MOSS3; 33.55% in sample MOSS2). Asteraceae Asteroideae are also well represented (min. 4.43% in sample MOSS1; max. 9.68% in sample MOSS2), as are Ericaceae (min. 2.53% in sample MOSS1; max. 6.45% in sample MOSS2), Apiaceae (min. 2.03% in sample MOSS3 ; max. 4.43% in sample MOSS1), and to a lesser extent Liliaceae, Lamiaceae, Fabaceae, Brassicaceae, Scrophulariaceae, Rosaceae. The group has minimum percentages of 29.95% in sample MOSS1, maximum percentages of 52.40% in sample MOSS2 (Figs. 20, 22), and an average of 38.10%.

Among the Xerophytes, the only taxon present is *Artemisia*, with minimum values in sample MOSS2 (0.48%) and maximum values in sample MOSS3 (3.24%) (Figs. 20, 22), with an average of 1.72%.

4.4 Analysis of the pollen trap (Figs. 21, 22)

A pollen trap from Lake Burano (TRAPY1 BUR1-22; Chapter 2, Fig. 3, Tab. 3), was analysed. It was installed inside the WWF Lago di Burano station (Fig. 22), and it was collected in December 2022.

The pollen analysis highlighted a clear predominance of Poaceae > 40 μm within the Anthropogenic group, accounting for 15.07% of the total pollen, alongside the presence of cereals (1.84%). Among anthropogenic taxa, *Olea* (3.68%) is also noteworthy, while *Vitis*, *Juglans*, and *Castanea* are also represented. Altogether, this group constitutes 22.06% of the total pollen found (Fig. 21).

Among Mediterranean elements (10.66%), the *Quercus ilex-coccifera* type is dominant (7.35%), with additional contributions from *Pistacia lentiscus*, *Phillyrea*, *Ligustrum*, and undetermined Oleaceae. Within the Sub-Mediterranean elements (9.19%), the main taxa are *Ostrya* (2.57%), *Quercus pubescens* type (1.84%), and *Carpinus orientalis* (1.84%), with lesser occurrences of *Corylus*, *Fraxinus*, *Quercus suber*, *Tilia*, *Sambucus*, and *Viburnum* (Fig. 21).

Pinus represents 6.62% of the total pollen. Among mountain elements, only *Fagus* is present (0.37%). The riparian taxa, representing just 1.84% of the total, are primarily *Salix* and *Alnus glutinosa*. The Helophytes (all Cyperaceae) represents 1.10% of the total. Among Halophytes/NAP (2.57%), Amaranthaceae are predominant. Within the Helophytes/NAP group (6.25%), Poaceae >20 μm are more prevalent than Poaceae <20 μm (Fig. 21).

The most represented group by far is Upland Herbs (37.87%), with Asteraceae Asteroideae (12.13%) as the dominant taxa, followed by Apiaceae (3.68%), and to a lesser extent Euphorbiaceae, Asteraceae Cichorioideae, Fabaceae, Lamiaceae, and Ranunculaceae. Xerophytes (1.47%) include only the genus *Artemisia* (Fig. 21).

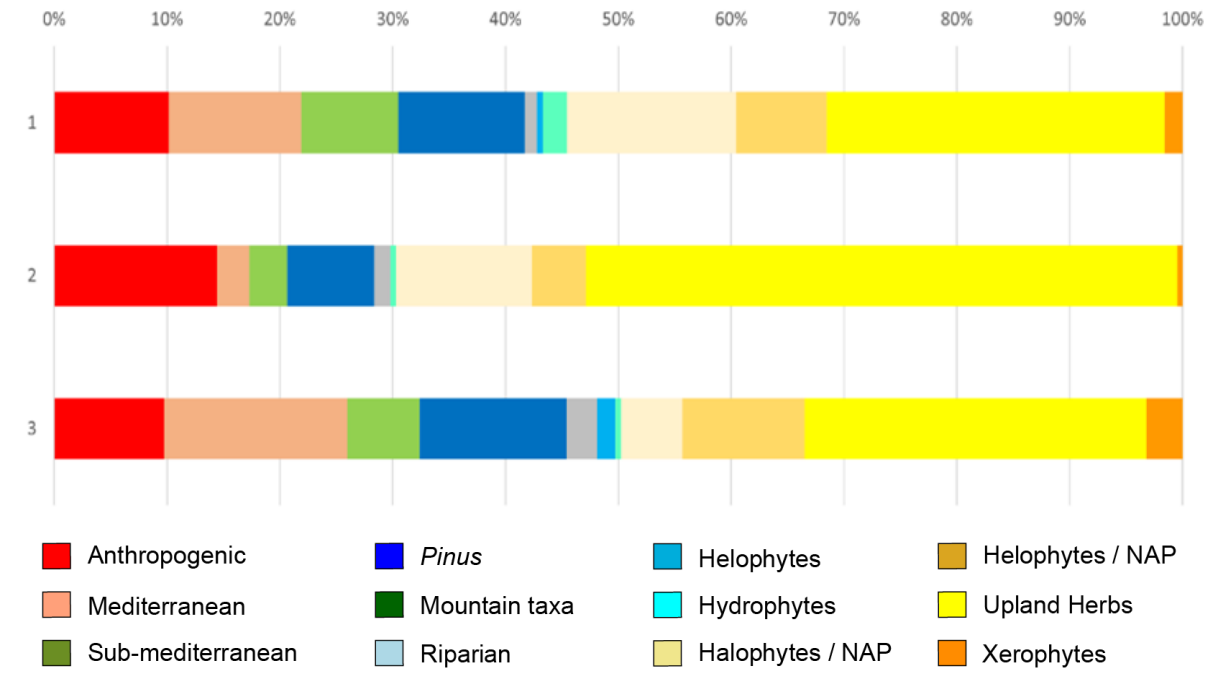

Fig. 20: Percentages of pollen content of moss samples from the Burano site, subdivided by informal palynological group. Y-axis labels: 1 = MOSS1 BUR1-23; 2 = MOSS2 BUR1-23; 3 = MOSS3 BUR1-23.

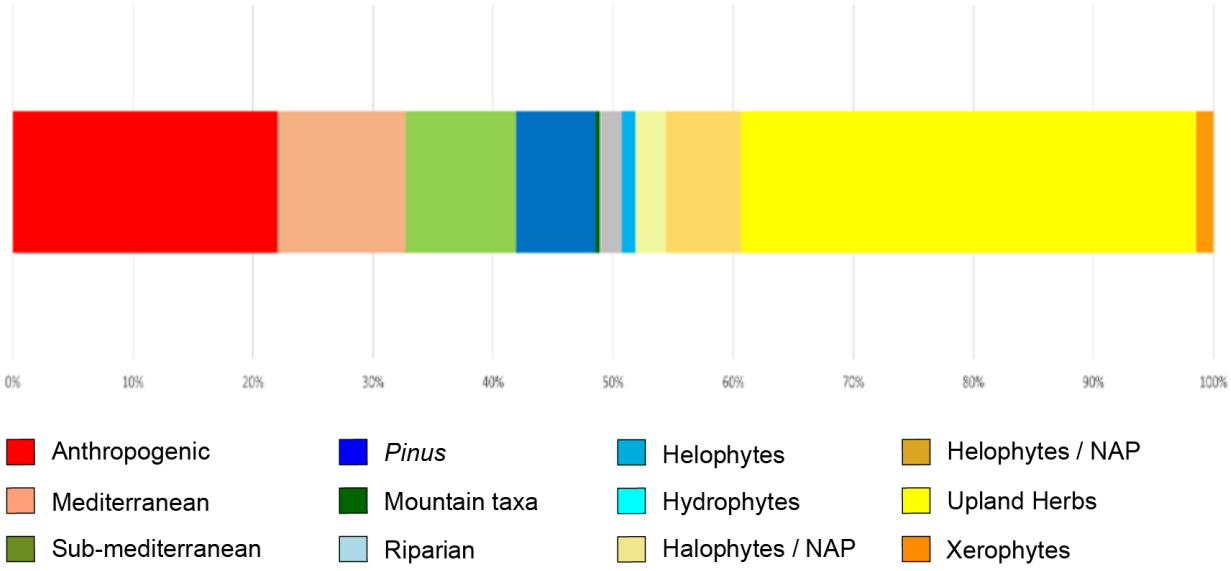

Fig. 21: Percentage of pollen content of the pollen trap (TRAPY1 BUR1-22) from the Burano site, subdivided by informal palynological group.

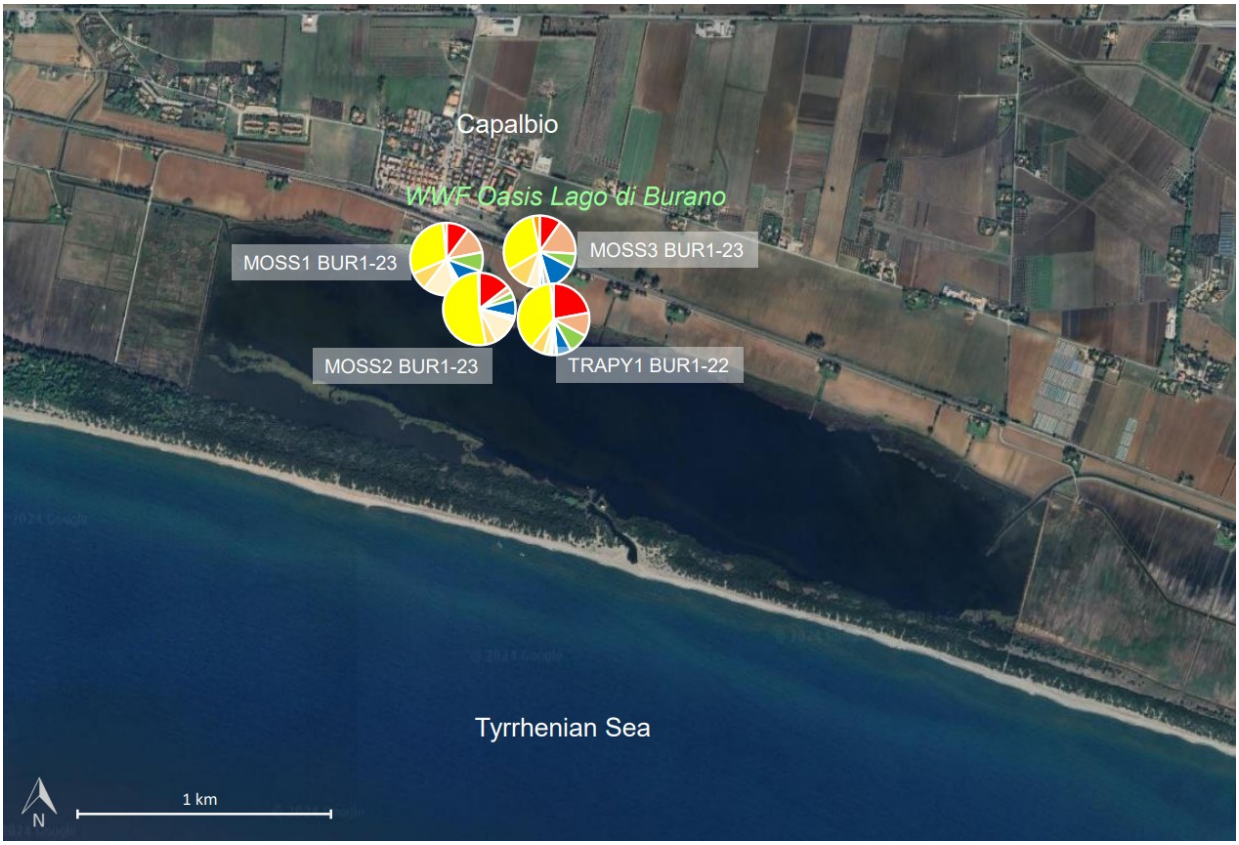

Fig. 22: Pie charts and geographical position of moss samples and of the pollen trap extracted at the Burano site.

5. Preliminary microplastics analysis on selected samples

Three samples of the LB5B core were analysed (MP-BUR-1, 9-18 cm deep; MP-BUR-2, 40-50 cm deep; MP-BUR-3, 81-89 cm deep; see Chapter 2, Tab. 4). The fragments were divided into two size categories (small: 63-125 μm; large: 125 μm-5mm) and classified by morphology based on visual observations with a stereomicroscope (Chapter 2, paragraph 2.5).

Microplastic fragments were detected in all three analysed samples. Tab. 3 shows the total number of fragments found, Tab. 4 shows the resulting number after subtracting the morphologies recorded in the control blanks (following Turner *et al.*, 2019, as explained in Chapter 2, paragraph 2.5), and Tab. 5 shows the concentration of the fragments (total number/sample weight) after the subtraction. The following graph (Fig. 23) visually represents the concentration of plastics detected in each analysed sample, along with their corresponding depth within the core.

The highest concentration (5.93 particles per gram) was recorded in the intermediate sample (MP-BUR-2) at 40-50 cm deep. The uppermost sample (MP-BUR-1) was found to be the second most abundant in microplastics (4.20 particles per gram), while the deepest one (MP-BUR-3) was found to be the least abundant (1.44 particles per gram) (Fig. 23).

The morphology of the fragments is variable (see Appendix III), and includes fibers (of variable length, blue, black, or red in colour), nylon-like transparent wires, irregularly shaped blue fragments, and various other elements such as spongy elements, masses of filamentous tangles, a blue grid-like fragment. In general, filamentous fibers are the most frequently found elements, especially the blue ones. The latter represents also the most common morphology found in the control blanks (Tabs. 3–5).

Total microplastics

Sample	MP-BUR-1		MP-BUR-2		MP-BUR-3	
Depth (cm)	9-18		40-50		81-89	
Fraction	B (125 µm-5 mm)	S (63-125 µm)	B (125 µm-5 mm)	S (63-125 µm)	B (125 µm-5 mm)	S (63-125 µm)
Blue fiber	21	11	33	20	12	1
Red fiber	4	1	4	3	2	
Black fiber			3	2		
Transparent wire (nylon-like)	5	6	9	2	2	
Blue fragment	1	2			1	2
Grey fragment						1
Dark yellow fragment						1
Dry mass (g)	8,1		9,1		9,0	
Total (n)	51		76		22	
Microplastics concentration (n/g)	6,30		8,35		2,44	

Tab. 3: Total number of microplastic fragments found in the LB5B core samples.

Total microplastics minus blank

Sample	MP-BUR-1	MP-BUR-2	MP-BUR-3
Depth (cm)	9-18	40-50	81-89
Fraction	all	all	all
Blue fiber	27	48	8
Red fiber	3	5	0
Black fiber		0	
Transparent wire (nylon-like)	1	1	0
Blue fragment	3		3
Grey fragment			1
Dark yellow fragment			1
Total (n) minus blank	34	54	13

Tab. 4: Number of microplastic fragments after subtracting the contaminant according to the method in Turner *et al.*, 2019.

Total microplastics minus blank concentration

Sample	MP-BUR-1	MP-BUR-2	MP-BUR-3
Depth (cm)	9-18	40-50	81-89
Fraction	all	all	all
Blue fiber	3,33	5,27	0,89
Red fiber	0,37	0,55	0,00
Black fiber		0,00	
Transparent wire (nylon-like)	0,12	0,11	0,00
Blue fragment	0,37		0,33
Grey fragment			0,11
Dark yellow fragment			0,11
Dry mass (g)	8,1	9,1	9,0
Total (n) minus blank	34	54	13
Total minus blank concentration (n/g)	4,20	5,93	1,44

Tab. 5: Concentration (total number/sample weight) of fragments by type, after subtracting the contaminant. Values are in number/g.

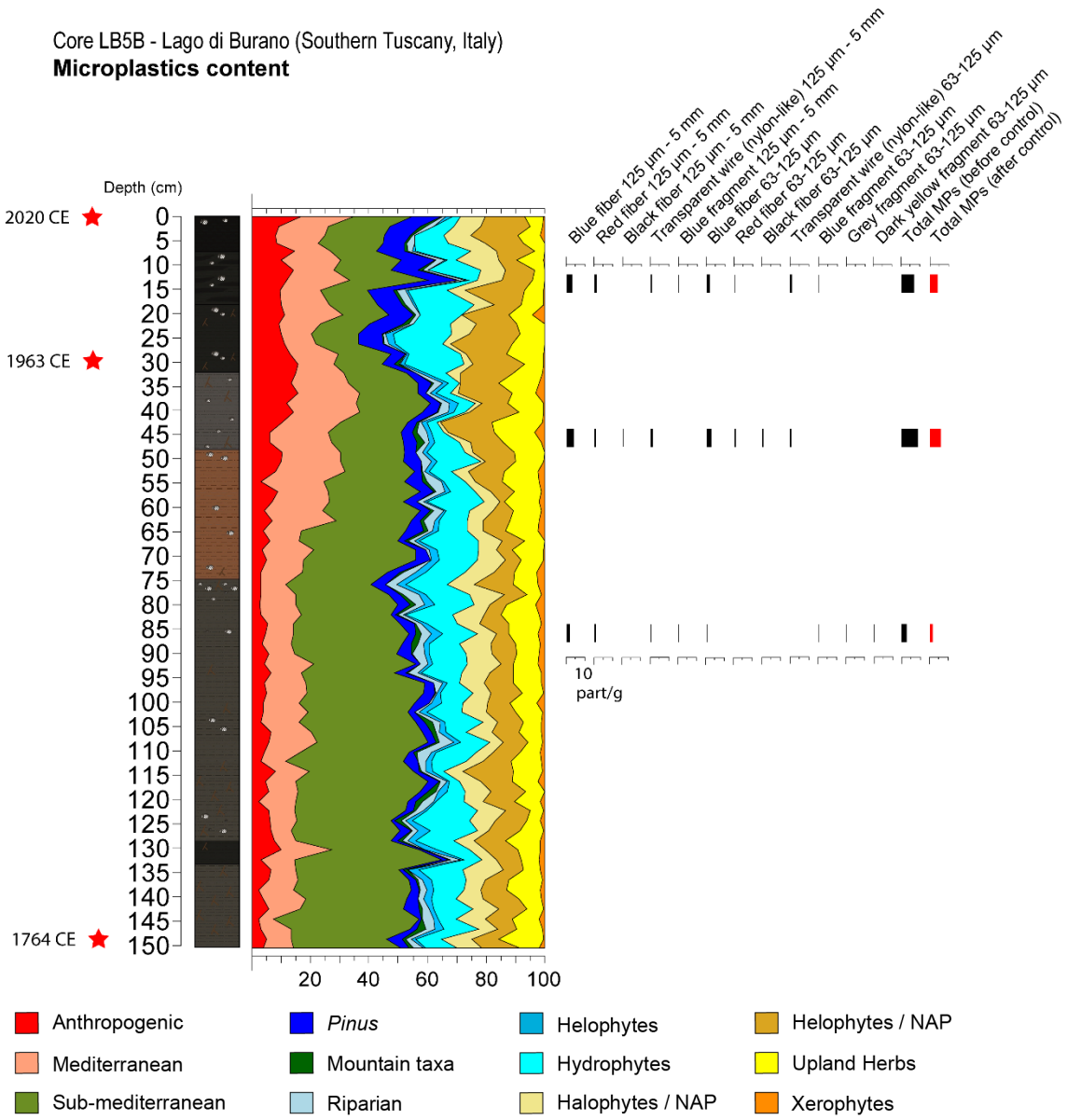

Fig. 23: Location and amount of microplastic findings along the core LB5B. Red bars on the right indicate the results after subtracting the contaminant according to the method in Turner *et al.*, 2019. Calibrated marine dates are reported.

Discussion

6. Strengths and weaknesses of the study

The palynological study of core LB5B from Lake Burano offers a record of recent vegetation dynamics and anthropogenic pressures in the southern Tuscan coastal sector. By integrating pollen, NPP, and sedimentological evidence, the sequence provides a basis for reconstructing the ecological history of this wetland.

The Burano sequence presents notable strengths. Its high-resolution sampling strategy (75 samples analysed, each representing a 2 cm interval) provides an unusually fine temporal detail for a Mediterranean lagoon sequence, allowing the detection of short-term ecological changes. The core is expected to cover at least the last ~250 years, a period marked by profound anthropogenic and ecological transformations. Furthermore, the Burano lagoon itself is a well-documented system, with abundant historical and ecological data that offer a valuable framework for interpreting the proxy record. These characteristics make the sequence particularly suited to linking microfossil evidence with known phases of land-use change, environmental stress, and management interventions.

The interpretation of this dataset, however, is subject to significant scientific limitations, foremost among them the chronological uncertainty. The available radiocarbon age control is sparse and not always consistent, resulting in a discontinuous and partly ambiguous temporal framework. Possible reworking of sediments, stratigraphic hiatuses, and mixing processes cannot be excluded, given the dynamic depositional setting of a shallow lagoon. These factors inherently reduce the temporal precision of paleo-environmental reconstructions and may account for the comparatively stable or muted trends observed in the biotic proxies.

In light of these constraints, the following discussion will deliberately adopt a cautious interpretive stance. Emphasis will be placed on those patterns that appear internally consistent and robust across multiple proxies, while more speculative interpretations will be explicitly qualified as uncertain. The goal is not to overstate the resolution of the dataset, but rather to delineate the main ecological tendencies that can be reliably inferred, acknowledging the limits of the available evidence.

7. *Interpretation of the chronological framework*

The chronological control of core LB5B is constrained by two radiocarbon dates and the combined ^{210}Pb-^{137}Cs-^{241}Am measurements (Tab. 2; Fig. 6). The radiocarbon sample at 101 cm depth yielded an age indistinguishable from modern, which is inconsistent with its stratigraphic position and is therefore interpreted as unreliable, most likely due to stratigraphic inversion or contamination by younger carbon. At 147 cm depth, a bulk-sediment sample containing inorganic carbon yielded a radiocarbon age of 870 ± 30 ^{14}C yr BP (Tab. 1). When calibrated, this corresponds to 1154 ± 107 CE using the terrestrial curve, and 1764 ± 144.5 CE using the marine calibration. Given the depositional context and the uncertainties associated with bulk dating, the marine calibration is regarded as more plausible, although still tentative.

The ^{137}Cs and ^{241}Am profiles provide an independent chronological anchor: the 1963 CE peak, corresponding to the maximum fallout from nuclear testing, was identified at 29 cm depth. Assuming the reliability of this signal, a mean sedimentation rate of ~4.98 mm/year can be inferred. This estimate is broadly consistent with the radiocarbon age obtained at 147 cm depth when using the marine calibration, which falls within the 18th century (Fig. 24).

The convergence of these independent constraints suggests that the sequence spans roughly the last three centuries, from the mid-18th century to the present. With the sampling resolution of 2 cm (75 samples in total), this corresponds to a temporal resolution on the order of a few years per level, which in principle allows the record to capture even relatively rapid environmental and anthropogenic events. Nonetheless, the chronological framework remains weakened by the reliance on a single reliable radiocarbon point, the use of bulk sediment for dating, and the assumption of linear sedimentation. The large uncertainty associated with the basal age, in particular, requires caution in any fine-scale chronological interpretation.

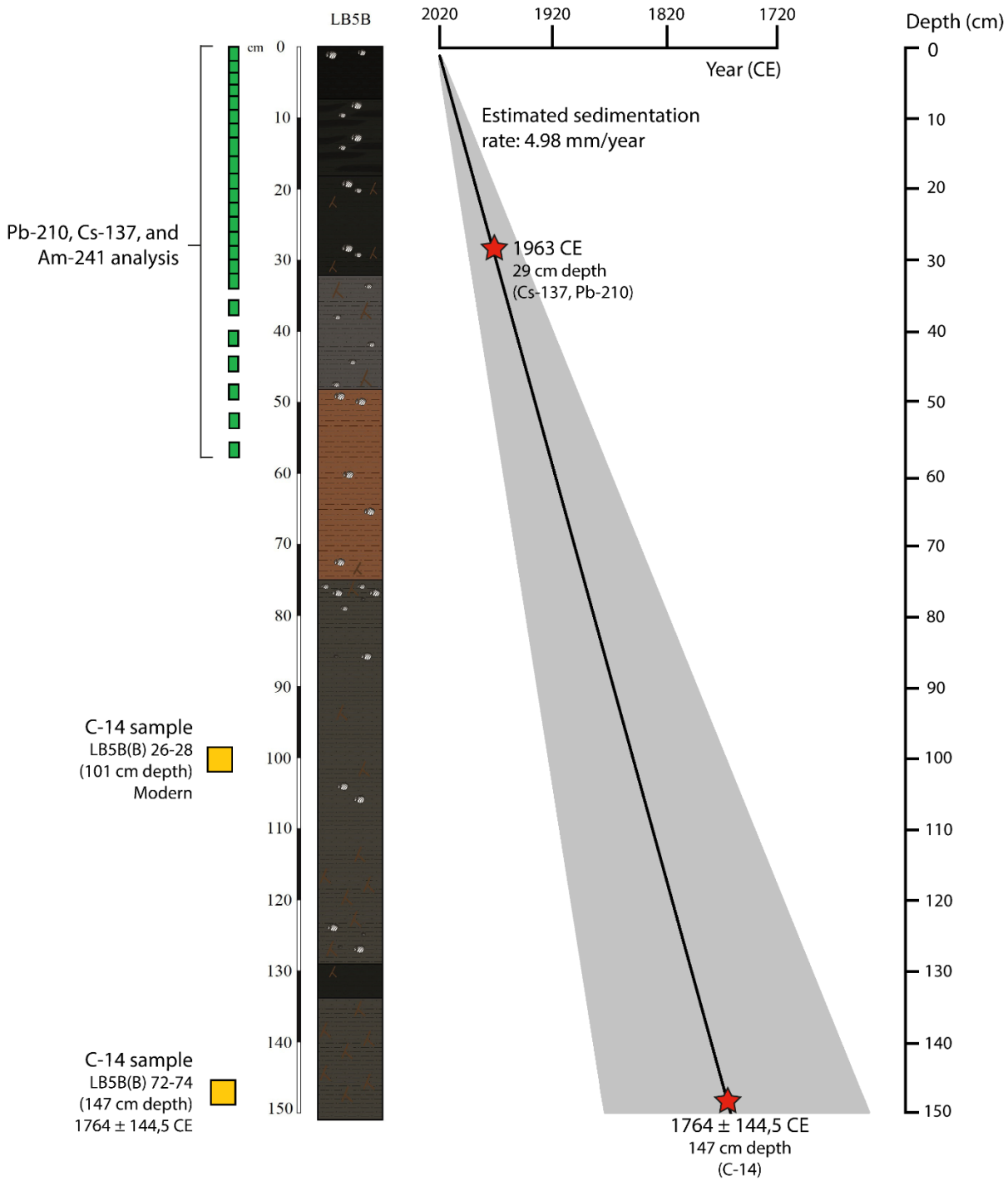

Fig. 24: Chronological constraints for core LB5B. Left: depths of radiocarbon (yellow squares) and $^{210}Pb/^{137}Cs/^{241}Am$ (green squares) samples. The 101 cm radiocarbon date is modern and interpreted as an inversion, while the 147 cm radiocarbon age (1764 ± 144.5 CE, marine calibration) is broadly consistent with the 1963 CE $^{210}Pb/^{137}Cs/^{241}Am$ marker at 29 cm depth. Right: tentative linear interpolation (black line) with uncertainty envelope (grey). This schematic does not represent a formal age-depth model but illustrates the overall compatibility of the chronological markers.

8. Interpretation of the fossil palynological record

8.1 Pollen assemblages and vegetation changes

The palynological sequence from core LB5B exhibits a relatively stable pattern, with no major or abrupt vegetation turnovers detected throughout the last three centuries (as constrained by the chronological framework outlined above). While minor variations in taxa proportions are present, they do not indicate large-scale shifts, suggesting that the overall landscape composition in the Burano basin has remained broadly consistent since the mid-18th century (Figs. 8–11).

The hierarchical cluster analysis (CONISS), applied to both individual taxa and ecological groups, nonetheless provides a formal subdivision into five pollen zones (BUR-1a, BUR-1b, BUR-2, BUR-3, BUR-4a, BUR-4b), each corresponding to subtle but consistent shifts in taxa proportions rather than to marked ecological thresholds (Figs. 12, 13).

1. At the base of the core (BUR-1a/b), Sub-Mediterranean arboreal taxa dominate the assemblages, particularly *Quercus pubescens* type, which reaches 30–40% of the arboreal pollen. This prevalence indicates the persistence of deciduous oak woodlands in the area during the mid- to late 18th century.
2. Moving upward through BUR-2 and BUR-3, a gradual decline in Sub-Mediterranean taxa is recorded, with *Q. pubescens* type falling to ~20% in the uppermost samples. This trend is counterbalanced by a modest increase in Mediterranean sclerophylls (notably *Quercus ilex-coccifera* type and *Pistacia*) and by the progressive appearance of cultivated taxa. The anthropogenic signal, though limited in amplitude, becomes clearer above ~52 cm (approximately the beginning of the twentieth century), with an increase in *Olea* and Poaceae and a simultaneous reduction of Sub-Mediterranean taxa. This corresponds well with the CONISS-defined transition into BUR-3, where Mediterranean elements and anthropogenic indicators outweigh the Sub-Mediterranean contribution.
3. In BUR-4a and BUR-4b, corresponding to the second half of the 20th century, the slight rise in *Pinus* percentages above 26 cm depth is especially noteworthy. While the Orbetello core shows a sharp rise in *Pinus* linked to the large-scale reforestation of the Duna Feniglia during the first decades of the 20th century, establishing a secure correlation with the Burano sequence remains challenging.

Indeed, the layer at 30 cm is precisely dated to 1963 CE by the ^{137}Cs peak, suggesting that the *Pinus* signal in Burano cannot be directly correlated with the Orbetello event, and might instead reflect local afforestation dynamics around the Burano basin or pollen input from more distant stands.

Herbaceous taxa as a whole display limited variation, with no consistent long-term trends. Minor oscillations are recorded in specific groups, but these do not translate into significant environmental changes. The persistence of halophytic Amaranthaceae, aquatic taxa such as *Ruppia*, and marsh indicators including *Phragmites* suggests continuity of lagoonal and wetland habitats throughout the core.

In synthesis, the combined pollen data and CONISS analysis suggest a vegetation landscape that has remained compositionally stable over the last three centuries. The dominant assemblage is a mixed broad-leaved forest composed of Mediterranean evergreen taxa (*Quercus ilex*, *Pistacia*) and Sub-Mediterranean deciduous oaks (*Q. pubescens* type). Olive cultivation expanded during the last century, marking the principal anthropogenic imprint, while aquatic and halophytic vegetation reflects the persistence of lagoonal habitats largely consistent with the current landscape of the Burano basin. The CONISS-defined zones therefore represent a statistical formalisation of gradual shifts in arboreal composition and human influence, rather than discrete ecological thresholds, and must be interpreted with caution given the limited chronological control.

8.2 NPPs and associated lagoonal trophic shifts

The analysis of NPPs provides independent evidence on trophic state, oxygenation, and hydrological variability within the Burano lagoon. These proxies complement the pollen record by capturing short-term ecological disturbances and offering insights into the dynamics of aquatic vegetation and microbial communities.

The NPP record from core LB5B is dominated by algal remains, dinocysts, fungal spores, and aquatic microfossils, which together provide critical insights into lagoonal trophic conditions and hydrological changes. While the background variability of most taxa remains moderate, several marked events punctuate the sequence (Figs. 14, 15).

The most conspicuous feature is the pronounced bloom of *Botryococcus* and *Euastrum* centred at ~40 cm depth. If the ^{137}Cs marker at 29 cm (1963 CE) is taken as a robust chronological anchor, this event can be placed in the early 1950s. The most plausible explanation is exceptional climatic stress, namely the July 1952 heatwave, when

maximum temperatures reached 36 °C in Tuscany. Although no instrumental record is available for Burano itself, multiple regional datasets document an intense early-July 1952 heat episode across Tuscany (e.g., +39.5 °C at the Firenze Ximeniano weather station on 6 July 1952; additional stations reporting July 1952 record highs). We therefore consider this mid-20th-century heat stress the most likely driver of the *Botryococcus–Euastrum* bloom, as it may have exacerbated water stratification and triggered algal proliferation. This interpretation is consistent with the *Annali Idrologici* (Condrò, 1952) for Tuscany, which report very high July temperatures at several stations across the region. At the same time, it cannot be excluded that reduced oxygenation of lagoon waters was also influenced by post-war transformations in the surrounding landscape. In particular, the intensification of agriculture and drainage interventions in the Maremma during the 1950s-1960s (Paolini, 2012; Saragosa, 2019) may have increased nutrient inputs and altered water circulation, processes that in other Tuscan lagoons such as Orbetello are well documented drivers of eutrophic crises (Lenzi *et al.*, 2003).

This bloom coincides with a striking decline of *Ruppia* between 44 and 36 cm depth, suggesting that submerged macrophyte communities were severely impacted. The almost complete disappearance of *Ruppia* may be explained by light limitation due to algal turbidity, by oxygen depletion, by salinity fluctuations, or by altered nutrient dynamics, all processes that have been shown to strongly affect *Ruppia* meadows under eutrophic conditions (Azzoni *et al.*, 2001). The coupling of algal proliferation and macrophyte collapse points to one of several major disturbance episodes that have affected the lagoon ecosystem during the 20th century.

Following this interval, a modest but consistent increase in foraminiferal linings is recorded. Given their general scarcity in brackish lagoonal deposits, this rise likely indicates a transient phase of enhanced marine influence or increased salinity. Such conditions may have followed the collapse of submerged vegetation, either as a result of altered lagoon-sea connectivity (e.g. dredging or management interventions) or as part of short-term hydroclimatic oscillations affecting water balance.

Beyond these mid-20th century disturbances, the NPP spectrum remains relatively stable. Dinocysts (including *Spiniferites* sp. and *Lingulodinium* sp.) occur sporadically, reflecting episodic marine incursions, while fungal spores (*Glomus*, Parasite eggs) and diatoms show only minor fluctuations. Overall, the NPP record highlights the exceptional significance of the *Botryococcus–Euastrum* bloom and the associated *Ruppia* collapse as key indicators of ecological stress, probably tied to a combination of anthropogenic and

climatic drivers. Analogous processes of eutrophication, driven by nutrient enrichment and limited exchange, have been extensively documented for the nearby Orbetello lagoon (Lenzi *et al.*, 2003), highlighting the sensitivity of coastal lagoons to small-scale changes in nutrient and hydrological balance.

8.3 Vegetation and NPPs trends in the climatic and historical context of the site

The palynological trends, the CONISS zonation, and the NPP evidence discussed above highlight a system marked by long-term stability but punctuated by subtle shifts in arboreal composition and by short-lived episodes of ecological stress. To interpret these signals more comprehensively, it is necessary to place them within the broader framework of historical land-use practices, hydrological management, and documented climatic variability in southern Tuscany. Such integration allows the Burano record to be evaluated not only as an isolated local archive, but as part of the wider dynamics affecting Tyrrhenian coastal lagoons during the last three centuries.

Taken together, the limited pollen variability, the statistically defined yet low-amplitude CONISS zones (BUR-1a to BUR-4b), and the few pronounced NPP excursions point to a landscape that remained compositionally stable but was periodically perturbed by 20th-century human interventions and short-lived climatic extremes in southern Tuscany. Regionally, the Orbetello-Burano system underwent major management changes since the early 1900s, most visibly the Feniglia dune reforestation: state expropriation (1910-1911) and long replanting campaigns (predominantly *Pinus pinea*) continued at least through the 1930s, creating ~430-460 ha of pinewood that still frames the lagoonal basins today. In the Burano record, however, the main *Pinus* increase appears later, suggesting that while the Feniglia plantations established the regional source of pine pollen, its detectable expansion in the core may reflect delayed dispersal and maturation of the pinewood, or additional reforestation phases and local landscape changes during the mid-20th century. This nuance cautions against interpreting the *Pinus* trend as a perfectly synchronous signal with Orbetello (presented in the following chapter), while still linking it to the broader history of coastal reforestation (Fondazione S. Giovanni Gualberto, 2000).

The pollen data show a gradual replacement of Sub-Mediterranean deciduous oaks by Mediterranean sclerophylls (decline of *Quercus pubescens*-type from ~30–40% to ~20% offset by *Q. ilex*-coccifera type, *Pistacia*) and a late anthropogenic imprint (rise of *Olea*,

Poaceae) that intensifies after World War II – precisely where CONISS places the BUR-3 to BUR-4a/b transitions (Figs. 12, 13). This pattern is consistent with documented 20th-century land-use intensification around Burano and the persistence of a coastal mosaic of maquis–pinewood–wetlands noted by floristic and reserve management surveys (Angiolini *et al.*, 2002; Piano antincendio boschivo (PAIB) 2022-2026). The increase of *Olea* and cereal-type pollen, together with ruderal and pasture indicators, suggests that agricultural expansion and more intensive land management played a central role in shaping the vegetation dynamics of the area during this phase.

The most diagnostic ecological disturbance in the core is the mid-20th-century bloom of *Botryococcus* and *Euastrum* (~40 cm) (Fig. 14), coeval with an almost complete collapse of *Ruppia* (~45-33 cm) (Fig. 8) and followed by a slight increase in foraminiferal linings. This disturbance episode, already detailed in the NPP section, highlights the sensitivity of the Burano lagoon to short-term ecological stress and marks one of the most significant shifts in the recent record.

Conservation reports and ecological surveys have long highlighted the vulnerability of the lagoon to eutrophication and shifts in water exchange regimes, particularly in relation to its shallow depth, limited tidal range, and strong dependence on canal connectivity (Lenzi & Angelini, 1985; Piano antincendio boschivo (PAIB) 2022-2026). These characteristics imply that even minor changes in nutrient input or circulation can trigger disproportionate ecological responses. Within this framework, the post-bloom increases in foraminifera observed in LB5B may be interpreted as a transient phase of enhanced salinity or marine connectivity following macrophyte collapse. Similar mechanisms have been invoked for other Tyrrhenian lagoons when artificial interventions or vegetation cycles altered water quality (D'Orefice *et al.*, 2020a; Krakimel, 2003; Lenzi *et al.*, 2003). These remain hypotheses, not assertions, given the chronological uncertainties of LB5B and the absence of direct hydrological records for Burano during the 1950s.

Finally, the long-view geomorphological setting of Burano suggests that, after the main Holocene phases of barrier-lagoon formation and sandspit closure, the last millennia, and particularly the last three centuries, were characterized by relative physical stability. In this context, human interventions such as reclamations, fishery infrastructures, and forestation projects became the main drivers of ecological change. This helps explain why pollen and NPP signals show gradual adjustments rather than major reorganizations, consistent with the persistence of a lagoon-wetland mosaic described by floristic surveys

and with the microtidal, low-energy character of the basin (Angiolini *et al.*, 2002; D'Orefice *et al.*, 2020a, 2022).

While the Burano record provides valuable insights into ecological dynamics over the last three centuries, its interpretation requires caution. Each linkage outlined above is contingent on the age model (^{137}Cs 1963 anchor; basal radiocarbon uncertainty) and on the non-uniqueness of NPP responses. Where climatic or management connections have been suggested (e.g., the 1952 heat event, exchange-driven salinity pulses), these should be regarded as plausible mechanisms supported by independent evidence rather than as deterministic drivers. The overall conclusion remains robust: minor, gradual compositional shifts, a mid-20th-century eutrophication/heat-stress episode, and no major reassembly of the Burano vegetation system during the last three centuries.

9. Surface samples

9.1 Granulometry and hydrodynamic implications (Figs. 16, 17)

The granulometric composition of the Burano surface sediments, dominated by silt with variable proportions of fine sand and clay, reflects the overall low-energy conditions of this microtidal lagoon. Beyond this general trend, the spatial distribution of grain sizes highlights the influence of basin morphology and local hydrodynamics.

Sediments collected closer to the shoreline are generally coarser, while those from more central positions are finer, indicating the expected reduction in energy and transport capacity with increasing distance from the margins. Exceptions to this pattern, such as the coarse fraction in sample 02 or the fine texture of sample 01, emphasise the role of site-specific factors, particularly the heterogeneous contribution of tributary inlets (Figs. 16, 17). The higher sand content in sample 07, for example, is plausibly linked to its proximity to the Scaricatore della Bassa, whereas the finer signature of sample 01 suggests a reduced sedimentary impact of the Fosso del Melone (Figs. 16, 17).

These observations underscore the dynamic equilibrium between localised sediment inputs and the overall depositional stability of the basin. While the biological proxies indicate compositional continuity of vegetation and aquatic assemblages, granulometric variability demonstrates how minor changes in hydrodynamic conditions or point-source inputs can modulate the physical characteristics of lagoonal deposits. This highlights the

importance of integrating granulometric evidence with palynological and NPP data, as it captures the small-scale heterogeneity of depositional processes that may not be reflected in the biotic record. Overall, the granulometric data confirm the low-energy depositional setting of the Burano lagoon and the limited spatial variability in sedimentary processes.

9.2 Surface samples comparison (Figs. 18, 19, 25)

The analysis of surface samples from Lake Burano was undertaken to establish a modern analogue for the fossil pollen record and to evaluate how well the uppermost levels of core LB5B capture present-day vegetation and depositional conditions. These samples represent the current pollen rain and sedimentary input across the lagoon, providing a baseline against which recent changes in the stratigraphic sequence can be assessed. This comparison is particularly relevant in a shallow, micro-tidal system like Burano, where short-term hydrological variability, vegetation dynamics, and human management may generate spatial heterogeneity not easily detectable in a single sediment core.

The seven surface samples from Burano shows a broadly uniform composition across the lagoon, with a predominance of herbaceous taxa (average ~34%) and a consistent representation of arboreal groups (Figs. 18, 19). Among herbaceous plants, the Halophytes/NAP and Helophytes/NAP groups stand out, though their values vary across samples: Halophytes/NAP reach up to 32.7% in sample PS-POL-BUR 06, almost entirely due to Amaranthaceae, while Helophytes/NAP average 8–9% but fall to just 2% in PS-POL-BUR 03, likely reflecting its central position far from reedbeds. Hydrophytes, including *Ruppia*, are present with variable percentages (up to 6.7%), confirming the persistence of aquatic vegetation within the lagoon, though at locally heterogeneous abundances (Figs. 18, 19, 25).

Within the arboreal assemblage, anthropogenic taxa represent a relatively high fraction (16.3%), primarily *Olea* (~12%), accompanied by sporadic *Eucalyptus* pollen. The latter reaches locally elevated percentages (8.1% in PS-POL-BUR 01), probably due to nearby ornamental trees or plantations, while being absent from most other samples. The Mediterranean arboreal group is dominated by *Quercus ilex-coccifera* type, whereas Sub-Mediterranean taxa are represented mainly by *Quercus pubescens* type and *Quercus suber*. *Pinus* is consistently present at modest levels (~7%), and upland herbs are represented primarily by Ericaceae, Asteraceae Asteroideae, and *Plantago lanceolata* type (Figs. 18, 19, 25).

Comparison with the upper levels of core LB5B indicates a strong continuity between recent surface deposition and the fossil pollen record of the past decades. The ecological groups represented in the cumulative surface spectrum largely mirror those in the uppermost core samples, with Mediterranean and Sub-Mediterranean arboreal taxa maintaining similar proportions and with anthropogenic indicators dominated by *Olea*. The main divergence concerns the Halophytes/NAP group, which appears more variable and locally more abundant in the surface samples than in the corresponding upper levels of LB5B. This difference can be plausibly explained by short-term ecological fluctuations in halophyte vegetation near lagoon margins, where Amaranthaceae are highly responsive to salinity and moisture variations.

Overall, the close correspondence between surface spectra and the uppermost core levels supports the reliability of the recent pollen record, indicating that the topmost part of the sequence faithfully reflects the modern vegetation and depositional setting of Lake Burano. Minor discrepancies, such as the higher halophytic signal in specific surface samples, underscore the localised influence of shoreline vegetation and highlight the importance of integrating spot surface data with stratigraphic sequences.

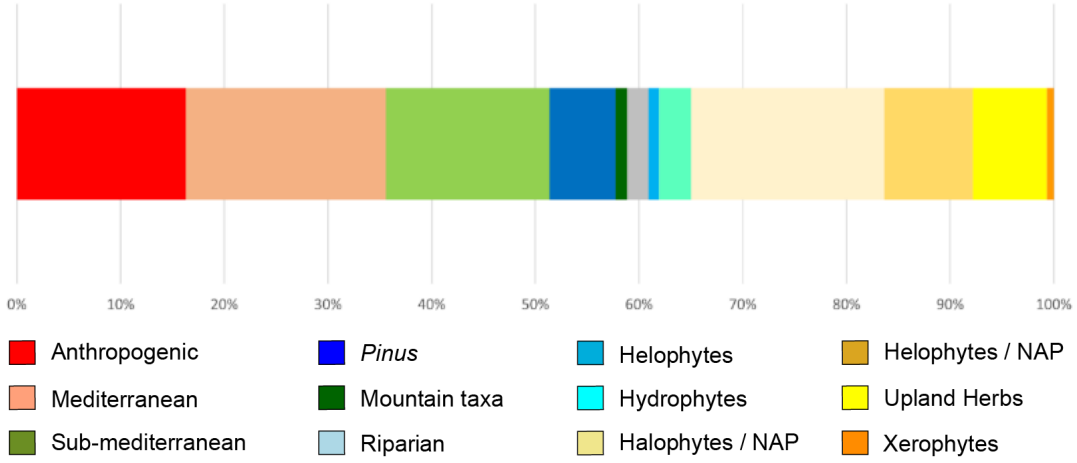

Fig. 25: Cumulative percentage of pollen content of surface samples from the Burano site, subdivided by informal palynological group.

9.3 Moss samples and pollen trap (Figs. 20–22, 26, 27)

The moss samples collected around Burano provide a complementary perspective to the lagoonal surface sediments, capturing pollen deposition over a broader areal source rather than strictly within-basin dynamics. Their spectra are characterized by a markedly higher

proportion of herbaceous taxa (averaging ~60%), with Upland Herbs consistently contributing at least 30% of the total and reaching more than 50% in MOSS2 BUR1-23. Within this group, Asteraceae Cichorioideae are particularly abundant, varying from ~15% to over 30% between samples. Arboreal taxa are present but comparatively less represented: *Quercus ilex-coccifera* type dominates the Mediterranean group, while Sub-Mediterranean oaks show minor values, with *Quercus pubescens* type absent from MOSS2 BUR1-23. Anthropogenic indicators are also noteworthy, particularly *Olea*, which rises to ~19% in MOSS2, compared to an average of ~11% in the other two samples. These patterns highlight the patchiness of extra-lagoon vegetation signals, strongly influenced by local pollen rain and landscape heterogeneity (Fig. 26).

The pollen trap reinforces this interpretation, recording the most recent deposition signal with a still higher herbaceous component (66%). Upland Herbs again dominate (38%), and anthropogenic inputs are clearly visible, with cereals and large Poaceae exceeding 16% of the total. This indicates that the modern pollen rain is strongly shaped by agricultural activity and ruderal vegetation in the surrounding matrix, as well as by ongoing olive cultivation. The arboreal component is comparatively subdued, with Mediterranean and Sub-Mediterranean taxa underrepresented relative to the lagoon sediments and moss samples (Fig. 27).

Taken together, the moss samples and the pollen trap illustrate the difference between extra-lagoonal and strictly lagoonal signals: while surface sediments integrate a more stable, basin-focused record of vegetation and aquatic communities, mosses and the trap highlight the strong influence of terrestrial pollen rain and short-term anthropogenic pressures. Their inclusion thus complements the fossil record from a monitoring perspective, documenting the structure of the modern pollen rain and offering a reference

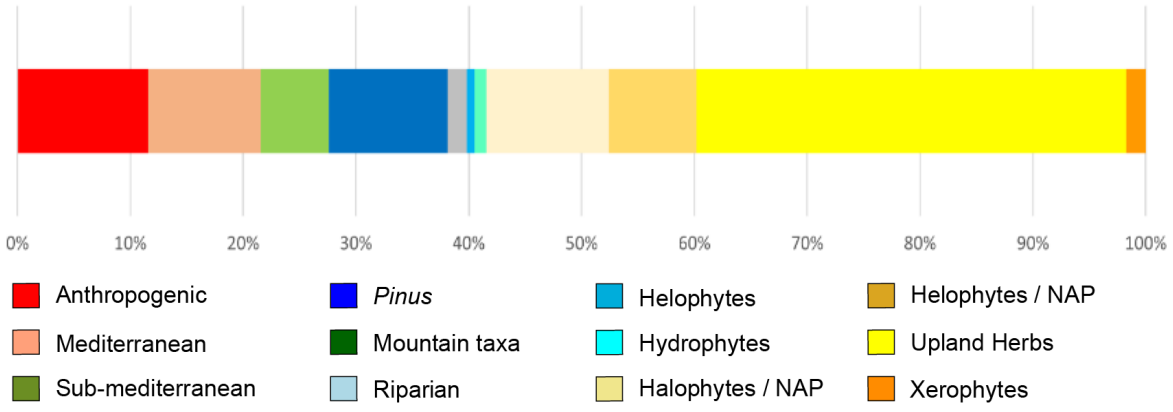

Fig. 26: Cumulative percentage of pollen content of moss samples from the Burano site, subdivided by informal palynological group.

framework for interpreting the most recent environmental and anthropogenic signals preserved in the sediments.

In this light, the comparison between the lagoonal surface spectra and the upper levels of core LB5B offers a contextual reference rather than a direct validation, indicating general correspondence with present-day vegetation patterns while highlighting the broader signal captured by moss samples and the pollen trap.

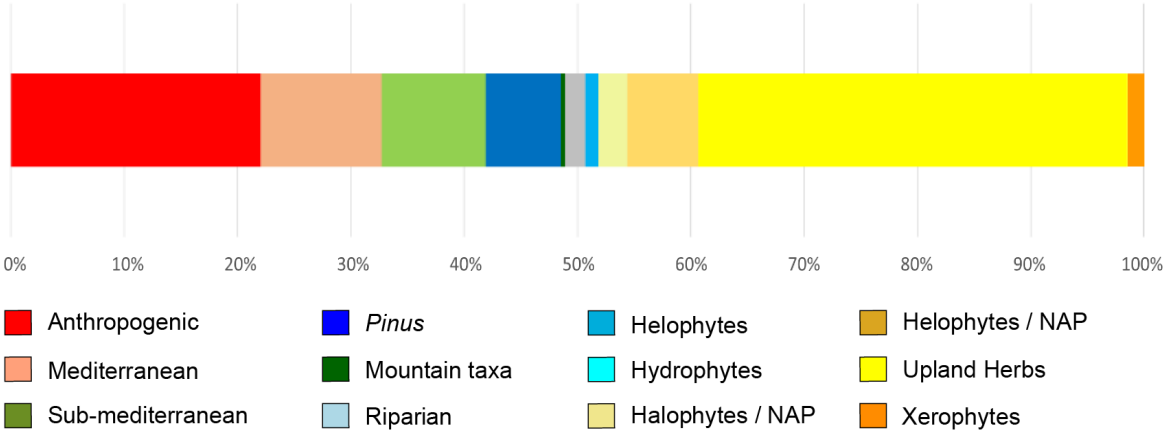

Fig. 27: Cumulative percentage of pollen content of the pollen trap from the Burano site, subdivided by informal palynological group.

10. Microplastic evidence and anthropogenic pressure

The analysis of microplastics in core LB5B revealed the presence of synthetic particles in all three investigated intervals (9-18 cm, 40-50 cm, and 81-89 cm), even after the exclusion of morphologies consistent with laboratory contaminants recorded in the procedural blanks (Tabs. 3–5; Fig. 23). Fibers, fragments, and filamentous aggregates were the most frequently observed morphologies, in line with reports from other lacustrine and lagoonal systems (Imhof *et al.*, 2013; Turner *et al.*, 2019). Although some fragments appeared optically more degraded than others (see Appendix III), this cannot be straightforwardly interpreted as evidence of older deposition, since post-depositional alteration, reworking, or contamination during sampling and preparation may generate similar patterns (Löder & Gerdts, 2015).

In the two upper intervals (9-18 cm and 40-50 cm) (Fig. 23), the concentration and typology of microplastics are coherent with the expected signal for the 20th century. The maximum concentration observed at 40-50 cm (5.93 particles/g) plausibly reflects an enhanced input during the mid-20th century, consistent with the onset of widespread

plastic use and the intensification of local anthropogenic pressure on coastal systems. At Burano, the lagoon's limited tidal exchange and proximity to agricultural and touristic activities increase its vulnerability to pollutant accumulation, a pattern also documented in other Mediterranean lagoons (e.g., Orbetello: Lenzi *et al.*, 2003). This interpretation aligns with studies in other lacustrine sequences, which consistently record a steep rise in microplastic deposition after the 1950s, tightly linked to the global "Great Acceleration" (Bancone *et al.*, 2020; Turner *et al.*, 2019).

Comparable findings have been reported along the southern Tuscan coast, where sediment surveys consistently identify fibers as the dominant microplastic form, exceeding 88% of items in some samples (Cannas *et al.*, 2017). Similarly, investigations near the Cecina River estuary show concentrations of 72-191 items/kg, with input strongly linked to riverine discharge and surrounding agro-industrial activities (Blašković *et al.*, 2018). These analogues reinforce the interpretation of Burano as a sensitive receptor of land-based microplastic pollution, shaped both by its catchment and by restricted water renewal.

The detection of microplastics at 81-89 cm depth (Fig. 23) is particularly problematic. According to the ^{210}Pb-^{137}Cs chronology, supported by the basal radiocarbon date, this interval would correspond approximately to the mid-19th century (~1840s). This finding is difficult to reconcile with the historical timeline of synthetic polymer production, which only began on an industrial scale in the early 20th century (Bancone *et al.*, 2020; Corcoran *et al.*, 2015). Comparable findings of fibers in late 19th-century sediments have also been reported from lake cores in London, although in that case the authors attributed these occurrences primarily to laboratory contamination rather than genuine early deposition (Turner *et al.*, 2019).

Several explanations must therefore be considered:

1. Environmental contamination during sampling or preparation – despite careful control, low counts close to blank values suggest that some fibers may result from background contamination, especially given the ubiquity of airborne synthetic particles (Bancone *et al.*, 2020).
2. Post-depositional migration or sediment mixing – vertical translocation through bioturbation, physical reworking, or anthropogenic disturbance could have displaced microplastics downward, as reported in other shallow lagoonal and lacustrine systems (Gimiliani *et al.*, 2020). If such mixing occurred, it could have affected not only the plastics but also other fine particles, including pollen.

However, the palynological record of LB5B does not show evidence of homogenization or distortion of pollen assemblages, suggesting that any downward transport of microplastics was probably localized and limited in extent.

3. Primary deposition of early polymeric materials – although unlikely, a genuine early occurrence cannot be entirely ruled out, as the optical appearance of some fragments (see Appendix III) suggests differential degradation rather than contamination. If confirmed, this would provide a minimum chronological constraint corresponding to the early phase of synthetic compound introduction, potentially offering an additional anchor point for the depth-age model.

Given the available evidence, the second explanation – partial downward migration within a mixed surface layer – appears the most plausible. The combination of bioturbation, hydrological oscillations, and human disturbance in a shallow lagoon environment could readily explain the apparent stratigraphic offset without invoking genuine pre-industrial deposition.

The original aim of introducing microplastic analysis was to provide an additional chronological proxy for the Burano sequence, complementing radiometric methods. In principle, the first appearance of plastics offers a clear stratigraphic marker for the Anthropocene (Zalasiewicz *et al.*, 2019). However, the unexpected detection of particles at the bottom of the analysed sequence demonstrates that, in this case, microplastics cannot be used as a secure chronological tool. Instead, they highlight potential disturbances to the sedimentary archive, calling into question the robustness of the age-depth model.

In conclusion, the microplastic data from Burano highlight both the potential and the limitations of this emerging proxy. The upper intervals coherently reflect the 20th-century rise in synthetic pollution, confirming the site's sensitivity to anthropogenic inputs, while the anomalous occurrence at depth underlines the need for cautious interpretation. The results reinforce the importance of integrating microplastic analysis with independent sedimentological and palynological evidence to distinguish between depositional and post-depositional processes. Future work, including compositional analysis of the recovered fragments and extension of sampling to deeper layers, will be crucial to disentangle *in situ* deposition from contamination or post-depositional reworking, and to clarify the interpretive value of microplastics in lagoonal stratigraphy.

11. Synthesis and interpretive cautions

The multiproxy analysis of core LB5B from Lake Burano depicts a system characterised by relative stability over the past three centuries. Palynological assemblages consistently indicate the persistence of a mixed Mediterranean / Sub-Mediterranean woodland matrix, complemented by lagoonal herbaceous communities (halophytes, helophytes, hydrophytes), with only modest increases in anthropogenic indicators such as *Olea* and *Eucalyptus* in the uppermost levels. Non-pollen palynomorphs document limited but significant short-term trophic perturbations, most notably the mid-20th-century bloom of *Botryococcus* and *Euastrum*, plausibly triggered by the exceptional July 1952 heatwave, possibly compounded by eutrophication and reduced oxygenation. Granulometric and surface-sample analyses corroborate this general stability, showing textural patterns coherent with lagoonal morphology and a strong continuity between modern spectra and the uppermost sections of LB5B.

At the same time, several uncertainties must be acknowledged. The chronological framework is constrained by a single ^{137}Cs marker (1963 CE) and a basal radiocarbon date affected by wide calibration ranges, while the unexpected detection of microplastics at depth points to possible sediment reworking. Consequently, the exact timing of observed biotic shifts remains tentative, and causal attributions (climatic versus Anthropogenic forcing) must be treated as hypotheses rather than deterministic conclusions.

Overall, the Burano record provides a cautiously reliable reconstruction of minor ecological adjustments in a lagoonal system under combined climatic and anthropogenic pressures, but no evidence of major vegetational turnover. In the broader comparative framework, Burano appears to represent a relatively stable lagoonal archive, whose modest ecological changes will be further contextualised alongside the parallel but distinct trajectories recorded at Orbetello and Orti-Bottagone.

Chapter 4

Orbetello Lagoon

Introduction

The Orbetello Lagoon, located along the southern coast of Tuscany (Chapter 2, Fig. 4), is a shallow transitional water body of high ecological and socio-economic importance. Over the past five decades, the lagoon has experienced significant ecological changes, driven primarily by eutrophication, which in turn has profoundly affected its submerged vegetation dynamics. This site also holds significant naturalistic value and is characterized by rich floristic and faunistic biodiversity, including rare associations of brackish lagoon vegetation. These areas also serve as important stopover sites along migratory routes for numerous bird species, such as flamingos. For this reason, the area is protected under several international conventions, and hosts the WWF Oasis of Laguna di Orbetello.

1. Environmental and cultural context

1.1. Geography and climate

The Orbetello lagoon is a coastal brackish and shallow water body, with an average depth of about 1 m. It is separated from the Tyrrhenian Sea by two sandy tombolos, the Giannella to the northwest and the Feniglia to the southeast, while the promontory of Monte Argentario encloses it from the west.

A narrow artificial isthmus, on which the town of Orbetello is situated, divides the lagoon into two interconnected sub-basins: the Laguna di Ponente (15.25 km², to the west) and the Laguna di Levante (10.00 km², to the east). The water body overall covers a total area of approximately 27 km². The lagoon is connected to the sea through three artificial

Fig. 1: Satellite image of Orbetello Lagoon, where the Orbetello peninsula divides the lagoon into a western portion (Laguna di Ponente) and an eastern one (Laguna di Levante) (modified from Google Earth 2023).

channels (Canale di Nassa, Canale di Fibbia, Canale di Ansedonia), which allow for limited hydrological exchange and are critical for maintaining the lagoon's salinity, ecological balance, and fisheries productivity (Fig. 1). Due to limited natural water exchange, the basin is highly sensitive to nutrient loading and anthropogenic pressures (ARPAT, 2025).

Historical climate data from Orbetello (1951-1980) indicate an average annual temperature of 16°C, with minimum monthly temperatures never below 0°C, and an annual average precipitation of 710 mm. Rainfall is concentrated in the autumn months, particularly in November (116.7 mm), while the summer months show minimal precipitation, as low as 9.5 mm in July, which is typical of a Mediterranean rainfall pattern (e.g. Angiolini *et al.*, 2002) (Fig. 2).

Based on long-term climatic data from the Orbetello meteorological station, as reported by WeatherSpark (www.weatherspark.com), average daily high temperatures peak in

August at approximately 30 °C, while the coldest month is January, with average lows around 4-5 °C. Precipitation is unevenly distributed throughout the year, with the wettest months typically occurring between October and December. Annual precipitation averages around 800-900 mm, with a pronounced summer dry season.

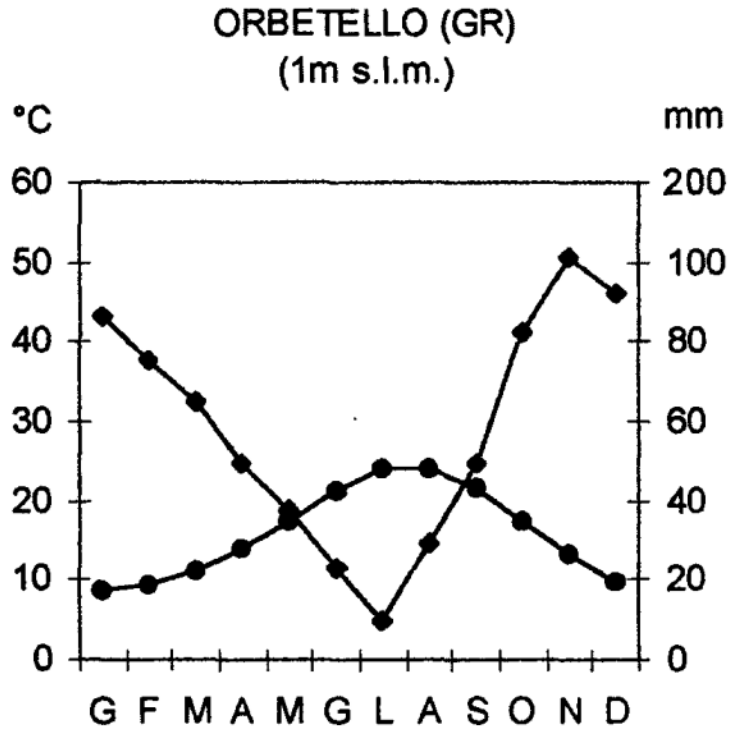

Fig. 2: Thermo-pluviometric diagram of Orbetello (from Angiolini *et al.*, 2002).

1.2. Geological and environmental history

The Orbetello Lagoon formed in response to post-glacial sea-level rise following the Last Glacial Maximum. The rising sea inundated low-lying coastal depressions, giving rise to lagoonal environments such as Orbetello (Mazzini *et al.*, 1999).

Recent geomorphological interpretations suggest that the Orbetello coastal system, characterized by the double tombolo formation of Giannella and Feniglia, developed through complex interactions between marine transgression, sediment supply, and barrier dynamics (Brocard *et al.*, 2024). The central segment, associated with a Pleistocene residual high, likely functioned as a natural sediment trap, promoting differential deposition on its eastern and western flanks. This process ultimately led to the development of the distinctive double-barrier morphology, with two elongated sand spits enclosing the Orbetello lagoon from both sides.

Stratigraphic and sedimentological evidence indicates that the formation of these tombolos occurred progressively during the mid to late Holocene (Mazzini *et al.*, 1999). Substantial parts of both barriers were likely emergent and partially connected to the mainland between approximately 4,800 and 3,000 years ago. The full stabilization and closure of the lagoon, effectively transforming it into a semi-enclosed coastal basin, likely occurred between the Late Bronze Age and Early Iron Age (~3,100–2,900 cal yr BP), though additional sedimentary consolidation may have continued into the Roman period. These findings underscore the importance of long-term coastal progradation, sea-level stabilization, and sediment infill in shaping the current geomorphology of the Orbetello lagoon (Brocard *et al.*, 2024).

The evolution of these tombolos has been linked to sediment inputs from the Albegna and Osa rivers, as well as marine longshore drift, highlighting the interplay between fluvial and coastal dynamics. The geomorphological evidence aligns with regional sea-level rise data and indicates that tombolo development occurred in phases, initially as submerged sandbars that later accreted into stable barrier structures (Pasquetti *et al.*, 2020).

The morphological evolution of the Orbetello coastal system is closely tied to its geological substrate. The central sandy platform where the town of Orbetello stands corresponds to a Pleistocene coastal deposit attributed to the Orbetello synthem, associated with Marine Isotope Stage (MIS) 5e, as documented by stratigraphic and geomorphological studies (Pasquetti *et al.*, 2020). This Pleistocene unit is composed of well-cemented beach and dune sands, subsequently overlain by Holocene deposits such as sands, gravels, and alluvial inputs, mainly from the Albegna River system (Pasquetti *et al.*, 2020). These deposits provide the foundation upon which the lagoonal environment has evolved.

According to Brocard *et al.* (2024), the Orbetello double tombolo developed around a pre-existing central isthmus of MIS 5 age, which acted as a barrier to longshore drift and facilitated the sedimentary accretion on both sides. The Giannella and Feniglia tombolos formed during the mid-to-late Holocene as regressive strandplains, developing laterally from this central core in response to Holocene sea-level stabilization, combined with sediment supply dynamics. The central isthmus, functioning as a sediment trap, promoted differential deposition along the eastern and western flanks, shaping the characteristic double-barrier morphology of the system.

Paleoenvironmental reconstructions by D'Orefice *et al.* (2022) indicate that from 4000 years BP onwards the two tombolos developed, progressively enclosing a wide lagoon

and significantly altering the local hydrodynamics. The complete closure of the lagoon occurred only after 3500 BP (a slightly earlier indication than the 3100–2900 BP closure proposed by Brocard *et al.*, 2024). Their synthesis of sedimentary, palynological, and archaeological data reveals that coastal evolution over the last 8000 years was influenced by both natural and anthropogenic drivers, including climatic fluctuations, land use, and settlement activities dating back to the Etruscan and Roman periods. Archaeological evidence from the surrounding area further confirms continuous human interaction with the lagoon since prehistoric times, with the exploitation of lagoonal and marine resources, salt production, and settlement development well attested throughout the Bronze Age and Classical periods (Cardosa & Dolfini, 2017).

The resulting semi-enclosed lagoonal system, supported by this composite geological and geomorphological framework, has undergone significant transformations from a shallow marine embayment to a highly compartmentalized wetland. These changes were further intensified by human modification and land reclamation during the modern era.

1.3. Modern environmental changes and management strategies

The submerged vegetation of the Orbetello Lagoon has undergone profound changes since the 1970s (Lenzi *et al.*, 1984). Earlier surveys indicated that the lagoon was predominantly colonized by seagrass species, mainly *Ruppia maritima*, *Ruppia cirrhosa*, and *Nanozostera noltii*, which formed extensive meadows in both lagoon basins (Cognetti *et al.*, 1978; Lenzi *et al.*, 1984). These seagrasses played a crucial role in stabilizing the sediments, oxygenating the benthic environment, and supporting high biodiversity. However, increasing nutrient loads from untreated urban wastewater, land-based fish farms, and agricultural runoff led to the proliferation of opportunistic macroalgae such as *Chaetomorpha linum*, *Cladophora vagabunda*, *Ulva rigida*, and *Gracilaria verrucosa* (Bombelli & Lenzi, 1996; Lenzi, 1992). Macroalgae, which thrive in nutrient-rich and oxygen-depleted conditions, gradually replaced seagrasses, particularly in the central and eastern parts of the lagoon.

The spatial distribution of submerged vegetation is determined by the interaction of hydrodynamic, chemical, and biological factors. Seagrasses, which are rooted in the substrate, prefer oxygenated, sandy environments low in organic matter and play a crucial role in stabilizing sediments and controlling nutrient dynamics through root-mediated oxygenation (Menéndez *et al.*, 2002; Viaroli *et al.*, 1996, 2008).

In contrast, macroalgae, which are typically unattached, thrive in nutrient-rich, fine sediments and can form dense mats that deplete oxygen, promote sulphate reduction, and generate toxic compounds such as hydrogen sulfide, thereby inhibiting seagrass growth (McGlathery, 2001). These processes create feedback mechanisms that favour macroalgal dominance. Comparative studies have shown that seagrass-dominated areas maintain higher redox potentials than macroalgae-dominated sediments and lower ammonium concentrations in sediments, highlighting the role of vegetation type in shaping sediment biogeochemistry and overall lagoon ecosystem health (Renzi *et al.*, 2007).

The dominance of macroalgae linked to eutrophication has triggered dystrophic crises in the Orbetello Lagoon, most notably during 1992-1993, when excessive algal blooms led to severe anoxic episodes, mass fish kills, and a collapse of benthic biodiversity (Lardicci *et al.*, 2001; Viaroli *et al.*, 2008). Although restoration measures (e.g., channel enlargement, removal of floating biomass, wastewater treatment) were implemented between 1994 and 1996, opportunistic species continued to dominate during summer seasons and structural parameters of benthic assemblages showed signs of ongoing stress (Lardicci *et al.*, 2001). Several studies have highlighted the eutrophic status of the lagoon, particularly in the 1990s and early 2000s. Investigations revealed high concentrations of dissolved inorganic nitrogen (DIN) and soluble reactive phosphorus (SRP), especially near persistent anthropogenic sources (Lenzi *et al.*, 2003).

Sediment analyses have shown that the Orbetello Lagoon functions as a nutrient sink, with organic-rich, reduced sediments especially in macroalgae-dominated areas (Azzoni *et al.*, 2001). These conditions promote internal nutrient release, particularly ammonium and phosphate, sustaining eutrophic states. Observations between 1999 and 2003 documented long water residence times and low redox potential, both contributing to persistent oxygen depletion and macroalgal dominance (Giusti & Marsili-Libelli, 2005). The presence of large fish farms, some of which discharged untreated effluents directly into the lagoon, contributed significantly to nitrogen and phosphorus inputs (Porrello *et al.*, 2003). Estimates suggested that land-based aquaculture alone accounted for approximately 265 kg of nitrogen and 13 kg of phosphorus per day (Lenzi *et al.*, 2009).

In response to these environmental challenges, the Orbetello Lagoon Environmental Reclamation Authority (OLERA) was established in the 1990s to implement a coordinated restoration strategy. The plan consisted of three main actions:

1. Macroalgae harvesting: mechanical removal of macroalgal biomass was initiated to reduce organic matter input and oxygen demand during decomposition. Boats

equipped with collection systems were employed during peak bloom periods (Lenzi *et al.*, 2003).

2. Artificial seawater pumping: given the limited tidal range and natural water exchange, artificial pumping systems were installed to enhance seawater input and reduce residence times. Water was pumped into the lagoon through the western canals and exited through the eastern canal, creating a one-way flow that improved oxygenation and nutrient flushing (Giusti & Marsili-Libelli, 2006).
3. Phytotreatment of wastewater: urban and aquaculture effluents were diverted to phytotreatment ponds (shallow marginal basins engineered to reduce nutrient loads through the uptake by aquatic macroalgae and the settling of suspended solids) before being discharged into the lagoon. Although not conventional constructed wetlands, these systems acted as nutrient buffers and contributed significantly to limiting the spread of pollutants from persistent anthropogenic sources (PAS) (Lenzi *et al.*, 2003).

Between the late 1990s and the early 2000s these interventions led to a marked improvement to both water quality and vegetation structure. Seagrasses began to recolonize sandy areas near the inlets, and the frequency of dystrophic events declined (Lenzi *et al.*, 2003). However, full recovery remained elusive, particularly in areas close to sources of persistent pollution.

To support adaptive management, several mathematical models, notably the "LaguSoft" model by Giusti and Marsili-Libelli (2005, 2006, 2010), have been developed to support adaptive management of the Orbetello Lagoon. Integrating hydrodynamics and ecological processes, LaguSoft reveals that vegetation patterns are driven by sediment conditions, nutrient levels, and wind-induced currents. The model emphasizes how seagrasses promote sediment oxygenation, creating feedback that support their persistence, while seawater pumping enhances their expansion by improving water quality. These insights have guided practical management decisions, including harvesting, pumping station placement, and wastewater treatment strategies.

In conclusion, although water quality and vegetation have been improved, the Orbetello Lagoon remains vulnerable to eutrophication due to residual nutrient loads and ongoing anthropogenic impacts. The benthic nutrient reservoir can still sustain algal blooms under favourable environmental conditions, with episodic dystrophic events remaining possible, especially during warm summers characterized by limited water circulation.

Long-term resilience requires integrated strategies, including sediment remediation (e.g., bioremediation, capping), reduced external nutrient inputs via improved wastewater

treatment, and sustainable agricultural and aquaculture practices. Expanding ecological models to account for climate change and socio-economic factors is also crucial. Finally, fostering active community involvement and environmental education will be essential to building public awareness and securing long-term support for conservation initiatives. Engaging local stakeholders not only enhances the effectiveness of restoration measures but also ensures that ecological stewardship becomes a shared responsibility. Ongoing monitoring and adaptive, science-based management remain essential for protecting the lagoon's ecological and economic value.

2. Chronological framework of the core OLP-11B

2.1. Radiocarbon dating

At the Orbetello site, the chronological framework was based on radiocarbon dating carried out by Christine Oberlin (Centre de Datation par le RadioCarbone, UMR 5138 "Archéométrie et Archéologie", Lyon, AMS ARTEMIS). Radiocarbon dating was performed on several cores, namely OLP-15, OLP-11B, OLP-14, OLL-6, OLL-7, OLL-9, OLL-11, OLL-12, OLL-13 (Fig. 3). Four samples of the OLP-11B core were analysed for radiocarbon dating, as indicated in Table 1. The origin of these samples is mixed; therefore, both the marine calibration (R ~450 y, ΔR=0, Oxcal v4.4.4, Marine data from Heaton *et al.*, 2020) and the terrestrial calibration (Reimer *et al.*, 2020) are reported in Table 1. Because chronological control relies on bulk-sediment samples, the resulting age estimates should be regarded as indicative.

Reference sample	Depth (cm)	Sample material	Uncalibrated Age (± error)	Calibrated Age (± error) (terrestrial)	Calibrated Age (± error) (marine)
Lyon-19771 (Sac-67918) *	80	Bulk	2895 ± 30 ^{14}C yr BP	1099,5 ± 108,5 BCE	551 ± 169 BCE
Lyon-19772 (Sac-67919) *	125	Bulk	3670 ± 30 ^{14}C yr BP	2046 ± 95 BCE	1463 ± 153 BCE
Lyon-19773 (Sac-67920) *	179	Bulk	4190 ± 30 ^{14}C yr BP	2765,5 ± 125,5 BCE	2130,5 ± 179,5 BCE
Lyon-19234 (GrM) *	215	Bulk: Fibers not visible to the naked eye	4180 ± 35 ^{14}C yr BP	2760 ± 128 BCE	2116,5 ± 184,5 BCE

Tab. 1: Radiocarbon dating analyses carried out on the OLP-11B core (Orbetello Lagoon). The asterisk indicates the date used for the construction of the age-depth model.

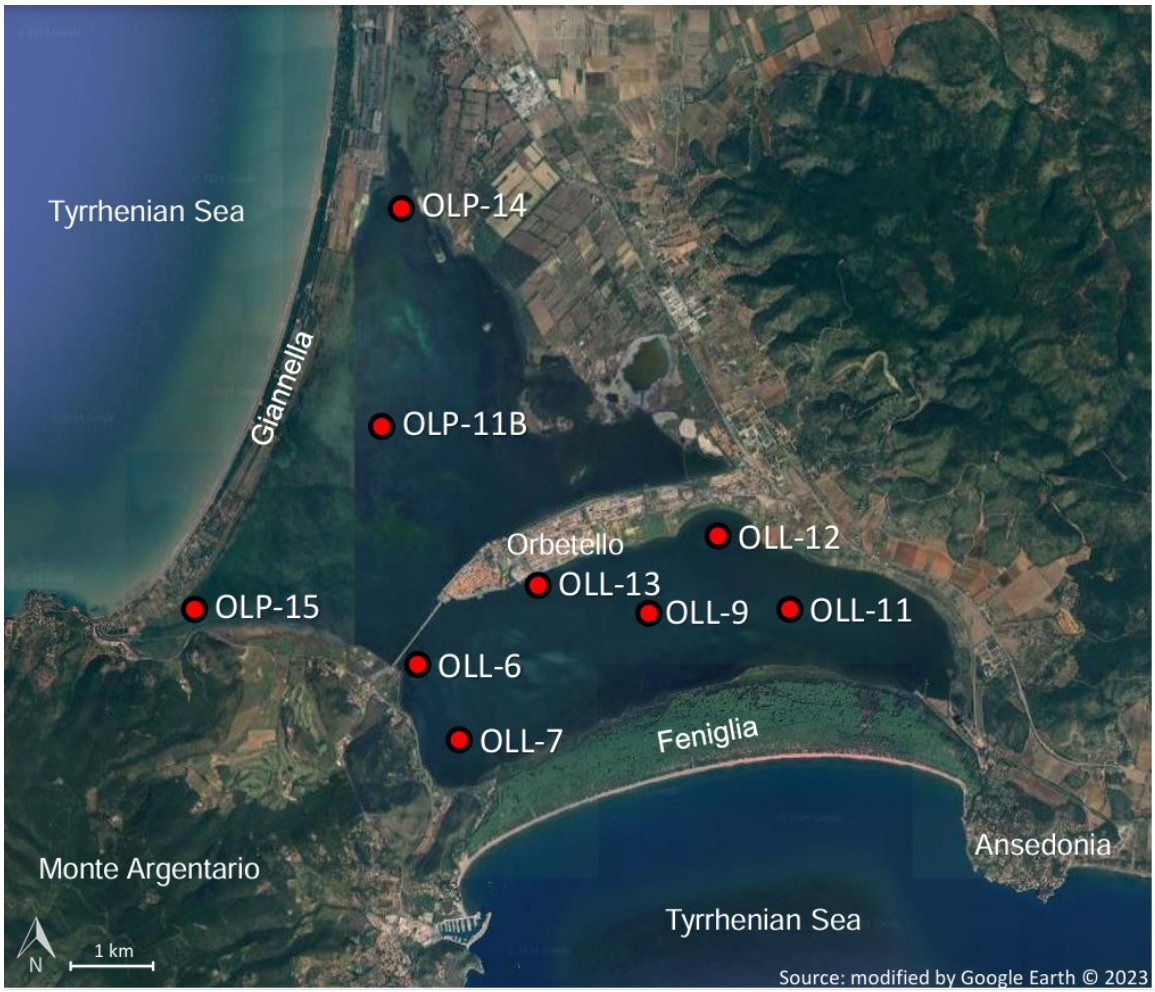

Fig. 3: Location of cores OLP-15, OLP-11B, OLP-14, OLL-6, OLL-7, OLL-9, OLL-11, OLL-12, and OLL-13 within the Orbetello Lagoon.

2.2. Lead-210, Caesium-137, and Americium-241 content analysis

Analyses on ^{210}Pb, ^{137}Cs, and ^{241}Am elements were conducted by Pierre Sabatier (EDYTEM Laboratory, Université Savoie Mont Blanc and CNRS, Le Bourget-du-Lac, France) on the OLP-11B core. The analysis was conducted on 11 consecutive samples (OLP-11B-(A) 0-2; OLP-11B-(A) 2-4; OLP-11B-(A) 4-6; OLP-11B-(A) 6-7,5; OLP-11B-(A) 7,5-9; OLP-11B-(A) 9-11; OLP-11B-(A) 11-13; OLP-11B-(A) 13-15; OLP-11B-(A) 15-17; OLP-11B-(A) 17-18,5; OLP-11B-(A) 18,5-20), covering the interval between 0 and 20 cm depth.

The analysis of ^{137}Cs, integrated with that of ^{241}Am, aimed to identify concentration peaks of these isotopes corresponding to key events in the second half of the 20th century, particularly those associated with nuclear weapons testing (1955 and 1963) and the Chernobyl nuclear disaster (1986) (Bruel & Sabatier, 2020). In this case, the ^{137}Cs and

^{241}Am activity profile does not display any discernible peaks, likely because they do not stratigraphically coincide with the specific layers sampled, but a clear ^{137}Cs increasing trend toward the top is visible (Fig. 4).

The ^{210}Pb dating method estimates sediment ages over the past 100-150 years by measuring excess ^{210}Pb from atmospheric deposition and applying decay models to infer sedimentation rates (as explained in more detail in paragraph 2.2 of chapter 3) (Bruel & Sabatier, 2020). In OLP-11B core the lead concentration profile shows a steadily decreasing trend with increasing depth from the top of the core (Fig. 4). No significant ^{210}Pb values were recorded below 13.5 cm depth, due to the excessive scarcity of this isotope beyond this depth, and they are therefore not represented in the graph below (Fig. 4). Since the concentration of ^{210}Pb in sediments decreases at a known rate, these data, when integrated with the results of the ^{137}Cs analysis, can provide an approximation of the sedimentation rate in this section of the core, which was estimated at 0.78 mm/year.

Using the mean sediment accumulation rate derived from the excess ^{210}Pb profile (SAR $\approx$ 0.78 mm yr^{-1}), a first-order age estimate can be obtained for the upper part of the core by simple linear back-calculation from the coring year (2020 CE). Under this assumption, a depth of ~10 cm corresponds to approximately 128 years of accumulation, placing this level close to 1900 CE. This estimate should be considered indicative, as it relies on a constant accumulation rate and is only valid within the shallow interval constrained by the ^{210}Pb measurements.

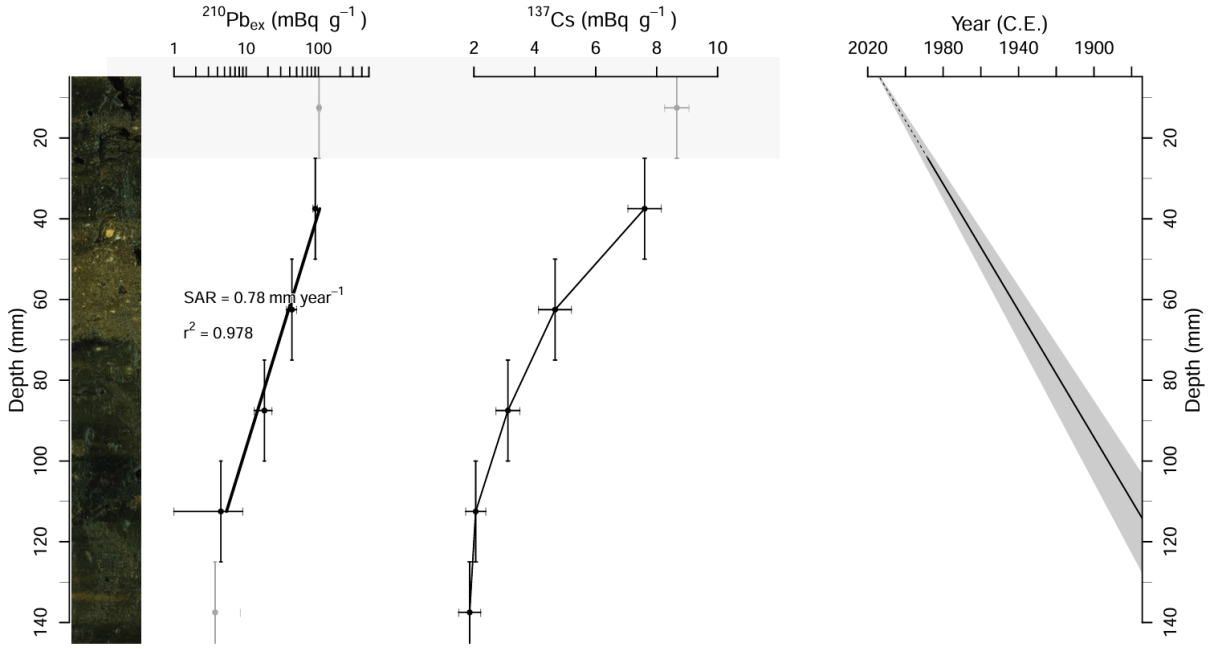

Fig. 4: Trend of ^{210}Pb and ^{137}Cs, with relative model age, on the first 14 cm of the OLP-11B core (image elaborated by Pierre Sabatier).

Results

3. Palynological analysis of the sediment core

3.1. Palynomorph concentrations

Concentrations of pollen and NPP in core OLP-11B display high variability throughout the sequence, with no sections characterized by consistently high or low values between adjacent samples. Concentrations range from a minimum of 5,227 to a maximum of 225,227 grains per gram of sediment, with a mean of 53,296 grains per gram (Fig. 5).

Overall, the preservation of grains is generally good. Pollen concentrations also vary considerably, reaching maxima of 76,688 grains/g, minima of 4,449 grains/g, and a mean of 34,979 grains/g. Concentration curves for individual ecological groups (Fig. 5) indicate that some peaks are specific to certain groups, while others affect multiple groups. Between 114 and 105 cm, there is a rapid increase in Mediterranean, Sub-Mediterranean, Montane, Riparian, and Upland Herbs taxa, with no changes observed in other groups. In contrast, the peak at 54-50 cm is primarily driven by *Pinus* and riparian taxa, with minor contributions from Mediterranean, Sub-Mediterranean, Anthropogenic, and Hydrophytes taxa. Some peaks are limited to only a few groups, such as the one between 20 and 17 cm, dominated by Hydrophytes (particularly *Ruppia* and *Lemna*) and Anthropogenic taxa. NPP concentrations are, on average, lower than those of pollen, with a mean of 18,317 grains/g. However, variability between samples is even greater, ranging from 320 to 166,896 grains/g. NPPs are relatively sparse throughout the core, except for higher concentrations between 189-179 cm, 150-107 cm (with the maximum peak at 129 cm), and 54-38 cm. The peak at 129 cm is entirely attributable to the abundance of indeterminate fungal spores (Fig. 5).

In summary, the palynomorph concentration profile exhibits complex patterns that differ among ecological groups, providing key insights into vegetation dynamics and environmental conditions during the deposition of the core.

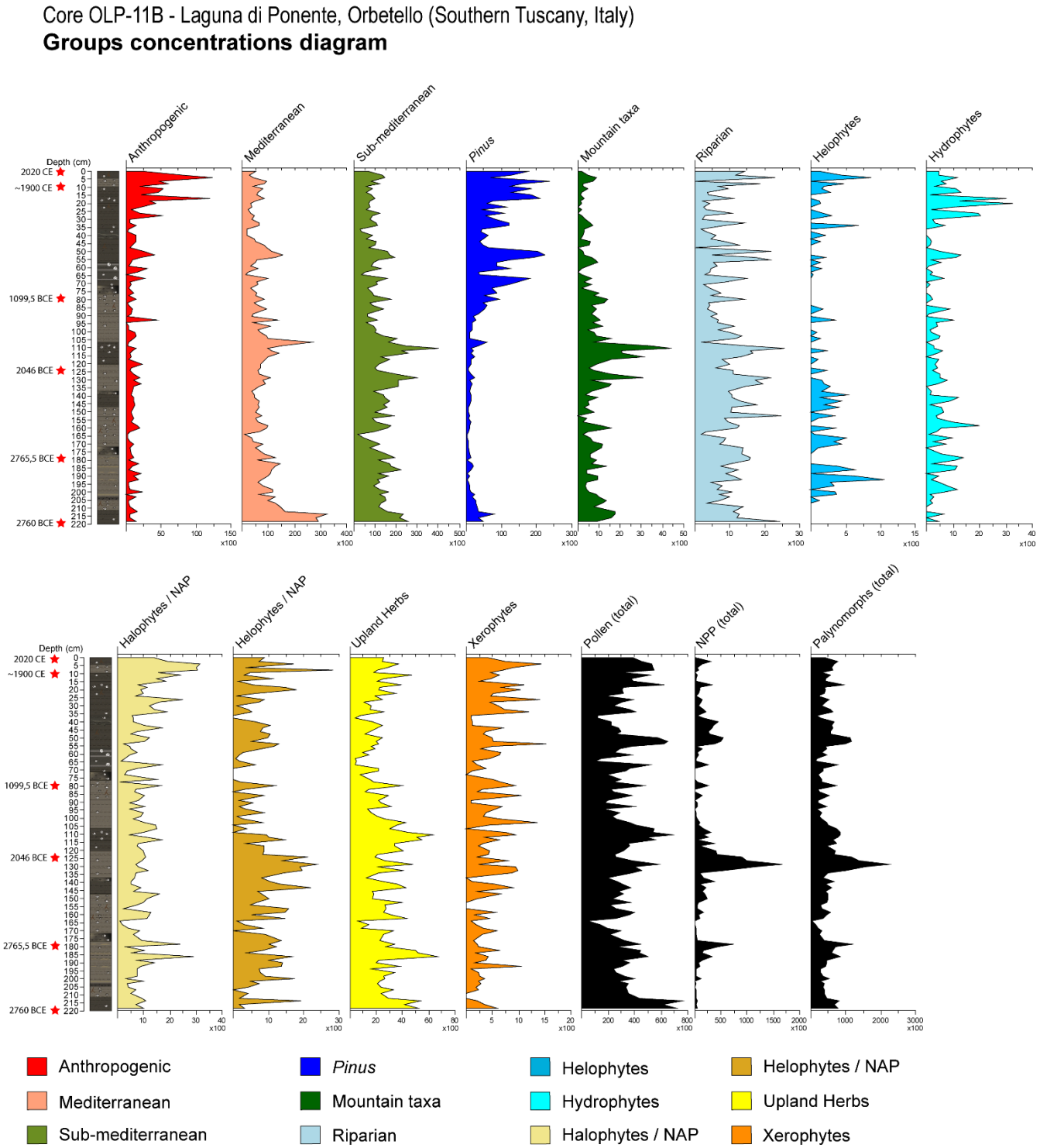

Fig. 5: Concentrations of selected informal palynological groups of the core OLP-11B. Calibrated terrestrial dates are reported.

3.2. Flora (Tab. 2 of Appendix I. Figs. 6, 7)

The analysis of core OLP-11B reveals a flora whose arboreal component is dominated primarily by species of the genus *Quercus*, and, in certain sections, by species of the genus *Pinus* (pine) (Fig. 6).

In particular, the *Quercus pubescens* (downy oak) and *Quercus ilex-coccifera* (holm/kermes oak group) types are by far the most represented, although *Quercus cerris* (Turkey oak) and *Quercus suber* (cork oak) are also consistently recorded throughout the record. Other Fagaceae present include *Castanea* (chestnut) and *Fagus* (beech). Among the Oleaceae, a significant presence of *Olea europaea* (olive), and *Fraxinus* – particularly the *F. excelsior* type (common ash) – is noted, with *Phillyrea* (mock privet) occurring to a lesser extent. *Pistacia* sp. (mastic/terebinth group) also occurs throughout the core. Within the Betulaceae, *Carpinus*, especially *Carpinus orientalis* (Oriental hornbeam), *Corylus* (hazel), and *Alnus* (alder) show a significant and ubiquitous presence. *Ostrya* (hop-hornbeam) and *Betula* (birch) are also detected, though in lower percentages.

Among the Ulmaceae, *Ulmus* (elm) appears consistently along the entire core, albeit with limited representation. Other arboreal taxa include scattered presences of *Juglans* (walnut), *Populus* (poplar), *Salix* (willow), *Sambucus* (elderberry), *Tilia* (linden), *Acer* (maple), *Buxus* (boxwood), and the non-native genus *Eucalyptus*. Among the gymnosperms, *Pinus* is present throughout the record and dominates in some sections, whereas *Abies* (fir) is recorded only occasionally, and *Picea* (spruce) even more rarely.

Shrubby taxa are represented notably by the Ericaceae, which are well documented across the entire core, while *Juniperus* (juniper) appears sporadically. Also recorded, though never in high percentages, are *Vitis* (grapevine), *Rhus* (sumac), *Cercis* (Judas tree), *Rhamnus* (buckthorn), *Viburnum* (viburnum), and *Cornus* (dogwood) (Fig. 6).

Among herbaceous taxa, the most common are the Amaranthaceae, Poaceae (grasses), and *Plantago* (plantain), particularly the *P. lanceolata* and *P. media* types. Asteraceae, especially *Artemisia* (mugwort), along with Brassicaceae, and occasionally *Rumex* (dock), are also well represented (Figs. 6, 7).

Additional families recorded in multiple samples include Euphorbiaceae (spurge), Rosaceae, Urticaceae, Ranunculaceae, Fabaceae – including the genus *Medicago* (medick) – Hypericaceae (gen. *Hypericum*, or St. John's wort), Araliaceae (gen. *Hedera*, or ivy), Polygonaceae, Iridaceae, Liliaceae, Lamiaceae, Apiaceae, Scrophulariaceae,

Cistaceae, and Ephedraceae (*Ephedra*, primarily the *E. fragilis* type or joint pine). A single grain belonging to family Solanaceae is also observed (Figs. 6, 7).

Among helophytic species, family Cyperaceae (sedges) is well represented, and the *Typha latifolia* type (broadleaf cattail) is also present. Within the aquatic group, the best-represented taxon is *Ruppia* (beaked tasselweed or widgeon grass), followed by *Alisma plantago* (water plantain), *Sparganium*/*Typha angustifolia* type (bur-reed/lesser bulrush), and *Lemna* (duckweed). Less abundant but present are *Potamogeton* (pondweed), *Myriophyllum* (water milfoil), *Sagittaria* (arrowhead), and *Callitriche* (water-starwort) (Fig. 6).

A total of 127 pollen taxa were identified. Specifically, 35 arboreal taxa, 7 shrub taxa, and 85 herbaceous taxa were recorded. The anthropogenic indicators group includes 10 taxa, Mediterranean 8 taxa, Sub-Mediterranean 18 taxa, Montane 4 taxa, Riparian 2 taxa, Helophytes 2 taxa, Hydrophytes 9 taxa, Halophytes/NAP 4 taxa, Helophytes/NAP 2 taxa, Upland Herbs 62 taxa, and Xerophytes 5 taxa. *Pinus* was counted separately.

Core OLP-11B - Laguna di Ponente, Orbetello (Southern Tuscany, Italy)

Single taxa diagram (exaggeration 8x)

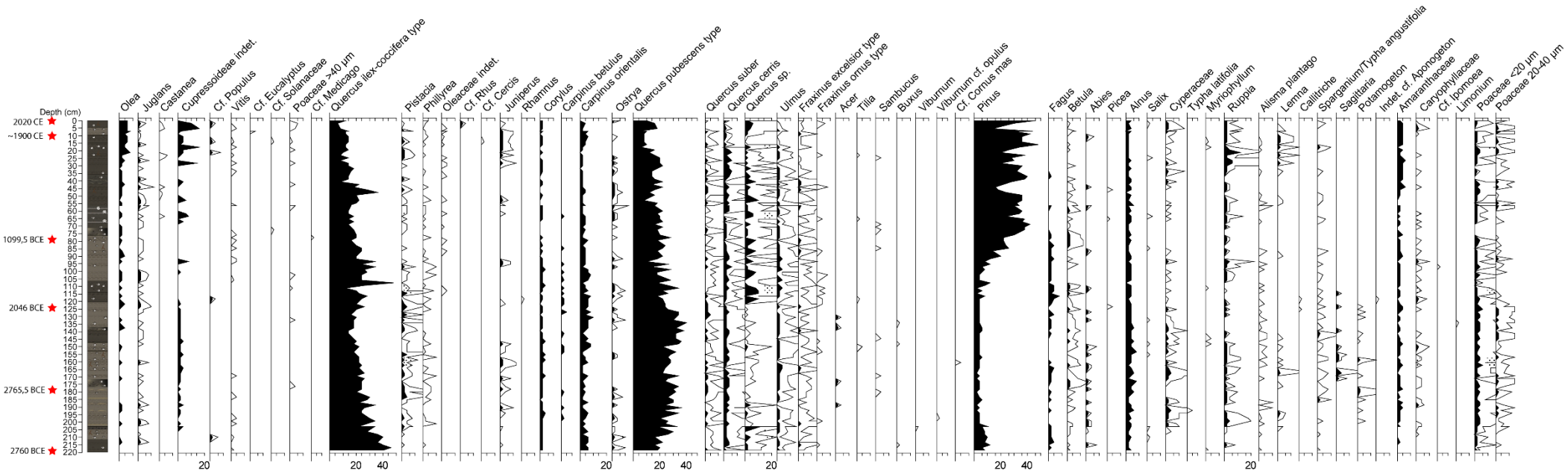

Fig. 6: Detailed palynological diagram of the core OLP-11B (exaggeration 8x). Calibrated terrestrial dates are reported.

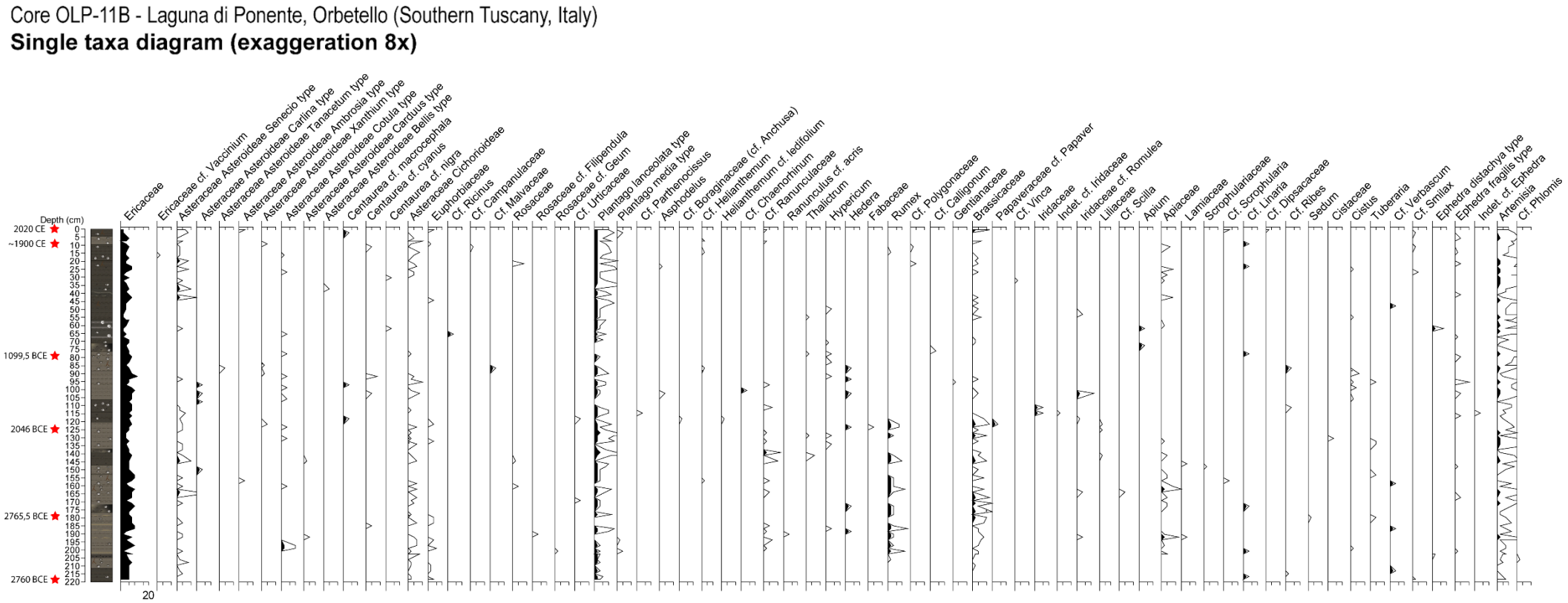

Fig. 7: Detailed palynological diagram of the core OLP-11B (exaggeration 8x). Calibrated terrestrial dates are reported.

3.3. Vegetation (Figs. 6–9)

The pollen record from core OLP-11B reveals a vegetation landscape consistently dominated by arboreal taxa, which account for an average of over 80% of total pollen throughout the sequence (Fig. 8A). Shrubby taxa average slightly above 5%, and herbaceous taxa just over 10%, with neither group showing substantial fluctuations along the core.

Basal Phase (core base to ~110 cm): in the lower part of the core, the arboreal assemblage is dominated by *Quercus ilex-coccifera* type and *Quercus pubescens* type. The *Q. ilex-coccifera* type reaches relatively high percentages (46-13% of total pollen), showing a gradual decrease upward. Other Mediterranean elements are scarce, with *Pistacia* as the only notable contributor. Anthropogenic taxa remain consistently low (<5%), with *Olea* and indeterminate Cupressoideae as the most represented. The *Q. pubescens* type is the second major component in this phase, ranging from 16% to 40% and displaying a clear upward trend toward the middle of the core. Among Sub-Mediterranean taxa, *Quercus suber*, *Quercus cerris*, *Corylus*, and *Ulmus* maintain relatively stable values (each ~2%), while *Carpinus orientalis* is more abundant (average 4.5%). Overall, the combined Mediterranean and Sub-Mediterranean elements represent approximately 75-80% of total pollen, forming nearly the entirety of the arboreal component (Figs. 6, 9). Other arboreal taxa occur at lower percentages: *Pinus* averages 4%, *Fagus* 2.3%, and *Alnus* 3.5%, with all remaining trees present in trace amounts (Fig. 6). Shrubby and herbaceous taxa are dominated by Amaranthaceae (average 4.4%), Ericaceae (6.3%, with a peak of 10.5%), Poaceae (2.8%), *Plantago lanceolata* type (0.6%), and *Artemisia* (1%). All other herbs occur at <0.5%. The only notable helophytic group, Cyperaceae, shows low but variable values (average 0.6%). Aquatic taxa average 1.4%, with *Ruppia* (0.4%) being the most frequent (Figs. 6, 7, 9).

Transitional Phase (~110–95 cm): values of *Q. pubescens* fluctuate, while *Q. ilex-coccifera* shows a marked peak, reaching 48% of total pollen (Fig. 6).

Pinus Expansion Phase (~95 cm to top): at ~95 cm, a pronounced compositional shift occurs. The previous dominance of *Q. ilex-coccifera* and *Q. pubescens* gives way to a marked increase in *Pinus*, which rises rapidly from ~4% to ~29% of total pollen between 95 and 73 cm depth. These high *Pinus* values persist through to the top of the core (Figs. 6, 8B, 9), while both *Q. ilex-coccifera* and *Q. pubescens* decline irregularly to ~15% each.

From 45 cm upward, Amaranthaceae increase slightly. *Ruppia* rises sharply between 28 and 18 cm, peaking at 10.8% before returning to background levels. *Olea* shows a clear increase from 20 cm, stabilizing at ~6.4% toward the top. Indeterminate Cupressoideae also display an upward trend in the uppermost layers, with distinct peaks at 28, 17, and 4 cm depth. Apart from these changes, the composition above 95 cm remains similar to that established during the *Pinus* expansion phase (Figs. 6, 7, 9).

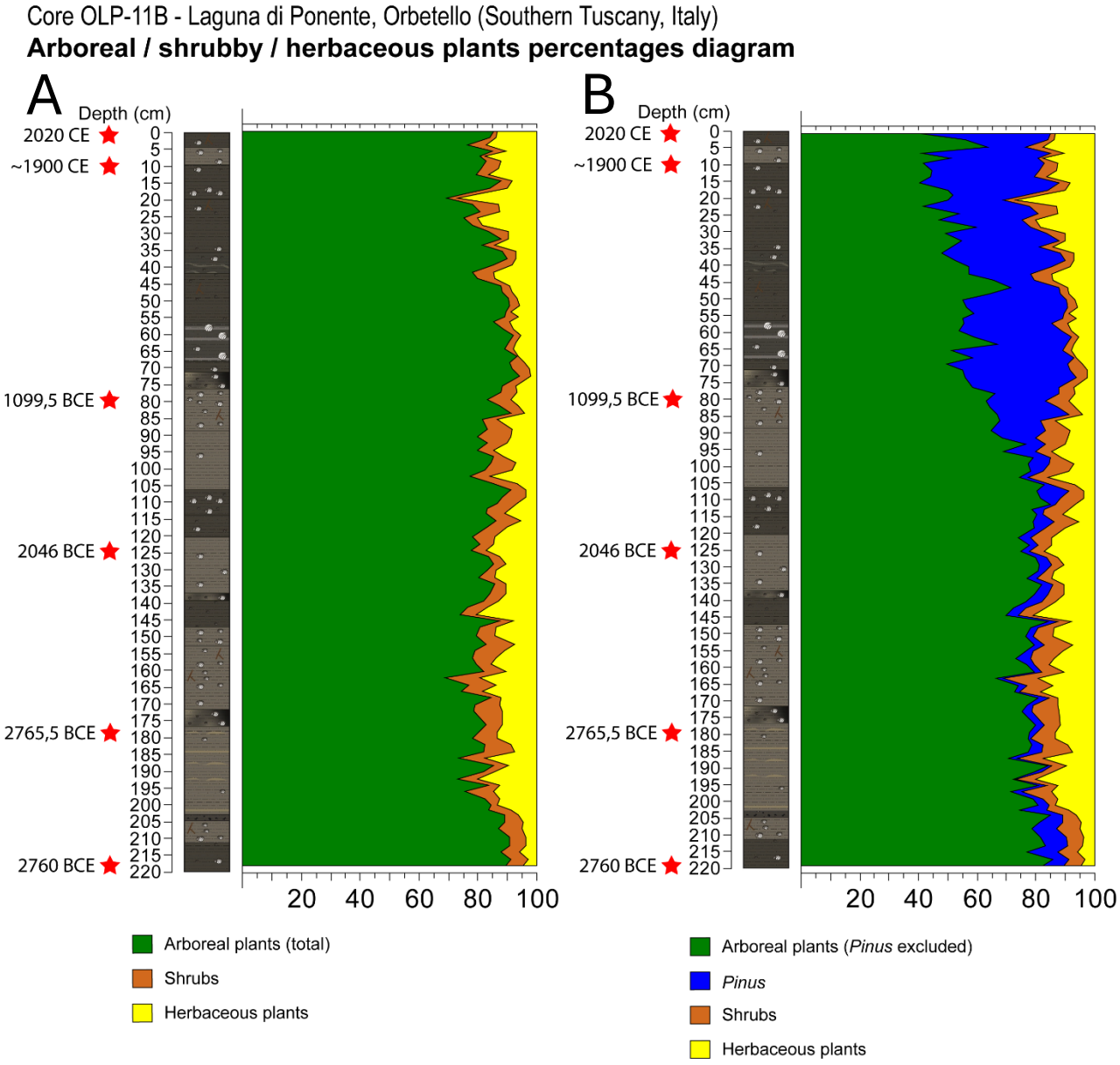

Fig. 8: Summary pollen diagram of arboreal / shrubby / herbaceous percentages of the core OLP-11B, cumulative (A), and with the detail of the percentage of *Pinus* in blue (B). Calibrated terrestrial dates are reported.

Core OLP-11B - Laguna di Ponente, Orbetello (Southern Tuscany, Italy)

Ecological groups diagram

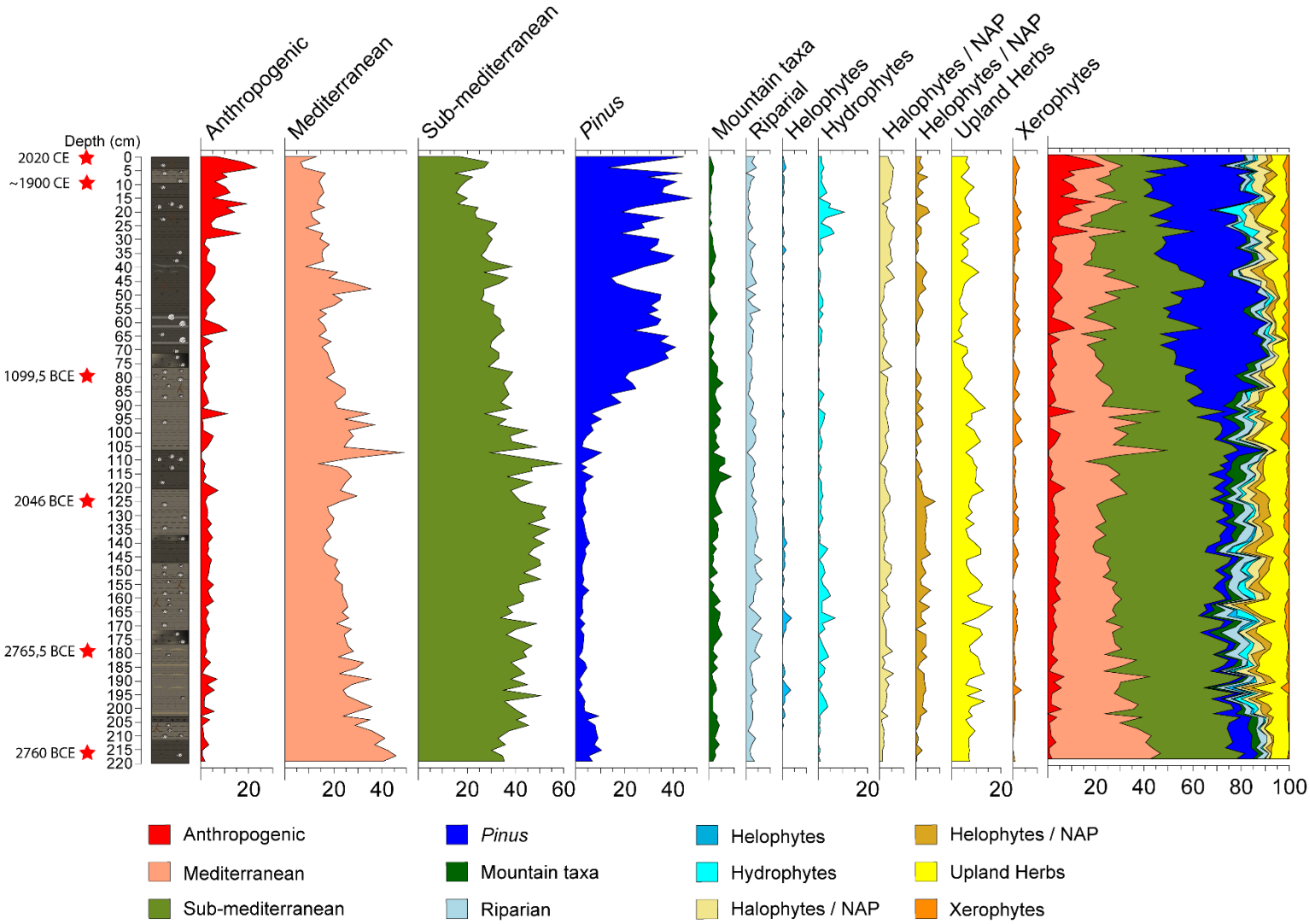

Fig. 9: Informal palynological groups percentages of the core OLP-11B. Calibrated terrestrial dates are reported.

3.4. Pollen zones description (Figs. 10, 11)

Based on the pollen analysis and the zonation produced by CONISS, the pollen record is divided into two main zones, ORB-1 and ORB-2, distinguished primarily by the abundance of *Pinus*: low in ORB-1 and markedly higher in ORB-2 (Figs. 10, 11). Within each main zone, subzones were identified based on more subtle compositional changes.

1. Subzone ORB-1a (219 cm to 201 cm) is dominated by *Quercus ilex-coccifera* type, showing a gradual decrease through the interval, and by slightly lower but increasing values of *Quercus pubescens* type. Other taxa include *Pinus*, Ericaceae, and Carpinus orientalis, each below 8% (*Pinus* averaging ~7.5%). All remaining taxa occur at very low percentages without notable changes.
2. Subzone ORB-1b (201 cm to 153 cm) retains *Q. ilex-coccifera* type and *Q. pubescens* type as the most represented taxa, but here *Q. pubescens* becomes dominant. Ericaceae remain the most common among minor taxa, followed by *Alnus*, which increases compared to the previous phase, and *C. orientalis*. At the onset of this subzone, *Pinus* declines sharply to low values (mean ~3%).
3. Subzone ORB-1c (153 cm to 123 cm) is marked by significant shifts in the three principal taxa. *Pinus* rises from low to dominant values; *Q. pubescens* type fluctuates but trends downward; *Q. ilex-coccifera* type increases slightly but remains variable. Ericaceae maintain non-negligible values, while *C. orientalis* and *Alnus* remain at low levels, with *Alnus* slightly decreasing. This subzone also records the highest representation of *Fagus*, although still in low abundance.
4. Subzone ORB-2a (123 cm to 92 cm) begins with consistently higher percentages of *Pinus* than in ORB-1c. *Q. ilex-coccifera* and *Q. pubescens* types remain substantial but slowly decline. Peaks of indeterminate Cupressaceae become increasingly frequent and pronounced toward the top of the subzone. Ericaceae decrease slightly, and Amaranthaceae show a modest increase toward the end, a trend that persists to the top of the core.
5. Subzone ORB-2b (92 cm to the top) maintains the general composition of ORB-2a but with further reductions in *Q. ilex-coccifera* and especially *Q. pubescens* types, while *Pinus* attains even higher average values. Anthropogenic indicators increase slightly, driven by a marked rise in *Olea* (from ~1.5% to ~6.4% on average) and by several peaks in indeterminate Cupressaceae. *C. orientalis* shows a slight increase, whereas *Q. cerris*, already rare, almost disappears. Ericaceae remain stable at slightly

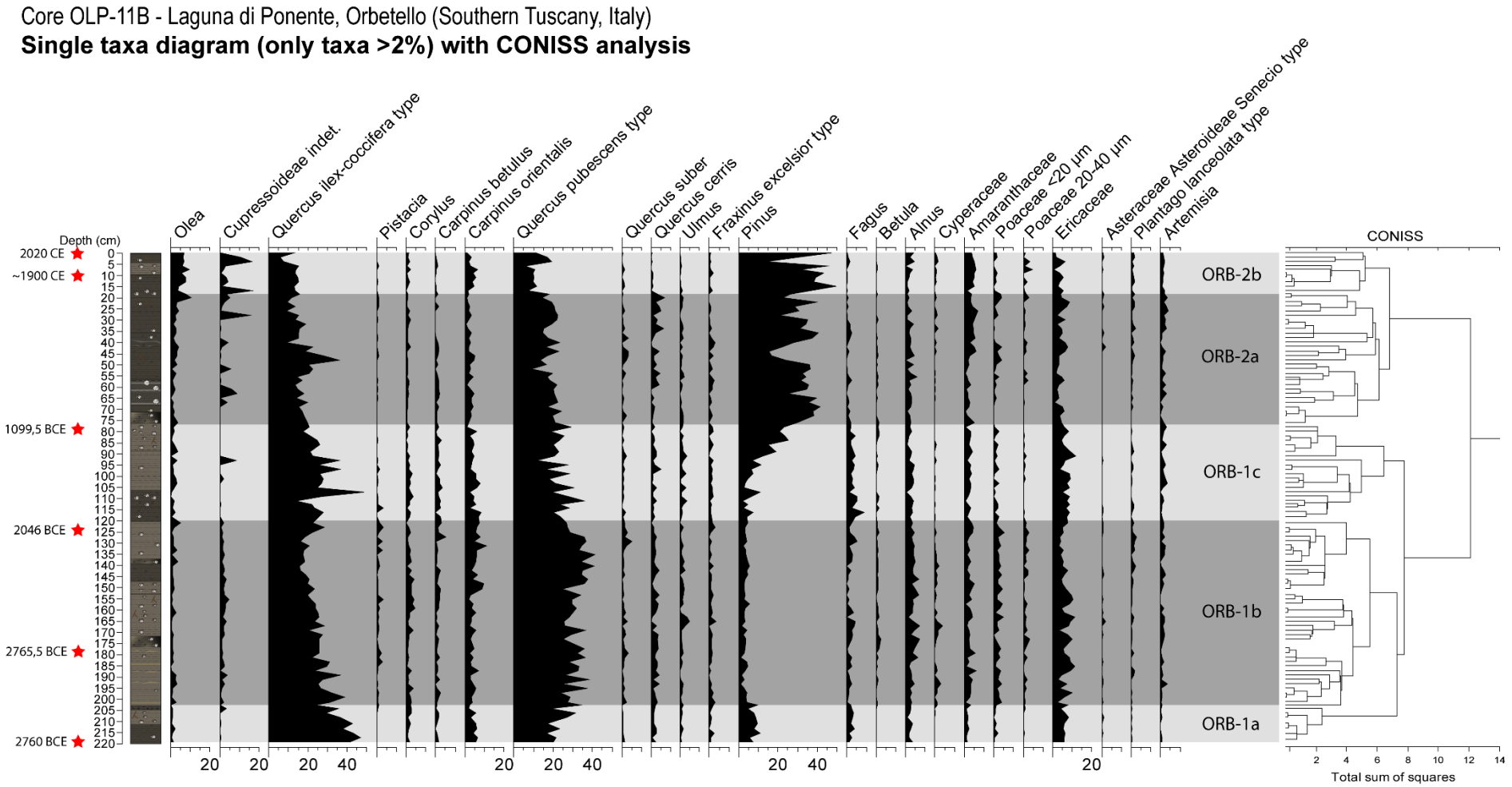

Fig. 10: Single taxa diagram with CONISS analysis and subdivisions of the zones. Only taxa reaching 2% in at least one sample were considered in the analysis. Calibrated terrestrial dates are reported.

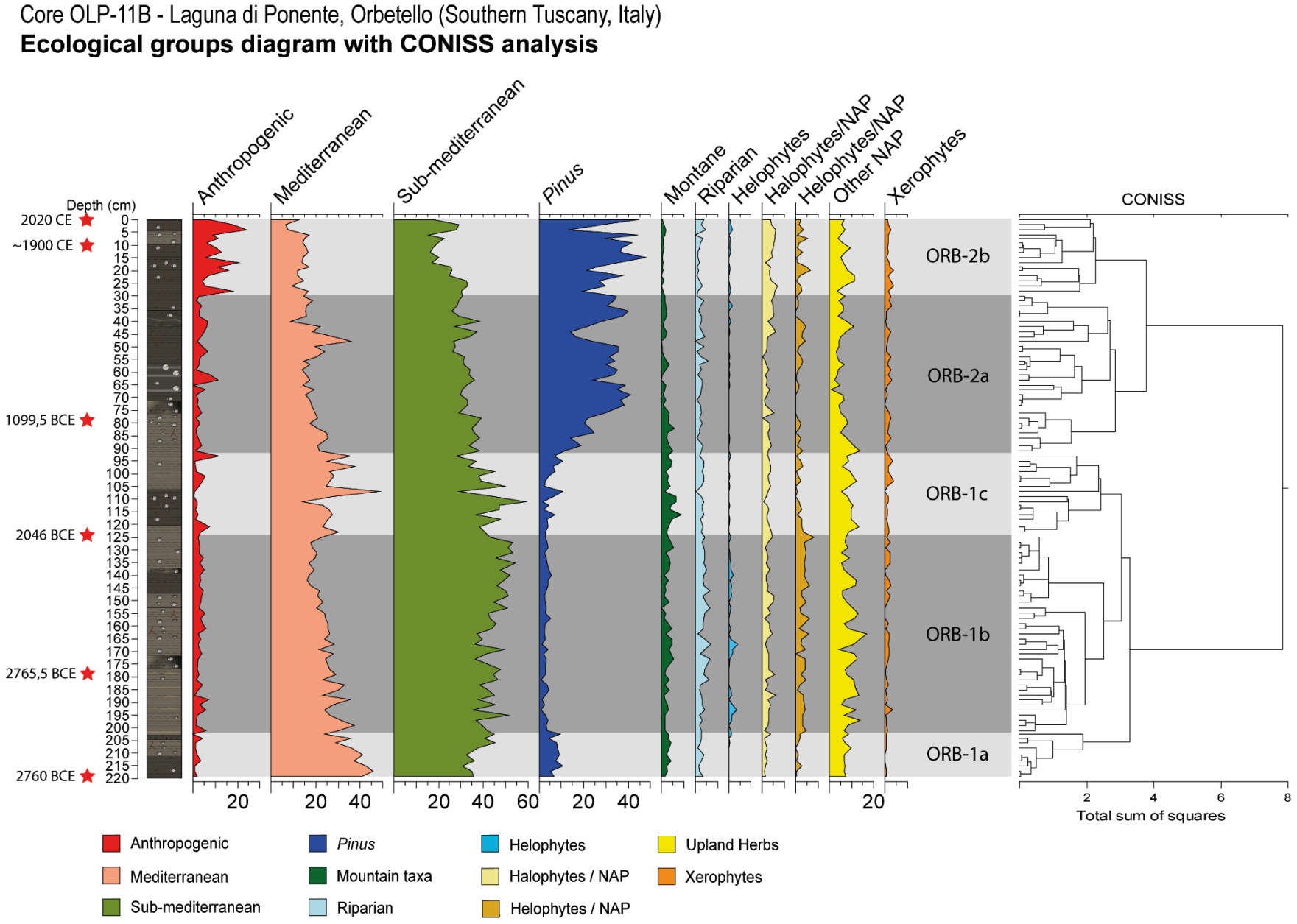

Fig. 11: Informal palynological groups diagram with CONISS analysis and subdivisions of the zones. Hydrophytes have not been considered in the analysis and thus are not represented in the graph. Calibrated terrestrial dates are reported.

lower levels than in ORB-1, and Amaranthaceae maintain the modest increase observed in the preceding subzone.

3.5. NPP (Figs. 12, 13)

NPPs are generally less abundant than pollen in the core, apart from three intervals – around 179 cm depth, between 150 and 107 cm, and between 54 and 38 cm – where NPPs percentages are more substantial and comparable to those of pollen (Fig. 13).

From the base up to a depth of approximately 202 cm depth, the NPP assemblage is dominated by *Botryococcus*, which accounts for an average of 50% of all NPPs. Dinocysts are present in significant percentages from the base to 193 cm (max 15% at 215 cm and 197 cm), with *Spiniferites* sp. as the dominant genus. Pteridophyte spores, particularly monolete types, are abundant throughout the section, averaging 19% and peaking at 50% at 213 cm. Fungal spores are absent in this basal phase (Fig. 12).

Between 202 and 123 cm, the assemblage undergoes a marked shift, with indeterminate fungal spores becoming the dominant NPP group. These exhibit considerable variability, with an average of 58% and values exceeding 90% around 146 and 180 cm. The highest value, 96.5%, is recorded at 129 cm. Other significant peaks of fungal spores with different morphologies are observed at 118-120 cm (indet. type 5, up to 35%) and at 118-111 cm (NPP morphotype 2, up to 69%). In this interval, *Botryococcus* becomes scarce, while indeterminate algae (Morphotype 1) occur sporadically, with minor peaks at 153, 135, and 114 cm. Foraminiferal linings show two distinct peaks at 173 cm (72%) and 169 cm (44%). Monolete spores also show a slight increase in this interval, with a local maximum of 34.5% at 155-173 cm depth (Fig. 12).

From 123 to 89 cm, coinciding with the decline of fungal spores, *Botryococcus* re-emerges with strongly fluctuating values and several local maxima, reaching up to 95% at 109 cm. Indeterminate algae continue to fluctuate, while dinocysts are relatively abundant between 103 and 78 cm, with a peak of 37.5% at 84 cm. Foraminiferal linings are generally less represented, except for a notable peak of 41% at 97 cm. *Pseudoschizaea*, generally rare throughout the core, shows an isolated and remarkable maximum of 75% at 89 cm (Fig. 12).

Between 89 and 63 cm, *Botryococcus* becomes highly variable and is entirely absent in several samples. This interval is characterized by notable percentages of indeterminate algae, peaking at 73%-89% at 86, 80, 73, and 67 cm, by frequent peaks in foraminiferal

linings (59%-67% at 71, 65, and 57 cm), and by a high occurrence of monolete spores (44.5% at 69 cm) (Fig. 12).

From 63 to 22 cm, *Botryococcus* rapidly increases and becomes overwhelmingly dominant, especially between 54 and 36 cm, where it averages 92%. This dominance extends, though slightly reduced, up to 22 cm. Other NPPs are minor components in this interval (Fig. 12).

In the uppermost section, from 22 cm to the top, *Botryococcus* declines significantly, except for isolated peaks at 17 cm and 2 cm. Marine influence is suggested by a brief increase in *Spiniferites* between 13 and 4 cm, reaching a maximum of 19% at 11 cm. Finally, indeterminate algae increase markedly, with an average of 38% and peaks of 68% at 20 cm and 66% at the top. Monolete spores are also abundant, averaging 32% (Fig. 12).

Core OLP-11B - Laguna di Ponente, Orbetello (Southern Tuscany, Italy)

Single taxa diagram (NPP) (exaggeration 8x)

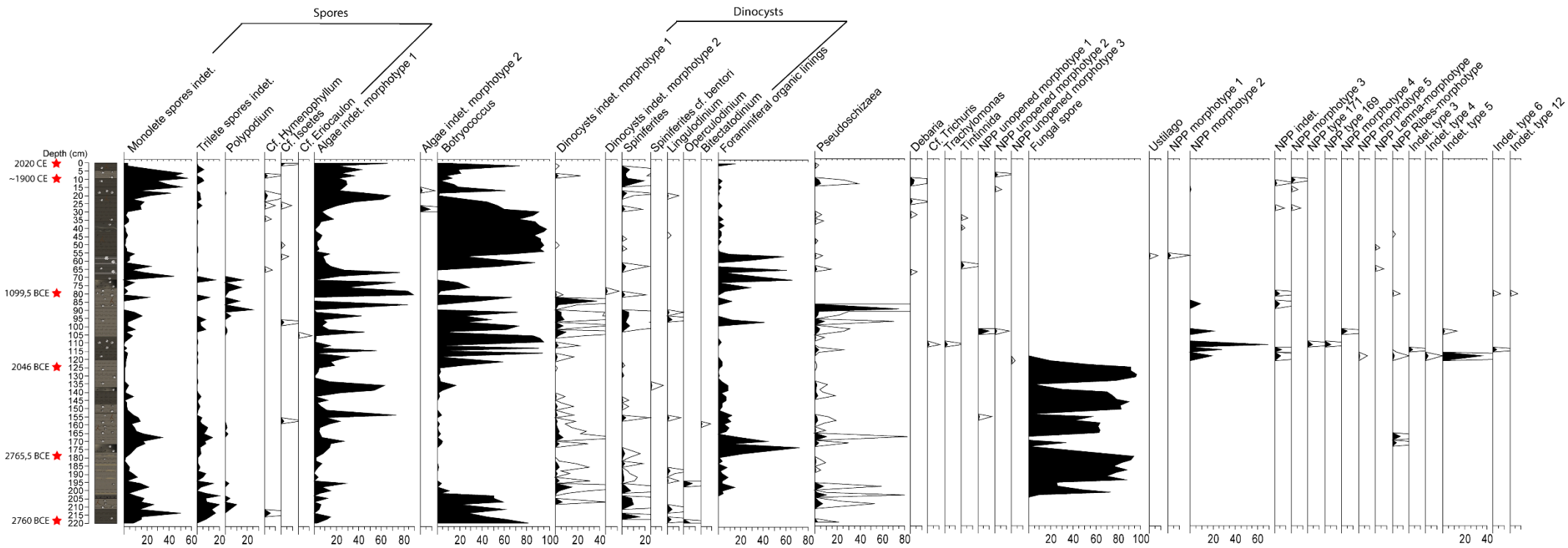

Fig. 12: Detailed palynological diagram of the core OLP-11B (exaggeration 8x), showing NPP taxa. Calibrated terrestrial dates are reported.

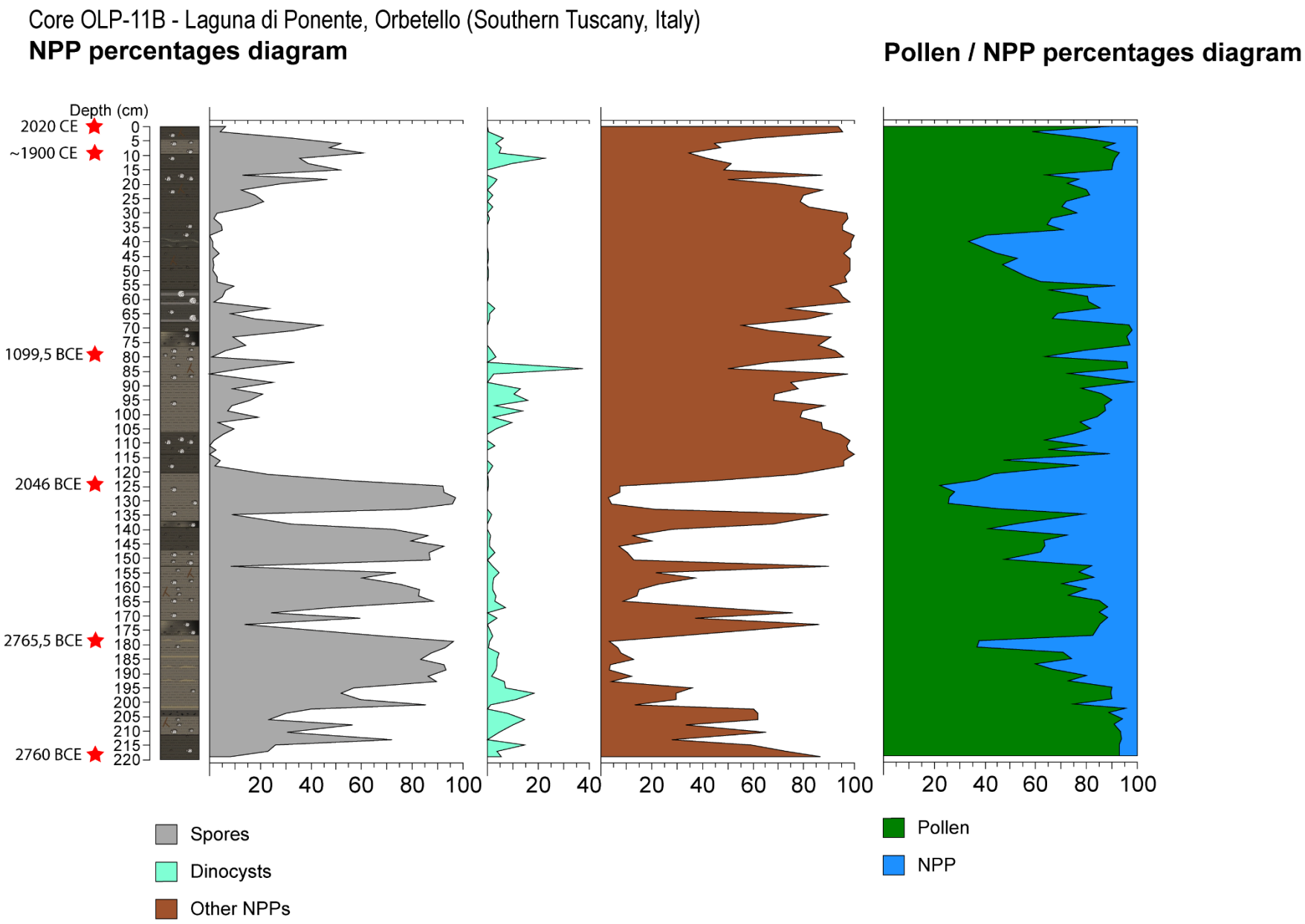

Fig. 13: Percentages of the different types of NPPs on the total NPPs (left); percentages of pollen and NPPs on the total palynomorphs (right) of the core OLP-11B. Calibrated terrestrial dates are reported.

4. Surface samples

4.1. Results of laser granulometric analysis (Figs. 14–16)

The granulometric composition of the fifteen surface samples taken from the Orbetello Lagoon was analysed (see Chapter 2, paragraph 2.6 for methodological details). Each sample was analysed three times, and the average result is shown in the following graphs (Figs. 14, 15). The samples were labelled using the code PS-POL-ORB 01 through PS-POL-ORB 15. For brevity, in this and the following paragraphs the prefix PS-POL-ORB is omitted, and only the numerical identifiers are used.

The samples exhibit highly variable grain-size compositions. In particular, the only predominantly clayey sample collected from the lagoon is 03. Samples 01 and 02 also show finer-than-average grain sizes, although with a slightly higher proportion of silt compared to clay. Samples 06 and 14, on the other hand, are clearly dominated by the silt fraction, with a noteworthy presence of clay (Fig. 16). Samples 01 and 02 exhibit a bimodal grain-size distribution, while 03, 06, and 14 display a unimodal or predominantly unimodal distribution (Figs. 14, 15).

Samples 04, 05, 10, 13, and 15 consist of sediment comprising various grain-size classes, among which the silt fraction is consistently dominant. The clay component is generally minor, with the exception of sample 04. In these samples, fine sand is present but relatively marginal, except in 05, where it is more prominent. Samples 04 and 05 also contain a notable proportion of coarse sand (> 2 mm) alongside the fine sand fraction (Fig. 16). Samples 04, 05, and 15 exhibit a bimodal distribution, with distinct peaks separating the silt/clay fraction from the sand fraction. Sample 13, by contrast, shows a unimodal distribution, with a more homogeneous grain-size profile and a peak located at the boundary between the silt and fine sand classes (approximately 60 μm). Sample 10 displays a less distinct bimodal distribution, with a fairly homogeneous profile marked by two minor peaks around 28 μm (silt) and 191 μm (fine sand) (Figs. 14, 15).

Finally, samples 07, 08, 09, 11, and 12 are predominantly composed of fine sand. Among these, sample 08 is composed almost entirely of fine sand, to the extent that palynological analysis could not be performed (Fig. 16). The grain-size distribution of all these samples is unimodal, with a peak falling within the fine sand class (Figs. 14, 15).

In general, samples with predominantly fine grain sizes (and a significant clay component) were collected from the northern sector of the Laguna di Ponente. In contrast,

the coarser samples were retrieved from the central sector of the Laguna di Levante and near the peninsula where the town of Orbetello is located, where a higher concentration of sand is evident (except for sample 15).

Samples collected from the westernmost corner of the Laguna di Ponente, near the sea connection via the Nassa channel, display highly variable grain sizes: 04 and 05 are markedly coarser, whereas 06 is finer (Fig. 16). The samples located near the inflow of the Canale di Fibbia (sample 03) and the Canale di Ansedonia (sample 14) do not appear to be significantly affected by this proximity, exhibiting a generally fine-grained texture (particularly sample 03, which shows the highest clay content overall) (Fig. 16).

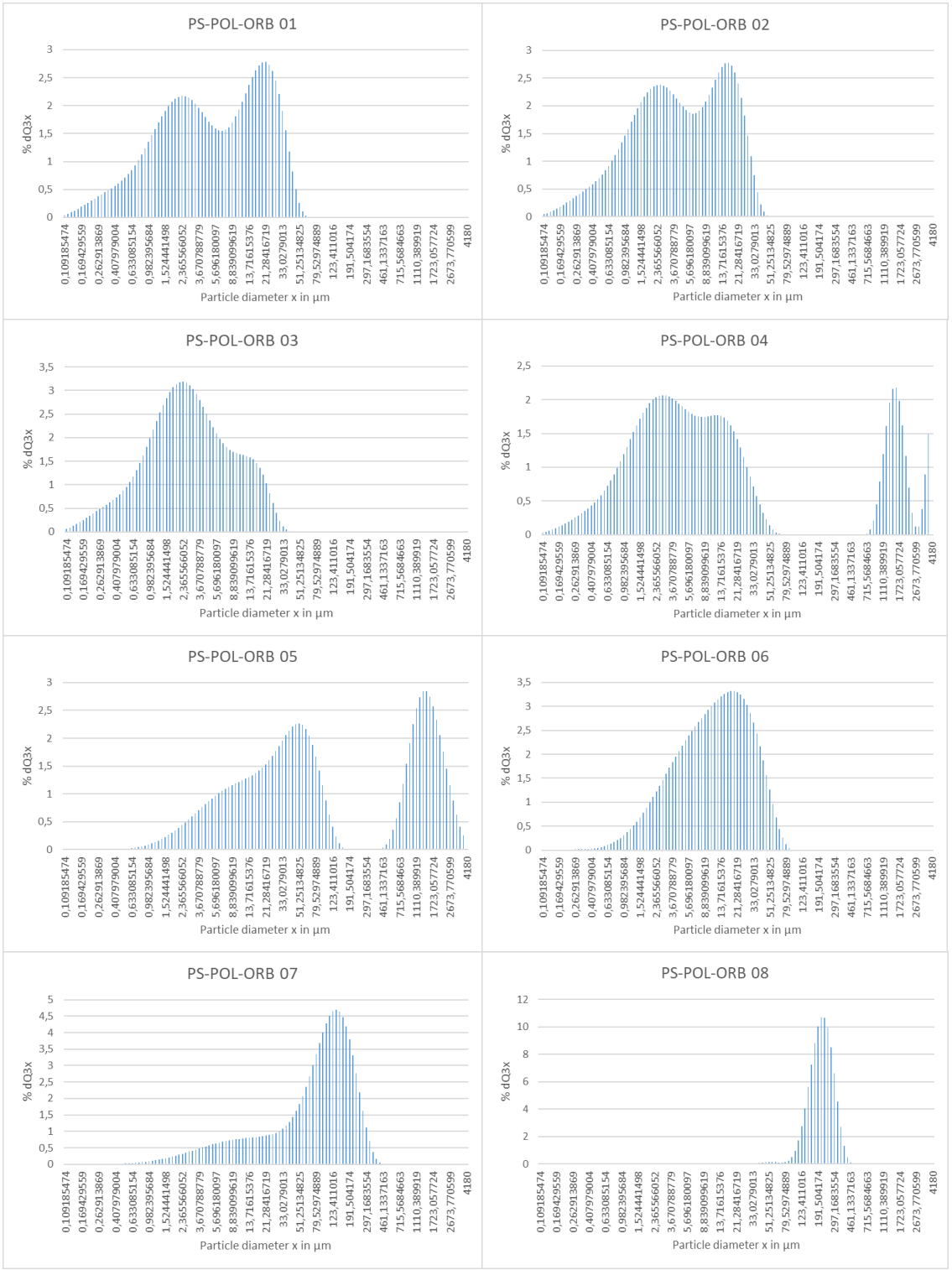

Fig. 14: Grain size profile of the surface sediments collected in the Orbetello site. Y- axis indicates the percentage of particles per grain size class; X-axis (in logarithmic scale) indicates the diameter of the particles in microns.

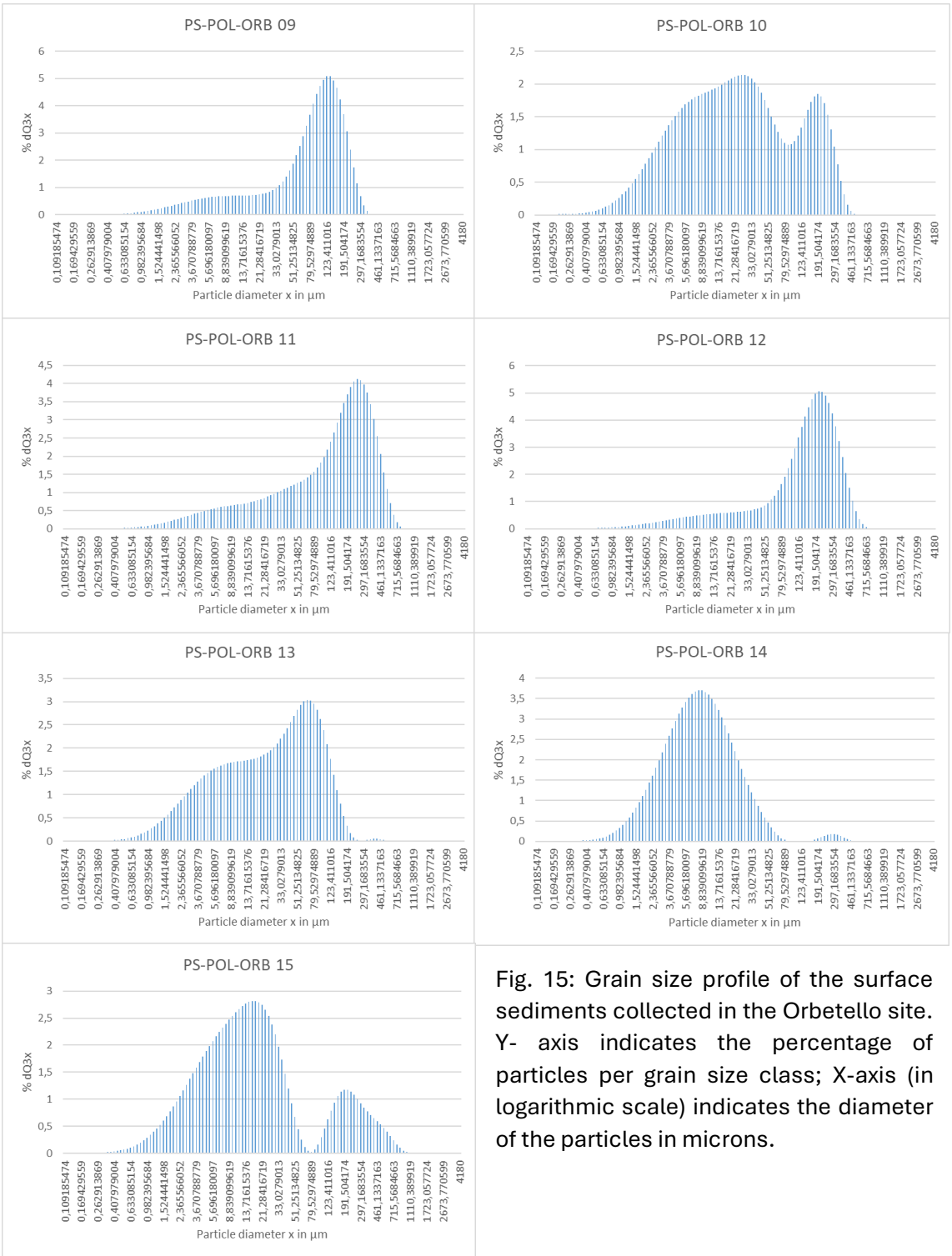

Fig. 15: Grain size profile of the surface sediments collected in the Orbetello site. Y- axis indicates the percentage of particles per grain size class; X-axis (in logarithmic scale) indicates the diameter of the particles in microns.

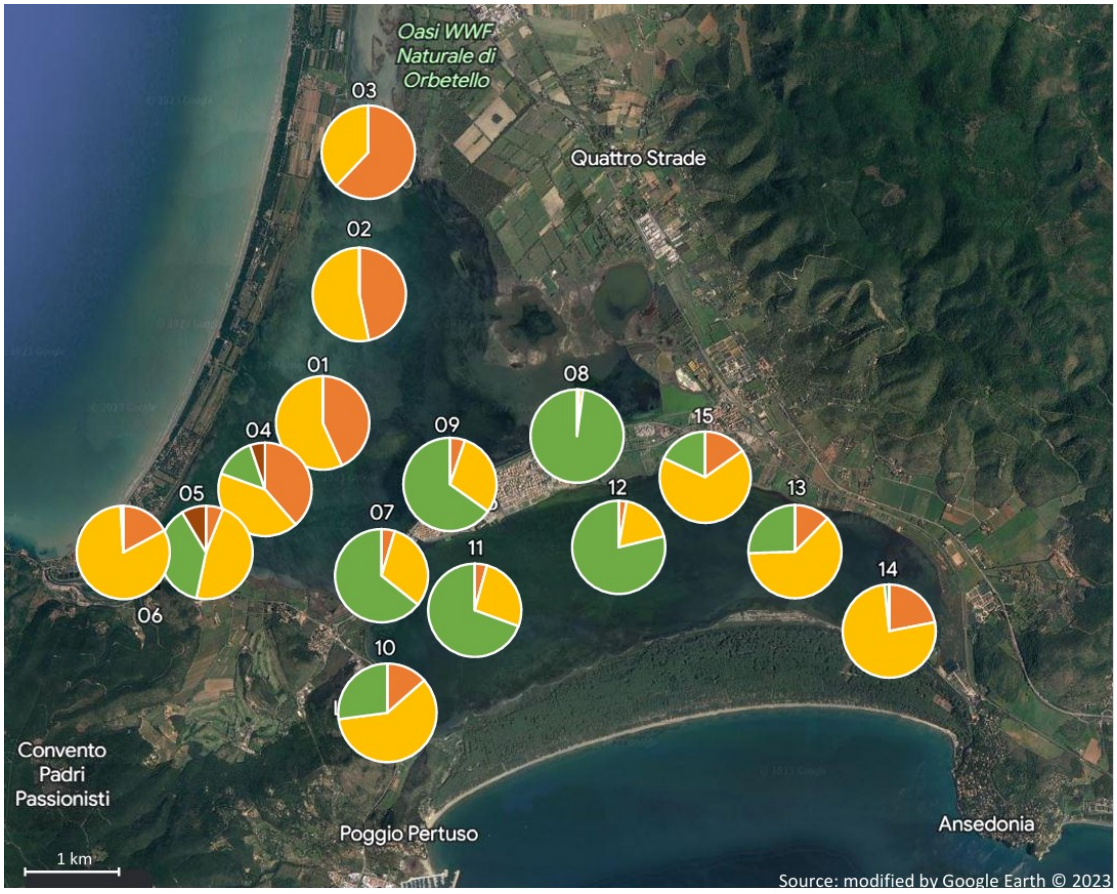

Fig. 16: Pie charts showing grain size profile of the surface sediments of Orbetello site. Legend: orange: clay (particle size < 4.0 μm); yellow: silt (particle size between 4.0 μm and 62.5 μm); green: fine sand (particle size between 62.5 μm and 2000 μm); brown: coarse sand (particle size > 2000 μm).

4.2. Palynological analysis of surface samples (Figs. 17, 18)

A total of 15 surface samples (Chapter 2, Fig. 4, Tab. 1), collected in both the western (Laguna di Ponente) and eastern (Laguna di Levante) parts of the lagoon, were analysed. Table 1 in Chapter 2 presents the list of collected surface samples, and Fig. 4 in the same chapter shows their location. Fourteen of the 15 samples collected and prepared were analysed under the optical microscope. One sample (08) was not suitable for the observation due to its predominantly sandy lithology, as confirmed by the granulometric analysis (see paragraph 4.1 and figs. 14–16).

The analysis of surface samples collected from both the Levante and Ponente basins of the Orbetello Lagoon reveals relatively uniform results throughout the lagoon (Figs. 17, 18). Anthropogenic taxa account for an average of 10.42% of the total and do not exhibit marked variation between samples (minimum 8.09% in sample 09; maximum 13.53% in

sample 15). Among them, *Olea* is the dominant element (it alone represents on average 7.89% of the total pollen and reaches about 11% in samples and 15), followed by indeterminate Cupressoideae (2.13% on average). The occurrence of other cultivated species and tree plantations is also documented, such as *Vitis*, *Juglans*, *Castanea*, *Eucalyptus* and cereals (Figs. 17, 18).

Sub-Mediterranean taxa (20.03% on average; minimum 14.19% in sample 01; maximum 25.49% in sample 07) and the Mediterranean taxa (17.71% on average; minimum 13.75% in sample 14; maximum 26.52% in sample 13) are the most represented groups after pine. Among the former, *Quercus pubescens* type is the prevalent one (11,53% of the total pollen on average), followed by *Carpinus orientalis* (2.76% on average). *Quercus suber*, *Q. cerris*, *Fraxinus* and *Corylus* are also abundant. Among the latter, *Quercus ilex-coccifera* type predominates (14,47% of the total pollen on average), but *Pistacia* and *Juniperus*, and to a lesser extent *Phillyrea*, also record a significant presence (Figs. 17, 18).

Pinus is the dominant genus as well as the leading ecological group in all analysed samples, with an average percentage of 32.70% (minimum 22.46% in sample 06; maximum values around 43% in both samples 01 and 14). Only in a few samples *Pinus* percentages, while still dominant, approximate those of Mediterranean elements (e.g., samples 05 and 13), Sub-Mediterranean elements (e.g., 04 and 09), or both these groups (06) (Figs. 17, 18).

The montane group is very poorly represented (0,60% on average, maximum 1.38% in sample 14), with *Fagus* and *Betula* being the most represented taxa, though *Abies* is also present. The riparian group, predominantly composed of *Alnus* and *Salix*, is similarly low in abundance, accounting for only 2.02% of the total (minimum 0.85% in sample 06; maximum 3.85% in sample 12) (Figs. 17, 18).

The herbaceous groups cumulatively represent 16.52% of the total. Helophytes are notably underrepresented (0.05%), although both Cyperaceae and *Typha latifolia* are present. This group is recorded exclusively in the samples 01, 05, and 13. Among the hydrophytes (1.80% on average; minimum 0.00% in sample 04; maximum 3.88% in sample 09), *Ruppia* is the most dominant taxon (1.22%), followed by *Sparganium* and *Lemna* (Figs. 17, 18).

In the halophyte/NAP category (6.16% on average; minimum 2.70% in sample 07; maximum 11.51% in sample 03), Amaranthaceae (6.09%) dominate over Caryophyllaceae, while helophytes/NAP account for 2.13% on average (minimum 0.32%

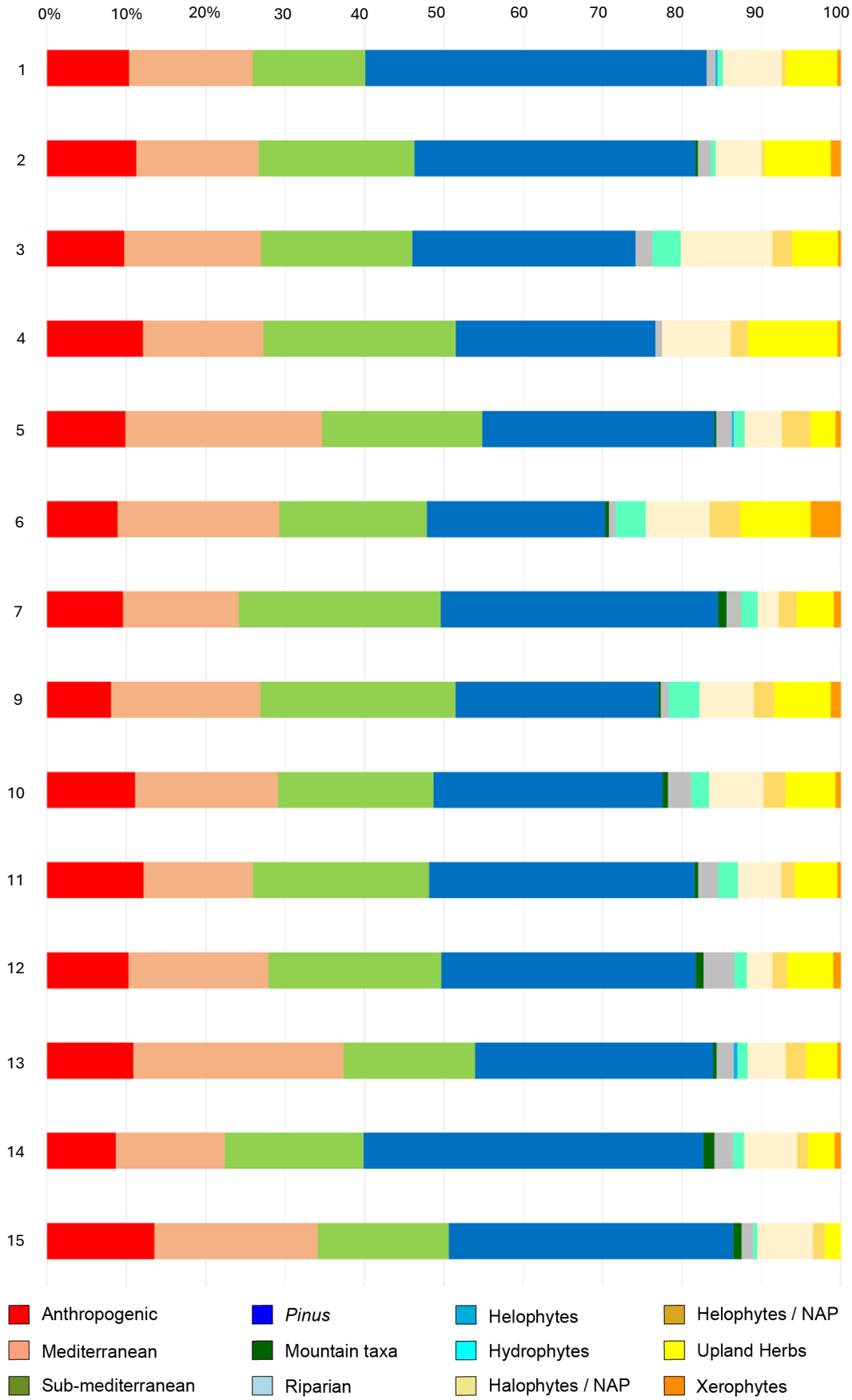

Fig. 17: Percentages of pollen content of surface samples from the Burano site, subdivided by ecological group. Y-axis labels: 1 = PS-POL-ORB 01; 2 = PS-POL-ORB 02; 3 = PS-POL-ORB 03; 4 = PS-POL-ORB 04; 5 = PS-POL-ORB 05; 6 = PS-POL-ORB 06; 7 = PS-POL-ORB 07; 9 = PS-POL-ORB 09; 10 = PS-POL-ORB 10; 11 = PS-POL-ORB 11; 12 = PS-POL-ORB 12; 13 = PS-POL-ORB 13; 14 = PS-POL-ORB 14; 15 = PS-POL-ORB 15.

in sample 02; maximum 3.81% in sample 06). Upland herbs (5.56% on average; minimum 2.01% in sample 15; maximum 11.26% in sample 04) are primarily composed of Ericaceae (2.24% on average), with smaller contributions from *Plantago lanceolata* type, Brassicaceae, *Rumex*, and Asteraceae Cichorioideae (all below 1%). Lastly, among xerophytes (0.82% on average, maximum 3.81% in sample 06), *Artemisia* is the most represented taxon (0.75%), though *Ephedra fragilis* is also attested (Figs. 17, 18).

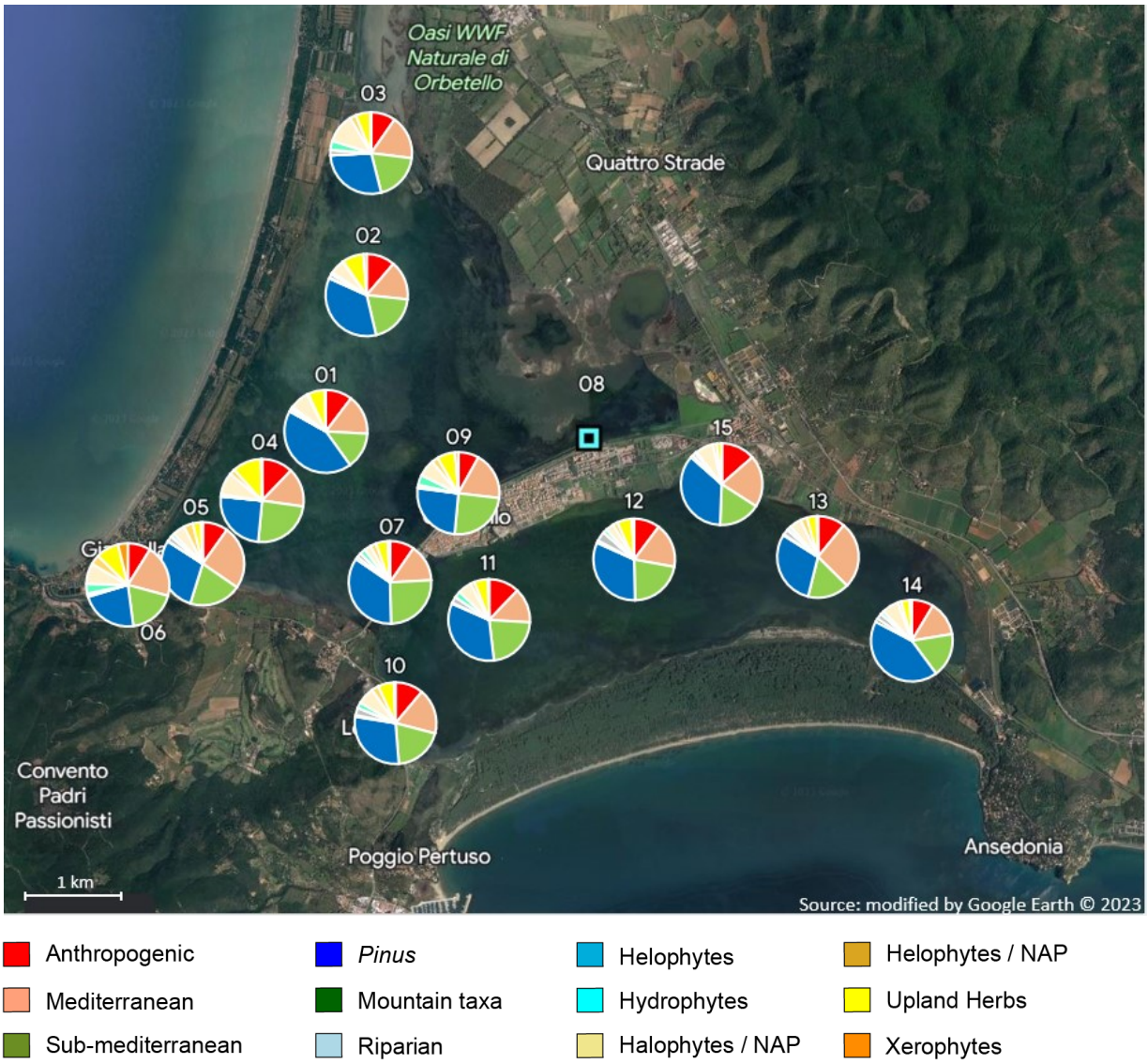

Fig. 18: Pie charts and geographical position of the surface samples extracted at the Orbetello site. Labels: 01 = PS-POL-ORB 01; 02 = PS-POL-ORB 02; 03 = PS-POL-ORB 03; 04 = PS-POL-ORB 04; 05 = PS-POL-ORB 05; 06 = PS-POL-ORB 06; 07 = PS-POL-ORB 07; 09 = PS-POL-ORB 09; 10 = PS-POL-ORB 10; 11 = PS-POL-ORB 11; 12 = PS-POL-ORB 12; 13 = PS-POL-ORB 13; 14 = PS-POL-ORB 14; 15 = PS-POL-ORB 15.

4.3. Analysis of moss samples (Figs. 19, 20)

2 moss samples (MOSS1 ORB1-23 and MOSS2 ORB1-23) from the site of Orbetello were analysed (Chapter 2, Fig. 4, Tab. 2). For brevity, the suffix ORB1-23 is omitted in the following sections.

The analysis of moss samples reveals that in both cases the dominant ecological group is *Pinus*, with an average percentage of 26.22% (27.44% in sample MOSS1 and 25.00% in MOSS2) (Figs. 19, 20). Among arboreal taxa, in addition to *Pinus*, Sub-Mediterranean elements are predominant, with significantly higher percentages in sample MOSS1 (14.42%) compared to MOSS2 (8.97%). In MOSS1, the most abundant taxon within this group is *Quercus pubescens* type (7.44%), followed by *Carpinus orientalis* (3.26%) and *Fraxinus excelsior* (1.40%), whereas in MOSS2, the percentage of *Quercus pubescens* type decreases to 2.24%, and *Carpinus orientalis* (2.88%) and *Fraxinus excelsior* (1.28%) remain relatively stable. Other taxa within this group are recorded in negligible percentages (Figs. 19, 20).

Mediterranean elements account for an average of 8.59% of the pollen (8.84% in MOSS1 and 8.33% in MOSS2), with the most represented taxa being *Quercus ilex-coccifera* type (4.55% on average), followed by *Pistacia lentiscus* (1.50%), *Myrtus* spp. (1.34%), and *Phillyrea* (1.03%). Anthropogenic elements contribute an average of 4.34%, mainly represented by *Olea* (3.46%), with occasional occurrences of *Eucalyptus* and *Juglans*. Montane elements (*Betula* and *Fagus*) are recorded only in sample MOSS2 (0.96%). The only riparian taxon identified, and at relatively low percentages, is *Alnus*, present in both samples with an average of 1.57% (Figs. 19, 20).

As expected, moss samples contain a higher proportion of herbaceous taxa compared to the lagoon samples. In particular, MOSS2 shows a greater proportion of herbaceous taxa (50.96% of total pollen) than MOSS1 (43.26%). The Halophytes/NAP group is more represented in MOSS1 (27.44%) than in MOSS2 (18.27%), and also shows a compositional difference between the two samples. In MOSS1, this group is composed almost entirely of Amaranthaceae (26.05% of the total), whereas in MOSS2, Caryophyllaceae (11.54%) dominate over Amaranthaceae (6.73%) (Figs. 19, 20).

In contrast, Helophytes/NAP account for higher percentages in MOSS2 (13.46%) than in MOSS1 (6.51%). The same pattern is observed for the Upland Herbs group, which is more abundant in MOSS2 (16.99%) compared to MOSS1 (8.84%). Among the latter, the most abundant taxon is *Plantago lanceolata* type (5.55% on average, reaching 7.37% in

MOSS2), followed by Asteraceae Cichorioideae (1.51% on average), Ericaceae (1.43%), and Brassicaceae (1.11%). Lastly, Xerophytes show negligible percentages (0.55% on average), including *Artemisia* and *Ephedra fragilis* type (Figs. 19, 20).

Helophytes (0.64%) and Hydrophytes (0.96%) are recorded at minimal levels only in sample MOSS2. In this sample, the relative abundance of the Hydrophyte taxa *Potamogeton* and, to a lesser extent, *Sagittaria* is noteworthy (Figs. 19, 20).

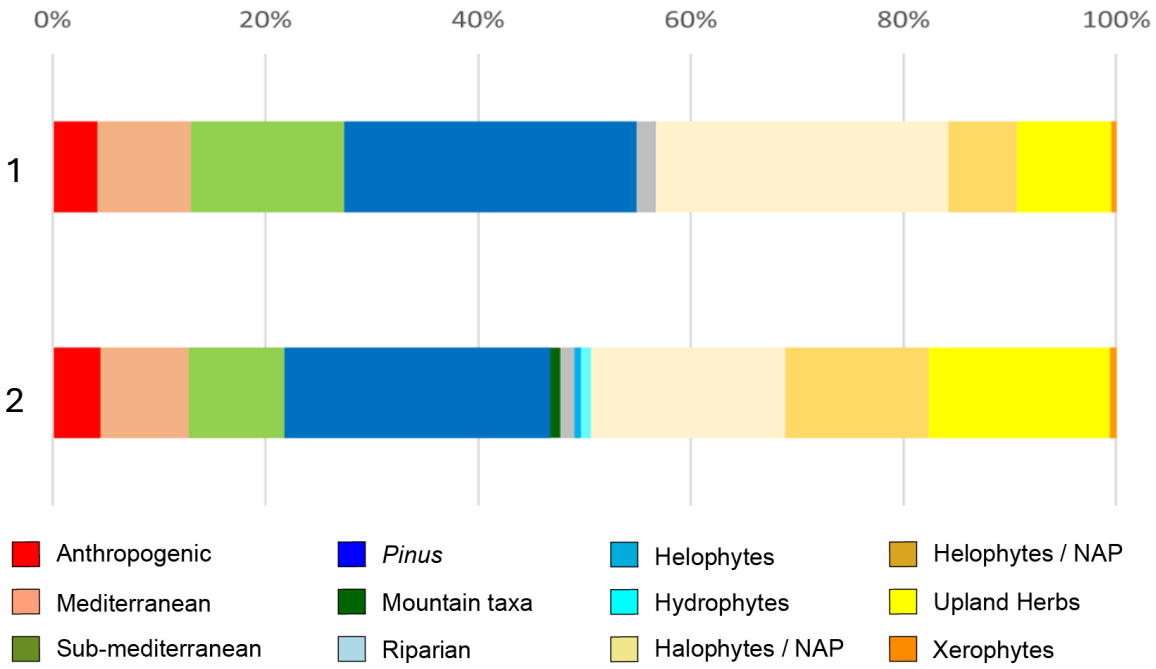

Fig. 19: Percentages of pollen content of moss samples from the Orbetello site, subdivided by informal palynological group. Y-axis labels: 1 = MOSS1 ORB1-23; 2 = MOSS2 ORB1-23.

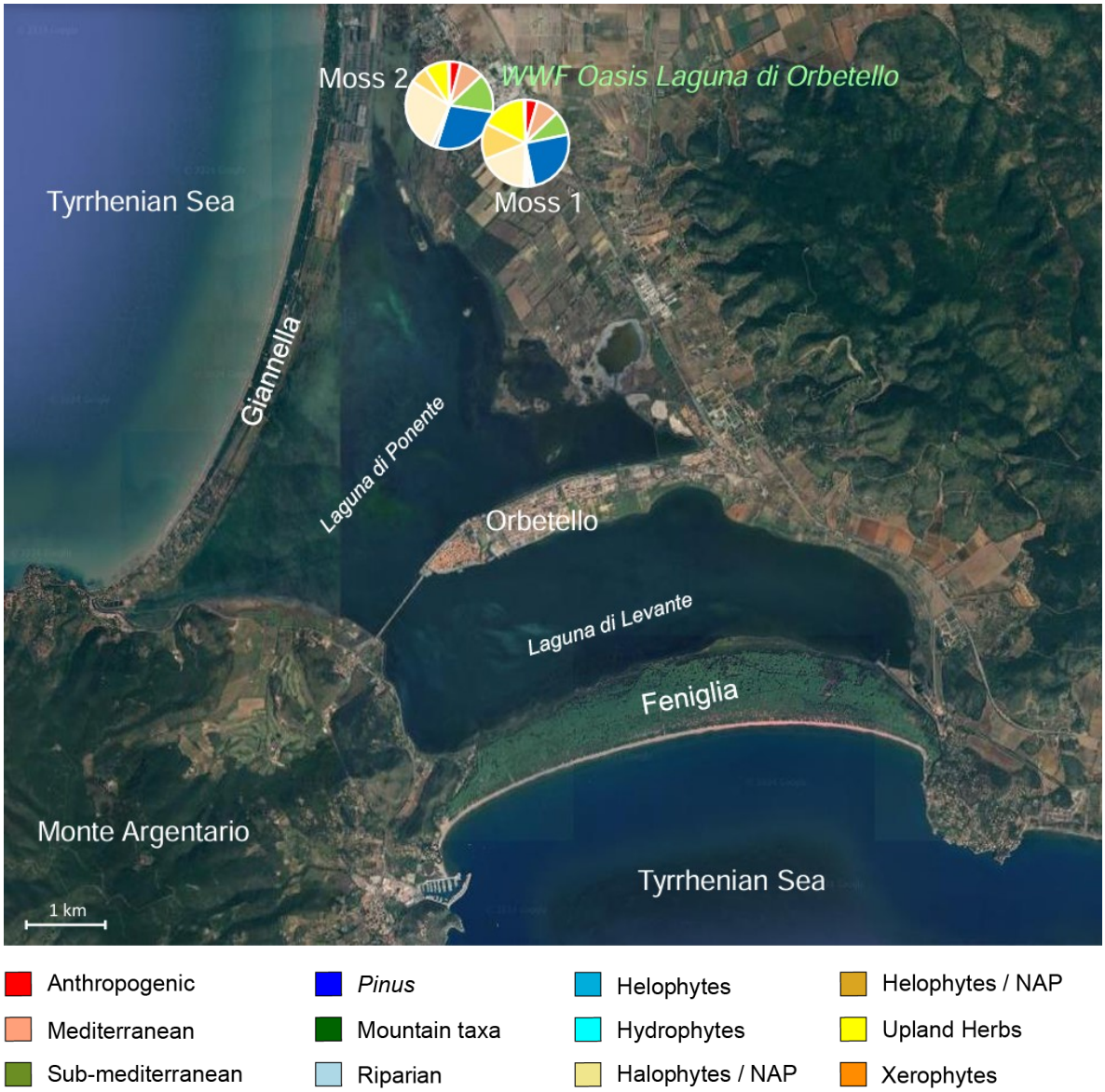

Fig. 20: Pie charts and geographical position of moss samples collected at the Orbetello site.

5. Microplastics analysis on selected samples

The microplastic content of six samples was analysed (MP-ORB-1, 7.5-18.5 cm deep; MP-ORB-2, 24-34 cm deep; MP-ORB-3, 52-63 cm deep; MP-ORB-4, 84-95 cm deep; MP-ORB-5, 129-140 cm deep; MP-ORB-6, 193-199 cm deep; see Chapter 2, Tab. 4). The fragments were divided into two size categories (small: 63-125 µm; large: 125 µm-5 mm) and classified by morphology based on visual observations with a stereomicroscope (see Chapter 2, paragraph 2.5).

The analysis detected the presence of microplastics in all six samples (Tabs. 2–4). Tab. 2 shows the total number of fragments found in all samples, Tab. 3 shows the resulting number after subtracting the morphologies recorded in the control blanks (following Turner *et al.*, 2019, as explained in Chapter 2, paragraph 2.5), and Tab. 4 shows the concentration of the fragments (total number/sample weight) after the subtraction. The following graph (Fig. 21) visually represents the concentration of plastics detected in each analysed sample, along with their corresponding depth within the core.

The uppermost sample (MP-ORB-1) recorded the highest concentration of microplastics in the entire core, with 11.77 particles per gram of sediment after contaminant subtraction. Sample MP-ORB-4 (the fourth from the bottom), collected at a depth of approximately 90 cm, also yielded a notably high concentration, with 6.67 particles per gram of sediment. In contrast, lower concentrations were recorded in samples MP-ORB-2 (2.68 particles per gram), MP-ORB-3 (1.79 particles per gram), and MP-ORB-5 (2.93 particles per gram). The deepest sample, MP-ORB-6, had the lowest concentration, at 0.68 particles per gram. This value indicates concentrations very similar to those of the control sample; however, even in this sample more than one blue fiber and more than one blue fragment were detected, even after contaminant subtraction (Tab. 4; Fig. 21).

Blue fibers were the most abundant morphotype. They were present in every sample and were particularly dominant in samples MP-ORB-1, MP-ORB-2, and MP-ORB-5, representing 77%, 73%, and 86% of the total fragments found, respectively. Other common morphotypes included transparent filaments (nylon-like), especially abundant in sample MP-ORB-1, followed by black or red fibers. Additionally, several irregular blue fragments were observed, along with a sponge-like agglomeration, a coarse yellow fabric, a blue filamentary mass, and a red fabric fiber (Fig. 21). See the Appendix III for the photos of different morphologies.

Total microplastics

Sample	MP-ORB-1		MP-ORB-2		MP-ORB-3		MP-ORB-4		MP-ORB-5		MP-ORB-6	
Depth (cm)	7,5-18,5		24-34		52-63		84-95		129-140		193-199	
Fraction	B (125 µm-5 mm)	S (63-125 µm)	B (125 µm-5 mm)	S (63-125 µm)	B (125 µm-5 mm)	S (63-125 µm)	B (125 µm-5 mm)	S (63-125 µm)	B (125 µm-5 mm)	S (63-125 µm)	B (125 µm-5 mm)	S (63-125 µm)
Blue fiber	33	28	7	14	6	10	31	17	5	25	4	6
Red fiber	3	1	1	2	2	4	8	3	2	4		1
Black fiber		7	2	5		2	7	4		3		1
Transparent wire (nylon-like)	13	8	1	10	4	2	5	13	2	3	1	
Blue fragment		2		1			2	3				2
Sponge-like agglomeration			1									
Coarse yellow fabric					1							
Blue filamentary mass						1						
Red fabric fiber							1					
Transparent fragment							1					
Dry mass (g)	6,2		8,2		9,5		10,8		9,9		10,3	
Total (n)	95		44		32		95		44		15	
Microplastics concentration (n/g)	15,32		5,37		3,37		8,80		4,44		1,46	

Tab. 2: Total number of microplastic fragments found in the OLP-11B core samples.

Total microplastics minus blank

Sample	MP-ORB-1	MP-ORB-2	MP-ORB-3	MP-ORB-4	MP-ORB-5	MP-ORB-6
Depth (cm)	7,5-18,5	24-34	52-63	84-95	129-140	193-199
Fraction	all	all	all	all	all	all
Blue fiber	56	16	11	43	25	5
Red fiber	2	1	4	9	4	0
Black fiber	2	2	0	6	0	0
Transparent wire (nylon-like)	11	1	0	8	0	0
Blue fragment	2	1		5		2
Sponge-like agglomeration		1				
Coarse yellow fabric			1			
Blue filamentary mass			1			
Red fabric fiber				1		
Transparent fragment				0		
Total (n) minus blank	73	22	17	72	29	7

Tab. 3: Number of microplastic fragments after subtracting the contaminant according to the method in Turner *et al.*, 2019.

Total microplastics minus blank concentration

Sample	MP-ORB-1	MP-ORB-2	MP-ORB-3	MP-ORB-4	MP-ORB-5	MP-ORB-6
Depth (cm)	7,5-18,5	24-34	52-63	84-95	129-140	193-199
Fraction	all	all	all	all	all	all
Blue fiber	9,03	1,95	1,16	3,98	2,53	0,49
Red fiber	0,32	0,12	0,42	0,83	0,40	0,00
Black fiber	0,32	0,24	0,00	0,56	0,00	0,00
Transparent wire (nylon-like)	1,77	0,12	0,00	0,74	0,00	0,00
Blue fragment	0,32	0,12		0,46		0,19
Sponge-like agglomeration		0,12				
Coarse yellow fabric			0,11			
Blue filamentary mass			0,11			
Red fabric fiber				0,09		
Transparent fragment				0,00		
Dry mass (g)	6,2	8,2	9,5	10,8	9,9	10,3
Total (n) minus blank	73	22	17	72	29	7
Total minus blank concentration (n/g)	11,77	2,68	1,79	6,67	2,93	0,68

Tab. 4: Concentration (total number/sample weight) of fragments by type, after subtracting the contaminant. Values are in number/g.

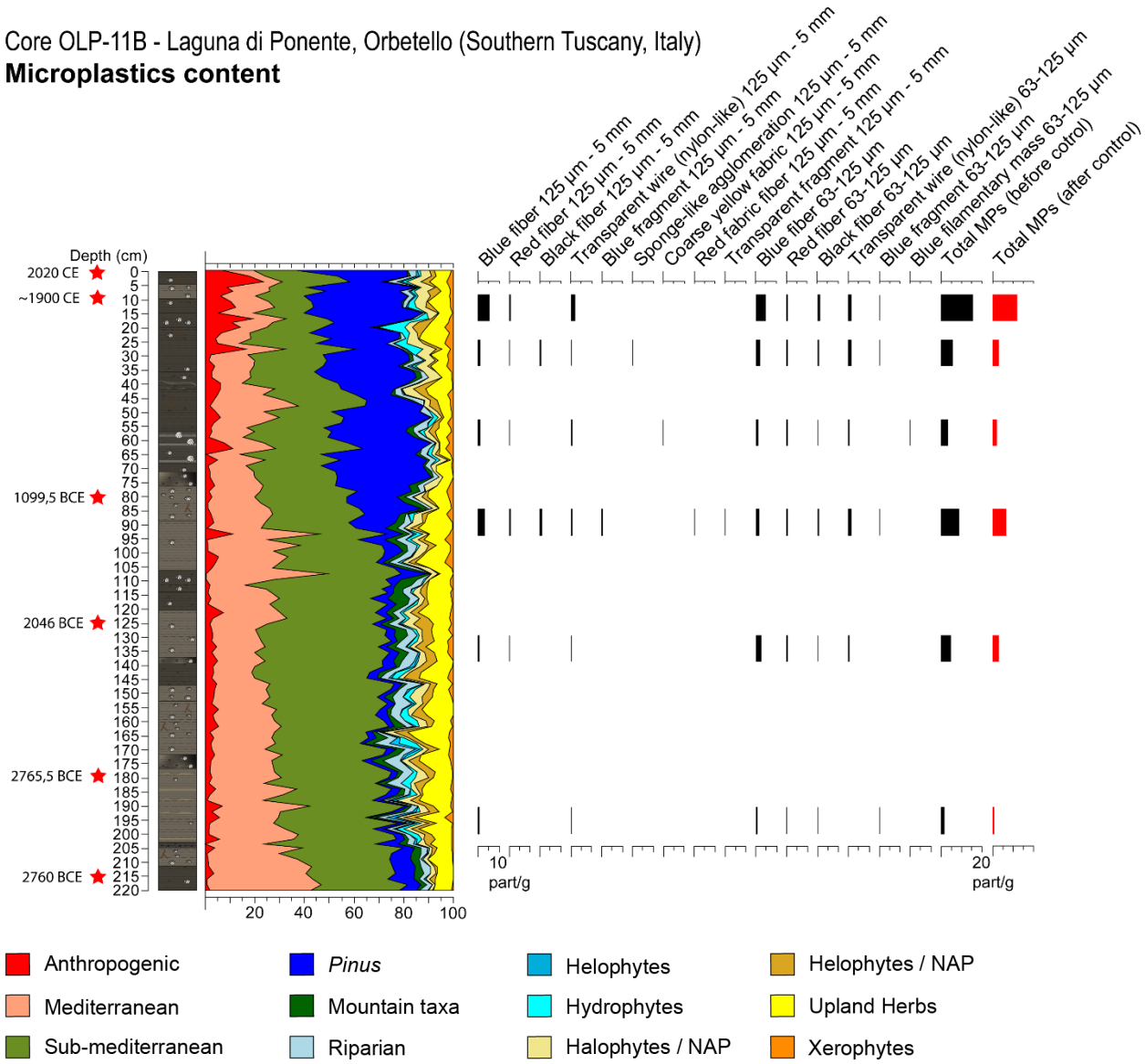

Fig. 21: Location and amount of microplastic findings along the OLP-11B core. Red bars on the right indicate the results after subtracting the contaminant according to the method in Turner *et al.*, 2019. Calibrated terrestrial dates are reported.

6. *Prospective application of Amino Acid Racemization*

Thirty selected samples from the OLP-11B core have been subjected to amino acid racemization analysis (analysis performed by the Departamento de Ingeniería Geológica y Minera, Universidad Politécnica de Madrid). This method has provided an independent estimate of sedimentation rates, which has contributed to the interpretation of the core discussed in the following section. However, only preliminary results were made available and are therefore not presented here as a dedicated dataset, thereby allowing for future work to further explore and integrate these data.

Discussion

7. Strengths and weaknesses of the study

The Orbetello Lagoon is a unique coastal system of central Tuscany, enclosed by the tombolos of Feniglia and Giannella and subdivided into two main basins (Ponente and Levante) with restricted connections to the Tyrrhenian Sea. This geomorphological setting has long conditioned hydrodynamics, sedimentation, and ecological processes, while at the same time supporting centuries of intensive exploitation through fisheries, saltworks, and land reclamation. Today the lagoon represents both a biodiversity hotspot of international value (Ramsar site, WWF Oasis) and one of the best-studied Mediterranean lagoons, where recurrent dystrophic crises and remediation strategies have turned it into a natural laboratory for lagoon management (Giusti & Marsili-Libelli, 2006; Lardicci *et al.*, 2001; Lenzi *et al.*, 2003).

The palynological study of sediment core OLP-11B and of the surface samples from the Orbetello Lagoon was designed to reconstruct vegetation dynamics, lagoonal eutrophication, and anthropogenic impacts affecting one of the most intensively managed wetlands of the Tyrrhenian coast. By combining pollen, NPPs, granulometric evidence, and microplastic records, the aim is to place the ecological history of the lagoon into a broader framework of land-use change, hydrological management, and climatic variability. Particular attention is directed to the identification of signatures of anthropogenic eutrophication and dystrophic crises, which are well documented for Orbetello in the historical and ecological literature, and to the relationship between vegetation changes and large-scale land-use transformations around the basin.

The Orbetello record offers several important strengths. First, it represents one of the few multiproxy sequences available for a Mediterranean lagoon with such a well-documented ecological and management history. The integration of biological and sedimentological indicators allows the comparison of fossil signals with independent historical and environmental records, providing a rare opportunity to evaluate how human interventions, such as reclamation works, dredging, and afforestation, are expressed in the stratigraphic archive. The high sampling density (2 cm intervals, 109 samples analysed) enhances temporal resolution and enables the detection of short-term ecological disturbances,

including dystrophic crises. Moreover, the parallel analysis of surface samples strengthens the connection between modern vegetation patterns and recent sedimentary processes, improving the interpretative framework for the fossil record. Together, these features make the Orbetello sequence a valuable reference for understanding recent lagoonal evolution along the Tyrrhenian coast.

The interpretation of these results, however, is strongly constrained by the chronological framework. Radiocarbon dating of bulk sediments yielded contrasting results depending on whether a terrestrial or marine calibration is applied, reflecting the likely presence of mixed sources of organic matter. In addition, the age obtained at 80 cm depth is poorly correlated and must be treated with caution, while deeper dates (below 125 cm) extend into the Bronze Age (~2500 BCE), raising the hypothesis of either a major hiatus or a dramatic reduction in sedimentation rate. These scenarios are difficult to reconcile with the relatively uniform pollen signal observed throughout the lower portion of the core.
Conversely, the upper part of the sequence shows a sharp rise in *Pinus*, plausibly related to the afforestation of the Feniglia dune in the early 20th century, but this interpretation conflicts with the radiocarbon chronology. The detection of microplastics at depth further complicates the picture, pointing to possible sediment reworking or post-depositional mixing. The ^{210}Pb-^{137}Cs-^{241}Am profiles add little resolution, lacking distinctive peaks and therefore not providing secure chronological anchors.
Given these uncertainties, the sequence is approached as a record potentially composed of two distinct segments: a basal portion with an apparent mid-third millennium BCE age, and an upper portion reflecting modern or sub-recent dynamics, with the possibility of hiatuses and internal mixing in both. As such, the discussion will focus on the clearest ecological signals and on the consistency between microfossil evidence and independent historical or ecological information, while explicitly acknowledging the severe limits of the chronological control.

8. *Interpretation of the chronological framework*

The chronological reconstruction of core OLP-11B is affected by multiple limitations and requires cautious interpretation. The ^{210}Pb-^{137}Cs-^{241}Am profiles (Fig. 4) do not display clear stratigraphic markers, as observed for Burano, and thus cannot independently anchor the uppermost sediments to absolute chronological horizons. Nevertheless, both ^{210}Pb and ^{137}Cs show consistent down-core declines that may still provide a tentative indication of sediment accumulation rates in the upper ~20 cm. These signals should be regarded as approximate and interpreted with caution, but they remain valuable as supporting evidence when integrated with radiocarbon results and ecological proxies. Based on the excess ^{210}Pb profile, a mean sedimentation rate of ~0.78 mm/year can be tentatively inferred for the uppermost section of the core (Fig. 4). While this estimate is affected by considerable uncertainty, it suggests relatively slow recent accumulation, broadly consistent with the restricted hydrodynamics of the lagoonal setting.

Radiocarbon dating offers a broader temporal reference but introduces its own set of uncertainties. The analysed samples consist of bulk sediment, likely of mixed continental and marine origin, which complicates calibration and prevents the choice of a single unambiguous curve. Both terrestrial and marine calibrations were therefore considered, but they diverge substantially (Tab. 1).

Among the dated levels, the sample at 80 cm depth (OLP11BB 60-62) yielded an age that is poorly correlated with the independent amino acid racemization (AAR) results (reported here qualitatively), and is therefore regarded as unreliable. By contrast, the deeper radiocarbon determinations (from 125 cm downward) show internal consistency and, importantly, are broadly coherent with the AAR-derived sedimentation trends. A full integration of AAR outcomes with radiocarbon and ^{210}Pb-derived constraints will require a dedicated dataset and may further refine sedimentation dynamics in the Orbetello record. Taken together, these data suggest very ancient basal ages, extending back to ~2500 BCE at the bottom of the core (Fig. 22). This interpretation, however, is difficult to reconcile with the remarkably stable pollen signal in the lower sequence, which shows minimal vegetation change over what would, under such a chronology, correspond to several centuries. Two hypotheses remain open: (I) the presence of a major hiatus separating the lower and upper portions of the core, or (II) an extremely reduced sedimentation rate during the late Holocene. At present, neither scenario can be resolved with certainty.

Modern indicators observed within the sequence also have important chronological implications. In particular, the detection of microplastics at nearly 2 m depth in Orbetello raises significant chronological concerns, as it suggests either downward displacement of recent particles, post-depositional mixing, or potential inconsistencies in the age-depth framework. Likewise, the persistence of pollen assemblages dominated by clearly modern anthropogenic and Mediterranean taxa within intervals that would otherwise be interpreted as older highlights the need for caution when extrapolating sedimentation rates beyond the uppermost dated section.

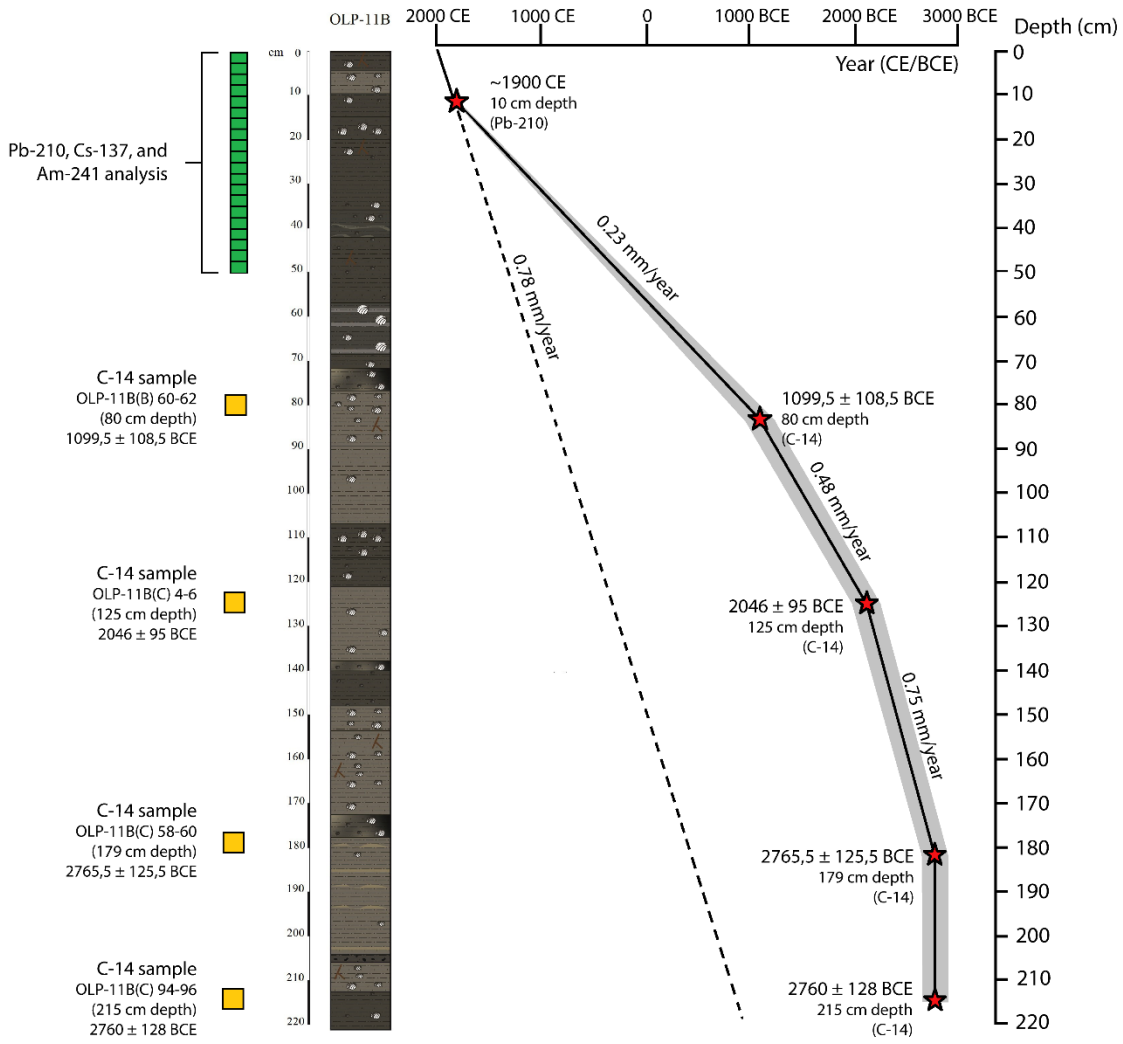

Fig. 22: Tentative graphical interpolation of the radiocarbon chronology for core OLP-11B under terrestrial calibration. Depths of all samples submitted for ^{14}C dating (yellow squares), as well as for ^{210}Pb, ^{137}Cs, and ^{241}Am analyses (green squares), are indicated on the left. For ^{14}C samples, calibrated terrestrial ages are reported.
The linear connection of calibrated ages illustrates the overall discrepancy between the lower sequence (which yields ages clustering around ~2500 BCE at the base) and the upper portion of the core, where independent ecological and historical evidence (e.g. *Pinus* expansion, microplastic detection) points to a much more recent age. This representation should not be considered a formal age-depth model, but an illustrative tool to visualise the inconsistencies affecting the chronological framework.

Additional contradictions emerge when comparing the upper pollen record with the radiocarbon chronology. A relatively sharp increase in *Pinus* above ~95 cm strongly suggests a recent ecological change, plausibly linked to the documented reforestation of the Feniglia dune in the early 20th century (Bellarosa *et al.*, 1996; Fondazione S. Giovanni Gualberto, 2000; Rossi, 2017). This attribution, however, is chronologically incompatible with the radiocarbon ages at similar depths. Independent evidence from the detection of microplastics in OLP-11B also indicates that at least the upper part of the core must be modern, further undermining a literal acceptance of the ^{14}C ages.

Overall, these data point to a problematic chronology, where reworking and partial mixing of sediments cannot be excluded for both the upper and lower portions. It is plausible that the sequence above ~95 cm reflects late 19th-20th century conditions, while the lower part may represent an older deposit that has been secondarily incorporated or disturbed. Figure 22 provides a tentative graphical interpolation of the radiocarbon chronology under terrestrial calibration; this representation should not be considered a formal age-depth model, but rather an illustrative tool to visualise the discrepancy between the radiocarbon dataset and the ecological proxies.

In conclusion, while a basal age around ~2500 BCE appears consistent across several radiocarbon determinations and is further supported by the amino acid racemization results, the integrity of the sequence as a continuous archive remains doubtful. Reworking and partial mixing of sediments cannot be excluded in either the upper or lower portions. It is therefore plausible that the section above ~95 cm reflects late 19th-20th century conditions, while the lower part represents an older deposit incorporated into the sequence under complex taphonomic processes. For this reason, the discussion of vegetation, NPPs, and surface assemblages will proceed by emphasising stratigraphically robust patterns, relying primarily on the internal coherence of palynological and sedimentological proxies while remaining cautious in attributing absolute ages.

9. Interpretation of the fossil palynological record

9.1. Pollen assemblages and vegetation changes

The pollen record of core OLP-11B reveals an overall stable floristic composition, dominated throughout by Mediterranean and Sub-Mediterranean woodland elements, with only limited long-term variability (Figs. 6–11).

1. In Zone ORB-1 (subzones a-c), extending from the base to ~95 cm, the assemblage is characterized by a balanced co-dominance of *Quercus ilex-coccifera* and *Q. pubescens* types, reflecting mixed evergreen-deciduous woodlands typical of the central Tyrrhenian lowlands. Minor but consistent taxa include *Carpinus orientalis*, *Corylus*, *Ulmus*, and *Pistacia*, together accounting for much of the Sub-Mediterranean component. Arboreal pollen exceeds 80% of the total, while herbaceous taxa (mainly Amaranthaceae, Poaceae, and *Plantago lanceolata* type) remain subordinate. The wetland signal, dominated by Cyperaceae and *Ruppia*, indicates stable lagoonal-marshy conditions along the margins. This lower interval thus depicts a persistent Mediterranean woodland landscape with little internal variability.
2. The transition to Zone ORB-2 (from ~95 cm upward) marks the major floristic change in the sequence, defined by the sharp expansion of *Pinus* (up to >40%), replacing *Quercus* as the dominant taxon. This signal is stratigraphically abrupt and suggests a major ecological reorganisation of the local landscape. Given its magnitude and the timing inferred from ecological evidence, this increase is plausibly associated with the reforestation of the Feniglia dune initiated in the early 20th century (Bellarosa *et al.*, 1996; Rossi, 2017). The expansion of *Pinus* thus appears to be the primary vegetation change captured in the upper part of the core, corroborating the hypothesis of recent sediment deposition in this interval despite the chronological uncertainties discussed above. Subzones ORB-2a-b retain broadly similar compositions, but show progressive increases in *Olea* (to ~13%), suggesting a long-standing signal of olive cultivation in the Orbetello hinterland, and recurrent peaks of indeterminate Cupressoideae at 28, 17, and 4 cm. These discontinuous signals plausibly relate to ornamental or shelterbelt plantings typical of 20th-century coastal management and urban landscaping in Tuscany (Bellarosa *et al.*, 1996; Fiaschi *et al.*, 2024; Lenzi *et al.*, 2009). Other

cultivated or synanthropic taxa (Cerealia-type, *Plantago lanceolata* type, *Eucalyptus*) occur sporadically or at low levels.

Within Zone ORB-2, two marked *Ruppia* peaks between 28 and 20 cm coincide with short-lived hydrophyte expansions, possibly reflecting temporary phases of improved water quality before the eutrophic crises described for the Orbetello Lagoon (Lenzi *et al.*, 1984, 2009). Similar fluctuations have been described in other Mediterranean lagoons, where the persistence of *Ruppia* meadows is strongly conditioned by water quality and sediment chemistry (Azzoni *et al.*, 2001). While direct correlation to the Orbetello record remains uncertain, these findings suggest that the pollen peaks may reflect temporary episodes of favourable ecological conditions, followed by decline under eutrophic stress.

Overall, the pollen zones delineated by CONISS capture a long-term ecological stability punctuated by a pronounced *Pinus* expansion and localized 20th-century anthropogenic inputs. The persistence of *Olea* confirms continuous olive cultivation in the Orbetello hinterland, while lagoonal and halophytic taxa document enduring wetland conditions modulated by recent eutrophication dynamics.

9.2. NPPs and associated lagoonal trophic shifts

In contrast to the pollen spectra, which display relatively modest variation, the NPP record of core OLP-11B reveals a much more dynamic ecological history, with marked fluctuations in algal, fungal, and other aquatic proxies (Figs. 12, 13).

1. At the base of the record (subzone ORB-1a; 219-201 cm), *Botryococcus* dominates the assemblage, averaging ~50% and locally exceeding 60%. This dominance is coupled with frequent dinocysts, especially *Spiniferites*, and abundant pteridophyte spores, suggesting relatively stable lagoonal waters with moderate marine influence.
2. Within subzones ORB-1b/c (201-123 cm), a major ecological turnover occurs: fungal spores become the overwhelmingly dominant component, frequently exceeding 90% (max. 96.50% at 129 cm). The collapse of *Botryococcus* in this interval, combined with the explosive rise of fungal morphotypes (including NPP Morphotype 2), points to a substantial ecological reorganisation of the lagoon. Such a fungal bloom could be related to increased organic matter loading, oxygen depletion, or episodic dystrophic events, phenomena already recognised in the

ecological history of Orbetello (Lardicci *et al*., 2001). The occurrence of foraminiferal linings at 173 and 169 cm, reaching 72% and 44% respectively, may also indicate episodes of stronger marine exchange during this ecologically stressed phase.

3. In subzone ORB-2a (123-92 cm), *Botryococcus* reappears with highly fluctuating values, reaching a maximum of 95% at 109 cm. This resurgence coincides with a gradual decline of fungal spores and the appearance of repeated peaks in dinocysts (up to 37.50% at 84 cm), suggesting alternation between phases of freshwater algal proliferation and increased marine connectivity.
4. At the onset of subzone ORB-2b (92 cm to the top), an isolated but pronounced *Pseudoschizaea* maximum (75% at 89 cm) represents a unique signal of potential ecological instability or unusual depositional conditions, possibly linked to transient stress episodes in the lagoon. Between 92 and 63 cm, *Botryococcus* remains highly unstable, in places entirely absent, while indeterminate algae show recurrent peaks (up to 89%). This phase also records multiple maxima in foraminiferal linings (59-67% between 71 and 57 cm), consistent with more open lagoonal circulation, and a conspicuous increase in monolete spores.

   The interval from 63 to 22 cm is marked by the overwhelming dominance of *Botryococcus*, which averages >90% between 54 and 36 cm. These extremely high abundances are commonly interpreted as reflecting quasi-lacustrine conditions characterised by strong water-column stratification, reduced mixing, and enhanced algal productivity. In coastal lagoons, this signal typically develops during phases of restricted circulation and oxygen depletion, when surface waters remain eutrophic while bottom waters become poorly ventilated. Therefore, the *Botryococcus* plateau is consistent with a stratified, dystrophic lagoonal state, possibly intensified by 20th-century anthropogenic pressures. Other NPPs are comparatively rare during this phase.

   In the uppermost sediments (22 cm to the core top), *Botryococcus* declines sharply, replaced by high abundances of indeterminate algae (average ~38%, peaking to 66%) and renewed presence of dinocysts (up to 19% Spiniferites at 11 cm), hinting at recent phases of increased marine input and altered trophic dynamics.

Overall, the NPP record indicates more numerous and abrupt ecological shifts than the pollen record, with *Botryococcus* oscillations and fungal spore blooms acting as the

clearest markers of lagoonal trophic instability. In particular, the transition at ~202 cm, from *Botryococcus* dominance to fungal spore expansion, and the later *Botryococcus* resurgence followed by modern algal fluctuations, point to recurrent reorganisations of the lagoonal ecosystem under both natural and anthropogenic drivers.

9.3. Vegetation and NPPs trends in the climatic and historical context of the site

The interpretation of the OLP-11B sequence requires situating the palynological and NPP signals within the broader framework of climatic oscillations and historical land-use practices. In the basal portion of the core, the persistence of a stable Mediterranean woodland signal, with mixed evergreen and deciduous oaks and constant *Olea*, suggests continuity of vegetation without marked anthropogenic disruption. If the terrestrial calibration of radiocarbon ages is adopted, this interval may extend back to the mid- to late third millennium BCE, potentially encompassing the 4.2 ka event.

This arid phase, widely recognised across the central Mediterranean between 39° and 43° N as a temporary decline in arboreal pollen and an opening of the forest cover, is not clearly expressed in the Orbetello record, which instead maintains high and stable tree pollen values (Figs. 8, 9). Such stability could be explained either by chronological uncertainties, by taphonomic smoothing due to low sedimentation rates, or by the relative resilience of coastal lowland vegetation compared to upland sites more sensitive to aridification (Di Rita & Magri, 2019). While this limits the use of Orbetello as a firm chronological marker for the 4.2 ka event, the absence of an evident signal is consistent with the variable regional imprint of this climatic anomaly, which was strong in southern Italy but less pronounced in Tuscany and further north (Di Rita & Magri, 2019).

Moving upward in the sequence, the progressive increase of *Olea* and sporadic records of other synanthropic taxa point to the steady presence of olive cultivation in the Orbetello hinterland since at least the classical period, in line with archaeological and historical evidence of Etruscan and Roman agricultural exploitation of the coastal plains (Cardosa & Dolfini, 2017; Perkins, 2017). The remarkable stability of the pollen spectrum until ~95 cm is therefore more likely to reflect either a very compressed chronology or a depositional hiatus, rather than a genuine absence of anthropogenic impact.

The sharp expansion of *Pinus* above 95 cm provides a more reliable chronological anchor (Figs. 6, 8, 9). This change is best interpreted as the palynological signature of the large-scale reforestation of the Feniglia tombolo initiated in the early 20th century (Bellarosa

et al., 1996; Rossi, 2017), a management practice that created a continuous *Pinus pinea* woodland still framing the lagoon today. The coincident appearance of Cupressoideae peaks in the upper part of the sequence corroborates this interpretation, as they likely reflect local ornamental and shelterbelt plantings typical of the same period (Lenzi *et al*., 2009). These signals provide an independent palynological confirmation that the upper ~95 cm of the core correspond to the last century, consistent with the ^{210}Pb-derived sedimentation rates.

The NPP record further refines this interpretation (Fig. 12). The massive dominance of *Botryococcus* between 63 and 22 cm, with maxima exceeding 90%, corresponds closely to the dystrophic crises and eutrophication episodes historically documented for Orbetello in the 20th century (Lardicci *et al.*, 2001). In turn, the subsequent decline of *Botryococcus* in the uppermost levels, accompanied by a resurgence of dinocysts and indeterminate algae, matches ecological reports of recent management interventions aimed at restoring marine exchange and mitigating eutrophication (Lenzi *et al.*, 2003, 2009; Nuccio *et al.*, 2003; Renzi, 2022). These measures, including enhanced seawater pumping, macroalgal harvesting, and wastewater treatment, profoundly altered lagoonal circulation and nutrient dynamics, and their legacy is consistent with the ecological shifts visible in the most recent sediments. However, the association of individual NPP peaks with precisely dated historical events must be regarded as methodologically fragile, even in the upper part of the core. The ^{210}Pb-^{137}Cs-^{241}Am profiles do not provide punctual chronological anchors, and the estimated sedimentation rate implies that a few centimetres of sediment may integrate several years to decades of ecological signal.

Within this framework, the *Botryococcus* plateau is consistent with the eutrophic conditions that culminated in the severe anoxic crises of 1992-93 (Lardicci *et al.*, 2001), while the later decline of *Botryococcus* and renewed marine signatures can plausibly be linked to remediation measures introduced from the mid-1990s onwards (Lenzi *et al.*, 2003, 2009; Nuccio *et al.*, 2003; Renzi, 2022). Nevertheless, these correspondences can only be framed at a decadal scale: the resolution of the core precludes one-to-one matching between single peaks in the palynological record and discrete historical events.

In sum, the combined pollen and NPP evidence strengthens the chronological hypothesis that identifies the upper metre of the sequence with the last ~100 years. Conversely, the deep basal ages inferred from radiocarbon may be partly artefactual, reflecting bulk sediment biases or hiatuses. While the Orbetello record does not clearly capture the 4.2

ka event, the absence of a strong aridification signal is compatible with its geographically variable expression across the Tyrrhenian sector, and thus does not contradict the possibility that the sequence indeed reaches back to the Bronze Age.

At the same time, the palynological data alone do not resolve the chronological uncertainty, and alternative depositional models, potentially very different from the one adopted here, cannot be excluded. The above-cited hypotheses must therefore be tested and refined through additional analyses of the sedimentary material capable of providing more robust chronological constraints.

10. Surface samples

10.1. Granulometry and hydrodynamic implications (Figs. 14–16)

The granulometric spectra of Orbetello surface sediments reveal a heterogeneous mosaic, reflecting the morphological complexity of the lagoon and its differentiated hydrodynamic regimes. Fine-grained samples, particularly the clay-rich deposits of the northern Laguna di Ponente (e.g. sample PS-POL-ORB 03), indicate zones of reduced energy and limited circulation, consistent with the more sheltered morphology of this sector. Similarly, the relatively high clay content near the Canale di Ansedonia and Canale di Fibbia (samples PS-POL-ORB 14 and PS-POL-ORB 03) suggests depositional settings where fine particles can accumulate despite proximity to fluvial inputs (Fig. 16).

By contrast, the prevalence of sandy and silty-sandy textures in the central Laguna di Levante and around the Orbetello peninsula points to more energetic hydrodynamic conditions. These coarser assemblages are plausibly linked to stronger tidal flushing, wave reworking, or anthropogenically enhanced water exchanges, which characterise this sector of the lagoon. The marked bimodality observed in some samples (e.g. PS-POL-ORB 04, PS-POL-ORB 05, PS-POL-ORB 15) further supports episodic sediment reworking, with alternation between fine settling and the introduction of coarse material.

The sharp contrast between the silt/sand-dominated Laguna di Levante and the clay/silt-dominated Laguna di Ponente confirms the asymmetric dynamics imposed by the lagoon's double-tombolo morphology. The Laguna di Levante, more exposed and connected to channels with active management, retains coarser deposits, while the Laguna di Ponente functions as a trap for finer sediments (Fig. 16). This spatial differentiation is essential for interpreting the fossil core OLP-11B: samples with higher

clay and silt fractions offer analogues for quieter depositional settings, while sandy units correspond to higher-energy or exchange-influenced phases.
In sum, the surface granulometry of Orbetello not only reflects the present-day hydrodynamic compartmentalisation of the basin but also provides a key to recognising analogous textural signatures in the stratigraphic record.

10.2. Surface samples comparison (Figs. 17, 18, 23)

The surface samples consist of surface sediments reaching a depth between 2 and 10 cm. Based on the sedimentation rate inferred from ^{210}Pb and ^{137}Cs analysis carried out on the OLP-11B core, these samples likely represent the pollen composition deposited in the basin over the past decades. The uncertain chronological framework of the OLP-11B core does not preclude the possibility that the uppermost 10 cm of the lagoon sediments were deposited much more recently, potentially reflecting only the most recent years of accumulation.
The analysis of surface samples from both the Levante and Ponente sectors of the Orbetello Lagoon indicates a relatively homogeneous pattern across the entire lagoon system. This uniformity is, at least in part, attributable to artificial interventions involving the resuspension of soft surface sediments, which affected the uppermost 3-4 cm of sediment (Renzi, 2022). These interventions were implemented to promote the mineralization of labile organic matter and thus mitigate episodes of algal eutrophication that have repeatedly impacted the lagoon over the past decades. The effect of this intervention on the accuracy of the analysis in representing the lagoon's vegetation requires further investigation. However, considering that these surface samples are collected up to depths of 10 cm and given the spatial distance between sampling points within the lagoon, we can reasonably assume that the variation in sample composition at least partially reflects the differences in vegetation across the various locations around the lagoon.

All samples exhibited high percentages of *Pinus*, which is the most represented taxon, averaging 32.70% (Fig. 23). This high percentage is primarily attributed to the pine forests surrounding the lagoon, particularly the Duna Feniglia forest, which borders the southern side of the lagoon. Smaller pine patches are also found on the Duna Giannella, bordering the northwestern side of the lagoon, and on the slopes of Monte Argentario. This elevated percentage is one of the main differences between the results from Orbetello

and those from the nearby Burano site, where the influence of the Feniglia pine forest is diminished and where pollen dispersal from this area is limited by the presence of two small promontories in the Ansedonia region.

If we consider the differences between the individual samples and their position in the lagoon (Figs. 17, 18), we notice that the samples showing on average the highest percentage of *Pinus* are those closest to the Duna Feniglia, which hosts a large pine forest. The PS-POL-ORB 01 (43.02%) and PS-POL-ORB 14 (42.83%) samples appear to be the richest in pine. In the latter case this is due to the proximity to the Feniglia pine forest, while in the former case this high percentage can likely be attributed to the proximity to some spots on the Giannella dune. For the same reason, sample PS-POL-ORB 02 also has slightly higher than average percentages of pine. In fact, despite the Giannella dune being less forested and more anthropized compared to the Feniglia, small pine plantations can still be found along its western coast and within some campsites (Figs. 17, 18).

The presence of large tracts of cultivated areas in the northern section of the Giannella tombolo likely explains the relatively high herbaceous pollen percentages in sample PS-POL-ORB 03. By contrast, samples PS-POL-ORB 05 and PS-POL-ORB 06 show higher values of evergreen oaks (*Quercus ilex*, represented in the Sub-Mediterranean group in the graph), consistent with the forests covering the eastern slope of Monte Argentario (as illustrated in the habitat map in Viciani *et al.*, 2018) (Figs. 17, 18).

In addition to these features, the cumulative diagram highlights that herbaceous taxa represent on average ~16% of the assemblages, with a prevalence of halophytic elements (mainly Amaranthaceae) alongside upland herbs (Fig. 23). This confirms the influence of both lagoonal margins and surrounding open habitats. When comparing the two basins, the Levante and Ponente sectors show broadly similar floristic compositions, yet the

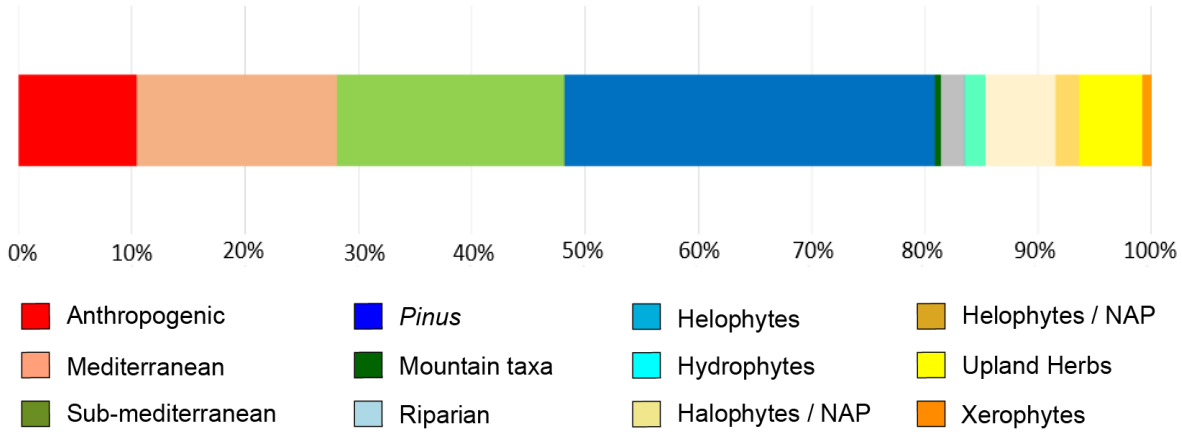

Fig. 23: Cumulative percentage of pollen content of surface samples from the Orbetello site, subdivided by informal palynological group.

slightly higher percentages of *Pinus* and evergreen oaks in the eastern stations suggest a stronger imprint of the Feniglia forest and Monte Argentario woodlands, whereas the Ponente sector locally records higher herbaceous values, reflecting the more cultivated landscape of the Giannella tombolo (Fig. 18).

The pollen composition of the PS-POL-ORB 01 and PS-POL-ORB 02 samples, as well as the overall average composition across the lagoon, closely mirrors that of the uppermost layers of the OLP-11B core, which was collected in close proximity. This similarity suggests that the core has not experienced any erosion of its superficial layers. This convergence between surface spectra and the uppermost core levels provides a coherent picture of the modern pollen rain in Orbetello, reinforcing the evidence for the strong ecological footprint of 20th-century reforestation and land use around the lagoon.

10.3. Moss samples (Figs. 19, 20, 24)

The two moss polsters collected around the Orbetello Lagoon (MOSS1 ORB1-23 and MOSS2 ORB1-23) provide a valuable comparison with the lagoonal surface samples, capturing pollen rain directly from the terrestrial vegetation mosaic. Both assemblages are dominated by arboreal taxa, with *Pinus* as the single most abundant component (average 26.22%), reflecting the pervasive influence of the pine forests of Feniglia and Giannella, as well as scattered stands on Monte Argentario (Viciani *et al.*, 2018).

Mediterranean elements (average 8.59%) are mainly composed of *Quercus ilex-coccifera* type, accompanied by *Pistacia*, *Myrtus*, and *Phillyrea*. Sub-Mediterranean taxa are also well represented (average 11.70%, primarily *Quercus pubescens*-type, *Carpinus orientalis*, and *Fraxinus excelsior*) (Fig. 24).

Indicators of human activity are consistently present, with *Olea* reaching 3.46% on average, together with sporadic traces of *Eucalyptus* and *Juglans*, confirming the persistence of cultivated and synanthropic taxa in the pollen rain. Montane (*Betula*, *Fagus*) and riparian (*Alnus*) elements occur at low percentages, indicating minimal input from distant or riverine sources (Fig. 24).

A distinctive feature of the moss assemblages is their markedly higher proportion of herbaceous taxa compared with lagoon sediments, reaching 43% in MOSS1 and 51% in MOSS2. The two samples also differ internally: MOSS1 is dominated by Amaranthaceae (26.05%), whereas MOSS2 shows a more diversified composition, with substantial Caryophyllaceae (11.54%) alongside upland and ruderal taxa such as *Plantago lanceolata*

type (7.37%), Asteraceae Cichorioideae, and Ericaceae. Hydrophytic elements are virtually absent, occurring only sporadically in MOSS2. These contrasts suggest that the moss spectra capture a stronger input from terrestrial and ruderal vegetation than the lagoonal sediments, reflecting the direct influence of the surrounding vegetation mosaic (Fig. 24).

Taken together, these patterns highlight the complementary role of moss polsters, which provide a more sensitive record of local vegetation heterogeneity compared to lagoonal surface samples. While both archives consistently capture the dominance of *Pinus* and the importance of Mediterranean and Sub-Mediterranean woodland elements, mosses emphasise fine-scale variations in herbaceous and anthropogenic indicators, offering a terrestrial counterpart to the aquatic-biased pollen signal of surface sediments.

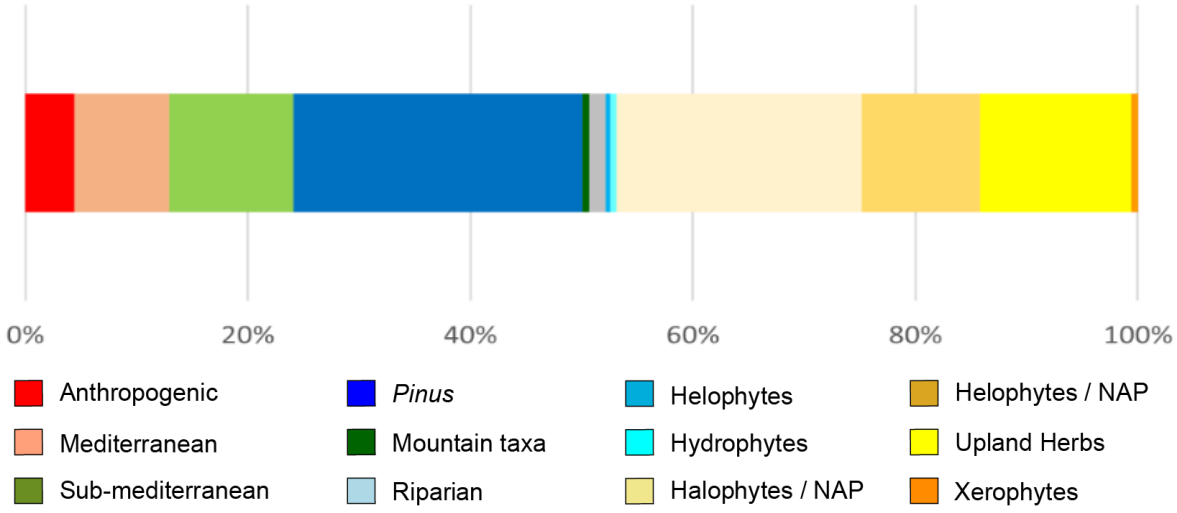

Fig. 24: Cumulative percentage of pollen content of moss samples from the Orbetello site, subdivided by informal palynological group.

10.4. Integrated comparison of core, surface, and moss records

The combined evidence from core OLP-11B, surface sediments, and mosses provides a coherent picture of the modern pollen rain in the Orbetello system while also highlighting differences linked to the specific taphonomic pathways of each archive. The uppermost levels of the core and the surface sediments show strong convergence, with *Pinus* overwhelmingly dominant, accompanied by Mediterranean and Sub-Mediterranean taxa such as *Quercus ilex* and *Olea*. This consistency confirms that the core has preserved its surficial layers and that both records integrate the dominant pollen sources from the Feniglia and Giannella pinewoods, as well as long-standing olive cultivation.

The moss samples, in contrast, amplify the terrestrial and ruderal component, with much higher percentages of herbaceous taxa (up to 51%), including Amaranthaceae, Caryophyllaceae, and *Plantago lanceolata* type. Hydrophytic elements are negligible in moss samples, in stark contrast with lagoonal sediments, where *Ruppia* and *Phragmites* appear regularly, albeit at modest levels. These differences underscore the complementary nature of the archives: lagoon sediments capture the integrated aquatic-terrestrial pollen rain over time, whereas moss polsters act as sensitive local collectors of airborne and ground-level input from nearby vegetation patches.

Taken together, the three archives allow for a more robust reconstruction of vegetation and land-use dynamics in Orbetello. The coherence between core and surface sediments underlines the stability of the recent pollen rain, while the moss spectra emphasise the heterogeneity of the surrounding vegetation mosaic, providing independent confirmation of the strong anthropogenic imprint on the landscape.

11. Microplastics evidence and anthropogenic pressure

The analysis of six sediment samples from the OLP-11B core revealed the consistent presence of microplastics throughout the profile, from the surface layers down to the deepest sample analysed at 193-199 cm (Tabs. 2–4; Fig. 21). Concentrations vary markedly, with the highest values recorded in the uppermost sample (11.77 particles/g) and at ~90 cm depth (6.67 particles/g), whereas intermediate levels range between 1.79 and 2.93 particles/g. The basal sample shows the lowest concentration (0.68 particles/g), yet even here multiple blue fibers and fragments were detected after contaminant subtraction, confirming that the signal is not an artefact of laboratory contamination.

Morphologically, the assemblage is strongly dominated by blue fibers, representing over 70% of all fragments in several samples. Other categories include transparent nylon-like filaments, black and red fibers, blue and transparent fragments, and more unusual morphotypes such as sponge-like agglomerations, coarse fabrics, and filamentary masses (Fig. 21). This morphological heterogeneity is consistent with mixed sources of plastic input, including textiles, packaging, and fishing-related materials, all of which are documented pressures on the Orbetello lagoon system (Renzi, 2022).

From a stratigraphic perspective, the detection of microplastics at nearly 2 m depth raises significant chronological concerns. According to the radiocarbon chronology with

terrestrial calibration, such levels would correspond to the mid-second millennium BCE, i.e. long before the invention of synthetic polymers. This paradox has been observed in other sedimentary archives (Bancone *et al.*, 2020; Turner *et al.*, 2019), and several mechanisms may explain it: vertical migration of particles through bioturbation and physical mixing, partial sediment reworking, or contamination introduced during coring or handling (Gimiliani *et al.*, 2020). The high concentrations in the topmost layers, on the other hand, clearly reflect intensified anthropogenic pressure over the last century, consistent with the global trajectory of plastic production and dispersal (Fytianos *et al.*, 2021).

Overall, the Orbetello record supports the interpretation of microplastics as sensitive proxies of recent anthropogenic impact, complementing ecological and geochemical indicators of lagoonal degradation. At the same time, their occurrence in the deepest horizons underscores the methodological and interpretative challenges of using microplastics as chronological markers. While they corroborate the hypothesis that the upper metre of the core corresponds to the last century, they do not resolve – and may even complicate – the debate over the absolute age of the basal deposits. Future work, including polymer identification and particle ageing analysis, will be essential to disentangle depositional from post-depositional signals and to refine the chronological significance of the Orbetello microplastic record.

12. Synthesis and interpretive cautions

The Orbetello multiproxy record offers a coherent picture of long-term ecological stability punctuated by clear signals of anthropogenic and lagoonal change. Arboreal taxa dominate consistently throughout the sequence, with Mediterranean and Sub-Mediterranean woodlands providing the backbone of the pollen rain. Within this framework, three features stand out as the most robust signals: the abrupt expansion of *Pinus*, tentatively attributed to the 20th-century reforestation of the Duna Feniglia; the persistent though fluctuating representation of *Olea*, attesting to long-standing olive cultivation in the hinterland; and the NPP assemblages, which capture repeated episodes of lagoonal stress, from fungal blooms to *Botryococcus* proliferations and ephemeral *Ruppia* peaks. Together, these markers highlight the intertwined effects of natural lagoonal dynamics and human interventions.

At the same time, significant uncertainties remain. The deep chronology inferred from radiocarbon, amino acid racemization, and sedimentation rates cannot yet be reconciled unambiguously, raising the possibility of hiatuses or reworking in the lower part of the core. The detection of microplastics even at great depth likewise complicates the chronological framework, leaving open the question of post-depositional mixing and the true antiquity of basal sediments. Distinguishing between localised vegetation inputs (e.g. Cupressoideae peaks from ornamental plantings) and broader regional signals also requires caution.

In this light, the Orbetello record provides a valuable but non-deterministic archive: it captures clear ecological reorganisations, especially in the modern period, but its long-term chronology and the precise timing of some signals remain provisional. The comparison with Burano and Orti-Bottagone will help place these findings in a broader regional context, testing whether the stability, eutrophication signals, and anthropogenic imprints observed at Orbetello represent shared trajectories across Tyrrhenian lagoons or instead reflect site-specific histories.

Chapter 5

Orti-Bottagone Marshes

Introduction

The Orti-Bottagone wetland is located on the coastal plain of southern Tuscany, near the town of Piombino, within the Cornia River alluvial plain (Fig.1; Chapter 2, Fig. 5). The site lies a few meters above sea level (Viciani & Lombardi, 2001), in proximity to the Tyrrhenian coastline, and is part of a broader sedimentary basin formed by Quaternary fluvio-deltaic and coastal processes (Amorosi *et al.*, 2004; Bianchini *et al.*, 2005). The remaining wetland area currently extends over 90 hectares, and is located in a coastal alluvial plain on a soft clay or clay-peat substrate, characterized by shallow groundwater tables (Viciani & Lombardi, 2001). It is enclosed within the Natural Reserve "Padule di Orti-Bottagone", a protected area of high ecological value.
Near the WWF Oasis lies the former Tor del Sale power plant, operating from 1977 to 2012 and now undergoing decommissioning and redevelopment with an environment-focused approach. Its chimneys have been demolished, and the site is part of sustainability projects, including a collaboration with the WWF to create oases/nesting areas.

1. Environmental and cultural context

1.1 Geography, geological context and climate

The area falls within a sub-humid to semi-arid climatic type according to the Thornthwaite climate classification (Thornthwaite & Mather, 1957), characterized by relatively low overall humidity, a moderate winter water surplus, and a prolonged dry summer period. The nearest thermo-pluviometric station is located in Follonica, indicating an average annual rainfall of 635 mm (predominantly concentrated in the colder seasons, while sum-

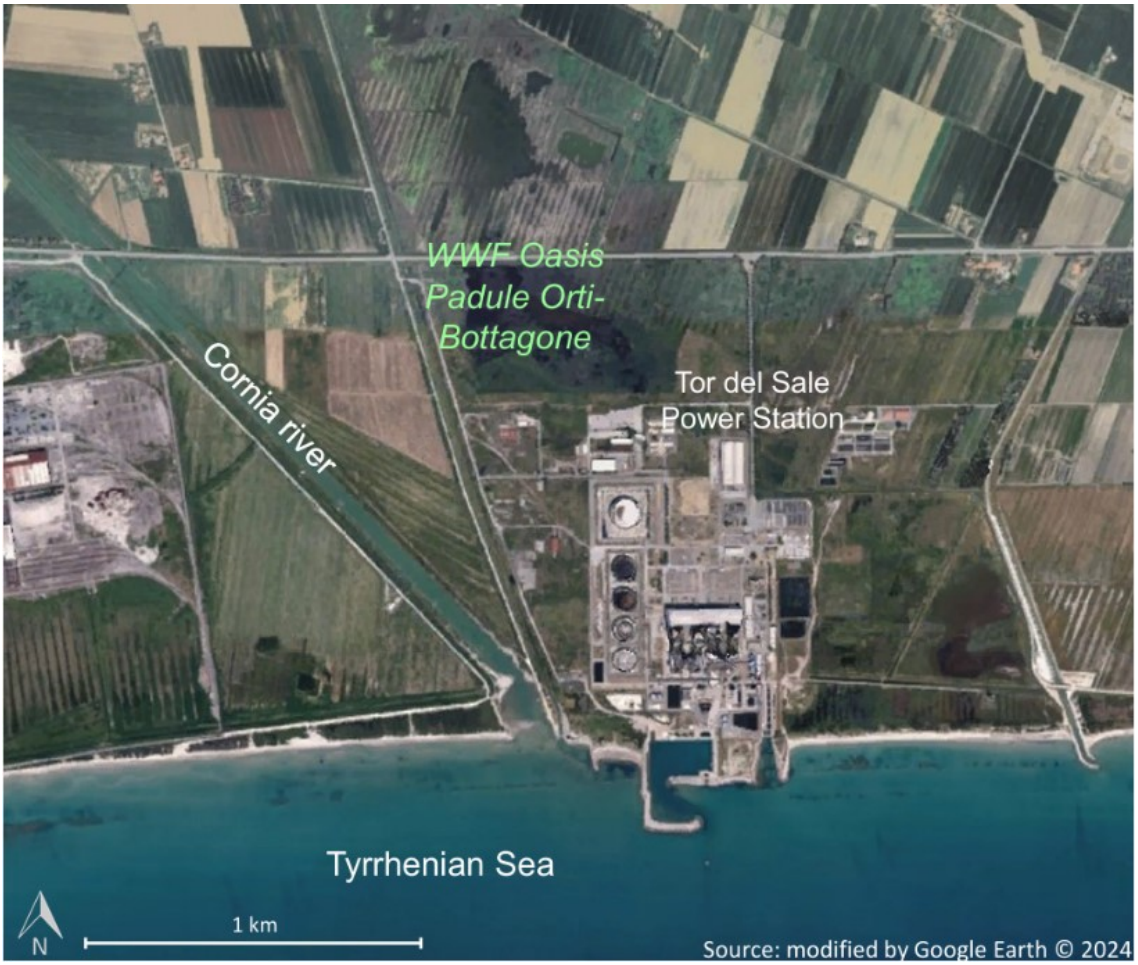

Fig. 1: Satellite image of the Orti-Bottagone site (modified from Google Earth 2023).

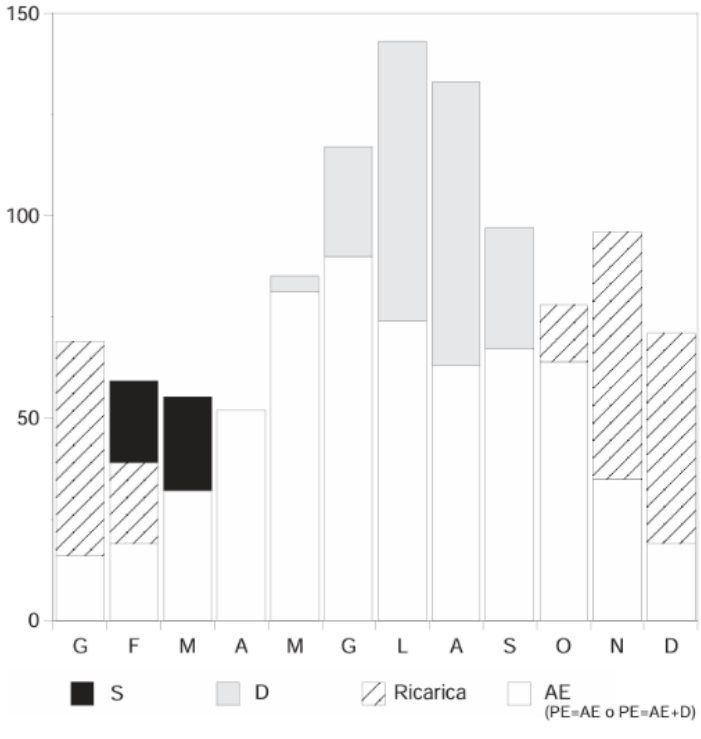

Fig. 2: Monthly water balance at the Follonica meteorological station (from Viciani & Lombardi, 2001). X-axis shows the months of the year; Y-axis indicates water quantities in millimetres. The legend identifies: S (black) = water surplus; D (light grey) = water deficit; Recharge (hatched) = soil water recharge; AE (outlined bars) = Actual Evapotranspiration.

mer droughts are common), and a mean annual temperature of 15.5 °C (Viciani & Lombardi, 2001) (Fig. 2). Wind exposure, saline intrusion, and high evapotranspiration influence both soil characteristics and plant communities, contributing to the establishment of halophilous and hygrophilous ecosystems (Paolini, 2012; Viciani & Lombardi, 2001).

Geologically, the Padule di Orti-Bottagone lies within the Cornia coastal plain, a sector of the broader Piombino-Follonica basin (Bianchini *et al.*, 2005; Pieruccini & Susini, 2020). This area is underlain by Mesozoic to Cenozoic basement rocks and is covered by a thick sequence of Quaternary sediments, shaped by fluvial, alluvial, and coastal processes associated with glacio-eustatic fluctuations and tectonic subsidence (Bianchini *et al.*, 2005; Pieruccini & Susini, 2020). Bianchini *et al.* (2005) describe the hydrogeological system as composed of three main aquifers, with the shallowest one being of particular importance for wetland hydrology. This aquifer consists of sandy to silty sediments with occasional peat and clay intercalations, indicative of a dynamic depositional environment influenced by both marine and continental inputs.

1.2 Overview of the current vegetation

The Orti-Bottagone Reserve exhibits a complex mosaic of vegetation types shaped by hydrological variability, geomorphology, and anthropogenic history. It includes brackish marshes, reed beds, wet meadows, salt pans, and remnants of Mediterranean shrublands (Saragosa, 2019).

Viciani & Lombardi (2001) identified over 300 plant species within the reserve, including those typical of hygrophilous and halophilous environments. Dominant formations include extensive stands of *Phragmites australis*, *Typha angustifolia*, and *Bolboschoenus maritimus*, particularly in permanently or seasonally inundated areas. Salt-tolerant taxa such as *Salicornia fruticosa*, *Sarcocornia perennis*, and *Limonium narbonense* are widely distributed across more saline and periodically exposed zones. Mediterranean shrubs such as *Pistacia lentiscus*, *Phillyrea angustifolia*, and *Myrtus communis* persist on slightly elevated ground or dune remnants.

The site also hosts rare or endangered species, including *Limonium etruscum* and *Cressa cretica*, emphasizing its conservation relevance. Anthropogenic pressures, including past agricultural drainage and the continued influence of nearby industrial activities, have

caused partial degradation and fragmentation of native plant communities (Paolini, 2012; Saragosa, 2019).

1.3 Geological and environmental history during Holocene

The coastal plain of the Cornia River, including the Padule Orti-Bottagone area, has undergone significant geological and geomorphological transformations over the Holocene, primarily governed by eustatic sea-level changes, sedimentary dynamics, and human-induced modifications. As shown by Pieruccini & Susini (2020), this area has undergone landscape transformations since the end of the Last Glacial Maximum (LGM), particularly in response to post-glacial marine transgressions and the progressive infilling of fluvial-coastal basins. This evolution is representative of broader processes observed along the Tyrrhenian coast of central Italy and offers valuable insight into the interactions between coastal progradation, lagoonal dynamics, fluvial processes, and anthropogenic interventions (Amorosi *et al.*, 2004; Pieruccini & Susini, 2020).

During the early Holocene, rapid eustatic sea-level rise – averaging approximately 1 cm per year between 10,000 and 7,000 cal yr BP (Lambeck *et al.*, 2011; Vacchi *et al.*, 2016) – drove the transgression of marine waters into the lower portions of the Cornia and Pecora river valleys. These low-gradient valleys, carved during the Late Pleistocene sea-level lowstand, served as natural sediment traps that were progressively infilled with estuarine and lagoonal facies. Sedimentary records from the Cornia plain, including those retrieved near the Orti-Bottagone wetland, testify to the presence of fine-grained, organic-rich clays and silts deposited in brackish lagoonal conditions (Pieruccini & Susini, 2020).

From approximately 7000 to 5000 cal yr BP, the transgression slowed and gradually transitioned into a phase of relative sea-level stability. This facilitated the lateral progradation of coastal barriers and beach ridges, which progressively isolated lagoonal basins from direct marine influence. In the Orti-Bottagone area, this process is reflected in the transition from brackish to freshwater marsh and swamp environments, accompanied by the development of thick peat layers, palustrine deposits, and fluvial overbank facies (Amorosi *et al.*, 2004; Pieruccini & Susini, 2020). These deposits suggest a reduction in salinity and an increase in alluvial input, associated with a more stable coastline.

Throughout the mid- to late Holocene, fluvial activity from the Cornia River contributed significantly to sediment accretion in the coastal plain. Meandering channels deposited

silty and sandy overbank sediments over earlier lagoonal deposits, often leading to the burying of wetland environments (Amorosi *et al.*, 2004; Pieruccini & Susini, 2020). Soil formation processes, such as hydromorphic gleysol development and incipient pedogenesis, are locally detectable and reflect episodic landscape stability and reduced sedimentation rates (Amorosi *et al.*, 2004; Pieruccini *et al.*, 2023).

Geomorphologically, stratigraphic data from multiple sediment cores drilled across the Cornia plain, including in the vicinity of the Orti-Bottagone wetland, reveal a complex sequence of sedimentary facies. These include lagoonal muds, organic-rich swamp deposits, and coarse-grained fluvial sediments, which reflect the vertical aggradation of floodplain environments over earlier lagoonal substrates (Pieruccini *et al.*, 2023). The sedimentary cores extracted in the most distal parts of the plane show that the lagoonal environment in that area had already been replaced by floodplain sedimentation as early as the third millennium BCE, highlighting the early onset of coastal progradation and compartmentalization of lagoonal basins (Pieruccini & Susini, 2020).

The Orti-Bottagone site is located within the western sector of the Cornia plain, near what historical cartography (e.g., *Catasto Leopoldino*) identifies as one of two main paleo-lagoons. Sediment cores extracted in this region show evidence of low-energy lagoonal facies during the Roman and early Medieval periods, which were subsequently replaced by swamp and floodplain environments during the Middle Ages. These findings point to a seaward regression of the lagoon, likely influenced by sediment inputs from the shifting channel belts of the paleo-Cornia system (Pieruccini & Susini, 2020). The dynamics of this regression were not linear. In many areas, shallow to deep swamps persisted for long periods, and transitions to floodplain environments occurred gradually, often controlled by both natural sedimentation and human interventions such as drainage or channel diversion. Notably, the cores drilled near the barrier beach system at the river's mouth, contains thick gravelly deposits indicative of high-energy channel lags. These are overlain by finer floodplain sediments that suggest that this portion of the plain was already emergent and no longer affected by lagoonal processes by the second millennium BCE.

Cores closer to the present-day coastline still preserve fully lagoonal sequences, though they are now located several meters below current sea level, reflecting both relative sea-level rise and subsidence processes. These sequences also confirm that the extent of the Medieval lagoon was comparable to that shown in the 19th-century maps, although slightly reduced and fragmented into western and eastern basins, separated by barrier systems and alluvial fans (Clò *et al.*, 2024; Pieruccini *et al.*, 2023).

Overall, the stratigraphic record confirms a long-term infilling trajectory, characterized by a vertical succession from lagoon to swamp and finally to floodplain environments, consistent with a regressive depositional model. This pattern is common throughout the Tyrrhenian coastal plains but is particularly well-preserved and documented in the Cornia basin thanks to the combined use of sedimentological, chronological, and geomorphological data (Amorosi *et al.*, 2004; Pieruccini & Susini, 2020; Pieruccini *et al.*, 2023).

1.4 Archaeological history and human impact in the area

The Cornia River coastal plain, encompassing the Orti-Bottagone wetland, presents a long and complex history of human occupation and landscape transformation, with evidence dating back to the Late Prehistoric and Protohistoric periods (Biagi & Milletti, 2017; Giroldini, 2010). This region, located between the metalliferous hills and the Tyrrhenian coast, has been continuously influenced by both cultural and environmental drivers that shaped its evolution from the Iron Age to the modern era (Buonincontri *et al.*, 2020; Dallai *et al.*, 2024, 2025; Pieruccini *et al.*, 2023).

The earliest signs of structured human settlement in the Cornia Plain and nearby Populonia are evident from the Final Bronze Age, but it is particularly during the Early Iron Age that anthropogenic activity intensifies. Excavations at Poggio delle Granate and Piano delle Granate, near Populonia, have revealed necropoleis dating to the 9th-7th centuries BCE (Biagi & Milletti, 2017). These funerary sites, characterized by tumulus burials and rich grave goods, indicate the emergence of a socially stratified and organized community, likely connected to the proto-urban centre of Populonia. This period marks the consolidation of the Etruscan city of Populonia as a regional hub for metallurgy, trade, and ritual activities. Control over resources and the exploitation of metal ores from the Colline Metallifere fueled the rise of this centre, influencing the settlement dynamics of the broader Cornia plain (Giroldini, 2010). The landscape around Orti-Bottagone likely served as both a resource hinterland and a buffer zone, with extensive coastal wetlands that once surrounded the Etruscan city, offering ecological niches for hunting, fishing, and agriculture (Di Paola, 2018).

During the Roman period, the Cornia Plain underwent significant infrastructural and agricultural development. Archaeological evidence (including traces of centuriation, ancient road alignments, and hydraulic works) combined with paleoenvironmental data (from sediment cores, palynological analyses, and geoarchaeological observations),

indicate the establishment of centuriation systems, road networks, and hydraulic management schemes aimed at reclaiming and organizing the landscape (Pieruccini *et al.*, 2023). The Romans built roads, aqueducts, and canal systems, some of which may have extended into or near the Orti-Bottagone sector, although direct archaeological evidence in the wetland itself remains scarce.

Pollen data and sedimentary sequences suggest extensive deforestation and a reduction in arboreal cover during this period, consistent with intensive agricultural exploitation and livestock grazing (Buonincontri *et al.*, 2020; Di Pasquale *et al.*, 2014; Pieruccini *et al.*, 2021). This transformation was accompanied by increased erosion and sedimentation, indicating a more open and anthropized landscape.

Following the decline of the Roman administration, the Cornia plain experienced episodes of reforestation, combined with renewed anthropogenic disturbance. The Early Middle Ages were marked by a relative reduction in anthropic pressure, allowing some natural rewilding of the landscape. However, from the 9th century onward, monastic estates and feudal authorities began to reorganize land use. By the High Middle Ages, paleoenvironmental records from sediment cores and charcoal analyses in the Tyrrhenian Tuscany lowlands reveal charcoal layers, fire residues, and renewed deforestation episodes, reflecting the resumption of slash-and-burn agriculture and forest clearance (Buonincontri *et al.*, 2020; Whitlock & Larsen, 2001). These dynamics are also linked to the expansion of the metallurgical economy in the inland hills and the consolidation of agrarian villages (Dallai *et al.*, 2024). Geoarchaeological and geomorphological analyses carried out in the Orti-Bottagone basin highlight fluctuating human pressure, with alternating phases of marsh expansion and agricultural exploitation, reconstructed through the integration of geomorphological mapping, historical cartography, and archaeological surveys (Pieruccini *et al*., 2023). This variability reflects broader economic and demographic patterns across Tuscany and the Tyrrhenian coastal corridor.

The early modern period saw increasing interest in draining the wetlands and converting them into arable land, a goal only partially achieved before the 20th century. Large-scale reclamation efforts in the Fascist era ultimately reshaped parts of the coastal plain, but Orti-Bottagone retained its palustrine character due to geomorphological constraints and persistent groundwater emergence (Paolini, 2012).

More recently, the area surrounding the wetland has been exposed to industrial development, especially around Piombino and its port, yet the Padule di Orti-Bottagone itself has been preserved as a protected natural reserve. Despite this legal protection,

threats from pollution, habitat fragmentation, and hydrological alterations persist (Dallai *et al.*, 2024; Pieruccini *et al.*, 2023).

1.5 Recent anthropogenic impact and conservation challenges

The Orti-Bottagone Reserve lies in one of the most industrialized and anthropogenically modified zones of the Tuscan coast. As highlighted by Paolini (2012), the proximity of the Piombino industrial complex, the port infrastructure, and the historical presence of land reclamation activities have all exerted pressure on the wetland's ecological integrity. Currently under legal protection and recognized as a Site of Community Importance (SCI), the area is also managed as a WWF Oasis and since 2013 is designated as a Ramsar wetland site of international importance (Padule Orti-Bottagone, Site no. 2571). Nevertheless, it faces several threats, including groundwater overexploitation, pollution from industrial runoff, and land-use change in the surrounding landscape. Climate change further exacerbates these issues by intensifying seasonal droughts, salinity intrusion, and extreme weather events.

Despite these pressures, the site remains a critical biodiversity hotspot and ecological corridor within the fragmented coastal landscape. The integration of paleoenvironmental knowledge (Amorosi *et al.*, 2004; Clò *et al.*, 2024; Pieruccini *et al.*, 2023) into conservation strategies is essential for adaptive management and restoration planning. It allows the reconstruction of baseline conditions and the identification of ecological thresholds, providing a foundation for informed, resilient preservation measures.

2. *Chronological framework of the core POP22-01*

2.1 Radiocarbon dating

At the Orti-Bottagone site, the chronological framework is based on radiocarbon dating carried out by Christine Oberlin (Centre de Datation par le RadioCarbone, UMR 5138 "Archéométrie et Archéologie", Lyon, AMS ARTEMIS).

Radiocarbon dating was carried out on 14 samples (Tab. 1) taken from core POP22-01 (Fig. 3) between 211 and 1286 cm. Most of the samples consisted of degraded vegetal fibers, while a seed, a bone fragment, and two wood fragments were also analysed. A terrestrial calibration was applied.

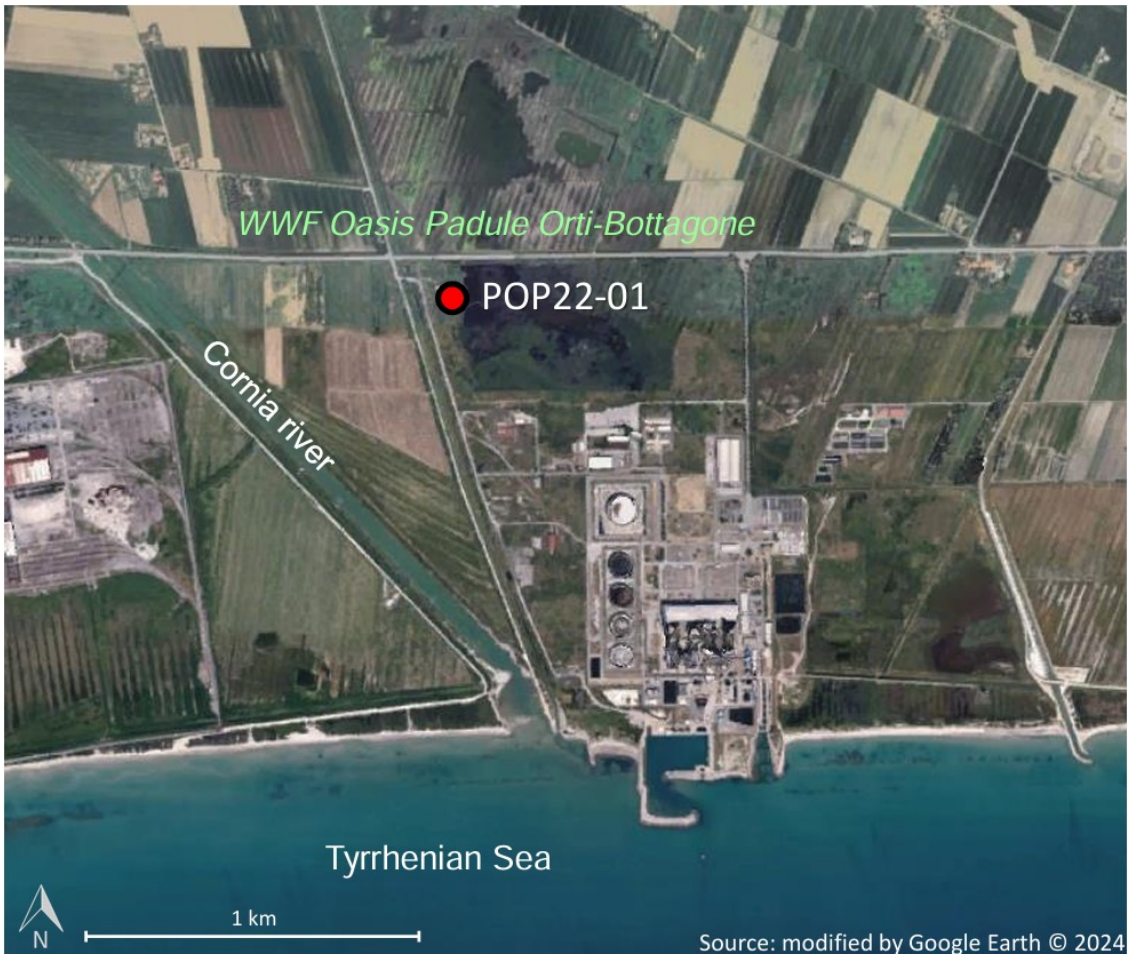

Fig. 3: Location of core POP22-01 within the Orti-Bottagone site.

Reference sample	Depth (cm)	Sample material	Uncalibrated Age (± error)	Calibrated Age	Calibration
Lyon-20448	211	Seed	195 ± 30 ^{14}C yr BP	1646-1950 CE	Terrestrial
Lyon-20449	289	Plant material	1675 ± 30 ^{14}C yr BP	256-530 CE	Terrestrial
Lyon-20450	348.5	Plant material	1340 ± 30 ^{14}C yr BP	645-775 CE	Terrestrial
Lyon-20790	361	Plant material	1520 ± 30 ^{14}C yr BP	436-637 CE	Terrestrial
Lyon-20451	361	Bone	3815 ± 30 ^{14}C yr BP	2434-2142 BCE	Terrestrial
Lyon-20453	412	Plant material	2905 ± 30 ^{14}C yr BP	1209-1009 BCE	Terrestrial
DeA-47727	432	Plant material	3394 ± 25 ^{14}C yr BP	1747-1617 BCE	Terrestrial
Lyon-20791	442	Plant material	1720 ± 30 ^{14}C yr BP	250-411 CE	Terrestrial
Lyon-20455	496	Plant material	1080 ± 30 ^{14}C yr BP	892-1023 CE	Terrestrial
Lyon-20792	553.5	Plant material	1050 ± 30 ^{14}C yr BP	895-1035 CE	Terrestrial
Lyon-20457	599	Plant material	155 ± 30 ^{14}C yr BP	1665-1950 CE	Terrestrial
DeA-47728	657	Plant material	4825 ± 28 ^{14}C yr BP	3649-3528 BCE	Terrestrial
DeA-47726	1091	Wood	7298 ± 33 ^{14}C yr BP	6226-6077 BCE	Terrestrial
DeA-47725	1286	Wood	7372 ± 40 ^{14}C yr BP	6373-6085 BCE	Terrestrial

Tab. 1: Radiocarbon dating analyses carried out on the POP22-10 core (Orti-Bottagone Marshes).

Results

3. Palynological analysis of the sediment core

3.1 Preservation and concentration of pollen and NPP

Pollen concentration in core POP22-01 shows strong variability, with overall low values throughout most of the sequence, interrupted by a few distinct samples that display marked peaks. Palynomorph concentrations range from a maximum of 124,803 grains per gram of sediment to a minimum of 8,668 grains per gram, with an average of 27,935 grains per gram. The preservation state of palynomorphs in the samples is generally good. Most of the palynomorphs observed consist of pollen grains, which register maximum concentration values of 123,030 grains per gram, minimum values of 8,149 grains per gram, and an average of 26,217 grains per gram.

As illustrated in Fig. 4, the concentration trends are largely similar across ecological groups, though a few samples deviate markedly from the general pattern. Within a general trend of moderately low concentrations, the first significant peak from the bottom of the core occurs at 902 cm depth and involves Mediterranean taxa, Sub-Mediterranean taxa, Montane taxa, Upland Herbs, Riparian elements, and to a lesser extent, Helophytes/NAP. At this depth, anthropogenic taxa exhibit a slight increase, followed by a more prominent peak at 866 cm The same set of groups shows a further concentration peak at 770 cm, while other ecological categories remain relatively stable. Helophytes, in contrast to other groups, display an independent trend in this interval, highlighted by a minor peak between 850 and 838 cm.

A broader and more pronounced peak is observed at 570 cm depth, involving nearly all ecological groups. This increase is especially marked in *Pinus*, Montane taxa, and Helophyte curves. A subsequent, slightly less marked peak at 405 cm again affects all groups to varying degrees, but it is particularly pronounced for Anthropogenic taxa, Helophytes, and Xerophytes (the latter of which show their only substantial variation at this depth). Hydrophytes exhibit a distinct pattern, with peaks that coincide with those of

Core POP22-01 - Padule Orti-Bottagone (Southern Tuscany, Italy)
Ecological groups concentrations diagram

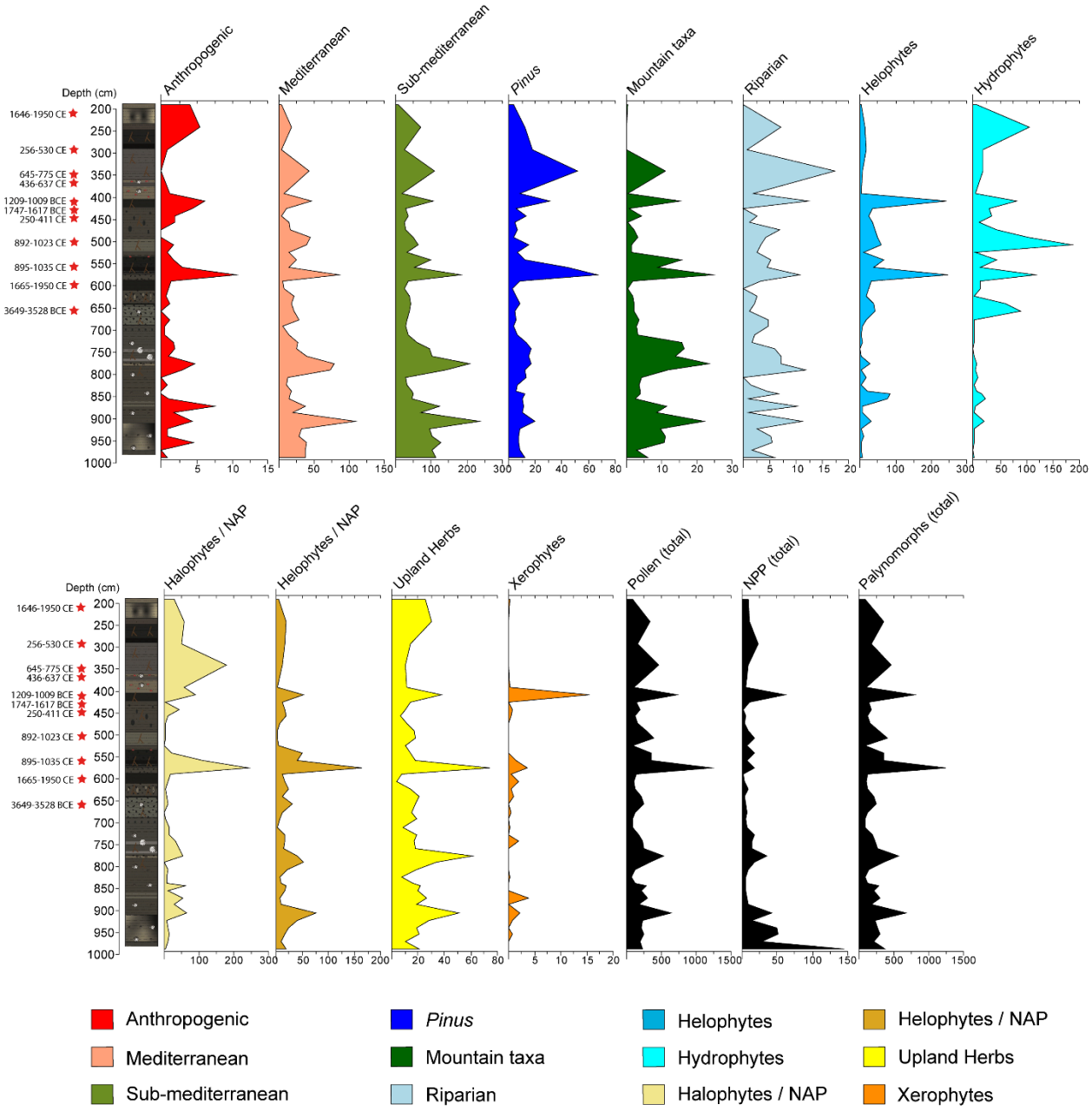

Fig. 4: Concentrations of selected informal palynological groups of the core POP22-01. Calibrated terrestrial dates are reported. The pollen diagram in this and in the following figures includes only the interval covered by the palynological sampling. Therefore, the deeper radiocarbon determinations at 1091 and 1286 cm are not shown because palynological analyses did not extend below the plotted interval.

other groups at 570 and 405 cm, as well as unique peaks – partially mirrored by Helophytes – at 654 cm and especially at 504 cm.

At 338 cm depth, several groups show increased concentrations. This peak is especially marked in *Pinus*, Riparian taxa, and Helophytes/NAP; it is also visible in Montane, Mediterranean, and Sub-Mediterranean taxa, but absent in other groups. In the uppermost

section of the core, particularly at 238 cm, there is a renewed increase in the concentration of Anthropogenic, Riparian, Hydrophyte, and Upland Herb taxa, while the remaining groups show a general declining trend.

Non-pollen palynomorph concentrations are consistently lower than those of pollen throughout the core, with an average of 1,718 grains per gram, a maximum of 14,440 grains per gram, and a minimum of 180 grains per gram. The deepest sample, at 982 cm, exhibits the highest NPP concentration, attributable to a substantial presence of dinocysts, which are considerably more concentrated in the basal portion of the core, particularly from the bottom to 934 cm. After this interval, their abundance sharply declines and remains low for the rest of the core.

3.2 Flora (Tab. 3 of Appendix I. Figs. 5, 6)

Core POP22-01 reveals a vegetation assemblage composed of arboreal, herbaceous, and aquatic species, which vary considerably in relative abundances throughout the stratigraphic sequence (Figs. 5, 6).

Among the arboreal taxa, the Fagaceae family is predominant. Within this group, the most abundant taxon is *Quercus pubescens* type (downy oak), particularly in the deeper sections of the core, between 982 and 672 cm depth. This is followed in abundance by *Quercus ilex-coccifera* type (holm oak/kermes oak). Other Fagaceae taxa, such as *Fagus* (beech), *Quercus suber* (cork oak), *Quercus cerris* (Turkey oak), and *Castanea* (chestnut), are also present, albeit in significantly lower percentages. Among the Betulaceae, though never dominant, the following taxa are observed: *Corylus* (hazel), *Carpinus betulus* (European hornbeam), *Carpinus orientalis* (oriental hornbeam), and *Alnus* (alder), with *Ostrya* (hop-hornbeam) and *Betula* (birch) occurring in lesser proportions. Within the Oleaceae, *Olea* (olive), *Fraxinus excelsior* (ash), and *Phillyrea* are represented (Fig. 5).

The presence of *Pinus* (pine) is significant among the Pinaceae, while *Abies* (fir) is less frequent but still well-represented. In contrast, *Picea* (spruce) is distinctly rare. Other relevant arboreal taxa include *Pistacia lentiscus* (mastic tree), *Ulmus* (elm), and *Tilia* (lime), whereas *Juglans* (walnut), *Acer* (maple), *Sambucus* (elder), and undetermined Salicaceae are only sporadically recorded (Fig. 5).

Among shrub taxa, Ericaceae is the most prominent group. *Vitis* (grapevine) is sparsely represented but distributed throughout the core. Occasional occurrences include *Rhus* (sumac), *Tamarix* (tamarisk), *Viburnum*, and *Ziziphus* (jujube) (Fig. 5).

Among herbaceous taxa, Amaranthaceae is the most abundant family, followed by Poaceae (grasses), Asteraceae Cichorioideae, Caryophyllaceae, Brassicaceae, and *Plantago lanceolata* type (ribwort plantain). Less abundant, but consistently present, are Asteraceae Asteroideae, indeterminate Cupressoideae, Ranunculaceae, and Fabaceae. Among Xerophytes, Artemisia is recorded along the entire core, and *Ephedra fragilis* is also attested. Very rare occurrences are noted for Euphorbiaceae, Saxifragaceae, Malvaceae, Rosaceae, Cistaceae, Convolvulaceae, Hypericaceae (gen. *Hypericum*, or St. John's wort), Araliaceae (gen. *Hedera*, or ivy), Polygonaceae, Rutaceae (gen. *Ruta*, or rue), Geraniaceae, Dipsacaceae (gen. *Scabiosa*), Plumbaginaceae (gen. *Armeria*, or thrift), Cannabaceae, Iridaceae, Apiaceae, Scrophulariaceae, Crassulaceae, and Smilacaceae (gen. *Smilax*, or catbriers) (Figs. 5, 6).

Among the Helophytes, Cyperaceae (sedges) are abundant and well-represented throughout the core. Among Hydrophytes, *Sparganium*/*Typha angustifolia* (bur-reed/lesser bulrush) and *Sagittaria* (arrowhead) are highly abundant. *Lemna* (duckweed) and *Ruppia* (beaked tasselweed or widgeon grass) follow in frequency, whereas *Typha latifolia* (broadleaf cattail), *Myriophyllum* (watermilfoil), *Alisma plantago* (water plantain), and *Potamogeton* (pondweed) are observed occasionally (Fig. 5).

Among cultivated plants, in addition to the previously mentioned occurrences of *Castanea* and *Vitis*, cereal-type pollen (i.e., Poaceae >40 μm; Andersen, 1979; Beug, 2004) is also recorded (Fig. 5).

Core POP22-01 - Padule Orti-Bottagone (Southern Tuscany, Italy)

Single taxa diagram (exaggeration 8x)

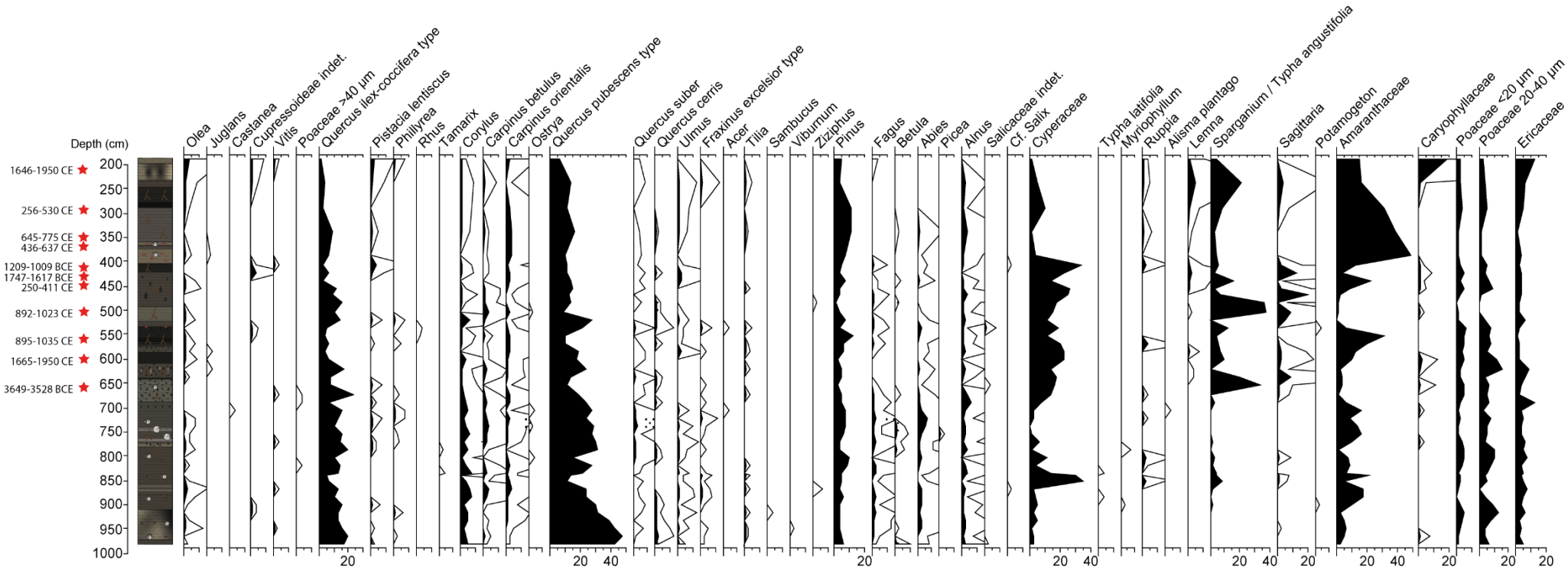

Fig. 5: Detailed palynological diagram of the core POP22-01 (exaggeration 8x). Calibrated terrestrial dates are reported.

Core POP22-01 - Padule Orti-Bottagone (Southern Tuscany, Italy)

Single taxa diagram (exaggeration 8x)

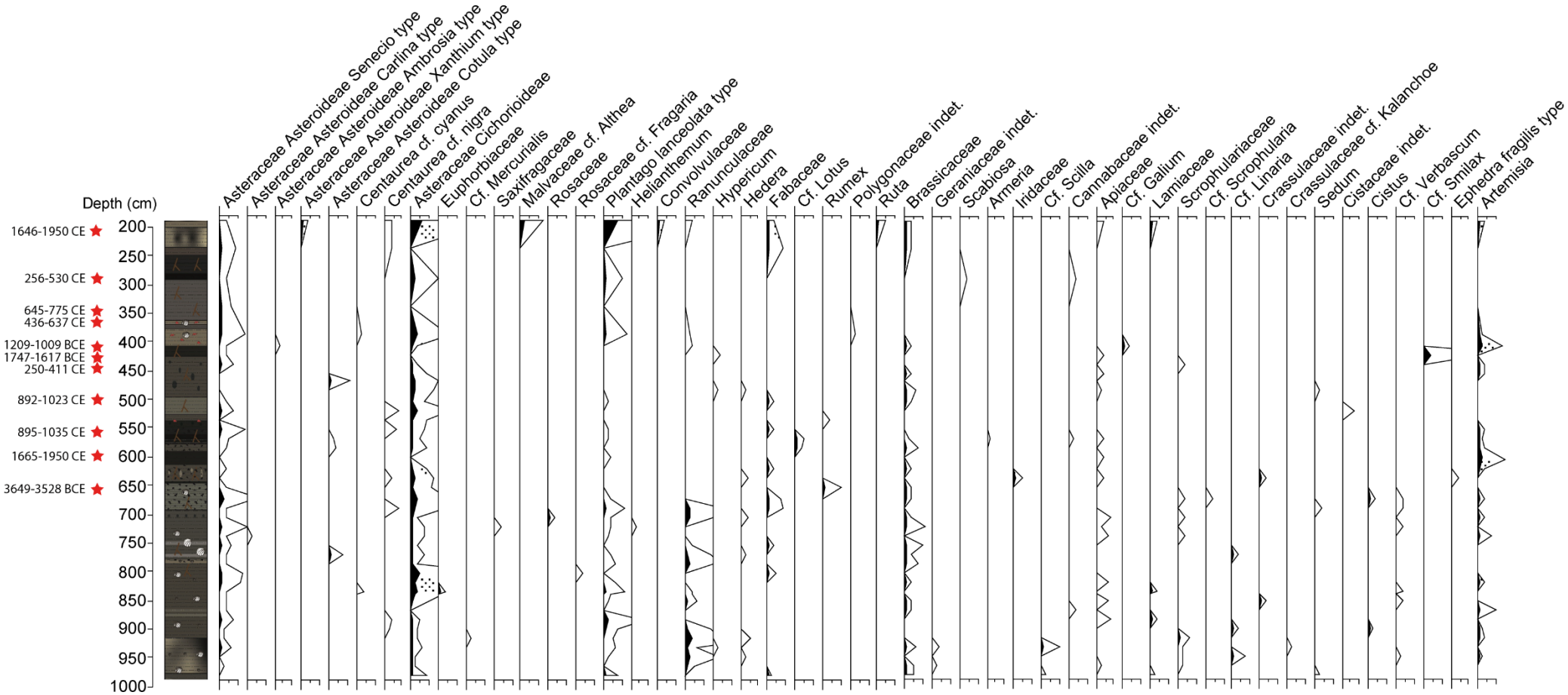

Fig. 6: Detailed palynological diagram of the core POP22-01 (exaggeration 8x). Calibrated terrestrial dates are reported.

3.3 Vegetation (Figs. 5–8)

The vegetation recorded in core POP22-01 exhibits a relatively balanced distribution between arboreal and herbaceous species (Fig. 7), with a slight predominance of arboreal taxa in the lower sections of the core, below 672 cm depth, and a minor dominance of herbaceous taxa in the uppermost part, above 672 cm. From 982 to 672 cm, the mean percentage of arboreal species is 62.68%, reaching a maximum of 81.68% in the deepest samples. Conversely, from 672 to 188 cm, the average percentage of arboreal taxa decreases to 36.66%, with a minimum value of 23.79% observed in the uppermost sample. Shrubby taxa maintain low percentages throughout, with a mean slightly above 4% and never exceeding 12% (Fig. 7).

The deepest portion of the core, from the base to approximately 654 cm, is dominated by deciduous and evergreen oaks. *Quercus pubescens* type is the most abundant taxon, with an average value of 27.62% of the total pollen within this interval, reaching a peak of 48.14% in the lowermost section. However, this taxon shows a clear declining trend from the base toward the top of the interval. *Quercus ilex-coccifera* type is the second most abundant taxon, with an average of 13.56%, and, unlike *Quercus pubescens* type, it does not display a significant decreasing trend. In the short interval between 838 and 850 cm, both taxa experience an abrupt decline (*Q. pubescens* type drops to ~12%; *Q. ilex-coccifera* type to ~6%), followed by a rapid recovery to their previous average values. This decline and recovery are reflected also in the concentration values of the two taxa within this interval.

This event coincides with a temporary peak in Cyperaceae (up to approximately 33%). In the basal half of the core, the third most important arboreal taxon is *Pinus*, maintaining a stable average of 5% with minimal variation. Within the same interval, low but consistent occurrences of *Corylus* (3.66% on average), *Abies* (2.39%), and *Alnus* (2.13%) are also significant. Among the herbaceous taxa, Amaranthaceae (8.84%), Poaceae (8.79%), Ericaceae (4.65%), and the already mentioned Cyperaceae (6.86%) are dominant, although they never reach high values. All other taxa remain below 2% on average in this section (Figs. 5, 6, 8).

From approximately 700 to 400 cm depth, all major arboreal taxa slightly reduce their relative abundance compared to the lower portion of the core. *Quercus pubescens* type maintains significant but lower values (15.36%), as does *Quercus ilex-coccifera* type (8.92%). *Pinus* shows only slight variation from the previous interval (4.56% on average).

Corylus, *Abies*, and *Alnus* all decrease to between 1% and 2%, as do *Carpinus betulus* and *Carpinus orientalis* among other arboreal taxa. In contrast, this interval sees a marked increase in Cyperaceae, which maintains relatively high and stable values (18.12% on average). Hydrophytes also increase in relative abundance, particularly due to marked peaks of *Sparganium/Typha angustifolia* (mean 11.17%, with peaks up to 37.45%) and occasional high percentages of *Sagittaria* (peaks up to 19.91%). Unlike Cyperaceae, both *Sparganium/Typha angustifolia* and *Sagittaria* display fluctuating patterns with large sample-to-sample variability, rather than a consistent increasing trend. Amaranthaceae exhibit a pattern similar to that of hydrophytes, with marked fluctuations (mean 8.10%). Among other herbaceous taxa, Poaceae show only a slight increase (9.50%) and relatively stable values, while Ericaceae decrease slightly (3.73%). Apart from Asteraceae Cichorioideae (1.20%), all other taxa remain below 1% (Figs. 5, 6, 8).

In the uppermost section of the core (400–188 cm), *Quercus pubescens* type further declines (11.27%), and *Quercus ilex-coccifera* type drops more significantly (to 4.76%). In contrast, *Pinus* shows a modest increase (mean 7.38%), particularly between 288 and 338 cm. *Olea* increases (1.11% average), reaching a maximum of 3.40% in the uppermost sample. Among other arboreal species, only *Carpinus orientalis* (2.89%) and *Alnus* (1.60%) exceed 1%. Cyperaceae show a sharp and sudden decrease, with a mean of 3.57%. Hydrophytes, after an initial decline, increase again at 238 cm due to a peak in *Sparganium/Typha angustifolia* (20.83% of total pollen), and to a lesser extent *Lemna* (5.21%) and *Sagittaria* (4.17%). A particularly notable feature of this section is the steep rise in Amaranthaceae, which increase rapidly and reach a peak of 49.67% at 388 cm. In the overlying samples, their values gradually decline, yet they still maintain relatively high averages (~25%) throughout the upper part of the core. The uppermost sample also shows a significant spike in Caryophyllaceae (18.45%), well above previous values where this taxon rarely exceeded 1%. Poaceae remain stable at low percentages (5.27%), whereas Ericaceae show a slight increase (5.10% on average) compared to the previous interval. Among the taxa recorded during this phase, only Asteraceae Cichorioideae (2.06%) and *Plantago lanceolata* type (2.06%) exceed an average of 1%. Among Xerophytes, the most represented taxon is *Artemisia* (mean 0.29%, maximum 2.10%), with occasional occurrences of *Ephedra fragilis* type (Figs. 5, 6, 8).

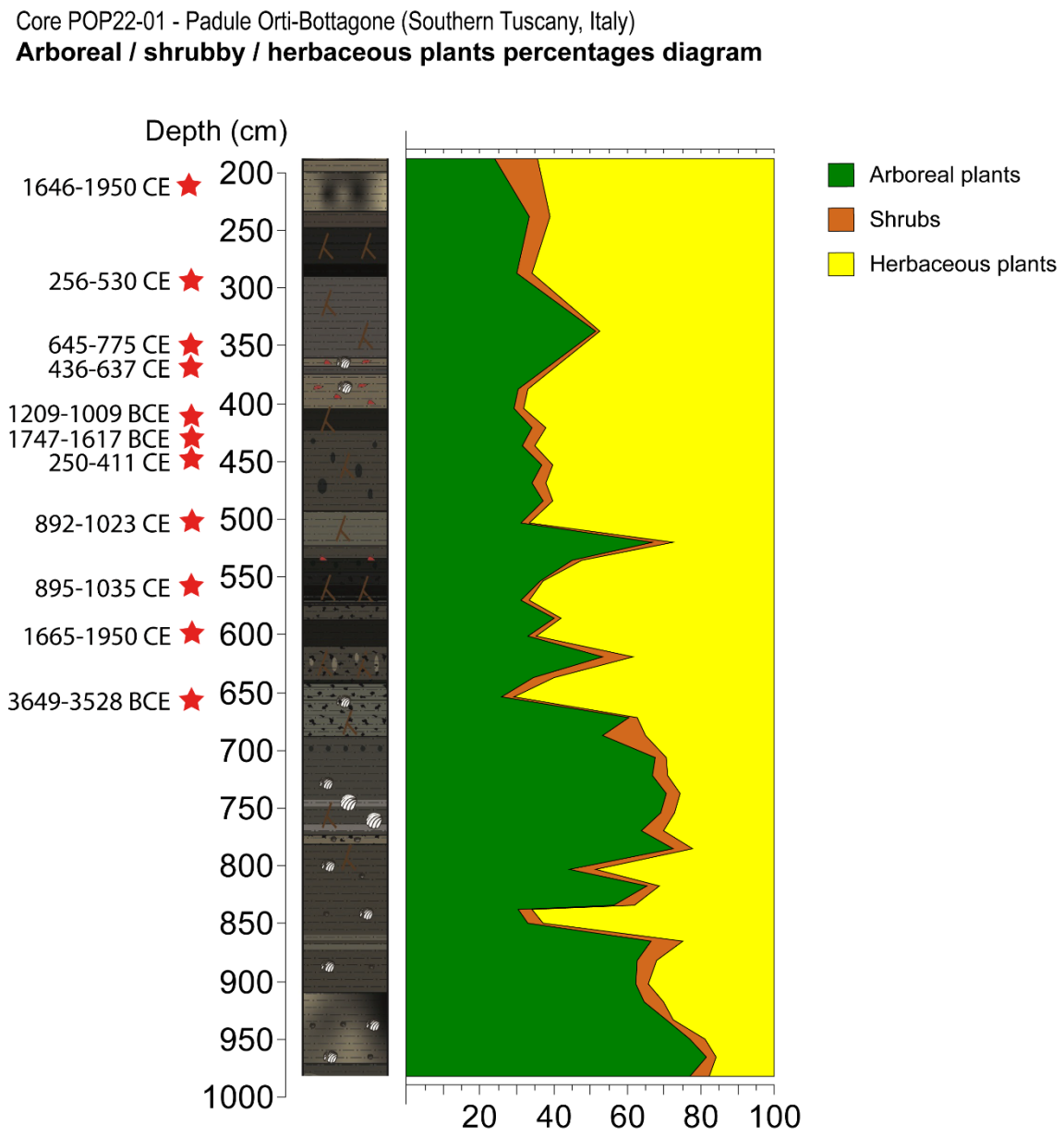

Fig. 7: Summary pollen diagram of arboreal / shrubby / herbaceous percentages of the core POP22-01. Calibrated terrestrial dates are reported.

Core POP22-01 - Padule Orti-Bottagone (Southern Tuscany, Italy)

Ecological groups diagram

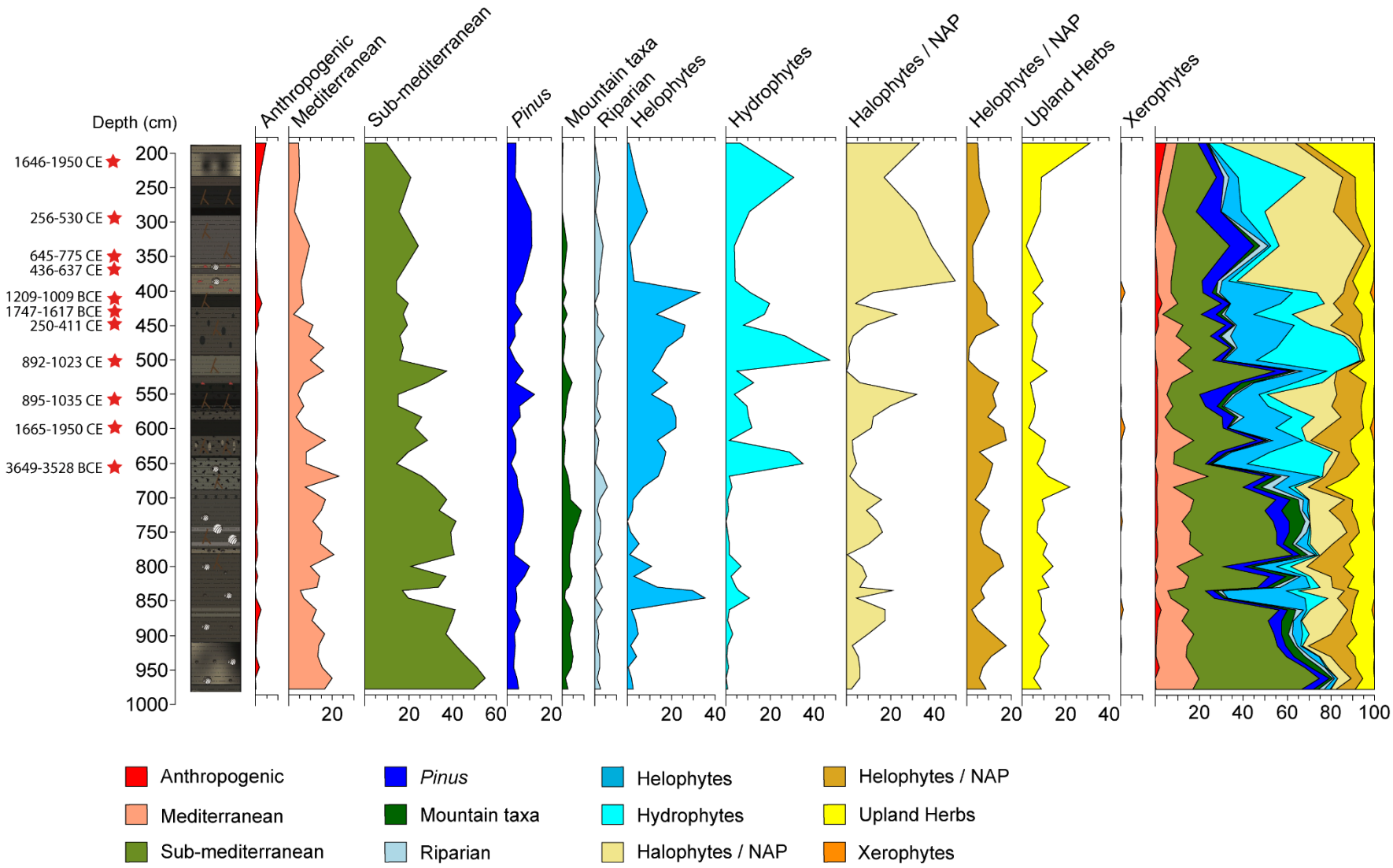

Fig. 8: Informal palynological groups percentages of the core POP22-01. Calibrated terrestrial dates are reported.

3.4 Pollen zones description (Figs. 9, 10)

The CONISS analysis allowed for the identification of three major pollen zones in the POP22-01 palynostratigraphic sequence (Figs. 9, 10). As with the previously discussed sites, the Hydrophytes group was excluded from the analysis to avoid the influence of an excessively local signal.

1. Zone POB-1 (982 cm to 672 cm) reveals an environment largely dominated by Mediterranean and Sub-Mediterranean elements, particularly by deciduous and evergreen oaks (*Quercus pubescens* type and *Quercus ilex-coccifera* type). Of these, *Quercus pubescens* type shows a strong dominance at the bottom of the core (constituting nearly half of the total pollen), before rapidly declining while still maintaining significant percentages (approximately 25% on average). *Pinus* shows a consistent occurrence around 5%. Other arboreal species, with the partial exception of *Corylus*, do not show significant percentages. Among montane species, *Abies* is the most frequent, though it never exceeds 7%.

   Within the herbaceous taxa, Helophytes/NAP and Upland Herbs exhibit relatively stable percentages, averaging around 9% throughout this interval. By contrast, Halophytes/NAP, here represented almost entirely by Amaranthaceae, show comparable mean values but considerably higher variability, ranging from near absence in some samples to over 20% of total pollen in others (e.g., at 838 cm).Helophytes are notably reduced (on average around 3%) in subzones POB-1c and POB-1a, whereas they reach very high values, exceeding30% of the total between 838 and 850 cm (POB-1b). This interval is distinct from both the preceding and succeeding subzones – which are relatively similar in their pollen spectra – specifically because of this peak in Helophytes, entirely attributable to the family Cyperaceae. This event coincides with a decline in the pollen of Sub-Mediterranean elements and a less pronounced decrease in Mediterranean, riparian, and montane elements. *Pinus* and the herbaceous groups do not appear to undergo significant changes, except for the Helophytes/NAP, which display a fluctuating pattern (Figs. 9, 10).
2. Zone POB-2 (672 cm to 405 cm) is characterized by a decline in Sub-Mediterranean elements, particularly *Quercus pubescens* type, which stabilizes at an average of 21.39% of the total pollen. Montane elements also decrease significantly, from an average of 4.02% in the previous interval to 1.73%. Mediterranean elements likewise

exhibit a slight decline, averaging 9.50%, while *Pinus* stabilizes at 4.56%. Sub-Mediterranean elements also show greater percentage variability than in the previous phase, particularly with relatively high values around 485 cm. The riparian group, by contrast, remains largely stable at low percentages, consistent with the previous zone.

This zone is also characterized by an expansion of the Helophytes – mostly composed of Cyperaceae – which continues until around 400 cm, averaging 18.12%. Among other herbaceous groups, Halophytes/NAP – again almost entirely represented by Amaranthaceae – show a slight decrease in percentages, but more notably, exhibit greater fluctuations than in the basal section of the core, with intervals of very low presence alternating with sharp peaks. Specifically, this group records two main peaks, at 554 cm (31.80%) and 437 cm (22.86%). Between these depths, however, its values drop sharply, with a complete absence at 520 cm. Helophytes/NAP also show variable percentages in this pollen zone. They decrease notably between 520 and 469 cm (dropping below 1% at 504 cm), coinciding with the above-mentioned reduction in Halophytes/NAP and relatively elevated Helophyte values. Upland Herbs exhibit a slight decline compared to the previous zone, without showing significant changes or clear trends during this phase (Figs. 9, 10).

3. Zone POB-3 (405 cm to 188 cm) is marked by the persistent decline of Mediterranean (averaging 5.66%) and Sub-Mediterranean (16.92%) elements. Among Mediterranean taxa, this trend is largely due to the decrease in *Quercus ilex-coccifera* type. Among Sub-Mediterranean taxa, *Quercus pubescens* type continues the decline observed in earlier phases and stabilizes at around 11%. There is also a slight increase in *Carpinus orientalis*, though it remains at very low percentages. Montane elements also decrease significantly in this phase, averaging less than 1% of the total, with declining occurrences of *Abies* and the near disappearance of *Fagus*. In contrast, *Pinus* shows a slight increase compared to earlier phases, averaging 7.38%. Anthropogenic taxa also increase, largely due to the rise of *Olea*, and their values double compared to previous phases, reaching an average of 1.57%. Riparian elements, however, do not show any significant changes.

   Among herbaceous taxa, Helophytes show a pronounced decrease compared to the previous zone, dropping to 3.57%. Halophytes/NAP, especially Amaranthaceae, show a sharp rise, peaking at nearly 50% of the pollen in the 388 cm sample and then gradually declining toward the top. In the uppermost sample (188 cm depth),

Caryophyllaceae exhibit a sharp increase, reaching 18.45%, and combining with similar values of Amaranthaceae.

Helophytes/NAP maintain stable percentages in this zone but are lower than in previous zones, averaging 5.27%. In this phase, both Poaceae <20 μm and Poaceae 20–40 μm follow comparable trends. Upland Herbs increase to an average of 12.09%, higher than in earlier zones, and show a strong upward trend toward the top of the core, reaching 31.07% of the pollen in the most superficial sample. This increase is initially driven by a rise in Ericaceae starting at 288 cm, followed in the uppermost sample (188 cm) by increases in Asteraceae Cichorioideae and *Plantago lanceolata* type. Xerophytes do not exhibit significant variations throughout the core, maintaining average percentages below 0.50% across all zones (Figs. 9, 10).

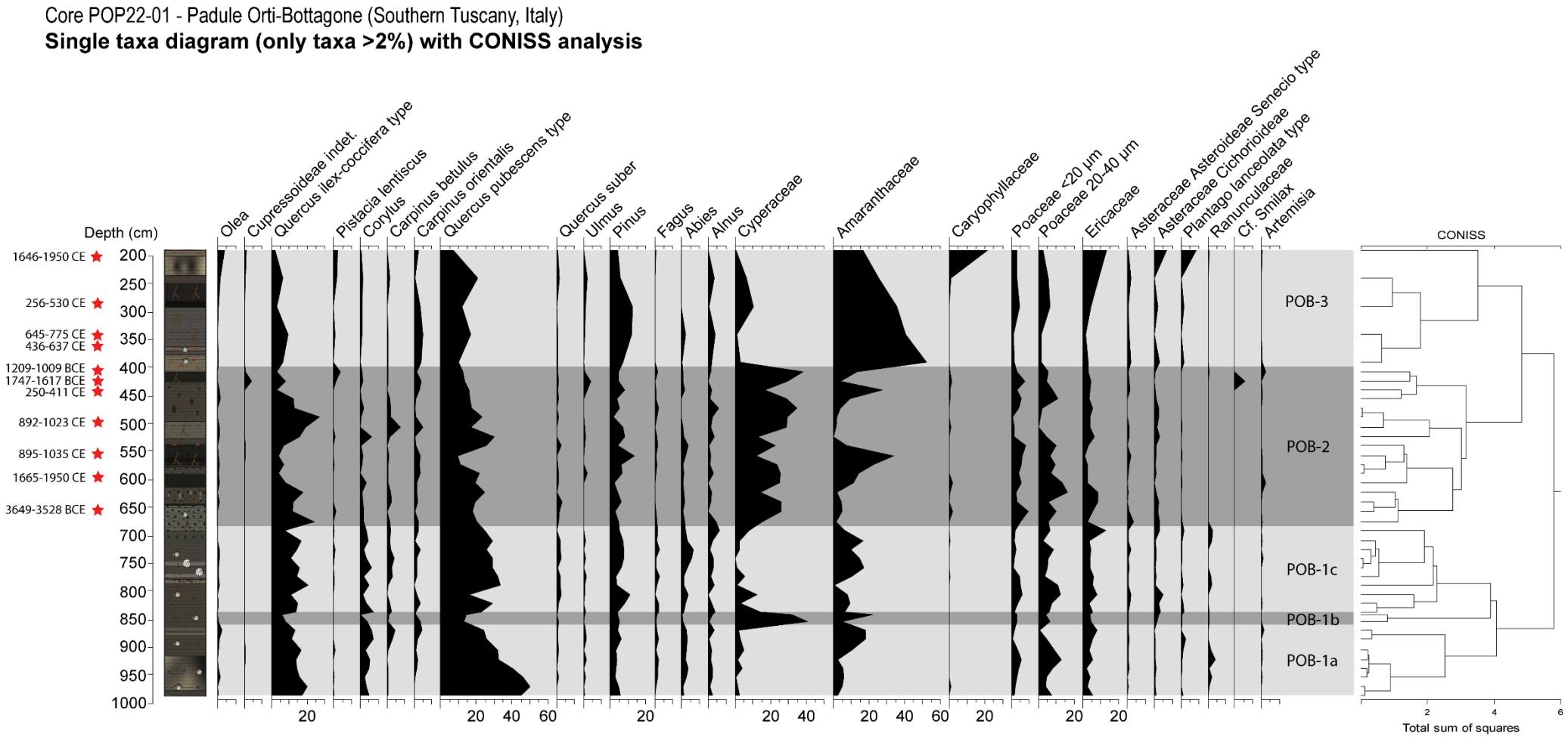

Fig. 9: Single taxa diagram with CONISS analysis and subdivisions of the zones. Only taxa reaching 2% in at least one sample were considered in the analysis. Calibrated terrestrial dates are reported.

Core POP22-01 - Padule Orti-Bottagone (Southern Tuscany, Italy)

Ecological groups diagram with CONISS analysis

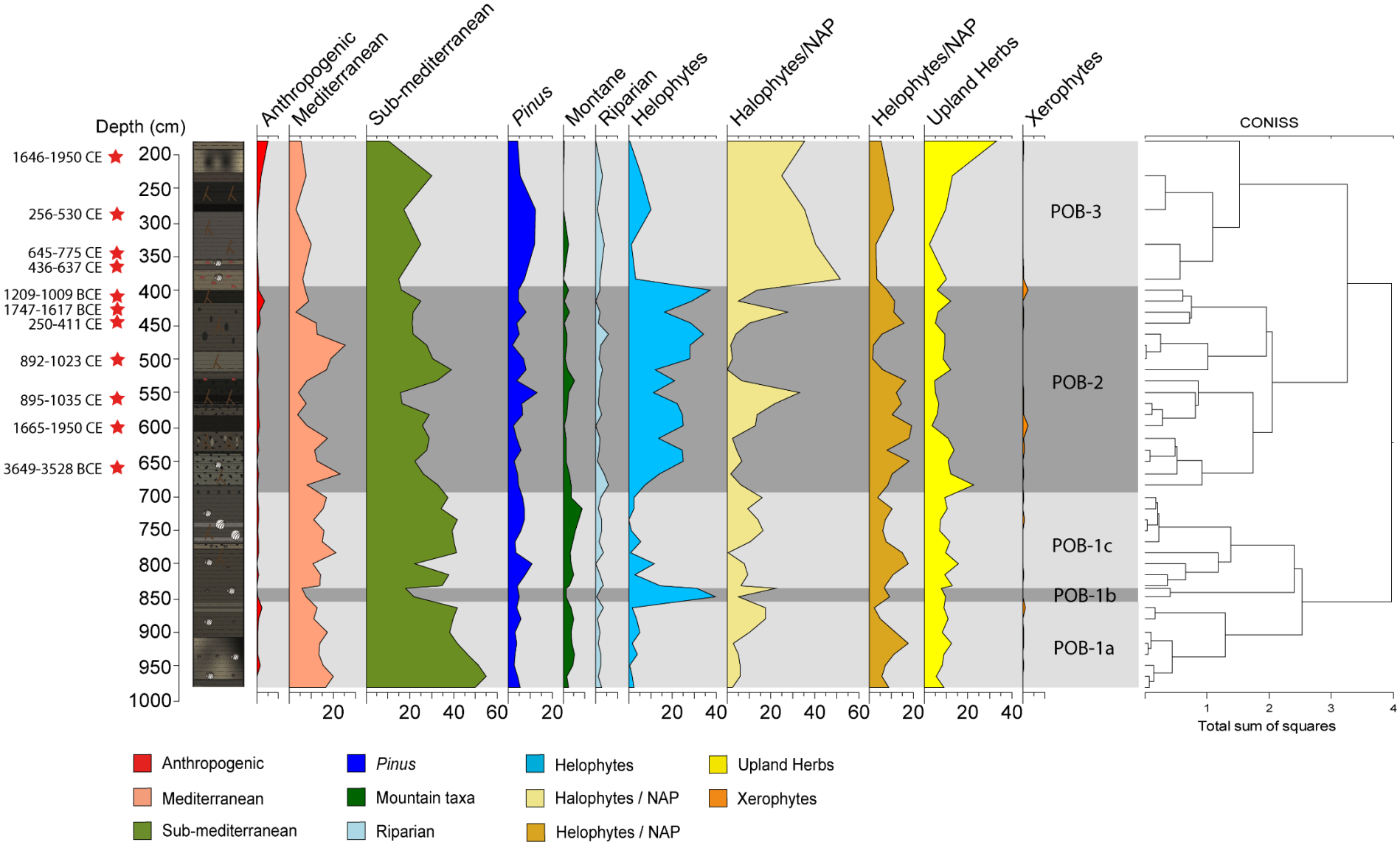

Fig. 10: Informal palynological groups diagram with CONISS analysis and subdivisions of the zones. Hydrophytes have not been considered in the analysis and thus are not represented in the graph. Calibrated terrestrial dates are reported.

3.5 NPP (Fig. 11, 12)

In core POP22-01, non-pollen palynomorphs (NPPs) are significantly less abundant than pollen (Fig. 11), averaging 7.23% of all palynomorphs. Only the basal samples (between 982 and 934 cm depth) exhibit higher NPP proportions, averaging 21.77%, while samples above 934 cm show a stable average of 4.54% with no marked variation along the core (Fig. 11).

The elevated NPP percentage near the core bottom is related to high dinocyst concentrations. Between 982 and 934 cm, indeed, indeterminate dinocysts (Dinocysts indet. morphotype 1) average 53.74% of NPPs, peaking at 64.29% at 934 cm. Other dinocysts are also abundant: *Lingulodinium* averages 20.71% of total NPP in this interval, with a maximum of 42.71% at the deepest sample (982 cm), while *Spiniferites* reaches 11.38% on average and peaks at 42.11% at 902 cm. In this same interval, a pronounced peak of *Botryococcus* (66.67%) is also recorded, stratigraphically restricted to 918 cm, while the taxon is absent in the immediately preceding and following samples. Also at 918 cm, dinocyst indet. type 2 appears at 6.67%, otherwise absent throughout the core. In this interval fern spores (pteridophyte spores) are present and rapidly increasing monolete spores are scarce from the bottom until 934 cm, then rise sharply to peaks of 30.00% at 882 cm and 50.00% at 850-838 cm (Fig. 12).

In the sections above 934 cm, dinocyst percentages gradually decline, though with high variability, and disappear by 706 cm. Indeterminate dinocysts reappear only at 504 cm. Between 882 and 586 cm, *Pseudoschizaea* occurs in noteworthy and highly variable percentages, exhibiting substantial fluctuations even between adjacent samples. The taxon displays peaks at 40-50% of NPPs at 882, 803, 688, 654, 620, and 586 cm depth. *Botryococcus* is absent throughout this section, except for a 50.00% peak at 786 cm that complements the one at 918 cm. Indeterminate algae (algae indet. morphotype 1) are highly discontinuous, absent in many samples but reaching percentages around 40% at 850, 637, and 554 cm. During this phase, relatively high percentages of both monolete and trilete spores are recorded, with mean values for each group around 34% within this interval. These two groups show episodes of pronounced dominance in the NPP assemblage: monolete spores exhibit numerous peaks reaching or exceeding 50% (in addition to the one previously noted at 850-838 cm, also at 688-672 cm and 554-570 cm), while trilete spores reach even higher values, exceeding 50% at 754, 520, and 485 cm, 60% at 818-834 cm and 672-654 cm, and attaining a maximum of 83.33% at the peak

recorded at 602 cm. These phases of rapid increase are almost always followed by sharply lower percentages in subsequent samples, and in some cases, the taxon is entirely absent. Among other spore types, *Polypodium* shows sporadic increases, with isolated peaks ranging from 7% to 10% at 882, 803, and 706 cm, and later exceeding 20% at 620 cm and 485-469 cm. Finally, a single occurrence of foraminiferal linings is observed at 536 cm, where they account for 20% of the NPPs (Fig. 12).

In the upper section of the core, above 504 cm, a new slight increase in indeterminate dinocyst percentages is observed, with peaks ranging between 10% and 20% at 504, 421-405, 288, and 188 cm. *Pseudoschizaea* shows a sharp increase starting from 520 cm, reaching 42.86% at 453 cm. Thereafter, the genus exhibits strong fluctuations up to the top of the core, attaining 30.00% at 188 cm. Indeterminate algae experience a very abrupt increase beginning at 421 cm, reaching around 55% of total NPPs at 405 and 288 cm. From 421 cm to the top of the core, they maintain an average of 30%, albeit with notable variability. In this section, *Botryococcus* reappears at low percentages at 421 cm and 288 cm. Additionally, the genera *Spirogyra* and *Cosmarium* are documented at 238 cm and 188 cm, respectively. Pteridophyte spores continue to show high and highly variable values. Monolete spores display distinct peaks at 437-421 cm (reaching 53.33%) and at 238 cm (reaching 66.67%). Trilete spores again account for 50.00% of total NPPs at 437 cm and 42.86% at 338 cm (Fig. 12).

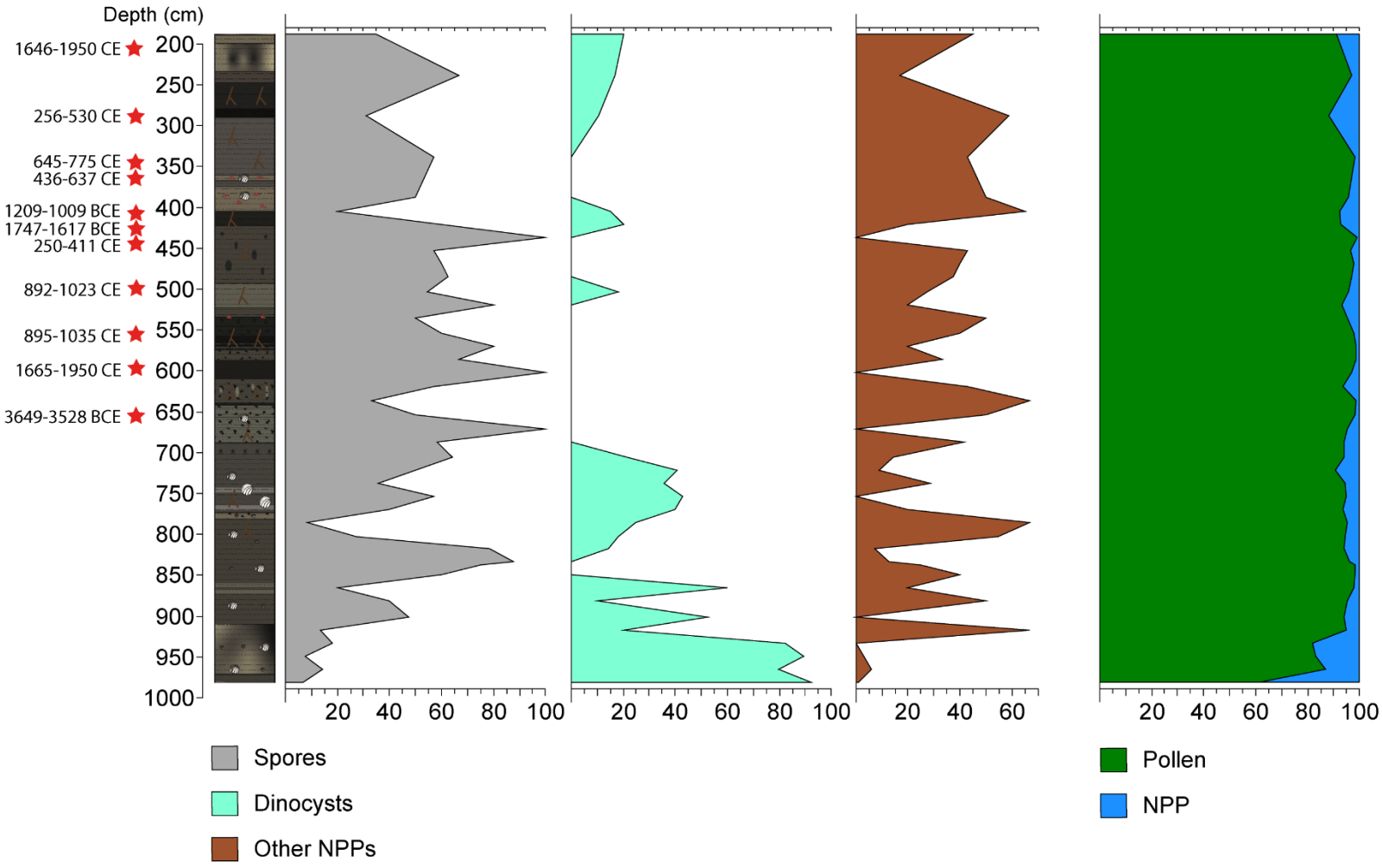

Fig. 11: percentages of various types of NPPs on the total NPPs (left); percentages of pollen and NPP on the total palynomorphs of the core POP22-01 (right). Calibrated terrestrial dates are reported.

Core POP22-01 - Padule Orti-Bottagone (Southern Tuscany, Italy)

Single taxa diagram (NPP)

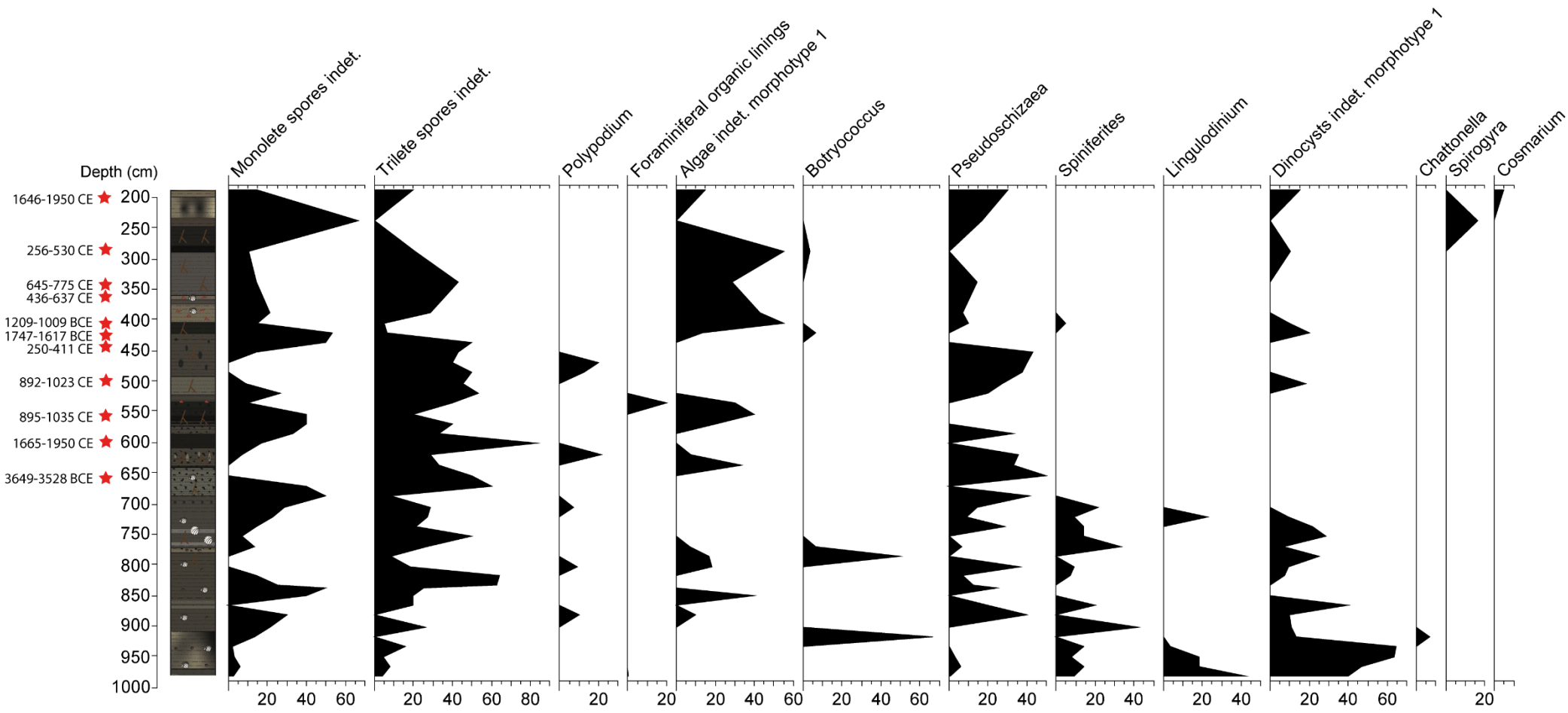

Fig. 12: Detailed palynological diagram of the core POP22-01, showing NPP taxa. Calibrated terrestrial dates are reported.

4. *Surface samples*

4.1 Palynological analysis of moss samples (Figs. 13–16)

Five moss samples from the Orti-Bottagone site were collected and analysed (Fig. 16; Chapter 2, Fig. 5, Tab. 2)). Three were collected in January 2022 (MOSS1 OBS1-22, MOSS 2 OBS1-22, MOSS3 OBS1-22) and two (MOSS1 OBS1-23, MOSS2 OBS1-23) in January 2023. For brevity, the acronym OBS is omitted in the following section.

All samples show comparable proportions of arboreal and herbaceous taxa. Arboreal taxa are slightly predominant only in MOSS1 1-22 (where they account for 57.01% of the total pollen) and in MOSS2 1-23 (64.47%).

All samples (Figs. 13, 14) show a tree pollen composition essentially dominated by four species: *Olea*, *Quercus ilex-coccifera* type, *Quercus pubescens* type, and *Pinus*. In samples MOSS1 1-23 and MOSS2 1-23, *Pistacia lentiscus* also appears in notable amounts among the Mediterranean elements.

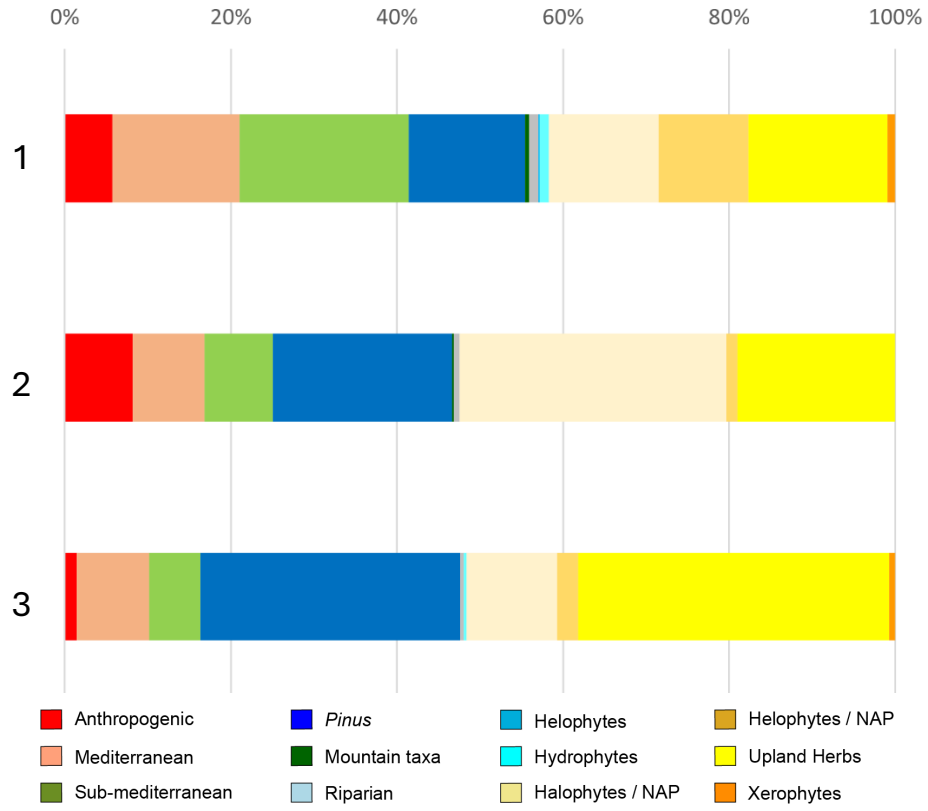

Fig. 13: Percentages of pollen content of moss samples collected in 2022 from the Orti-Bottagone site, subdivided by informal palynological group. Y-axis labels: 1 = MOSS1 OBS1-22; 2 = MOSS2 OBS1-22; 3 = MOSS3 OBS1-22.

Anthropogenic species contribute variably to the total pollen, with 5.73% in MOSS1 1-22, 8.21% in MOSS2 1-22, and 1.45% in MOSS3 1-22. In the 2023 samples, they reach 1.98% in MOSS1 1-23 and 6.02% in MOSS2 1-23. In all cases, *Olea* is the dominant element of this group, though indeterminate Cupressoideae, *Juglans*, and cereals are also recorded.

Mediterranean species are well represented in all samples, though with considerable variation. They account for 15.29% in MOSS1 1-22, decreasing to 8.64% in MOSS2 1-22 and remaining similar in MOSS3 1-22 (8.73%). In the later samples, MOSS1 1-23 and MOSS2 1-23, values are 6.75% and 16.91% respectively. Within this group, the most abundant taxon is *Quercus ilex-coccifera* type, followed by *Pistacia lentiscus*. Also present are *Phillyrea*, *Tamarix*, *Ligustrum*, *Pistacia terebinthus*, and *Myrtus*.

Sub-Mediterranean species stand out as one of the most significant arboreal groups, particularly in MOSS1 1-22, where they constitute 20.38% of the total pollen. Their percentages decline noticeably in MOSS2 1-22 (8.21%) and MOSS3 1-22 (6.18%). In MOSS1 1-23 and MOSS2 1-23, Sub-Mediterranean taxa account for 9.92% and 12.32%, respectively. The dominant taxon in this group is *Quercus pubescens* type, accompanied by *Carpinus orientalis*, *Fraxinus excelsior*, *Quercus suber*, and *Corylus*, as well as other taxa present in minor percentages.

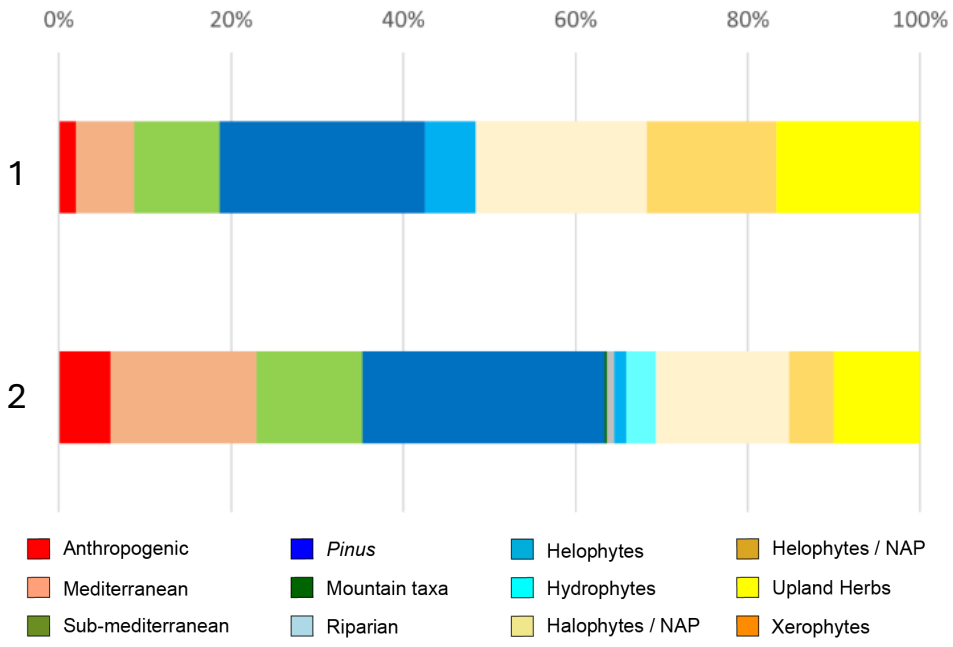

Fig. 14: Percentages of pollen content of moss samples collected in 2023 from the Orti-Bottagone site, subdivided by informal palynological group. Y-axis labels: 1 = MOSS1 OBS1-23; 2 = MOSS2 OBS1-23.

The genus *Pinus* is the dominant arboreal taxon in all samples. It records its highest value in MOSS3 1-22 (31.27%) and maintains significant values across the samples: 14.01% in MOSS1 1-22, 21.60% in MOSS2 1-22, 23.81% in MOSS1 1-23, and 28.08% in MOSS2 1-23. In the latter two samples, it also represents the dominant ecological group when herbaceous taxa are included. Other arboreal plant groups are poorly represented in all samples, with average percentages below 1%: montane elements peak at 0.48% (in MOSS1 1-22), while riparian species range between 0% and 1.11%.

Among herbaceous species, Helophytes are virtually absent in the 2022 samples but are present at 5.95% in MOSS1 1-23 and 1.43% in MOSS2 1-23. The group is represented solely by the Cyperaceae family. Hydrophytes are also reduced, with the highest value recorded in MOSS2 1-23 (3.44%), and appear scarce or absent in the other samples. They include the genera *Sparganium*/*Typha angustifolia* type, *Potamogeton*, and *Sagittaria*.

Halophytes/NAP are represented in all samples, with moderately significant but highly variable percentages. The maximum value is recorded in MOSS2 1-22 (32.18%), while they are lower in MOSS1 1-22 (13.22%) and MOSS3 1-22 (10.91%). The 2023 samples show slightly higher percentages (19.84% in MOSS1 1-23, 15.47% in MOSS2 1-23). The group is composed almost exclusively of Amaranthaceae, which clearly dominate its composition, but Caryophyllaceae and the genus *Limonium* are also present. Helophytes/NAP show very variable values across samples, being high in MOSS1 1-23 (15.08%) and MOSS1 1-22 (10.83%), and much lower in MOSS2 1-22 (1.30%), MOSS3 1-22 (2.55%), and MOSS2 1-23 (5.16%).

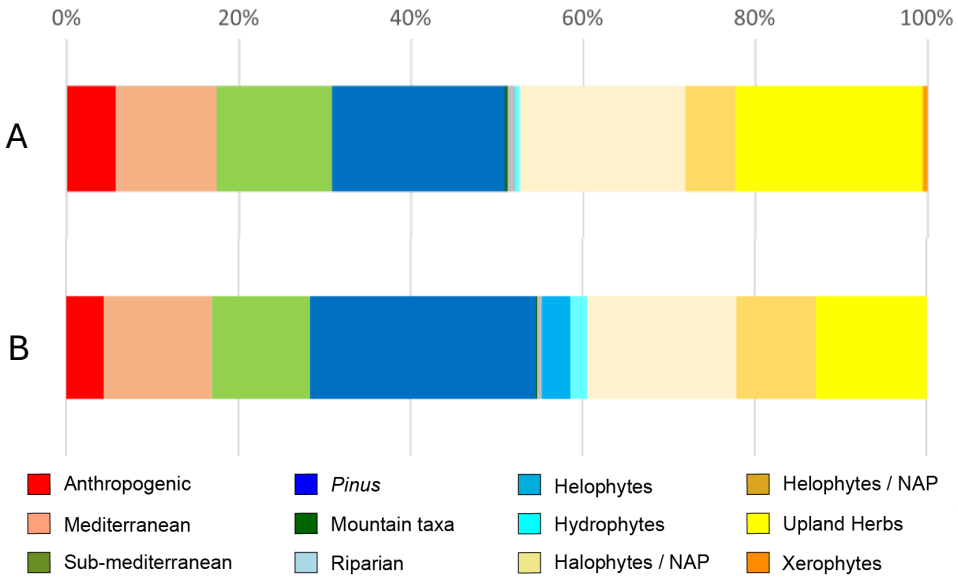

Fig. 15: Cumulative percentage of pollen content of moss samples collected in 2022 (A) and 2023 (B) in the Orti-Bottagone site, subdivided by informal palynological group.

Upland Herbs are a significantly represented group. MOSS2 1-22 registers the highest percentage (32.18%). MOSS1 1-22, MOSS3 1-22, and MOSS1 1-23 show values between 16% and 19%, while the lowest value is in MOSS2 1-23 (10.03%). The most represented taxa include Asteraceae Cichorioideae, Apiaceae (more abundant in the 2022 samples, averaging over 5% of total pollen), *Plantago lanceolata* type, Brassicaceae, and Ericaceae (especially in MOSS1 1-22). Asteraceae Cichorioideae show significant percentages in all samples, but display a marked increase in MOSS3 1-22 (22.55%). All other Upland Herbs taxa average below 1%. Xerophytes are very poorly represented (<1%) in MOSS1 1-22 and MOSS3 1-22, and absent in the remaining samples. This group includes *Artemisia* and *Ephedra fragilis* type (Figs. 13, 14).

The comparative analysis of the cumulative pollen composition in mosses collected from the site in 2022 and 2023 (Fig. 15) reveals a picture of substantial stability, with some slight compositional differences. In both years, the predominant ecological groups are *Pinus*, Halophytes/NAP, Helophytes/NAP, and Upland Herbs, together accounting for the majority of the pollen content. However, 2023 shows a slight increase in *Pinus* compared to 2022, accompanied by a modest increase in Helophytes and Hydrophytes, which were nearly absent in the previous year. The Helophytes/NAP group also shows a slight increase.

Conversely, the percentages of Halophytes/NAP and, more markedly, Upland Herbs decrease in 2023. The contribution of anthropogenic species also appears slightly reduced in 2023, though still visible in both years. Mediterranean and Sub-Mediterranean components remain relatively stable, while montane taxa, riparian species, and Xerophytes continue to be consistently marginal in both years.

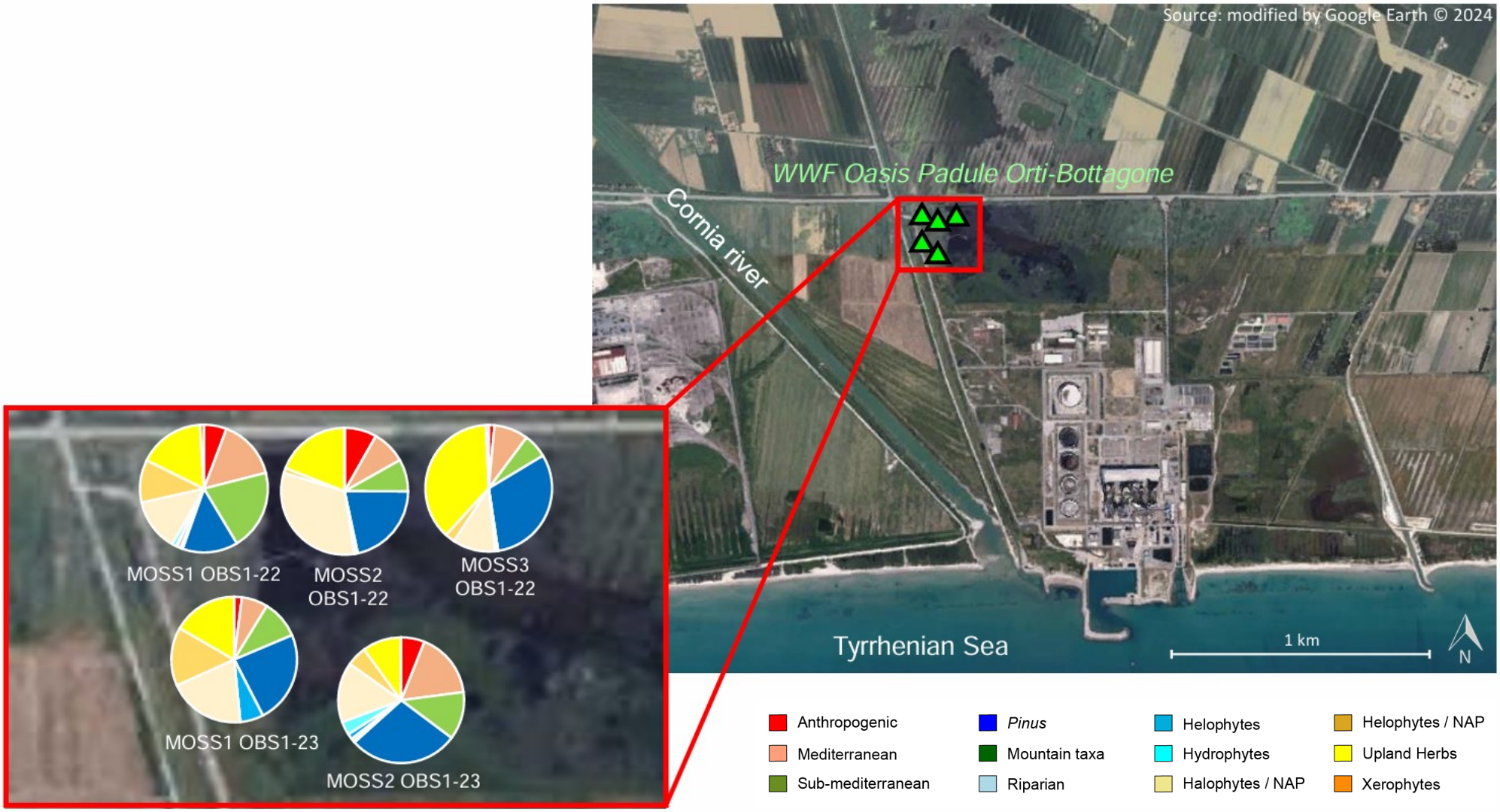

Fig. 16: Pie charts and geographical position of moss samples collected at the Orti-Bottagone site.

Discussion

5. *Strengths and weaknesses of the study*

The Orti-Bottagone record, obtained from the Cornia River coastal plain, aims to reconstruct long-term vegetation, hydrological, and anthropogenic dynamics within one of the most transformed areas of the Tyrrhenian coastal landscape. Located between the Cornia River mouth and the Gulf of Follonica, the present WWF wetland preserves a remnant of the once extensive Tuscan coastal marshlands, whose stratigraphy reflects the interplay of natural and human-driven processes such as drainage, agriculture, and industrial activity. This complex history makes Orti-Bottagone a key site for exploring human-environment interactions and Holocene landscape evolution in southern Tuscany.

This study presents several notable strengths. The Orti-Bottagone core represents one of the few continuous sedimentary archives available for the Cornia coastal plain, and its depth extends the temporal framework of comparison beyond that of Burano and Orbetello, offering complementary insights at the millennial scale. The integration of multiple proxies (pollen, NPPs, and ostracods) adds interpretative reliability, allowing the cross-validation of salinity and trophic changes through independent biological indicators. Finally, the site's geomorphological and environmental setting, situated at the convergence of fluvial, lagoonal, and anthropogenic processes, makes Orti-Bottagone an exceptional observatory for exploring how small coastal wetlands record the cumulative effects of climate variability, land-use change, and geomorphological evolution in the lower Cornia basin.

The discussion that follows, however, must contend with significant chronological limitations. Radiocarbon dating of bulk sediment samples provided inconsistent or contradictory results. Given the depositional setting, a terrestrial calibration was adopted as the most conservative option, though the possibility of reworked or stratigraphically displaced organic fractions cannot be excluded. The absence of independent chronological markers (e.g., ^{210}Pb, ^{137}Cs, amino acid racemization) further complicates the establishment of a robust age-depth model. Potential sedimentary hiatuses or variable accumulation rates cannot be excluded, and therefore the temporal resolution of the record remains highly uncertain.

Considering these constraints, the interpretation will focus on the most coherent stratigraphic and palynological patterns, while avoiding deterministic chronological assignments. Emphasis will be placed on stratigraphically robust vegetation shifts, lagoonal and wetland proxies, and their possible correspondence with broader climatic oscillations or historically documented anthropogenic interventions. The aim is to extract reliable signals from the available multiproxy evidence, while explicitly acknowledging the interpretative limits imposed by the uncertain dating framework.

6. Interpretation of the chronological framework

6.1 Challenges in establishing a reliable chronology

The chronological reconstruction of core POP22-01 is hampered by significant uncertainties. Radiocarbon dating of sediment samples produced inconsistent and sometimes contradictory results (Tab. 1), with inversions that complicate the establishment of a coherent age-depth model. Unlike the Orbetello and Burano sequences, no ^{210}Pb-^{137}Cs-^{241}Am profiles were obtained for the uppermost sediments, and no auxiliary markers such as amino acid racemization or microplastic profiles are available. This absence of independent chronological anchors leaves radiocarbon as the sole dating tool, despite its evident limitations in this depositional context.

In principle, ^{210}Pb-^{137}Cs-^{241}Am activity profiles can provide robust constraints on sediment accumulation rates within the uppermost sediments (i.e., the last ~100–150 years). For the Orti-Bottagone record, however, this approach was not prioritised for two main reasons. First, based on the preliminary stratigraphic and paleoenvironmental assessment, the sequence was expected to be generally ancient, and therefore radionuclide dating, being essentially restricted to very recent sediments, would have provided information limited to the immediate core top, with little relevance for constraining the deeper part of the record. Second, palynological sampling was intentionally focused on the interval between ~2 and 10 m in order to target older phases and intercept the Ancient period; consequently, any ^{210}Pb/^{137}Cs signal attributable to twentieth-century deposition would likely have been confined to the uppermost section, which was not the primary target of the palynological investigation. Moreover, because Orti-Bottagone is an onshore, reclaimed setting, the shallowest interval may not fully represent continuous primary deposition, but could be affected by surface disturbance and reworking, further

limiting the interpretative value of short-lived radionuclide profiles. Future work dedicated to the topmost section, with high-resolution sampling, would nonetheless be valuable to test the preservation of recent radionuclide markers and to independently constrain recent sedimentation and possible surface mixing processes at this site.

In the present setting of the Cornia alluvial plain, where the core site corresponds to a freshwater marshland, a terrestrial calibration has been adopted as the most appropriate option. Although geomorphological reconstructions indicate that the Cornia plain experienced lagoonal and coastal influence during parts of the Holocene (Amorosi *et al.*, 2004; Pieruccini & Susini, 2020; Pieruccini *et al.*, 2023), the modern continental environment of the Padule di Orti-Bottagone supports the use of a terrestrial calibration. Nevertheless, the possibility of reworked organic material of mixed origin (whether transported from upstream or derived from earlier lagoonal phases) must be considered when evaluating the basal radiocarbon ages.

These limitations imply that the sequence may span several millennia, but the depth-age relationship remains open to alternative hypotheses, including the possibility of major hiatuses or episodes of extremely low sedimentation. At present, no single chronological model can be considered definitive, and the results should be interpreted in terms of broad temporal trends rather than precise absolute ages. In this framework, the palynological record must be integrated with independent evidence, particularly the ostracod assemblages studied in parallel and regional stratigraphic reconstructions of the Cornia plain.

Together, these proxies provide critical constraints on environmental changes and help mitigate the uncertainty of the radiocarbon-based chronology. For these reasons, all paleoecological trends discussed below must be interpreted with caution and only at broad temporal scales. While the sequence captures long-term patterns of vegetation and environmental change, it does not currently permit fine chronological attribution or one-to-one correlation with external historical or climatic events.

6.2 Assessment of the radiocarbon chronology

Given the contradictory outcomes of the radiocarbon series, a dedicated assessment is necessary to evaluate the stratigraphic reliability of the dated levels. Overall, the sequence suggests three distinct stratigraphic domains with differing reliability.

In the upper portion of the core (0-432 cm), the radiocarbon ages are broadly consistent with stratigraphic order, indicating a general increase in age with depth. Minor reversals

occur, such as at 289 cm, where the age (256-530 CE) is slightly older than those immediately below (645-775 CE at 348.5 cm and 436-637 CE at 361 cm). More critically, the determination on bone at 361 cm (2434-2142 BCE) is entirely inconsistent with the surrounding levels (Tab. 1). Given both its anomalous position and its different nature compared to the other samples (plant remains), this age is best interpreted as intrusive, likely reflecting the reworking of older material into younger sediments. Despite these irregularities, the upper 4 m of the core can be treated as a broadly coherent sequence, although with recognized uncertainties.

A second stratigraphic unit between 442 and 599 cm yields ages that are strikingly out of order, showing progressively younger ages with increasing depth (250-411 CE at 442 cm down to 1665-1950 CE at 599 cm) (Tab. 1). This inversion strongly suggests that this part of the sequence is reworked, most plausibly representing a displaced or redeposited block of upper sediments emplaced at greater depth. For this reason, the chronological information from this interval cannot be considered stratigraphically reliable.

At greater depth (≥657 cm), a third unit is marked by radiocarbon ages that are both internally consistent and stratigraphically ordered. The ages range from 3649-3528 BCE at 657 cm to 6226-6077 BCE and 6373-6085 BCE at 1091 and 1286 cm, respectively, with the latter two determinations based on wood fragments (Tab. 1). The consistency of these ages, together with the nature of the dated material, provides moderate-to-high confidence that the base of the core reaches into the early Holocene, around the 7th millennium cal BCE. It should be noted that the palynological analyses cover the interval between 188 and 982 cm, while the two deepest radiocarbon determinations (1091 and 1286 cm) are stratigraphically below the pollen record. For the purposes of the palaeoecological discussion, the basal reference is therefore provided by the 1091 cm age (6226-6077 cal BCE), which represents the closest chronological anchor to the lowermost palynological sample (Tab. 1).

The recognition of these three domains has direct implications for the palaeoecological discussion. The interval 0-432 cm can be used with caution to reconstruct late Holocene vegetation dynamics, albeit with some local reversals and potential outliers. The section 442-599 cm, by contrast, should be treated as a disturbed interval with no chronological value. Finally, the sediments below ~657 cm provide the most reliable long-term framework, extending back to the mid-early Holocene, and thus represent a critical archive for reconstructing the earlier phases of environmental and vegetation history in the Cornia coastal plain.

7. Interpretation of the fossil palynological record

7.1 Pollen assemblages and vegetation changes

The pollen sequence of core POP22-01 reveals three main stratigraphic zones (POB-1 to POB-3) that reflect marked environmental and ecological transitions (Figs. 5–10).

1. POB-1 (982-688 cm, basal unit): the lowest part of the sequence is dominated by arboreal taxa, particularly deciduous oaks (*Quercus pubescens* group) and evergreen oaks (*Q. ilex-coccifera* type), which together form a stable Mediterranean/Sub-Mediterranean woodland signal. Conspicuous peaks of Cyperaceae, combined with the persistent presence of dinoflagellate cysts, indicate the influence of lagoonal or brackish environments during this early phase. Within this interval, alternating phases of halophyte expansion (notably Amaranthaceae) and hydrophyte proliferation (with a distinct episode of Cyperaceae dominance between 850 and 838 cm) suggest short-lived oscillations in salinity and water depth. This pattern suggests that the core site was initially located within a shallow coastal system, subject to marine inputs but fringed by extensive woodland.
2. POB-2 (688-405 cm, intermediate unit): a major reorganization occurs in the middle part of the core. Arboreal pollen declines, while Cyperaceae expand markedly, accompanied by repeated increases in hydrophytes, especially *Sparganium/Typha angustifolia* and to a lesser extent *Sagittaria*. Two main hydrophytic/helophytic phases can be distinguished: the first between 672 and 602 cm, and the second between 536 and 405 cm. The latter in particular is marked by an initial expansion of *Sparganium/Typha angustifolia* followed by a predominance of Cyperaceae. These hydrophytic phases alternate with renewed expansions of Amaranthaceae (notably between 602 and 536 cm), marking a sequence of shifting dominance between freshwater swamp vegetation and halophytic communities. These changes point to the progressive infilling of the coastal system and the establishment of freshwater swamp environments. The vegetation signal indicates a transitional phase from a lagoonal-brackish habitat toward a predominantly palustrine setting.
3. POB-3 (405–188 cm, upper unit): the upper sequence is characterized by a further decline in arboreal taxa and a strong expansion of non-arboreal pollen, especially

Amaranthaceae and Caryophyllaceae. Upland herbs (Asteraceae, Ericaceae, *Plantago lanceolata* type) also become more abundant, suggesting increasingly open landscapes around the basin. Anthropogenic indicators are frequent, with *Olea* reaching up to 11% and repeated occurrences of Cerealia-type pollen, documenting agricultural activities in the Cornia plain. As in the earlier units, hydrophytic taxa undergo marked oscillations, with *Sparganium/Typha latifolia* dominating from 288 to 238 cm, pointing to fluctuating freshwater conditions. The overall picture is one of intensified human impact on the surrounding vegetation, combined with evidence for fluctuating hydrological conditions within the wetland.

In sum, the pollen record documents a long-term transition from a coastal brackish system with surrounding oak woodlands (POB-1), to a freshwater swamp with alternating halophytic and hydrophytic phases (POB-2), and finally to an anthropogenically modified wetland embedded in an open cultural landscape (POB-3).

7.2 NPPs and associated lagoonal trophic shifts

The NPP record of core POP22-01, though less diverse than in the Orbetello and Burano sequences, provides important complementary information on the ecological history of the Cornia wetland (Figs. 11, 12).

1. In the basal unit (POB-1), dinoflagellate cysts occur repeatedly, corroborating the pollen evidence for lagoonal or brackish conditions during the early stages of sedimentation. Their association with Cyperaceae peaks suggests the persistence of transitional shore environments, where marine inputs alternated with freshwater influence.

   Notably, the Cyperaceae peak around 850-838 cm coincides with a sudden rise in *Pseudoschizaea*, a morphotype commonly regarded as an indicator of ecological instability. Its occurrence has been linked in different contexts to phases of increased catchment erosion, to stress in shallow aquatic settings (Van Geel, 2002), or to episodic hydrological disturbance such as fluctuating water levels (Gelorini *et al.*, 2011). In the Orti-Bottagone record, its abrupt peak may therefore signal a short-lived perturbation within an otherwise brackish-freshwater transitional setting, plausibly reflecting enhanced sediment input or transient water stress in the marsh environment.

Botryococcus appears only sporadically in this interval, indicating that eutrophic freshwater phases were occasional rather than dominant. The marked peaks at 918 and at 786 cm may reflect a brief eutrophic phase in standing freshwater bodies, possibly linked to reduced marine connectivity and transient water stagnation, before the subsequent establishment of swamp vegetation.

2. In the intermediate unit (POB-2), the disappearance of dinocysts coincides with the expansion of Cyperaceae and hydrophytes, marking the establishment of a stable freshwater swamp. *Botryococcus* remains rare, while non-pollen palynomorphs are dominated by *Pseudoschizaea* and unidentified algal morphotypes. Occasional peaks of pteridophyte spores, some exceeding 80% of total NPPs, may reflect episodes of hydrological stress or disturbance of the swamp margins.
3. In the upper unit (POB-3), the assemblage is dominated by pteridophyte spores and unidentified algal morphotypes, with occasional but noteworthy reappearances of *Botryococcus*. These sporadic algal increases suggest transient eutrophic phases within the wetland, possibly linked to anthropogenic nutrient inputs documented in the Cornia plain during historical times. The recurrence of spore peaks further supports the interpretation of unstable hydrological regimes in the recent past.

Overall, the NPP record aligns with the pollen-based reconstruction of environmental change. Dinocysts confirm the brackish conditions of the basal unit, while their disappearance and the spread of algal morphotypes point to the later dominance of freshwater swamp environments subject to episodic instability. Thus, the NPP record complements the pollen evidence by highlighting the ecological instability and alternation between oligotrophic and eutrophic states of the wetland.

7.3 Vegetation and NPPs trends in the climatic and historical context of the site

The integration of pollen and ostracod data from core POP22-01 provides a coherent picture of environmental dynamics in the Cornia coastal plain, despite the chronological uncertainties outlined above. The broad correspondence between the two proxies (Fig. 17) – with dinocysts and halophytic pollen dominating in the lower unit, and freshwater taxa expanding upward – suggests that the stratigraphic sequence, though affected by

possible reworking, preserves a meaningful record of local environmental change. This convergence reinforces the reliability of the palynological approach applied here.
A tentative comparison between the two proxies suggests that intervals dominated by halophytic vegetation in the pollen record tend to coincide with phases of increased eurihaline (*Cyprideis torosa*) and brackish-lagoonal marine (*Loxoconcha elliptica*, *Xestoleberis* spp.) ostracods, whereas phases characterized by freshwater swamp vegetation (Cyperaceae, *Sparganium/Typha angustifolia*) are broadly paralleled by higher proportions of freshwater to low-brackish taxa (*Candona* spp) (Fig. 17). Although the correlation is not perfectly synchronous at every transition, the overall coherence between pollen- and ostracod-based signals strengthens the interpretation of alternating salinity and hydrological regimes in the Cornia plain.

From a geological perspective, the observed alternation of halophytic and hydrophytic phases can be interpreted against the backdrop of the Holocene evolution of the Cornia plain. Stratigraphic reconstructions indicate that this sector of the Tuscan coast experienced repeated shifts between lagoonal and fluvial-marsh environments, driven by sea-level oscillations, deltaic progradation, and alluvial inputs (Amorosi *et al.*, 2004; Pieruccini & Susini, 2020; Pieruccini *et al.*, 2023).
In particular, the basal phases of POP22-01 are consistent with a shallow lagoonal-brackish setting, in line with the persistence of marine influence in the central-northern plain during the mid-Holocene. The subsequent dominance of hydrophytic pollen and low-brackish ostracods matches the progressive infilling of the lagoon and the transition to swamp environments, a trend also described in nearby sedimentary archives (Bianchini *et al.*, 2005; Zanon *et al.*, 2019). In this context, the alternation of halophytic and hydrophytic dominance within POB-2 could reflect the expression of major Holocene climatic oscillations, potentially including the 4.2 ka aridification event. Yet, given the weak chronological control of this section, any such attribution remains speculative.

If the early Holocene radiocarbon ages at the base of the core are accepted (ca. 7th millennium cal BCE), the sequence would also encompass a key transitional phase between the Neolithic and the onset of the Bronze Age in central Italy. This would place the earliest lagoonal signals of the Cornia plain within a broader framework of regional paleoenvironmental shifts, paralleled by other central Mediterranean records (Francke *et al.*, 2022; Zanon *et al.*, 2019).

Archaeological research confirms that the Val di Cornia was already frequented in these centuries, with evidence of early Neolithic communities exploiting the coastal resources and establishing small settlements in the hinterland. During the Bronze Age, the plain and its margins hosted more structured forms of occupation, as shown by funerary contexts and settlement traces linked to the wider network of exchanges across the Tyrrhenian basin (Dallai *et al.*, 2024; Pieruccini *et al.*, 2023). These data highlight the close relationship between the progressive infilling of lagoonal environments, the creation of fertile marshlands, and the strategies of prehistoric communities who inhabited and transformed this landscape.

At a broader historical scale, the record also intersects with phases of human activity in the Val di Cornia. The upper part of the sequence, where arboreal taxa decline and anthropogenic pollen (*Olea*, Cerealia-type) becomes frequent (Fig. 8), coincides with archaeological evidence for intensified land use from the Etruscan and Roman periods onwards (Biagi & Milletti, 2017, 2021; Dallai *et al.*, 2024; Di Pasquale *et al.*, 2014; Giroldini, 2010). The expansion of cultivated and ruderal taxa reflects the transformation of the coastal plain into a managed landscape, as confirmed by historical-archaeological studies of Populonia and its hinterland. In the Roman period, centuriation schemes documented in the Cornia plain testify to systematic planning and deforestation, consistent with the palynological signal of agricultural expansion. In later centuries, Medieval reclamation attempts and land-use practices further reshaped the area, as also mirrored in alternating signals of freshwater and halophytic vegetation (Clò *et al.*, 2024; Pieruccini *et al.*, 2021). Finally, in the modern period, despite repeated reclamation efforts, geomorphological constraints limited drainage success and extensive swamp environments persisted until recent centuries, a persistence mirrored in the pollen evidence for dominant hydrophytic taxa (Fig. 8). These oscillations reflect both natural hydrological variability and anthropogenic interventions on water circulation, consistent with the long history of human-environment interactions documented in this sector of Tuscany. Nevertheless, all chronological links to specific historical phases must be regarded as tentative, given the intrinsic uncertainty of the age model for core POP22-01.

Overall, while absolute dating remains fragile, the combined proxy evidence situates the Cornia plain within the broader trajectories of Holocene environmental change along the Tyrrhenian coast: from early lagoonal systems influenced by marine inputs to freshwater wetlands shaped by fluvial dynamics, and finally to a cultural landscape increasingly structured by human activities.

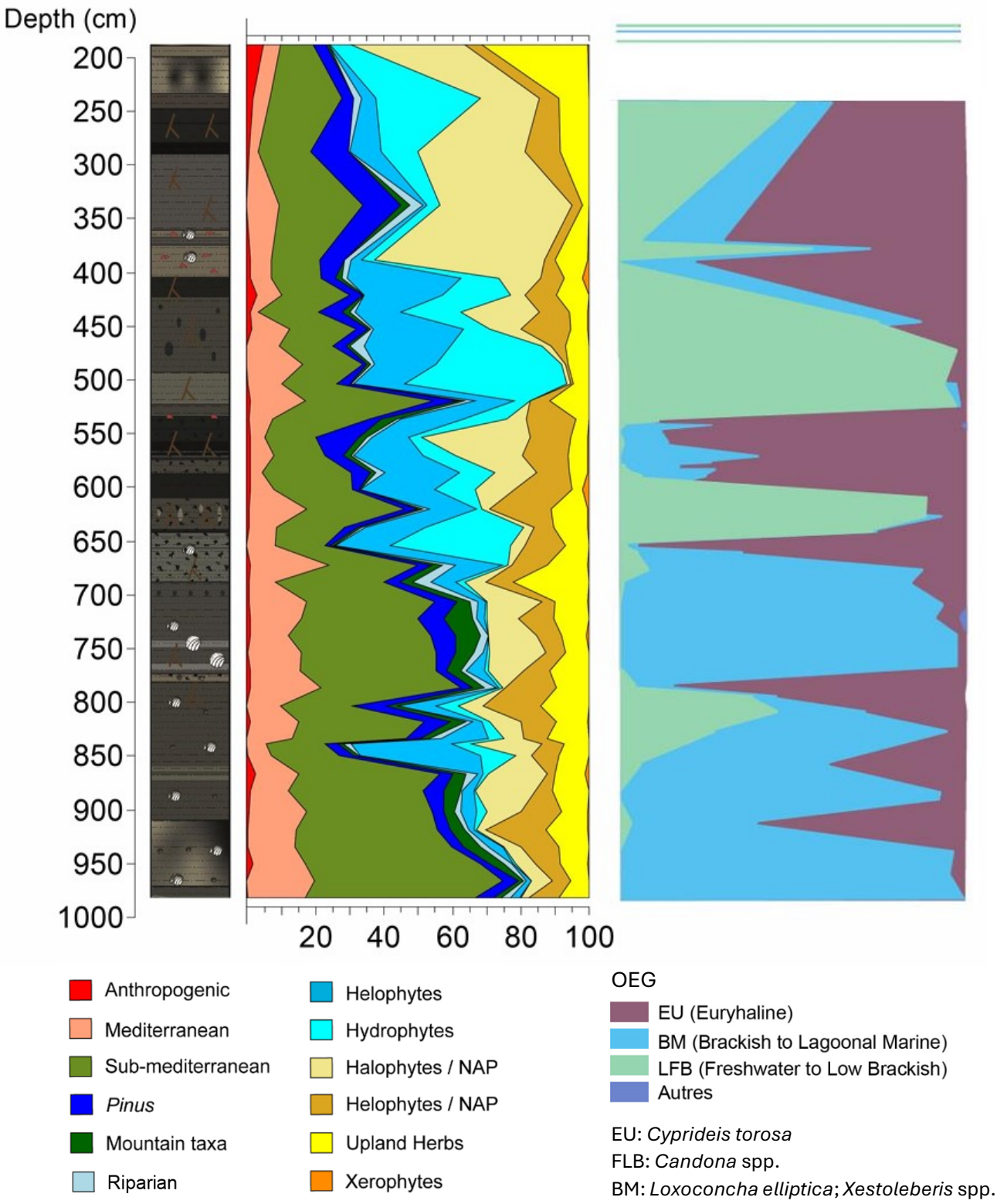

Fig. 17: Summary diagram of pollen informal palynological groups (left) and ostracod ecological groups (right) from core POP22-01 (Padule Orti-Bottagone). The ostracod diagram groups taxa into OEG, i.e., Ostracod Ecological Groups.
Ostracod spectrum modified from Cécile Vittori (2024).

8. Surface samples (mosses) (Figs. 13–16, 18, 19)

The analysis of the moss samples collected in 2022 and 2023 at Orti-Bottagone reveals a pollen spectrum dominated in its arboreal component by *Pinus*, *Olea*, and *Quercus* spp. (Figs. 18, 19), reflecting both the influence of widespread pine plantations and the persistence of Mediterranean/Sub-Mediterranean woodland patches in the surrounding area (Viciani & Lombardi, 2001). The consistent representation of olive pollen indicates the proximity of cultivated areas, while sporadic occurrences of Cerealia-type confirm the ongoing agricultural imprint on the coastal plain.

Halophytes (mainly Amaranthaceae) and upland herbs (particularly *Plantago lanceolata* type, Asteraceae Cichorioideae, and Apiaceae) are also frequent, highlighting the role of open disturbed habitats and the direct influence of the wetland-agricultural matrix that still characterizes the Orti-Bottagone site. Hydrophytic and helophytic taxa (Cyperaceae, *Sparganium/Typha angustifolia*, *Potamogeton*) further attest to the proximity of canals and residual marshland patches.

A comparison between the two sampling years shows a general stability in composition, with only minor shifts: an increase in *Pinus* in 2023, a slight decline in upland herbs, and variable halophyte frequencies. These limited changes are consistent with the relatively stable land-use and environmental configuration of the site in recent decades (Figs. 18, 19).

Overall, the surface samples capture the coexistence of natural, agricultural, and artificial components within the modern landscape of the Cornia plain. Importantly, they provide a valuable calibration for the uppermost part of the core, confirming that the dominance of pine, olive, and halophytic taxa in the recent pollen record is not an artifact of taphonomy but reflects the current vegetation mosaic and anthropogenic imprint of the area.

The strong representation of disturbance-related taxa, such as *Plantago*, Amaranthaceae, and Asteraceae Cichorioideae, further highlights the ecological impact of recent land-use practices. In addition to the agricultural signal, the ecological configuration of Orti-Bottagone has been strongly shaped first by the legacy of reclamation projects that redefined the coastal plain during the 20th century (Paolini, 2012), and later by the industrial expansion of the Piombino metallurgical district, which has added further layers of disturbance and transformation (Saragosa, 2019).

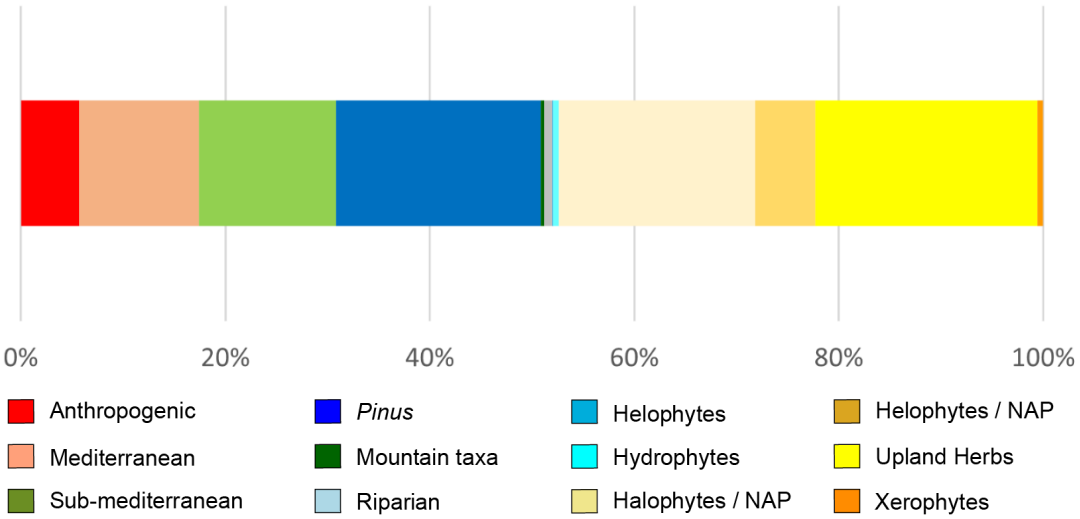

Fig. 18: Cumulative percentage of pollen content of moss samples collected in 2022 from the Orti-Bottagone site, subdivided by informal palynological group.

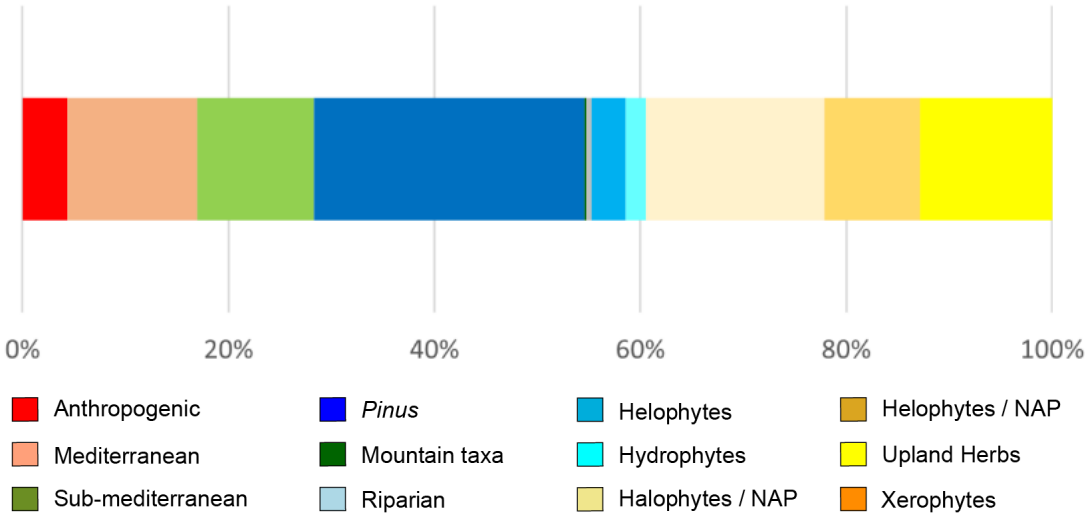

Fig. 19: Cumulative percentage of pollen content of moss samples collected in 2023 from the Orti-Bottagone site, subdivided by informal palynological group.

9. Synthesis and interpretive cautions

The POP22-01 sequence from Orti-Bottagone provides a rare long-term archive of environmental change in the Cornia coastal plain. Despite its limited resolution and fragile chronological framework, the record highlights a set of robust signals: the basal evidence for a lagoonal-brackish phase, the subsequent establishment of freshwater swamp conditions, and the eventual transformation into an open, anthropogenically shaped wetland. These transitions are broadly consistent with the known geomorphological evolution of the plain, where sea-level oscillations, deltaic progradation, and alluvial infilling alternated in shaping the landscape.

At the same time, major limitations persist. Radiocarbon inversions, the absence of independent chronological anchors, and the relatively coarse sampling strategy hinder the construction of a precise age-depth model. As a result, paleoecological patterns can only be interpreted at broad temporal scales, precluding any firm attribution to specific historical or climatic events. The pollen and NPP data, while internally coherent, thus need to be read as indicative of general trends rather than finely resolved episodes.

In a comparative perspective, Orti-Bottagone stands out for offering a deeper temporal window than Burano and Orbetello, potentially extending back to the early Holocene. However, this depth comes at the cost of lower chronological precision and reduced stratigraphic resolution. The value of the site lies therefore in complementing the more finely resolved but shorter sequences from the lagoons, allowing regional reconstructions to integrate both millennial-scale trends and centennial-scale dynamics. Together, these archives provide a more complete picture of the interplay between natural processes and human impact along the Tyrrhenian coast.

The forthcoming comparative synthesis across the three case studies will further assess these convergences and divergences, highlighting both shared regional trajectories and site-specific histories.

Chapter 6

Regional synthesis and conclusions

1. Objectives and regional framework

This thesis set out to investigate the environmental history of three key wetlands along the southern Tuscan coast – Burano, Orbetello, and Orti-Bottagone – through a multiproxy approach centred on pollen analysis and complemented by non-pollen palynomorphs, microplastics, and, where available, ostracods and other auxiliary indicators. The overarching goal was to reconstruct vegetation dynamics, trace the response of lagoonal and wetland ecosystems to both climatic oscillations and anthropogenic pressures, and evaluate the reliability and complementarity of different proxies in complex depositional contexts.

The southern Tuscan lagoons and wetlands represent a natural laboratory for exploring the long-term interplay between geomorphological processes, ecological transformations, and human activities. Their location along the Tyrrhenian coast has exposed them to millennial-scale sea-level changes, deltaic and fluvial inputs, and recurrent phases of reclamation and land use. At the same time, their proximity to major archaeological landscapes, from Etruscan and Roman Populonia to medieval and modern reclamation projects, provides a unique opportunity to link paleoenvironmental records with cultural trajectories.

Within this framework, the comparative study of Burano, Orbetello, and Orti-Bottagone allows us to move beyond single-site narratives. By placing the three cores side by side, it becomes possible to highlight common trends that reflect broader regional processes, as well as divergences that stem from local geomorphological or anthropogenic histories. The following sections synthesize these results and situate them within a wider Tyrrhenian and Mediterranean perspective.

2. *Chronological challenges and multiproxy constraints*

Establishing a robust chronological framework for coastal lagoon and wetland sequences is inherently challenging, as sedimentation may be discontinuous, affected by mixing and reworking, and characterised by strong spatial variability in accumulation rates. In this study, age control therefore relies on a combination of independent constraints, including radiocarbon dating, short-lived radionuclide profiles (^{210}Pb-^{137}Cs-^{241}Am) for the uppermost sediments where available, and complementary chronological information provided by amino-acid racemization (AAR) and stratigraphic coherence with sedimentological and palaeoecological signals.

The chronological control of the studied cores nevertheless remains limited by the small number of radiocarbon determinations per record, which restricts the robustness of age-depth reconstructions and increases the uncertainty associated with sedimentation-rate estimates and temporal correlations between sites. Especially in the cases of the Burano and Orbetello sites, radiocarbon dating was performed on bulk sediment samples (see Chapter 3, paragraph 2.1, and Chapter 4, paragraph 2.1) because no discrete terrestrial macro-remains or clearly identifiable short-lived organic material were consistently available in these lagoonal and wetland deposits, and because bulk material provided sufficient carbon for measurement across multiple stratigraphic levels. However, bulk sediments may incorporate mixed carbon sources (terrestrial and marine, as well as reworked or older organic matter), which makes the resulting ages potentially ambiguous. In addition, the choice between terrestrial and marine calibration curves (and the possible influence of reservoir effects) can lead to substantially different calibrated ages. For these reasons, the radiocarbon ages reported here should be considered as approximate chronological constraints, to be interpreted critically and in conjunction with independent evidence, including radionuclide trends, sedimentological markers, and the internal coherence of palynological and non-pollen palynomorph assemblages.

3. *Synthesis of site records*

Despite their differences in size, history, and stratigraphic resolution, the three investigated sites share several robust features that allow us to reconstruct common trajectories across the Tyrrhenian coastal wetlands.

To support this cross-site comparison, Tab. 1 provides a synthetic overview of the main climatic, historical and environmental events that frame the evolution of the southern Tuscan coastal basins and inform the interpretation of the pollen and NPP records. The table includes both drivers for which a clear imprint can be recognised in the analysed assemblages, and broader-scale processes documented in the regional literature that help contextualise site dynamics even when they are not directly captured by the studied cores. This distinction is particularly important where temporal coverage is restricted (e.g., the Burano LB5B core) or where chronological uncertainties prevent a precise alignment with discrete historical episodes. Therefore, the table should be read as a contextual framework guiding interpretation and comparison, rather than as a strict event-by-event correspondence with individual proxy fluctuations.

Fig. 1 provides a synthetic comparison of the three palynological records along a north–south transect of the southern Tuscan coastal basins (see Chapter 2, Fig. 1 for site locations). Because temporal coverage and chronological robustness differ between sequences, the proposed correlations should be considered conceptual rather than strictly isochronous. At the broadest scale, all sites document marked late historical to modern ecosystem shifts, expressed either through changes in arboreal versus open-land pollen signals or through pronounced variations in aquatic NPPs. The Orbetello record stands out for its dystrophic/eutrophic phases, highlighted by extreme *Botryococcus* dominance and the occurrence of microplastics, which suggest substantial recent disturbance and possible sediment mixing in the upper sequence. Burano, by contrast, captures only the uppermost portion of the sedimentary infill (marine-calibrated ~250 years) and provides a higher-resolution view of recent environmental dynamics. Orti-Bottagone offers a longer-term perspective on basin evolution, although the deepest radiocarbon constraints extend beyond the palynological log and therefore limit direct comparison at older depths. Overall, the comparison highlights shared trajectories of increasing anthropogenic influence and site-specific aquatic variability, while emphasising that local hydro-dynamics and site-specific taphonomic processes strongly modulate the expression of ecological change.

Time window	*Event type*	*Event (regional/local)*	*Sites mainly concerned*	*Main signals in pollen/NPP records*
~8000–7500 BP	Geomorphology / sea-level	Open lagoon phase in Tyrrhenian coastal basins	Burano (context)	Brackish/marine indicators possible (dinocysts), lagoonal taxa (D'Orefice *et al.*, 2020a) (context from literature; not recorded in this core)
~6000 BP	Geomorphology	Progressive lagoon closure and reduced marine exchange	Burano (context)	Shift towards more confined conditions; fewer marine indicators (D'Orefice *et al.*, 2020a) (context from literature; not recorded in this core)
~4000 BP	Geomorphology	Transition towards wetland/back-barrier environments	Burano (context)	Increased freshwater/wetland taxa; organic-rich deposits (D'Orefice *et al.*, 2020a) (context from literature; not recorded in this core)
~3000 BP onward	Human impact	Increasing anthropogenic pressure on coastal plains	Burano / Orbetello	More anthropogenic pollen (ruderal/grasslands, crops), coprophilous fungi
16th–19th centuries	Climate	Little Ice Age (regional cooling and hydroclimatic variability)	Regional	Possible shifts in hygrophilous taxa, erosion pulses, land-use sensitivity
Late 19th – first half 20th c.	Land-use / management	Major reclamation and drainage in Tuscan Maremma; wetlands transformed	Regional	Wetland contraction, increase of cultivated land signals, disturbance taxa (Novello, 2025)
Early 20th century	Ecosystem management	Reforestation/rehabilitation of Feniglia dune system	Orbetello	Rise of *Pinus* and planted dune vegetation; landscape stabilisation (local pollen rise)
1950s–present	Anthropocene proxy	Spread and accumulation of plastics in coastal environments	Burano / Orbetello	Microplastics occurrence; modern assemblage fingerprints
1970s–1990s	Eutrophication	Severe eutrophication and dystrophic crises culminating in 1992–1993 anoxic events	Orbetello	Very high *Botryococcus* / algae occurrence, fungal blooms, ecological instability (Lardicci *et al.*, 2001)
1994–1996 onward	Remediation	Mitigation measures: macroalgal harvesting, wastewater diversion, dredging/channel modifications	Orbetello	Decline of dystrophic signals; renewed marine influence (dinocysts/foraminiferal linings) (Lardicci *et al.*, 2001)
20th century (general)	Hydrosystem change	Increasing regulation of freshwater inputs, altered circulation, strong human control	Burano / Orbetello	Greater instability of NPPs, shifts in salinity proxies, episodic mixing/reworking

Tab. 1: main climatic, historical and environmental events that provide context for interpreting the pollen and NPP records from the southern Tuscan coastal basins. The table is intended as a conceptual framework for linking proxy changes to plausible regional and local drivers.

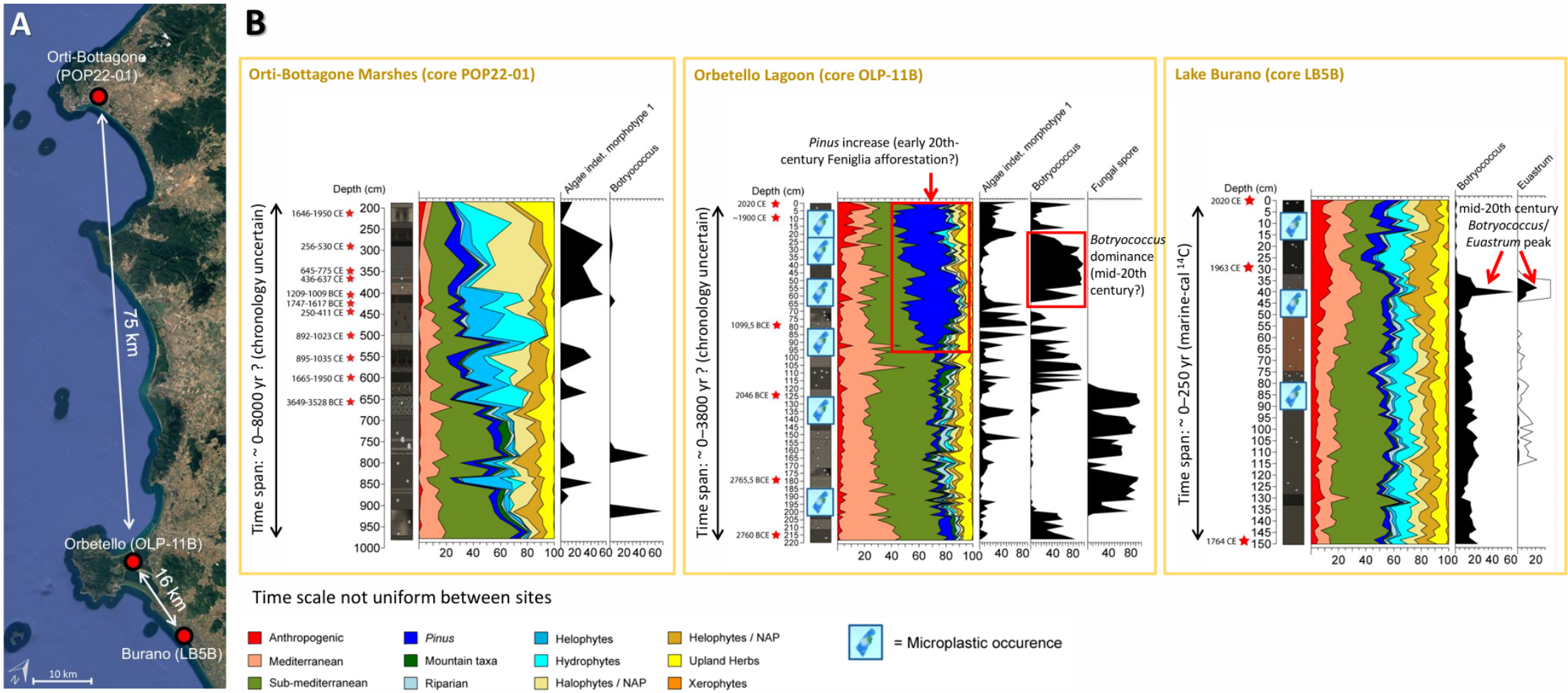

Fig. 1: Synthetic comparison of the three records and tentative correlations. (A) North–south transect along the southern Tuscan coast showing the location of the three study sites and the relative distances (see also Chapter 2, Fig. 1). (B) Side-by-side comparison of the three palynological records (pollen ecological groups and selected NPP indicators), displayed against depth for visual comparison; the position of the microplastic occurrences is also indicated; axes are not to scale and each record is placed within its own chronological constraints.

3.1. Shared trends

A persistent arboreal signal characterizes all three sequences, dominated by Mediterranean and Sub-Mediterranean taxa such as *Quercus ilex-coccifera* and *Quercus pubescens* types, and accompanied by *Pinus*, largely reflecting Mediterranean species, together with other thermophilus elements (Fig. 1B). This woodland background provides a relatively stable ecological framework, onto which both natural oscillations and anthropogenic imprints are superimposed. Among the latter, *Olea* represents the most consistent signal, showing recurrent expansions that coincide with phases of intensified human land use, particularly from historical times onward. Other markers of anthropogenic pressure, including Cupressaceae and *Eucalyptus*, appear in the upper parts of the sequences, reflecting modern introductions and reforestation practices.

Recent centuries are also marked in Burano and Orbetello, and more tentatively in Orti-Bottagone, by signs of eutrophication (Fig. 1B). These include the proliferation of aquatic macrophytes (*Ruppia*, *Sparganium/Typha angustifolia*) and non-pollen palynomorphs such as *Botryococcus*, pointing to nutrient enrichment and unstable hydrological regimes (Fig. 1B). Additional episodes of ecological stress are suggested by sudden peaks of *Pseudoschizaea*, *Euastrum* and other algal morphotypes, as well as sporadic increases in fungal spores, which together reinforce the evidence for repeated phases of disturbance and eutrophic instability in the lagoons.

The appearance of microplastics in the Orbetello and Burano cores adds a distinctly modern proxy, highlighting both the pervasiveness of contemporary anthropogenic pressures and the potential of these particles as stratigraphic markers for the Anthropocene (Fig. 1B).

3.2. Site-specific differences

Burano provides the most robust chronological framework, supported by consistent radiocarbon dating and auxiliary markers. Its stratigraphic resolution allows the recognition of a gradual trajectory of eutrophication, moving from lagoonal to increasingly freshwater and anthropogenically stressed conditions as reflected by changes in aquatic NPPs and pollen ecological groups (Fig. 1B), but without evidence of acute

dystrophic crises. This makes Burano a reliable reference sequence for understanding fine-scale paleoenvironmental dynamics on the Tyrrhenian coast.

Orbetello, by contrast, presents a more problematic chronology, with inversions and uncertainties in the deeper part of the core. Its ecological record is strongly marked by the 20th-century reforestation of the Feniglia tombolo with *Pinus*, producing an abrupt pollen signal that is not as clearly expressed in Burano (Fig. 1B). Moreover, Orbetello preserves clear evidence of dystrophic crises, consistent with historical documentation of fish kills and water management challenges in the lagoon. These features make Orbetello a crucial archive for understanding the intersection of environmental stress and human intervention in recent centuries.

Orti-Bottagone differs fundamentally from the two lagoons, being located in a reclaimed sector of the Cornia alluvial plain rather than in a coastal basin. Its chronology is fragile, hindered by radiocarbon inversions and the lack of independent chronological markers, and the sampling resolution is lower compared to Burano and Orbetello. Nevertheless, this core offers a unique contribution: its greater depth extends the temporal coverage into the early Holocene, thereby completing the regional framework (Fig. 1B). The sequence documents long-term transitions from lagoonal to swampy environments, followed by the imprint of anthropogenic land use in the upper layers. These features, although less finely resolved, provide essential context for interpreting millennial-scale trajectories in the coastal plain.

3.3. Comparative value

Taken together, the three records capture both the shared trajectories of Tyrrhenian wetlands and the distinct local pathways shaped by geomorphology and land use (Fig. 1). Burano contributes chronological reliability and fine ecological detail; Orbetello highlights the complex interplay of anthropogenic interventions and lagoonal instability; Orti-Bottagone, though less resolved, anchors the system within a deeper temporal framework, linking Holocene environmental change to the long history of human occupation in the Cornia plain.

4. Regional and comparative perspectives

The comparative analysis of the three sites highlights how broadly similar vegetation signals, notably the persistence of Mediterranean woodland and recurrent anthropogenic imprints, translate into different ecological trajectories depending on local geomorphology and management history (Fig. 1B). This shift in perspective, from shared background trends to basin-specific responses, is key to understanding the role of Tyrrhenian lagoons as sensitive archives of both natural variability and human impact. At the regional scale, the pollen data consistently document the interplay between enduring arboreal cover and successive waves of human-induced disturbance, including *Olea* cultivation, the spread of introduced taxa such as Cupressaceae and *Eucalyptus*, and the expansion of ruderal herbs associated with open environments and intensive land use.

Within this shared framework, however, the three sites illustrate different degrees of resilience to ecological stress, particularly eutrophication. Burano shows a gradual and progressive trend toward nutrient enrichment, without evidence of abrupt crises (Fig. 1B). Orbetello, by contrast, preserves clear signals of dystrophic episodes that align with historical documentation of fish kills and water management challenges (Lardicci *et al.*, 2001; Nuccio *et al.*, 2003) (Fig. 1B). Orti-Bottagone, while less finely resolved, highlights longer-term oscillations between halophytic and hydrophytic phases, consistent with geomorphological dynamics of the Cornia plain. This variability underscores how local morphology, hydrological connectivity, and human interventions modulate the ecological response of individual basins to similar pressures.

When placed in a broader Mediterranean framework, these records echo regional patterns described in other coastal archives. Episodes of arboreal decline, expansion of *Olea*, and the spread of open-land indicators parallel findings from pollen records in central and southern Italy (Calò *et al.*, 2012; Di Rita & Magri, 2012, 2019). Similarly, the strong imprint of 20th-century eutrophication in Orbetello resonates with ecological studies of other Mediterranean lagoons under heavy anthropogenic pressure (Lardicci *et al.*, 2001). Conversely, the lack of a clear palynological expression of the 4.2 ka event in these sequences highlights the heterogeneous expression of Holocene climatic anomalies in the Tyrrhenian sector, as already emphasized by Di Rita & Magri (2019).

Methodologically, the comparison across sites also underscores the strengths and limitations of the applied proxies. Pollen and NPPs remain the most robust indicators for reconstructing long-term vegetation dynamics and lagoonal responses, but their inter-

pretive power is constrained by chronological uncertainties, especially in Orbetello and Orti-Bottagone. Microplastics, tested in Burano and Orbetello, offer a promising marker of modern anthropogenic impact, but their occurrence at stratigraphically unexpected depths points to problems of reworking, contamination, or bioturbation, limiting their chronological reliability (Fig. 1B). Granulometric and geochemical data add critical contextual information on hydrodynamics and sediment sources, refining the interpretation of the palynological signal.

In sum, the integrated multi-proxy approach applied here highlights both the shared environmental trajectories of Tyrrhenian lagoons and the distinctive pathways followed by individual basins. This duality is central for interpreting the Holocene evolution of coastal wetlands in Tuscany: the common background trends provide a regional signal of climatic and anthropogenic forcing, while local divergences illuminate the role of geomorphology and human management in shaping site-specific ecological histories.

5. *Methodological conclusions and future perspectives*

This research highlights the strength of a multiproxy approach, combining palynological data (pollen and NPP) with complementary indicators to reconstruct the ecological history of three distinct wetland systems. The comparative perspective across Burano, Orbetello, and Orti-Bottagone demonstrates the value of analysing different archives within a single regional framework, which allows common patterns and local peculiarities to be disentangled.

At the same time, the study underscores the limitations imposed by uncertain chronologies, particularly where radiocarbon determinations alone proved inconsistent. The experience gained here shows that no single proxy can guarantee a robust depth-age model, but that integration can make the difference. The combined use of ^{210}Pb-^{137}Cs-^{241}Am with radiocarbon dating indeed provided a more reliable chronology in Burano, whereas its absence in Orti-Bottagone left major uncertainties unresolved. Future work should therefore seek to complement radiocarbon dating with additional chronological markers, including amino acid racemization, tephrochronology, or microplastic stratigraphy, wherever applicable, to improve temporal resolution.

Equally important is the integration of ecological proxies: the convergence of pollen, NPP, and ostracod records in Orti-Bottagone shows how independent lines of evidence

can validate the reconstruction of hydrological regimes, even where the stratigraphy is complex or partially reworked. Extending this strategy with geochemical and granulometric analyses would further clarify sedimentary processes and improve the interpretation of ecological signals.

Looking ahead, progress will depend on three main directions:

1. a stronger integration of geochemical analyses with biological and sedimentary proxies, in order to improve the interpretability of ecological shifts and the overall reconstruction of lagoonal dynamics;
2. the development of more robust chronological frameworks for each core, achieved by systematically combining multiple dating approaches, in order to reduce uncertainties and strengthen depth-age models;
3. a stronger focus on the effects of climate variability and human management on Tyrrhenian lagoons, with direct implications for both paleoenvironmental research and modern conservation policies.

In this sense, the three case studies presented here do not only document the past but also provide critical insights into the long-term resilience and vulnerability of coastal wetlands, offering a historical perspective that is directly relevant for the management and conservation of these ecosystems in the face of current and future environmental change.

References

Abidli, S., Antunes, J. C., Ferreira, J. L., Lahbib, Y., Sobral, P., & El Menif, N. T. (2018). Microplastics in sediments from the littoral zone of the north Tunisian coast (Mediterranean Sea). *Estuarine, Coastal and Shelf Science*, *205*, 1-9.

Aiello, G., Barra, D., De Pippo, T., Donadio, C., Miele, P., & Ermolli, E. R. (2007). Morphological and palaeoenvironmental evolution of the Vendicio coastal plain in the Holocene (Latium, Central Italy). *Alpine and Mediterranean Quaternary*, *20*(2), 185-194.

Amorosi, A., Ricci Lucchi, M., Sarti, G., Vaiani, S. C., Prandin, S., & Muti, A. (2004). Late Quaternary sedimentary evolution of the Piombino alluvial plain (western Tuscany) as revealed by subsurface data. *GeoActa*, *3*, 97-106.

Andersen, S. T. (1979). Identification of wild grass and cereal pollen. *Danmarks Geologiske Undersøgelse Årbog*, *1978*, 69-92.

Angiolini, C., Riccucci, C., & De Dominicis, V. (1998). Alcune specie di interesse fitogeografico rinvenute alla riserva naturale di Burano (Grosseto). *Botanica*, *15*(17), 63-66.

Angiolini, C., Riccucci, C., & De Dominicis, V. (2002). La flora vascolare della Riserva Naturale Lago di Burano (Grosseto, Toscana meridionale). *Webbia*, *57*(1), 115-152.

Ardizzone, G. D., Giardini, M., & Tripaldi, G. (1983). Nutrient pathways in the Burano Lagoon. *Rapp. P.-V. Réun. CIESM.*, *28*(6), 193-194.

Ariztegui, D., Chondrogianni, C., Lami, A., Guilizzoni, P., & Lafargue, E. (2001). Lacustrine organic matter and the Holocene paleoenvironmental record of Lake Albano (central Italy). *Journal of Paleolimnology*, *26*(3), 283-292.

ARPAT (2025), *Report mensile chimico e fisico Laguna di Levante e Ponente*, maggio 2025. Technical report.

Azzoni, R., Giordani, G., Bartoli, M., Welsh, D. T., & Viaroli, P. (2001). Iron, sulphur and phosphorus cycling in the rhizosphere sediments of a eutrophic *Ruppia cirrhosa* meadow (Valle Smarlacca, Italy). *Journal of Sea Research*, *45*(1), 15-26.

Badino, F., Bertini, A., Pili, M., Ciampalini, R., Vittori, C., Baroni, D., Goiran J.-P., Catelani, T. (submitted). Assessing ecological risk factors in Central Mediterranean coastal lagoons using a spatially integrated palynological approach. *Science of the Total Environment.*

Bakrač, K., Sirenko, O., Hruševar, D., Baniček, I., Novak, V., Kletečki, N., & Oros Sršen, A. (2024). First palynological results from Spila nad Procjepom cave, Mljet island (Croatia). *Geologia Croatica*, *77*(1), 29-39.

Bancone, C. E., Turner, S. D., Ivar do Sul, J. A., & Rose, N. L. (2020). The paleoecology of microplastic contamination. *Frontiers in Environmental Science*, *8*, 574008.

Bellarosa, R., Codipietro, P., Piovesan, G., & Schirone, B. (1996). Degradation, rehabilitation and sustainable management of a dunal ecosystem in central Italy. *Land Degradation & Development*, *7*(4), 297-311.

Bellotti, P., Calderoni, G., Carboni, M. G., Di Bella, L., Tortora, P., Valeri, P., & Zernitskaya, V. (2007). Late Quaternary landscape evolution of the Tiber River delta plain (Central Italy): new evidence from pollen data, biostratigraphy and 14C dating. *Zeitschrift für Geomorphologie*, *51*(4), 505-534.

Benjamin, J., Rovere, A., Fontana, A., Furlani, S., Vacchi, M., Inglis, R. H., Galili, E., Antonioli, F., Sivan, D., Miko, S., Mourtzas, N., Felja, I., Meredith-Williams, M., Goodman-Tcherno, B., Kolaiti, E., Anzidei, M., & Gehrels, R. (2017). Late Quaternary sea-level changes and early human societies in the central and eastern Mediterranean Basin: An interdisciplinary review. *Quaternary International*, *449*, 29-57.

Beug, H.-J. (2004). *Leitfaden der Pollenbestimmung für Mitteleuropa und angrenzende Gebiete*. Friedrich Pfeil Verlag.

Biagi, F., & Milletti, M. (2017). Nuovi dati sulla necropoli dell'età del Ferro di Poggio e Piano delle Granate a Populonia (LI). *Archeologia classica: rivista del dipartimento di scienze storiche archeologiche e antropologiche dell'antichità, 68*(7), 375-408.

Biagi, F., & Milletti, M. (2021). L'età del Ferro a Populonia: nuovi dati dall'abitato e dalla necropoli. *Mediterranea: XVIII, 2021*, 41-51.

Bianchini, G., Pennisi, M., Cioni, R., Muti, A., Cerbai, N., & Kloppmann, W. (2005). Hydrochemistry of the high-boron groundwaters of the Cornia aquifer (Tuscany, Italy). *Geothermics*, *34*(3), 297-319.

Bigi, L., & Rustici, L. (1984). *Regime idrico dei suoli e tipi climatici in Toscana*. Regione Toscana, Dipartimento Agricoltura e Foreste.

Blašković, A., Guerranti, C., Fastelli, P., Anselmi, S., & Renzi, M. (2018). Plastic levels in sediments close to Cecina river estuary (Tuscany, Italy). *Marine pollution bulletin*, *135*, 105-109.

Bombelli, V., & Lenzi, M. (1996). Italy—the Orbetello lagoon and the Tuscan coast. In A. A. (Eds.), *Marine benthic vegetation: recent changes and the effects of eutrophication* (pp. 331-337). Springer.

Brocard, G., Goiran, J.-P., Conforti, A., Preusser, F., Vitale, Q., Jouve, G., Darras, L., Benech, C., Vittori, C., Oberlin, C., Pons-Branchu, E., Mattio, L., de Grauuw, A., Leporatti-Persiano, M., De Giorgi A. U., & Bertini, A. (2024). Double tombolo formation by regressive barrier widening and landside submergence: The case of Orbetello, Italy. *Marine Geology*, *477*, 107415.

Bruel, R., & Sabatier, P. (2020). Serac: an R package for ShortlivEd RAdionuclide chronology of recent sediment cores. *Journal of Environmental Radioactivity*, *225*, 106449.

Buonincontri, M. P., Pieruccini, P., Susini, D., Lubritto, C., Ricci, P., Rey, F., Tinner, W., Colombaroli, D., Drescher-Schneider, R., Dallai, L., Marasco, L., Poggi, G., Bianchi, G., Hodges, R., & Di Pasquale, G. (2020). Shaping Mediterranean landscapes: The cultural impact of anthropogenic fires in Tyrrhenian southern Tuscany during the Iron and Middle Ages (800–450 BC/AD 650–1300). *The Holocene*, *30*(10), 1420-1437.

Calastri, C. (2019). L'urbanistica antica di Orbetello. *L'Argentariana*, *10*, 2-10.

Calò, C., Henne, P. D., Curry, B., Magny, M., Vescovi, E., La Mantia, T., Pasta, S., Vannière, B., & Tinner, W. (2012). Spatio-temporal patterns of Holocene environmental change in southern Sicily. *Palaeogeography, Palaeoclimatology, Palaeoecology*, *323*, 110-122.

Cannas, S., Fastelli, P., Guerranti, C., & Renzi, M. (2017). Plastic litter in sediments from the coasts of south Tuscany (Tyrrhenian Sea). *Marine Pollution Bulletin*, *119*(1), 372-375.

Cardosa, M., & Dolfini, A. (2017). Paesaggi d'Acque. La Laguna di Orbetello e il Monte Argentario tra Preistoria ed Età Romana.

Caroli, I., & Caldara, M. (2007). Vegetation history of Lago Battaglia (eastern Gargano coast, Apulia, Italy) during the middle-late Holocene. *Vegetation History and Archaeobotany*, *16*(4), 317-327.

Chiarantini, L., Benvenuti, M., Costagliola, P., Dini, A., Firmati, M., Guideri, S., Villa, I. M., & Corretti, A. (2018). Copper metallurgy in ancient Etruria (southern Tuscany, Italy) at the Bronze-Iron Age transition: a lead isotope provenance study. *Journal of Archaeological Science: Reports*, *19*, 11-23.

Clò, E., Furia, E., Florenzano, A., & Mercuri, A. M. (2024). Flora-vegetation history and land use in Medieval Tuscany: The palynological evidence of a local biodiversity heritage. *Quaternary International*, *705*, 1-15.

Cognetti, G., De Angelis, C. M., & Orlando, E. (1978). Situazione ecologica del Lago di Burano (GR). *WWF Serie Atti e Studi*, *3*.

Colombaroli, D., Marchetto, A., & Tinner, W. (2007). Long-term interactions between Mediterranean climate, vegetation and fire regime at Lago di Massaciuccoli (Tuscany, Italy). *Journal of Ecology*, *95*(4), 755-770.

Colombaroli, D., Vannière, B., Emmanuel, C., Magny, M., & Tinner, W. (2008). Fire—vegetation interactions during the Mesolithic—Neolithic transition at Lago dell'Accesa, Tuscany, Italy. *The Holocene*, *18*(5), 679-692.

Condrò, A. (1952). *Annali Idrologici (Parte Seconda)*. Istituto Poligrafico dello Stato. Technical report.

Corcoran, P. L. (2015). Benthic plastic debris in marine and freshwater environments. *Environmental Science: Processes & Impacts, 17*(8), 1363-1369.

Corretti, A., & Benvenuti, M. (2001). The Beginning of Iron Metallurgy in Tuscany, with Special Reference to" Etruria Mineraria". *Mediterranean Archaeology*, 127-145.

Cugny, C., Mazier, F., & Galop, D. (2010). Modern and fossil non-pollen palynomorphs from the Basque mountains (western Pyrenees, France): the use of coprophilous fungi to reconstruct pastoral activity. *Vegetation History and Archaeobotany*, *19*(5), 391-408.

Dallai, L., Buonincontri, M. P., Poggi, G., & Volpi, V. (2024). Paesaggio naturale ed antropico nell'area costiera della Toscana meridionale (Val di Cornia): sistemi di fonti, strumenti e metodi di studio per una nuova lettura storico-archeologica dell'ambiente e delle sue trasformazioni. *L'Archeologo Subacqueo*, *30*(76).

Dallai, L., Volpi, V., & Poggi, G. (2025). Liminal historical landscapes in southern Tuscany: a multidisciplinary approach for a new narrative. In *Waterscapes Archaeology: Multi-Scalar Human-Environment Interactions in Coastal Lagoons* (pp. 71-90). Archaeopress Publishing.

De Silva, M., Guarducci, A., & Rombai, L. (2018). Per un progetto di itinerari culturali della bonifica. La pianura di Grosseto nella cartografia dei secoli XV III-XX. Georeferenziazione e paesaggio storico.

Di Paola, G. M. F. (2018). Central place and liminal landscape in the territory of Populonia. *Land*, *7*(3), 94.

Di Pasquale, G., Buonincontri, M. P., Allevato, E., & Saracino, A. (2014). Human-derived landscape changes on the northern Etruria coast (western Italy) between Roman times and the late Middle Ages. *The Holocene*, *24*(11), 1491-1502.

Di Rita, F., & Magri, D. (2009). Holocene drought, deforestation and evergreen vegetation development in the central Mediterranean: a 5500 year record from Lago Alimini Piccolo, Apulia, southeast Italy. *The Holocene*, *19*(2), 295-306.

Di Rita, F., & Magri, D. (2012). An overview of the Holocene vegetation history from the central Mediterranean coasts. *Journal of Mediterranean Earth Sciences*, *4*, 35-52.

Di Rita, F., & Magri, D. (2019). The 4.2 ka event in the vegetation record of the central Mediterranean. *Climate of the Past*, *15*(1), 237-251.

D'Orefice, M., Bellotti, P., Bertini, A., Calderoni, G., Censi Neri, P., Di Bella, L., Fiorenza, D., Foresi, L. M., Louvari, M. A., Rainone, L., Vittori, C., Goiran, J. P., Schmitt, L., Carbonel, P., Preusser, F., Oberlin, C., Sangiorgi, F., & Davoli, L. (2020a). Holocene evolution of the Burano paleo-lagoon (Southern Tuscany, Italy). *Water*, *12*(4), 1007.

D'Orefice, M., Graciotti, R., Bertini, A., Fedi, M., Foresi, L. M., Ricci, M., & Toti, F. (2020b). Latest Pleistocene to Holocene environmental changes in the northern Tyrrhenian area (central mediterranean). A case study from southern Elba island. *Alpine and Mediterranean Quaternary*, *33*(1), 5-30.

D'Orefice, M., Bellotti, P., Bellotti, T., Davoli, L., & Di Bella, L. (2022). Natural and cultural lost landscape during the Holocene along the Central Tyrrhenian Coast (Italy). *Land*, *11*(3), 344.

Drescher-Schneider, R., de Beaulieu, J. L., Magny, M., Walter-Simonnet, A. V., Bossuet, G., Millet, L., Brugiapaglia, E., & Drescher, A. (2007). Vegetation history, climate and human impact over the last 15,000 years at Lago dell'Accesa (Tuscany, Central Italy). *Vegetation History and Archaeobotany*, *16*(4), 279-299.

Erdtman, G. (1952). *Pollen morphology and plant taxonomy. Angiosperms*. Chronica Botanica Co.

Erdtman, G. (1954). Pollen morphology and plant taxonomy. *Botaniska Notiser*, *107*, 65-81.

Erdtman, G. (1969). *An introduction to the study of pollen grains and spores*. Hafner.

Ermolli, E. R., & Di Pasquale, G. (2002). Vegetation dynamics of south-western Italy in the last 28 kyr inferred from pollen analysis of a Tyrrhenian Sea core. *Vegetation History and Archaeobotany*, *11*(3), 211-220.

Fiaschi, T., Bonari, G., Frignani, F., Gizzi, G., Landi, M., Magrini, S., Quilghini, G., Pafumi, E., Scoppola, A., & Angiolini, C. (2024). Vascular flora of the isthmus of Feniglia (southern Tuscany, Italy). *Italian Botanist*, *17*, 77-101.

Finsinger, W., Colombaroli, D., De Beaulieu, J. L., Valsecchi, V., Vannière, B., Vescovi, E., Chapron, E., Lotter, A. F., Magny, M., & Tinner, W. (2010). Early to mid-Holocene climate change at Lago dell'Accesa (central Italy): climate signal or anthropogenic bias? *Journal of Quaternary Science*, *25*(8), 1239-1247.

Fondazione S. Giovanni Gualberto (2000). La Toscana dei boschi. In A. A. Hofmann & D. Perulli (Eds.), *Attraverso le regioni forestali d'Italia*. Edizioni Vallombrosa.

Francke, A., Lacey, J. H., Marchegiano, M., Wagner, B., Ariztegui, D., Zanchetta, G., Kusch, S., Ufer, K., Baneschi, I., & Knödgen, K. (2022). Last Glacial central Mediterranean hydrology inferred from Lake Trasimeno's (Italy) calcium carbonate geochemistry. *Boreas*, *51*(1), 219-237.

Frias, J., Pagter, E., Nash, R., O'Connor, I., Carretero, O., Filgueiras, A., Viñas, L., Gago, J., Antunes, J., Bessa, F., Sobral, P., Goruppi, A., Tirelli, V., Pedrotti, M. L., Suaria, G., Aliani, S., Lopes, C., Raimundo, J., Caetano, M., Palazzo, L., de Lucia, G. A., Camedda, A., Muniategui, S., Grueiro, G., Fernandez, V., Andrade, J., Dris, R., Laforsch, C., Scholz-Böttcher, B. M., & Gerdts, G. (2018). Standardised protocol for monitoring microplastics in sediments. JPI-Oceans BASEMAN project. Technical report.

Fytianos, G., Ioannidou, E., Thysiadou, A., Mitropoulos, A. C., & Kyzas, G. Z. (2021). Microplastics in Mediterranean coastal countries: a recent overview. *Journal of Marine Science and Engineering*, *9*(1), 98.

Gelorini, V., Verbeken, A., van Geel, B., Cocquyt, C., & Verschuren, D. (2011). Modern non-pollen palynomorphs from East African lake sediments. *Review of Palaeobotany and Palynology*, *164*(3-4), 143-173.

Gimiliani, G. T., Fornari, M., Redígolo, M. M., Bustillos, J. O. W. V., de Souza Abessa, D. M., & Pires, M. A. F. (2020). Simple and cost-effective method for microplastic quantification in estuarine sediment: A case study of the Santos and São Vicente Estuarine System. *Case Studies in Chemical and Environmental Engineering*, *2*, 100020.

Giroldini, P. (2010). *La Pianura di Piombino in età antica: dinamiche di controllo e organizzazione territoriale.* Doctoral dissertation, University of Florence.

Giusti, E., & Marsili-Libelli, S. (2005). Modelling the interactions between nutrients and the submersed vegetation in the Orbetello Lagoon. *Ecological Modelling*, *184*(1), 141-161.

Giusti, E., & Marsili-Libelli, S. (2006). An integrated model for the Orbetello lagoon ecosystem. *Ecological Modelling*, *196*(3-4), 379-394.

Giusti, E., Marsili-Libelli, S., Renzi, M., & Focardi, S. (2010). Assessment of spatial distribution of submerged vegetation in the Orbetello lagoon by means of a mathematical model. *Ecological Modelling*, *221*(11), 1484-1493.

Grimm, E. (2015). *Tilia* and *TGView* version 2.0.41. Computer software. Illinois State Museum, Research and Collection Center.

Guarducci, A., Rombai, L., & Piccardi, M. (2021). Il paesaggio della Bonifica Grossetana: ricerca geostorica e candidatura UNESCO. *Atti e Memorie dell'Accademia Toscana di Scienze e Lettere La* Colombaria, *85*(71), 294-306.

Guideri, S., & Matteini, T. (2021). Cultivating Archaeological Landscape: Notes on a Mediterranean Applied Case Study. *Joelho-Journal of Architectural Culture*, (11-12), 101-120.

Head, M. J. (2019). Formal subdivision of the Quaternary System/Period: Present status and future directions. *Quaternary International*, *500*, 32-51.

Heaton, T. J., Köhler, P., Butzin, M., Bard, E., Reimer, R. W., Austin, W. E., Ramsey, C. B., Grootes, P. M., Hughen, K. A., Kromer, B., Reimer, P. J., Adkins, J., Burke, A., Cook, M. S., Olsen, J., & Skinner, L. C. (2020). Marine20—the marine radiocarbon age calibration curve (0–55,000 cal BP). *Radiocarbon*, *62*(4), 779-820.

Imhof, H. K., Ivleva, N. P., Schmid, J., Niessner, R., & Laforsch, C. (2013). Contamination of beach sediments of a subalpine lake with microplastic particles. *Current Biology*, *23*(19), R867-R868.

Jahns, S., & van den Bogaard, C. (1998). New palynological and tephrostratigraphical investigations of two salt lagoons on the island of Mljet, south Dalmatia, Croatia. *Vegetation History and Archaeobotany*, *7*(4), 219-234.

Jouve, G., Vittori, C., Brocard, G., Pili, M., Gonçalves, C., Goyon, A., Bomou, B., Jacq, K., Debret, M., Mattio, L., Darras, L., Benech, C., Vitale, Q., Bertini, A., Leporatti-Persiano, M., Cianchi, F., Oberlin, C., Sabatier, P., Mesnage, V., & Goiran, J.-P. (2022). *Stratigraphic record of lagoonal management since Antiquity: insights from sediment core analysis and sub-bottom profiling, lagoon of Orbetello, Italy* (No. ICG2022-333). Conference presentation abstract. ICG 2022. Copernicus Meetings.

Krakimel, J.-D. (2003). Impact of tourism on Mediterranean marine and coastal biodiversity. In *Project for the Preparation of a Strategic Action Plan for the Conservation of Biological Diversity in the Mediterranean Region (SAP BIO)*. Management plan.

Lambeck, K., Antonioli, F., Anzidei, M., Ferranti, L., Leoni, G., Scicchitano, G., & Silenzi, S. (2011). Sea level change along the Italian coast during the Holocene and projections for the future. *Quaternary International*, *232*(1-2), 250-257.

Langgut, D., Cheddadi, R., Carrión, J. S., Cavanagh, M., Colombaroli, D., Eastwood, W. J., Greenberg, R., Litt, T., Mercuri, A. M., Miebach, A., Roberts, C. N., Woldring, H., & Woodbridge, J. (2019). The origin and spread of olive cultivation in the Mediterranean Basin: The fossil pollen evidence. *The Holocene*, *29*(5), 902-922.

Lardicci, C., Como, S., Corti, S., & Rossi, F. (2001). Recovery of the macrozoobenthic community after severe dystrophic crises in a Mediterranean coastal lagoon (Orbetello, Italy). *Marine Pollution Bulletin*, *42*(3), 202-214.

Lenzi, M. (1984). Indagine sulla distribuzione delle macrofite nella laguna di Orbetello. *Quad. Mus. Stor. Nat. Livorno*, *5*, 37-55.

Lenzi, M., & Angelini, M. (1985). Indagine sulla macrovegetazione sommersa e sul carico microfitico dello stagno costiero di Burano. *Quad. Mus. Stor: Nat. Livorno*, *6*, 27-35.

Lenzi, M. (1992). Experiences for the management of Orbetello Lagoon: eutrophication and fishing. In *Marine coastal eutrophication* (pp. 1189-1198). Elsevier.

Lenzi, M., Palmieri, R., & Porrello, S. (2003). Restoration of the eutrophic Orbetello lagoon (Tyrrhenian Sea, Italy): water quality management. *Marine Pollution Bulletin, 46*(12), 1540-1548.

Lenzi, M., Birardi, F., Boddi, S., Roffilli, R., Solari, D., & Sartoni, G. (2009). The lagoon of Orbetello. In *Flora and Vegetation of the Italian Transitional Water Systems* (pp. 111-123). Lagunet, CORILA.

Lenzi, M., & Cianchi, F. (2022). Summer dystrophic criticalities of non-tidal lagoons: the case study of a Mediterranean lagoon. *Diversity*, *14*(9), 771.

Löder, M. G., & Gerdts, G. (2015). Methodology used for the detection and identification of microplastics—a critical appraisal. In Bergmann, Gutow, & Klages (Eds.), *Marine anthropogenic litter* (pp. 201-227). Springer.

Magny, M., de Beaulieu, J. L., Drescher-Schneider, R., Vannière, B., Walter-Simonnet, A. V., Millet, L., Bossuet, G., & Peyron, O. (2006). Climatic oscillations in central Italy during the Last Glacial–Holocene transition: the record from Lake Accesa. *Journal of Quaternary Science: Published for the Quaternary Research Association*, *21*(4), 311-320.

Magny, M., Vannière, B., de Beaulieu, J. L., Bégeot, C., Heiri, O., Millet, L., Peyron, O., & Walter-Simonnet, A. V. (2007a). Early-Holocene climatic oscillations recorded by lake-level fluctuations in west-central Europe and in central Italy. *Quaternary Science Reviews*, *26*(15-16), 1951-1964.

Magny, M., de Beaulieu, J. L., Drescher-Schneider, R., Vanniere, B., Walter-Simonnet, A. V., Miras, Y., Millet, L., Bossuet, G., Peyron, O., Brugiapaglia, E., & Leroux, A. (2007b). Holocene climate changes in the central Mediterranean as recorded by lake-level fluctuations at Lake Accesa (Tuscany, Italy). *Quaternary Science Reviews*, *26*(13-14), 1736-1758.

Magri, D. (1997). Middle and Late Holocene vegetation and climate changes in peninsular Italy. In *Third millennium BC climate change and Old World collapse* (pp. 517-530). Berlin, Heidelberg: Springer Berlin Heidelberg.

Magri, D. (1999). Late Quaternary vegetation history at Lagaccione near Lago di Bolsena (central Italy). *Review of Palaeobotany and Palynology*, *106*(3-4), 171-208.

Magri, D., & Sadori, L. (1999). Late Pleistocene and Holocene pollen stratigraphy at Lago di Vico, central Italy. *Vegetation history and archaeobotany*, *8*(4), 247-260.

Mariotti Lippi, M., Di Tommaso, P. L., Giachi, G., Mori Secci, M., & Paci, S. (2003). Archaeobotanical investigations into an Etruscan farmhouse at Pian d'Alma (Grosseto, Italy). *Atti della Società Toscana di Scienze Naturali residente in Pisa. Memorie. Serie B*, *109*, 159-165.

Mariotti Lippi, M., Guido, M., Menozzi, B. I., Bellini, C., & Montanari, C. (2007). The Massaciuccoli Holocene pollen sequence and the vegetation history of the coastal plains by the Mar Ligure (Tuscany and Liguria, Italy). *Vegetation History and Archaeobotany*, *16*(4), 267-277.

Mariotti Lippi, M., Mori Secci, M., Giachi, G., Bouby, L., Terral, J. F., Castiglioni, E., Cottini, M., Rottoli, M., & de Grummond, N. T. (2020). Plant remains in an Etruscan-Roman well at Cetamura del Chianti, Italy. *Archaeological and Anthropological Sciences*, *12*(1), 35.

Matthews, J. (1969). The assessment of a method for the determination of absolute pollen frequencies. *New Phytologist*, *68*(1), 161–166.

Mazzini, I., Anadon, P., Barbieri, M., Castorina, F., Ferreli, L., Gliozzi, E., Mola, M., & Vittori, E. (1999). Late Quaternary sea-level changes along the Tyrrhenian coast near Orbetello (Tuscany, central Italy): palaeoenvironmental reconstruction using ostracods. *Marine Micropaleontology*, *37*(3-4), 289-311.

McGlathery, K. J. (2001). Macroalgal blooms contribute to the decline of seagrass in nutrient-enriched coastal waters. *Journal of Phycology*, *37*(4), 453-467.

Menéndez, M., Hernandez, O., & Comin, F. A. (2002). Spatial distribution and ecophysiological characteristics of macrophytes in a Mediterranean coastal lagoon. *Estuarine, Coastal and Shelf Science*, *55*(3), 403-413.

Mensing, S. A., Tunno, I., Sagnotti, L., Florindo, F., Noble, P., Archer, C., Zimmerman, S., Pavon-Carrasco, F. J., Cifani, G., Passigli, S., & Piovesan, G. (2015). 2700 years of Mediterranean environmental change in central Italy: a synthesis of sedimentary and cultural records to interpret past impacts of climate on society. *Quaternary Science Reviews*, *116*, 72-94.

Mercuri, A. M., Sadori, L., & Uzquiano Ollero, P. (2011). Mediterranean and north-African cultural adaptations to mid-Holocene environmental and climatic changes. *The Holocene*, *21*(1), 189-206.

Ministero dell'Ambiente (1993). St*udio multidisciplinare per la tutela dell'ecosistema acquatico del Lago di Burano (GR)*. WWF Italia. Technical report.

Moore, P. D., Webb, J. A., & Collison, M. E. (1991). *Pollen analysis*. Blackwell Scientific Publications.

Murphy, L., Germaine, K., Kakouli-Duarte, T., & Cleary, J. (2022). Assessment of microplastics in Irish river sediment. *Heliyon*, *8*(7).

Nijboer, A. J. (2021). *Entanglements, elite prerogatives, migratory swallows, and the elusive transfer of technological know-how into the western Mediterranean, 1000–700 BC.* McDonald Institute for Archaeological Research.

Novello, E. (2025). Private interest and public policy: land reclamation in the Tuscan Maremma (1860s–1950s). *Rural History*, 1-23.

Nuccio, C., Melillo, C., Massi, L., & Innamorati, M. (2003). Phytoplankton abundance, community structure and diversity in the eutrophicated Orbetello lagoon (Tuscany) from 1995 to 2001. *Oceanologica Acta*, *26*(1), 15-25.

Paolini, F. (2012). Salting Fresh Waters. Industries, Tourism and the Environment on Tuscany's Central Southern Coast. *Storia e Futuro*, *29*, 1-20.

Pasquetti, F., Vaselli, O., Zanchetta, G., Nisi, B., Lezzerini, M., Bini, M., & Mele, D. (2020). Sedimentological, mineralogical and geochemical features of late Quaternary sediment profiles from the southern Tuscany Hg mercury district (Italy): evidence for the presence of pre-industrial mercury and arsenic concentrations. *Water*, *12*(7), 1998.

Pedrotti, F., Pedrotti, C. C., & Orsomando, E. (1979). The phytosociological map of Burano (Tuscany). *Webbia*, *34*(1), 529-531.

Pérez-Obiol, R., & Sadori, L. (2007). Similarities and dissimilarities, synchronisms and diachronisms in the Holocene vegetation history of the Balearic Islands and Sicily. *Vegetation History and Archaeobotany*, *16*(4), 259-265.

Perkins, P. (2017). The landscape and environment of Etruria. In Naso (Ed.), *Etruscology* (pp. 1239-1250). De Gruyter.

Piano antincendio boschivo (PAIB) di previsione, prevenzione e lotta attiva contro gli incendi boschivi Riserva Naturale Statale Lago di Burano 2022-2026. Management plan.

Pieruccini, P., & Susini, D. (2020). The Holocene sedimentary record and the landscape evolution along the coastal plains of the Pecora and Cornia rivers (Southern Tuscany, Italy): preliminary results and future perspectives. In Bianchi, Hodges (Eds.), *The nEU-Med project: Vetricella, an early medieval royal property on Tuscany's Mediterranean* (pp. 161-168). All'Insegna del Giglio.

Pieruccini, P., Susini, D., Buonincontri, M. P., Bianchi, G., Hodges, R., Lubritto, C., & Di Pasquale, G. (2021). Late Holocene human-induced landscape changes in Calcareous Tufa environments in Central Mediterranean valleys (Pecora river, Southern Tuscany, Italy). *Geomorphology*, *383*, 107691.

Pieruccini, P., Susini, D., Poggi, G., Bianchi, G., & Hodges, R. (2023). Geoarchaeology of the Cornia river coastal plain (Piombino, southern Tuscany, Italy). *Journal of Maps*, *19*(1), 2173677.

Porrello, S., Lenzi, M., Persia, E., Tomassetti, P., & Finoia, M. G. (2003). Reduction of aquaculture wastewater eutrophication by phytotreatment ponds system: I. Dissolved and particulate nitrogen and phosphorus. *Aquaculture*, *219*(1-4), 515-529.

Pranzini, E. (2001). Updrift river mouth migration on cuspate deltas: two examples from the coast of Tuscany (Italy). *Geomorphology*, *38*(1-2), 125-132.

Prayon, F. (2010), *Die Etrusker. Geschichte, Religion, Kunst* (2nd ed.). C. H. Beck.

Ramrath, A., Sadori, L., & Negendank, J. F. (2000). Sediments from Lago di Mezzano, central Italy: a record of Lateglacial/Holocene climatic variations and anthropogenic impact. *The Holocene*, *10*(1), 87-95.

Ravazzi, C., Marchetti, M., Zanon, M., Perego, R., Quirino, T., Deaddis, M., De Amicis, M., & Margaritora, D. (2013). Lake evolution and landscape history in the lower Mincio River valley, unravelling drainage changes in the central Po Plain (N-Italy) since the Bronze Age. *Quaternary International*, *288*, 195-205.

Reille, M. (1992). *Pollen et spores d'Europe et d'Afrique du Nord*. Laboratoire de Botanique historique et Palynologie.

Reille, M. (1995). *Pollen et spores d'Europe et d'Afrique du Nord, Supplement 1*. Laboratoire de Botanique historique et Palynologie.

Reille, M. (1998). *Pollen et spores d'Europe et d'Afrique du Nord, Supplement 2*. Laboratoire de Botanique historique et Palynologie.

Reimer, P. J., Austin, W. E., Bard, E., Bayliss, A., Blackwell, P. G., Ramsey, C. B., Butzin, M., Cheng, H., Edwards, R. L., Friedrich, M., Grootes, P. M., Guilderson, T. P., Hajdas, I., Heaton, T. J., Hogg, A. G., Hughen, K. A., Kromer, B., Manning, S. W., Muscheler, R., Palmer, J. G., Pearson, C., van der Plicht, J., Reimer, R. W., Richards, D. A., Scott, E. M., Southon, J. R., Turney, C. S. M., Wacker, L., Adolphi, F., Büntgen, U., Capano, M., Fahrni, S. M., Fogtmann-Schulz, A., Friedrich, R., Köhler, P., Kudsk, S., Miyake, F., Olsen, J., Reinig, F., Sakamoto, M., Sookdeo, A., & Talamo, S. (2020). The IntCal20 Northern Hemisphere radiocarbon age calibration curve (0–55 cal kBP). *Radiocarbon*, *62*(4), 725-757.

Renzi, M., Lenzi, M., Franchi, E., Tozzi, A., Porrello, S., Focardi, S., & Focardi, S. E. (2007). A forecast method of seagrass meadow compatibility in coastal shallow water bottom. *International Journal of Environment and Health*, *1*(3), 360-374.

Renzi, M. (2022). *La laguna di Orbetello: storia, ambiente, gestione e progetti futuri*. Effigi.

Rossi, F. (2017). Duna Feniglia – Sede Forestale (sito TF01). Un sito produttivo villanoviano. In N. Negroni Catacchio, M. Cardosa, & A. Dolfini (Eds.), *Paesaggi d'Acque. La laguna di Orbetello e il Monte Argentario tra Preistoria ed Età Romana* (pp. 230-251). Centro Studi di Preistoria e Archeologia.

Sadori, L., & Narcisi, B. (2001). The Postglacial record of environmental history from Lago di Pergusa, Sicily. *The Holocene*, *11*(6), 655-671.

Sadori, L., Zanchetta, G., & Giardini, M. (2008). Last Glacial to Holocene palaeoenvironmental evolution at Lago di Pergusa (Sicily, Southern Italy) as inferred by pollen, microcharcoal, and stable isotopes. *Quaternary International*, *181*(1), 4-14.

Sadori, L., Jahns, S., & Peyron, O. (2011). Mid-Holocene vegetation history of the central Mediterranean. *The Holocene*, *21*(1), 117-129.

Sadori, L., Mazzini, I., Pepe, C., Goiran, J. P., Pleuger, E., Ruscito, V., Salomon, F., & Vittori, C. (2016). Palynology and ostracodology at the Roman port of ancient Ostia (Rome, Italy). *The Holocene*, *26*(9), 1502-1512.

Sadori, L. (2018). The Lateglacial and Holocene vegetation and climate history of Lago di Mezzano (central Italy). *Quaternary Science Reviews*, *202*, 30-44.

Salvagnoli-Marchetti, A. (1859). *Rapporto a sua eccellenza il presidente del R. governo della Toscana sul bonificamento delle Maremme toscane dal 1828-29 al 1858-59 compilato dall'ispettore Antonio Salvagnoli Marchetti*. Tip. delle Murate.

Saragosa, C. (2019). La Costa della Maremma Toscana tra protezione e sviluppo. Da Piombino a Punta Civette. In *La costa della Maremma Toscana tra protezione e sviluppo* (pp. 67-84). Universitas Studiorum.

Seager, R., Osborn, T. J., Kushnir, Y., Simpson, I. R., Nakamura, J., & Liu, H. (2019). Climate variability and change of Mediterranean-type climates. *Journal of Climate*, *32*(10), 2887-2915.

Srihari, S., Subramani, T., Prapanchan, V. N., & Li, P. (2022). Human health risk perspective study on characterization, quantification and spatial distribution of microplastics in surface water, groundwater and coastal sediments of thickly populated Chennai coast of South India. *Human and Ecological Risk Assessment: An International Journal*, *29*, 222-244.

Thornthwaite, C. W., & Mather, J. R. (1957). Instructions and tables for computing potential evapotranspiration and the water balance. *Publications in Climatology, 10*(3), 1-311. Laboratory of Climatology.

Turner, S., Horton, A. A., Rose, N. L., & Hall, C. (2019). A temporal sediment record of microplastics in an urban lake, London, UK. *Journal of Paleolimnology*, *61*(4), 449-462.

Vacchi, M., Marriner, N., Morhange, C., Spada, G., Fontana, A., & Rovere, A. (2016). Multiproxy assessment of Holocene relative sea-level changes in the western Mediterranean: Sea-level variability and improvements in the definition of the isostatic signal. *Earth-Science Reviews*, *155*, 172-197.

Vacchi, M., Ghilardi, M., Melis, R. T., Spada, G., Giaime, M., Marriner, N., Lorscheid, T., Morhange, C., Burjachs, F., & Rovere, A. (2018). New relative sea-level insights into the isostatic history of the Western Mediterranean. *Quaternary Science Reviews*, *201*, 396-408.

Van Geel, B. (2002). Non-pollen palynomorphs. In Smol, Birks, Last, Bradley, Alverson (Eds.), *Tracking environmental change using lake sediments: terrestrial, algal, and siliceous indicators* (pp. 99-119). Springer.

Vannière, B., Colombaroli, D., Chapron, E., Leroux, A., Tinner, W., & Magny, M. (2008). Climate versus human-driven fire regimes in Mediterranean landscapes: the Holocene record of Lago dell'Accesa (Tuscany, Italy). *Quaternary Science Reviews*, *27*(11-12), 1181-1196.

Viaroli, P., Bartoli, M., Bondavalli, C., Christian, R. R., Giordani, G., & Naldi, M. (1996). Macrophyte communities and their impact on benthic fluxes of oxygen, sulphide and nutrients in shallow eutrophic environments. *Hydrobiologia*, *329*(1), 105-119.

Viaroli, P., Bartoli, M., Giordani, G., Naldi, M., Orfanidis, S., & Zaldivar, J. M. (2008). Community shifts, alternative stable states, biogeochemical controls and feedbacks in eutrophic coastal lagoons: a brief overview. *Aquatic Conservation: Marine and Freshwater Ecosystems*, *18*(S1), S105-S117.

Viciani, D., & Lombardi, L. (2001). La vegetazione del padule di Orti-Bottagone (Piombino, Toscana meridionale) e la sua importanza botanica ai fini conservazionistici. *Parlatorea*, *5*, 101-118.

Viciani, D., Dell'Olmo, L., Foggi, B., Ferretti, G., Lastrucci, L., & Gennai, M. (2018). Natura 2000 habitat of Mt. Argentario promontory (southern Tuscany, Italy). *Journal of Maps*, *14*(2), 447-454.

Walker, M., Head, M. J., Berkelhammer, M., Björck, S., Cheng, H., Cwynar, L., Fisher, D., Gkinis, V., Long, A., Lowe, J., Newnham, R., Rasmussen, S. O., & Weiss, H. (2018). Formal ratification of the subdivision of the Holocene Series/Epoch (Quaternary System/Period): two new Global Boundary Stratotype Sections and Points (GSSPs) and three new stages/subseries. *Episodes*, *41*(4), 213-223.

Whitlock, C., & Larsen, C. (2001). Charcoal as a fire proxy. In Smol, Birks, Last, Bradley, Alverson (Eds.), *Tracking environmental change using lake sediments: terrestrial, algal, and siliceous indicators* (pp. 75-97). Springer.

Wolfram, A. (1954). Versuche zur Trennung der Sporomorphen von organischen und anorganischen Beimengungen unter Berücksichtigung der Wirkung des Ultraschalls auf Kohlenmazerate. *Geologisches Jahrbuch*, *3*, 655-659.

Zalasiewicz, J., Waters, C. N., Ivar do Sul, J. A., Corcoran, P. L., Barnosky, A. D., Cearreta, A., Edgeworth, M., Gałuszka, A., Jeandel, C., Leinfelder, R., McNeill, J. R., Steffen, W., Summerhayes, C., Wagreich, M., Williams, M., Wolfe, A. P., & Yonan, Y. (2019). The geological cycle of plastics and their use as a stratigraphic indicator of the Anthropocene. *Anthropocene*, 28, 100224

Zanon, M., Unkel, I., Andersen, N., & Kirleis, W. (2019). Palaeoenvironmental dynamics at the southern Alpine foothills between the Neolithic and the Bronze Age onset. A multi-proxy study from Bande di Cavriana (Mantua, Italy). *Quaternary Science Reviews*, *221*, 105891.

Appendix I – Floristic lists

Site: Burano - Core: LB5B			
Taxa	**Family**	**Ecological group**	**Habit**
Sambucus	Adoxaceae	Sub-Mediterranean	Arboreal
Viburnum	Adoxaceae	Sub-Mediterranean	Shrubby
Alisma plantago	Alismataceae	Hydrophytes	Herbaceous
Sagittaria	Alismataceae	Hydrophytes	Herbaceous
Amaranthaceae indet.	Amaranthaceae	Halophytes / NAP	Herbaceous
Pistacia lentiscus	Anacardiaceae	Mediterranean	Arboreal
Pistacia terebinthus	Anacardiaceae	Mediterranean	Arboreal
Rhus	Anacardiaceae	Mediterranean	Arboreal
Apiaceae indet.	Apiaceae	Upland Herbs	Herbaceous
Lemna	Araceae	Hydrophytes	Herbaceous
Hedera	Araliaceae	Upland Herbs	Herbaceous
Artemisia	Asteraceae	Xerophytes	Herbaceous
Asteraceae Asteroideae *Ambrosia* type	Asteraceae	Upland Herbs	Herbaceous
Asteraceae Asteroideae *Carduus* type	Asteraceae	Upland Herbs	Herbaceous
Asteraceae Asteroideae *Carlina* type	Asteraceae	Upland Herbs	Herbaceous
Asteraceae Asteroideae *Cirsium* type	Asteraceae	Upland Herbs	Herbaceous
Asteraceae Asteroideae *Cotula* type	Asteraceae	Upland Herbs	Herbaceous
Asteraceae Asteroideae *Senecio* type	Asteraceae	Upland Herbs	Herbaceous
Asteraceae Asteroideae *Xanthium* type	Asteraceae	Upland Herbs	Herbaceous
Asteraceae Cichorioideae	Asteraceae	Upland Herbs	Herbaceous
Centaurea cf. *cyanus*	Asteraceae	Upland Herbs	Herbaceous
Centaurea cf. *nigra*	Asteraceae	Upland Herbs	Herbaceous
Alnus	Betulaceae	Riparian	Arboreal
Betula	Betulaceae	Mountain taxa	Arboreal
Carpinus betulus	Betulaceae	Sub-Mediterranean	Arboreal
Carpinus orientalis	Betulaceae	Sub-Mediterranean	Arboreal
Corylus	Betulaceae	Sub-Mediterranean	Arboreal
Ostrya	Betulaceae	Sub-Mediterranean	Arboreal
Brassicaceae indet.	Brassicaceae	Upland Herbs	Herbaceous
Cannabaceae indet.	Cannabaceae	Upland Herbs	Herbaceous
Celtis	Cannabaceae	Anthropogenic	Arboreal
Cf. *Knautia*	Caprifoliaceae	Upland Herbs	Herbaceous
Caryophyllaceae indet.	Caryophyllaceae	Halophytes / NAP	Herbaceous
Cistaceae indet.	Cistaceae	Upland Herbs	Herbaceous
Cistus	Cistaceae	Upland Herbs	Herbaceous
Cf. *Helianthemum*	Cistaceae	Upland Herbs	Herbaceous
Sedum	Crassulaceae	Upland Herbs	Herbaceous
Cupressoideae indet.	Cupressaceae	Anthropogenic	Arboreal
Juniperus	Cupressaceae	Mediterranean	Shrubby
Cyperaceae indet.	Cyperaceae	Helophytes	Herbaceous
Ephedra fragilis type	Ephedraceae	Xerophytes	Herbaceous

Ericaceae indet.	Ericaceae	Upland Herbs	Shrubby
Euphorbiaceae indet.	Euphorbiaceae	Upland Herbs	Herbaceous
Fabaceae indet.	Fabaceae	Upland Herbs	Herbaceous
Cf. *Lotus*	Fabaceae	Upland Herbs	Herbaceous
Castanea	Fagaceae	Anthropogenic	Arboreal
Fagus	Fagaceae	Mountain taxa	Arboreal
Quercus cerris	Fagaceae	Sub-Mediterranean	Arboreal
Quercus ilex-coccifera type	Fagaceae	Mediterranean	Arboreal
Quercus pubescens type	Fagaceae	Sub-Mediterranean	Arboreal
Quercus suber	Fagaceae	Sub-Mediterranean	Arboreal
Quercus sp.	Fagaceae	Sub-Mediterranean	Arboreal
Geraniaceae cf. *Erodium*	Geraniaceae	Upland Herbs	Herbaceous
Geraniaceae indet.	Geraniaceae	Upland Herbs	Herbaceous
Myriophyllum	Haloragaceae	Hydrophytes	Herbaceous
Cf. *Elodea*	Hydrocharitaceae	Hydrophytes	Herbaceous
Hypericum	Hypericaceae	Upland Herbs	Herbaceous
Iridaceae indet.	Iridaceae	Upland Herbs	Herbaceous
Juglans	Juglandaceae	Anthropogenic	Arboreal
Lamiaceae indet.	Lamiaceae	Upland Herbs	Herbaceous
Liliaceae indet.	Liliaceae	Upland Herbs	Herbaceous
Malvaceae indet.	Malvaceae	Upland Herbs	Herbaceous
Eucalyptus	Myrtaceae	Anthropogenic	Arboreal
Myrtaceae indet.	Myrtaceae	Mediterranean	Shrubby
Myrtus	Myrtaceae	Mediterranean	Shrubby
Fraxinus excelsior type	Oleaceae	Sub-Mediterranean	Arboreal
Fraxinus ornus type	Oleaceae	Sub-Mediterranean	Arboreal
Olea	Oleaceae	Anthropogenic	Arboreal
Phillyrea	Oleaceae	Mediterranean	Arboreal
Pinus	Pinaceae	*Pinus*	Arboreal
Callitriche	Plantaginaceae	Hydrophytes	Herbaceous
Plantago lanceolata type	Plantaginaceae	Upland Herbs	Herbaceous
Plantago media type	Plantaginaceae	Upland Herbs	Herbaceous
Plantago sp.	Plantaginaceae	Upland Herbs	Herbaceous
Poaceae >40 µm	Poaceae	Anthropogenic	Herbaceous
Poaceae <20 µm	Poaceae	Helophytes / NAP	Herbaceous
Poaceae 20<x<40 µm	Poaceae	Helophytes / NAP	Herbaceous
Cf. *Calligonum*	Polygonaceae	Upland Herbs	Herbaceous
Polygonum cf. *persicaria*	Polygonaceae	Upland Herbs	Herbaceous
Rumex	Polygonaceae	Upland Herbs	Herbaceous
Potamogeton	Potamogetonaceae	Hydrophytes	Herbaceous
Ranunculaceae indet.	Ranunculaceae	Upland Herbs	Herbaceous
Thalictrum	Ranunculaceae	Upland Herbs	Herbaceous
Ziziphus	Rhamnaceae	Sub-Mediterranean	Shrubby
Rosaceae cf. *Geum*	Rosaceae	Upland Herbs	Herbaceous
Rosaceae indet.	Rosaceae	Upland Herbs	Herbaceous
Rosaceae cf. *Spiraea*	Rosaceae	Upland Herbs	Herbaceous
Cf. *Galium*	Rubiaceae	Upland Herbs	Herbaceous

Ruppia	Ruppiaceae	Hydrophytes	Herbaceous
Ruta	Rutaceae	Upland Herbs	Herbaceous
Salicaceae indet.	Salicaceae	Riparian	Arboreal
Cf. *Salix*	Salicaceae	Riparian	Arboreal
Acer	Sapindaceae	Sub-Mediterranean	Arboreal
Saxifragaceae indet.	Saxifragaceae	Upland Herbs	Herbaceous
Cf. *Scrophularia*	Scrophulariaceae	Upland Herbs	Herbaceous
Scrophulariaceae indet.	Scrophulariaceae	Upland Herbs	Herbaceous
Cf. *Verbascum*	Scrophulariaceae	Upland Herbs	Herbaceous
Cf. *Smilax*	Smilacaceae	Upland Herbs	Herbaceous
Solanum cf. *nigrum*	Solanaceae	Anthropogenic	Herbaceous
Tamarix	Tamaricaceae	Mediterranean	Shrubby
Sparganium/Typha angustifolia	Typhaceae	Hydrophytes	Herbaceous
Typha latifolia	Typhaceae	Helophytes	Herbaceous
Ulmus	Ulmaceae	Sub-Mediterranean	Arboreal
Urticaceae indet.	Urticaceae	Upland Herbs	Herbaceous
Vitis	Vitaceae	Anthropogenic	Arboreal

Taxa	**Family**	**Category**	**Habit**
Monolete spore indet.	Various	Pteridophyte spore	/
Trilete spore indet.	Various	Pteridophyte spore	/
Polypodium	Polypodiaceae	Pteridophyte spore	/
Cf. *Hymenophyllum*	Hymenophyllaceae	Pteridophyte spore	/
Cf. *Isoetes*	Isoetaceae	Pteridophyte spore	/
Spiniferites	Uncertain	Dinocyst	/
Lingulodinium	Gonyaulacaceae	Dinocyst	/
Dinociste indet.	Various	Dinocyst	/
Dinociste indet. morphotype 2	Various	Dinocyst	/
Indet. cf. *Closterium*	Closteriaceae	Dinocyst	/
Zygnema type	Zygnemataceae	Dinocyst	/
Cf. *Glomus*	Glomeraceae	Fungal spore	/
Foraminiferal organic linings	Various	Other NPPs	/
Algae indet. morphotype 1	Uncertain	Other NPPs	/
Botryococcus	Botryococcaceae	Other NPPs	/
Pseudoschizaea	Uncertain	Other NPPs	/
Spirogyra	Zygnemataceae	Other NPPs	/
Cosmarium	Desmidiaceae	Other NPPs	/
Euastrum	Desmidiaceae	Other NPPs	/
Arcella	Arcellidae	Other NPPs	/
Parasite egg	Uncertain	Other NPPs	/
Resting egg	Uncertain	Other NPPs	/
Cf. Trichome type 2	Uncertain	Other NPPs	/
Diatom indet.	Various	Other NPPs	/
NPP *Ribes* type	Uncertain	Other NPPs	/
Indet. type128	Uncertain	Other NPPs	/

Tab. 1: list of taxa (both pollen and NPPs) found in the LB5B core.

Site: Orbetello - Core: OLP-11B			
Taxa	**Family**	**Ecological group**	**Habit**
Sambucus	Adoxaceae	Sub-Mediterranean	Arboreal
Viburnum	Adoxaceae	Sub-Mediterranean	Shrubby
Viburnum cf. *opulus*	Adoxaceae	Sub-Mediterranean	Shrubby
Alisma plantago	Alismataceae	Hydrophytes	Herbaceous
Sagittaria	Alismataceae	Hydrophytes	Herbaceous
Amaranthaceae indet.	Amaranthaceae	Halophytes / NAP	Herbaceous
Pistacia	Anacardiaceae	Mediterranean	Arboreal
Rhus	Anacardiaceae	Mediterranean	Arboreal
Apiaceae indet.	Apiaceae	Upland Herbs	Herbaceous
Cf. *Apium*	Apiaceae	Upland Herbs	Herbaceous
Cf. *Vinca*	Apocynaceae	Upland Herbs	Herbaceous
Indet. cf. Aponogeton	Aponogetonaceae	Hydrophytes	Herbaceous
Lemna	Araceae	Hydrophytes	Herbaceous
Hedera	Araliaceae	Upland Herbs	Herbaceous
Cf. *Scilla*	Asparagaceae	Upland Herbs	Herbaceous
Asphodelus	Asphodelaceae	Upland Herbs	Herbaceous
Artemisia	Asteraceae	Xerophytes	Herbaceous
Asteraceae Asteroideae *Ambrosia* type	Asteraceae	Upland Herbs	Herbaceous
Asteraceae Asteroideae *Bellis* type	Asteraceae	Upland Herbs	Herbaceous
Asteraceae Asteroideae *Carduus* type	Asteraceae	Upland Herbs	Herbaceous
Asteraceae Asteroideae *Carlina* type	Asteraceae	Upland Herbs	Herbaceous
Asteraceae Asteroideae *Cotula* type	Asteraceae	Upland Herbs	Herbaceous
Asteraceae Asteroideae *Senecio* type	Asteraceae	Upland Herbs	Herbaceous
Asteraceae Asteroideae *Tanacetum* type	Asteraceae	Upland Herbs	Herbaceous
Asteraceae Asteroideae *Xanthium* type	Asteraceae	Upland Herbs	Herbaceous
Asteraceae Cichorioideae	Asteraceae	Upland Herbs	Herbaceous
Centaurea cf. *cyanus*	Asteraceae	Upland Herbs	Herbaceous
Centaurea cf. *macrocephala*	Asteraceae	Upland Herbs	Herbaceous
Centaurea cf. *nigra*	Asteraceae	Upland Herbs	Herbaceous
Alnus	Betulaceae	Riparian	Arboreal
Betula	Betulaceae	Mountain taxa	Arboreal
Carpinus betulus	Betulaceae	Sub-Mediterranean	Arboreal
Carpinus orientalis	Betulaceae	Sub-Mediterranean	Arboreal
Corylus	Betulaceae	Sub-Mediterranean	Arboreal
Ostrya	Betulaceae	Sub-Mediterranean	Arboreal
Boraginaceae (Cf. *Anchusa*)	Boraginaceae	Upland Herbs	Herbaceous
Brassicaceae indet.	Brassicaceae	Upland Herbs	Herbaceous
Buxus	Buxaceae	Sub-Mediterranean	Arboreal
Campanulaceae indet.	Campanulaceae	Upland Herbs	Herbaceous
Caryophyllaceae indet.	Caryophyllaceae	Halophytes / NAP	Herbaceous
Cistaceae indet.	Cistaceae	Upland Herbs	Herbaceous
Cistus	Cistaceae	Upland Herbs	Herbaceous
Helianthemum	Cistaceae	Upland Herbs	Herbaceous
Helianthemum cf. *ledifolium*	Cistaceae	Upland Herbs	Herbaceous
Tuberaria	Cistaceae	Upland Herbs	Herbaceous

Cf. *Ipomoea*	Convolvulaceae	Halophytes / NAP	Herbaceous
Cornus cf. *mas*	Cornaceae	Sub-Mediterranean	Shrubby
Sedum	Crassulaceae	Upland Herbs	Herbaceous
Cupressoideae indet.	Cupressaceae	Anthropogenic	Arboreal
Juniperus	Cupressaceae	Mediterranean	Shrubby
Cyperaceae indet.	Cyperaceae	Helophytes	Herbaceous
Cf. Dipsacaceae indet.	Dipsacaceae	Upland Herbs	Herbaceous
Ephedra distachya type	Ephedraceae	Xerophytes	Herbaceous
Ephedra fragilis type	Ephedraceae	Xerophytes	Herbaceous
Indet. cf. *Ephedra*	Ephedraceae	Xerophytes	Herbaceous
Ericaceae indet.	Ericaceae	Upland Herbs	Shrubby
Ericaceae cf. *Vaccinium*	Ericaceae	Upland Herbs	Shrubby
Euphorbiaceae indet.	Euphorbiaceae	Upland Herbs	Herbaceous
Ricinus	Euphorbiaceae	Upland Herbs	Herbaceous
Cercis	Fabaceae	Mediterranean	Arboreal
Fabaceae indet.	Fabaceae	Upland Herbs	Herbaceous
Medicago	Fabaceae	Anthropogenic	Herbaceous
Castanea	Fagaceae	Anthropogenic	Arboreal
Fagus	Fagaceae	Mountain taxa	Arboreal
Quercus cerris	Fagaceae	Sub-Mediterranean	Arboreal
Quercus ilex-coccifera type	Fagaceae	Mediterranean	Arboreal
Quercus pubescens type	Fagaceae	Sub-Mediterranean	Arboreal
Quercus suber	Fagaceae	Sub-Mediterranean	Arboreal
Quercus sp.	Fagaceae	Sub-Mediterranean	Arboreal
Gentianaceae indet.	Gentianaceae	Upland Herbs	Herbaceous
Cf. *Ribes*	Grossulariaceae	Upland Herbs	Herbaceous
Myriophyllum	Haloragaceae	Hydrophytes	Herbaceous
Hypericum	Hypericaceae	Upland Herbs	Herbaceous
Iridaceae indet.	Iridaceae	Upland Herbs	Herbaceous
Juglans	Juglandaceae	Anthropogenic	Arboreal
Lamiaceae indet.	Lamiaceae	Upland Herbs	Herbaceous
Cf. *Phlomis*	Lamiaceae	Xerophytes	Herbaceous
Liliaceae indet.	Liliaceae	Upland Herbs	Herbaceous
Malvaceae indet.	Malvaceae	Upland Herbs	Herbaceous
Tilia	Malvaceae	Sub-Mediterranean	Arboreal
Eucalyptus	Myrtaceae	Anthropogenic	Arboreal
Fraxinus excelsior type	Oleaceae	Sub-Mediterranean	Arboreal
Fraxinus ornus type	Oleaceae	Sub-Mediterranean	Arboreal
Olea	Oleaceae	Anthropogenic	Arboreal
Oleaceae indet.	Oleaceae	Mediterranean	Arboreal
Phillyrea	Oleaceae	Mediterranean	Arboreal
Papaveraceae cf. *Papaver*	Papaveraceae	Upland Herbs	Herbaceous
Abies	Pinaceae	Mountain taxa	Arboreal
Picea	Pinaceae	Mountain taxa	Arboreal
Pinus	Pinaceae	*Pinus*	Arboreal
Callitriche	Plantaginaceae	Hydrophytes	Herbaceous
Cf. *Chaenorhinum*	Plantaginaceae	Upland Herbs	Herbaceous

Linaria	Plantaginaceae	Upland Herbs	Herbaceous
Plantago lanceolata type	Plantaginaceae	Upland Herbs	Herbaceous
Plantago media type	Plantaginaceae	Upland Herbs	Herbaceous
Limonium	Plumbaginaceae	Halophytes / NAP	Herbaceous
Poaceae >40 µm	Poaceae	Anthropogenic	Herbaceous
Poaceae <20 µm	Poaceae	Helophytes / NAP	Herbaceous
Poaceae 20<x<40 µm	Poaceae	Helophytes / NAP	Herbaceous
Calligonum	Polygonaceae	Upland Herbs	Herbaceous
Polygonaceae indet.	Polygonaceae	Upland Herbs	Herbaceous
Rumex	Polygonaceae	Upland Herbs	Herbaceous
Potamogeton	Potamogetonaceae	Hydrophytes	Herbaceous
Ranunculaceae indet.	Ranunculaceae	Upland Herbs	Herbaceous
Ranunculus cf. *acris* type	Ranunculaceae	Upland Herbs	Herbaceous
Thalictrum	Ranunculaceae	Upland Herbs	Herbaceous
Rhamnus	Rhamnaceae	Mediterranean	Shrubby
Rosaceae cf. *Filipendula*	Rosaceae	Upland Herbs	Herbaceous
Rosaceae cf. *Geum*	Rosaceae	Upland Herbs	Herbaceous
Rosaceae indet.	Rosaceae	Upland Herbs	Herbaceous
Ruppia	Ruppiaceae	Hydrophytes	Herbaceous
Cf. *Populus*	Salicaceae	Anthropogenic	Arboreal
Salix	Salicaceae	Riparian	Arboreal
Acer	Sapindaceae	Sub-Mediterranean	Arboreal
Cf. *Scrophularia*	Scrophulariaceae	Upland Herbs	Herbaceous
Scrophulariaceae indet.	Scrophulariaceae	Upland Herbs	Herbaceous
Cf. *Verbascum*	Scrophulariaceae	Upland Herbs	Herbaceous
Cf. *Smilax*	Smilacaceae	Upland Herbs	Herbaceous
Solanaceae indet.	Solanaceae	Anthropogenic	Herbaceous
Sparganium/Typha angustifolia	Typhaceae	Hydrophytes	Herbaceous
Typha latifolia	Typhaceae	Helophytes	Herbaceous
Ulmus	Ulmaceae	Sub-Mediterranean	Arboreal
Cf. Urticaceae indet.	Urticaceae	Upland Herbs	Herbaceous
Parthenocissus	Vitaceae	Upland Herbs	Herbaceous
Vitis	Vitaceae	Anthropogenic	Arboreal

Taxa	**Family**	**Category**	**Habit**
Monolete spore indet.	Various	Pteridophyte spore	/
Trilete spore indet.	Various	Pteridophyte spore	/
Polypodium	Polypodiaceae	Pteridophyte spore	/
Cf. *Hymenophyllum*	Hymenophyllaceae	Pteridophyte spore	/
Cf. *Isoetes*	Isoetaceae	Pteridophyte spore	/
Foraminiferal organic linings	Various	Other NPPs	/
Algae indet. morphotype 1	Uncertain	Other NPPs	/
Algae indet. motphotype 2	Uncertain	Other NPPs	/
Botryococcus	Botryococcaceae	Other NPPs	/
Pseudoschizaea	Uncertain	Other NPPs	/
Debarya	Uncertain	Dinocyst	/

Ustilago	Ustilaginaceae	Pteridophyte spore	/
Dinociste indet.	Various	Dinocyst	/
Dinociste baculata	Various	Dinocyst	/
Spiniferites	Uncertain	Dinocyst	/
Spiniferites cf. *bentori*	Uncertain	Dinocyst	/
Lingulodinium	Gonyaulacaceae	Dinocyst	/
Operculodinium	Uncertain	Dinocyst	/
Bitectatodinium	Uncertain	Dinocyst	/
Indet. fungal spore	Various	Fungal spore	/
Cf. *Trichuris*	Trichuridae	Other NPPs	/
Trachylomonas	Euglenaceae	Other NPPs	/
Tintinnids	Various	Other NPPs	/
Indeterminate inaperturate morphotype	Uncertain	Other NPPs	/
Verrucate inaperturate morphotype	Uncertain	Other NPPs	/
Spiny indeterminate morphotype	Uncertain	Other NPPs	/
Small hyaline NPP	Uncertain	Other NPPs	/
Small rounded NPP	Uncertain	Other NPPs	/
Indeterminate NPP	Uncertain	Other NPPs	/
Spiny NPP	Uncertain	Other NPPs	/
NPP morphotype 171	Uncertain	Other NPPs	/
NPP morphotype 169	Uncertain	Other NPPs	/
Process-bearing NPP	Uncertain	Other NPPs	/
Ascidian NPP	Uncertain	Other NPPs	/
NPP *Lemna* type	Uncertain	Other NPPs	/
NPP *Ribes* type	Uncertain	Other NPPs	/
Indet. hairy NPP	Uncertain	Other NPPs	/
Indet. type 4	Uncertain	Other NPPs	/
Indet. type 5	Uncertain	Other NPPs	/
Indet. type 6	Uncertain	Other NPPs	/
Indet. type 12	Uncertain	Other NPPs	/

Tab. 2: list of taxa (both pollen and NPPs) found in the OLP-11B core.

Site: Orti-Bottagone - Core: POP22-01			
Taxa	**Family**	**Ecological group**	**Habit**
Sambucus	Adoxaceae	Sub-Mediterranean	Arboreal
Viburnum	Adoxaceae	Sub-Mediterranean	Shrubby
Alisma plantago	Alismataceae	Hydrophytes	Herbaceous
Sagittaria	Alismataceae	Hydrophytes	Herbaceous
Amaranthaceae indet.	Amaranthaceae	Halophytes / NAP	Herbaceous
Pistacia lentiscus	Anacardiaceae	Mediterranean	Arboreal
Rhus	Anacardiaceae	Mediterranean	Arboreal
Apiaceae indet.	Apiaceae	Upland Herbs	Herbaceous
Lemna	Araceae	Hydrophytes	Herbaceous
Hedera	Araliaceae	Upland Herbs	Herbaceous
Cf. *Scilla*	Asparagaceae	Upland Herbs	Herbaceous
Artemisia	Asteraceae	Xerophytes	Herbaceous
Asteracea Asteroideae *Ambrosia* type	Asteraceae	Upland Herbs	Herbaceous
Asteracea Asteroideae *Carlina* type	Asteraceae	Upland Herbs	Herbaceous
Asteracea Asteroideae *Cotula* type	Asteraceae	Upland Herbs	Herbaceous
Asteracea Asteroideae *Senecio* type	Asteraceae	Upland Herbs	Herbaceous
Asteracea Asteroideae *Xanthium* type	Asteraceae	Upland Herbs	Herbaceous
Asteracea Cichorioideae	Asteraceae	Upland Herbs	Herbaceous
Centaurea cf. *cyanus*	Asteraceae	Upland Herbs	Herbaceous
Centaurea cf. *nigra*	Asteraceae	Upland Herbs	Herbaceous
Alnus	Betulaceae	Riparian	Arboreal
Betula	Betulaceae	Mountain taxa	Arboreal
Carpinus betulus	Betulaceae	Sub-Mediterranean	Arboreal
Carpinus orientalis	Betulaceae	Sub-Mediterranean	Arboreal
Corylus	Betulaceae	Sub-Mediterranean	Arboreal
Ostrya	Betulaceae	Sub-Mediterranean	Arboreal
Brassicaceae indet.	Brassicaceae	Upland Herbs	Herbaceous
Cannabaceae indet.	Cannabaceae	Upland Herbs	Herbaceous
Scabiosa	Caprifoliaceae	Upland Herbs	Herbaceous
Caryophyllaceae indet.	Caryophyllaceae	Halophytes / NAP	Herbaceous
Cistaceae indet.	Cistaceae	Upland Herbs	Herbaceous
Cistus	Cistaceae	Upland Herbs	Herbaceous
Helianthemum	Cistaceae	Upland Herbs	Herbaceous
Convolvulaceae indet.	Convolvulaceae	Upland Herbs	Herbaceous
Crassulaceae indet.	Crassulaceae	Upland Herbs	Herbaceous
Crassulaceae cf. *Kalanchoe*	Crassulaceae	Upland Herbs	Herbaceous
Sedum	Crassulaceae	Upland Herbs	Herbaceous
Cupressoideae indet.	Cupressaceae	Anthropogenic	Arboreal
Cyperaceae indet.	Cyperaceae	Helophytes	Herbaceous
Ephedra fragilis type	Ephedraceae	Xerophytes	Herbaceous
Ericaceae indet.	Ericaceae	Upland Herbs	Shrubby
Euphorbiaceae indet.	Euphorbiaceae	Upland Herbs	Herbaceous
Cf. *Mercurialis*	Euphorbiaceae	Upland Herbs	Herbaceous
Fabaceae indet.	Fabaceae	Upland Herbs	Herbaceous
Cf. *Lotus*	Fabaceae	Upland Herbs	Herbaceous

Castanea	Fagaceae	Anthropogenic	Arboreal
Fagus	Fagaceae	Mountain taxa	Arboreal
Quercus cerris	Fagaceae	Sub-Mediterranean	Arboreal
Quercus ilex-coccifera type	Fagaceae	Mediterranean	Arboreal
Quercus pubescens type	Fagaceae	Sub-Mediterranean	Arboreal
Quercus suber	Fagaceae	Sub-Mediterranean	Arboreal
Geraniaceae indet.	Geraniaceae	Upland Herbs	Herbaceous
Myriophyllum	Haloragaceae	Hydrophytes	Herbaceous
Hypericum	Hypericaceae	Upland Herbs	Herbaceous
Iridaceae indet.	Iridaceae	Upland Herbs	Herbaceous
Juglans	Juglandaceae	Anthropogenic	Arboreal
Lamiaceae indet.	Lamiaceae	Upland Herbs	Herbaceous
Malvaceae cf. *Althea*	Malvaceae	Upland Herbs	Herbaceous
Tilia	Malvaceae	Sub-Mediterranean	Arboreal
Fraxinus excelsior type	Oleaceae	Sub-Mediterranean	Arboreal
Olea	Oleaceae	Anthropogenic	Arboreal
Phillyrea	Oleaceae	Mediterranean	Arboreal
Abies	Pinaceae	Mountain taxa	Arboreal
Picea	Pinaceae	Mountain taxa	Arboreal
Pinus	Pinaceae	*Pinus*	Arboreal
Linaria	Plantaginaceae	Upland Herbs	Herbaceous
Plantago lanceolata type	Plantaginaceae	Upland Herbs	Herbaceous
Armeria	Plumbaginaceae	Upland Herbs	Herbaceous
Poaceae >40 µm	Poaceae	Anthropogenic	Herbaceous
Poaceae <20 µm	Poaceae	Helophytes / NAP	Herbaceous
Poaceae 20<x<40 µm	Poaceae	Helophytes / NAP	Herbaceous
Polygonaceae indet.	Polygonaceae	Upland Herbs	Herbaceous
Rumex	Polygonaceae	Upland Herbs	Herbaceous
Potamogeton	Potamogetonaceae	Hydrophytes	Herbaceous
Ranunculaceae indet.	Ranunculaceae	Upland Herbs	Herbaceous
Ziziphus	Rhamnaceae	Sub-Mediterranean	Shrubby
Rosaceae cf. *Fragaria*	Rosaceae	Upland Herbs	Herbaceous
Rosaceae indet.	Rosaceae	Upland Herbs	Herbaceous
Cf. *Galium*	Rubiaceae	Upland Herbs	Herbaceous
Ruppia	Ruppiaceae	Hydrophytes	Herbaceous
Ruta	Rutaceae	Upland Herbs	Herbaceous
Salicaceae indet.	Salicaceae	Riparian	Arboreal
Cf. *Salix*	Salicaceae	Riparian	Arboreal
Acer	Sapindaceae	Sub-Mediterranean	Arboreal
Saxifragaceae indet.	Saxifragaceae	Upland Herbs	Herbaceous
Cf. *Scrophularia*	Scrophulariaceae	Upland Herbs	Herbaceous
Scrophulariaceae indet.	Scrophulariaceae	Upland Herbs	Herbaceous
Cf. *Verbascum*	Scrophulariaceae	Upland Herbs	Herbaceous
Cf. *Smilax*	Smilacaceae	Upland Herbs	Herbaceous
Tamarix	Tamaricaceae	Mediterranean	Shrubby
Sparganium/Typha angustifolia	Typhaceae	Hydrophytes	Herbaceous
Typha latifolia	Typhaceae	Helophytes	Herbaceous

Ulmus	Ulmaceae	Sub-Mediterranean	Arboreal
Vitis	Vitaceae	Anthropogenic	Arboreal

Taxa	**Family**	**Category**	**Habit**
Monolete spore indet.	Various	Pteridophyte spore	/
Trilete spore indet.	Various	Pteridophyte spore	/
Polypodium	Polypodiaceae	Pteridophyte spore	/
Foraminiferal organic linings	Various	Other NPPs	/
Algae indet. morphotype 1	Uncertain	Other NPPs	/
Botryococcus	Botryococcaceae	Other NPPs	/
Pseudoschizaea	Uncertain	Other NPPs	/
Spirogyra	Zygnemataceae	Other NPPs	/
Cosmarium	Desmidiaceae	Other NPPs	/
Spiniferites	Uncertain	Dinocyst	/
Lingulodinium	Gonyaulacaceae	Dinocyst	/
Dinociste indet.	Various	Dinocyst	/
Dinociste indet. morphotype 2	Various	Dinocyst	/

Tab. 3: list of taxa (both pollen and NPPs) found in the POP22-01 core.

Appendix II – Photos

Fig. 1: the mechanical rotation core drill used for the extraction of sediment cores at Duna Feniglia (Orbetello site) (Photo: Matteo Pili).

Fig. 2: preliminary lithological description of a core extracted from Duna Feniglia (Orbetello site) (Photo: Cécile Vittori).

Fig. 3: plastic case for depositing and transporting the extracted cores. (Photo: Cécile Vittori).

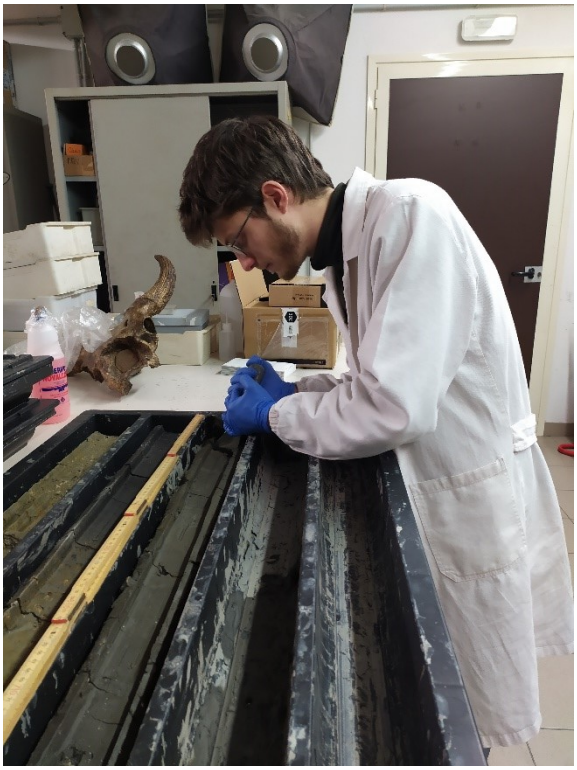

Fig. 4: sampling of the sediment core POP22-01. (Photo: Houssem Tabbabi).

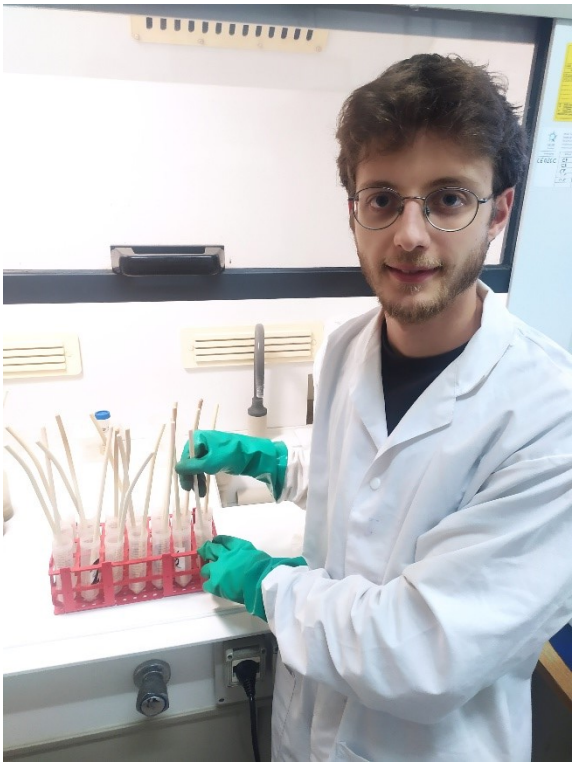

Fig. 5: chemical-physical treatment of the sediment samples in the laboratory. (Photo: Houssem Tabbabi).

Fig. 6: Leica ICC50 W microscope used for slide analysis. (Photo: Matteo Pili).

Fig. 7: NIKON Eclipse 50i microscope used for slide analysis. (Photo: Gabriele Niccolini).

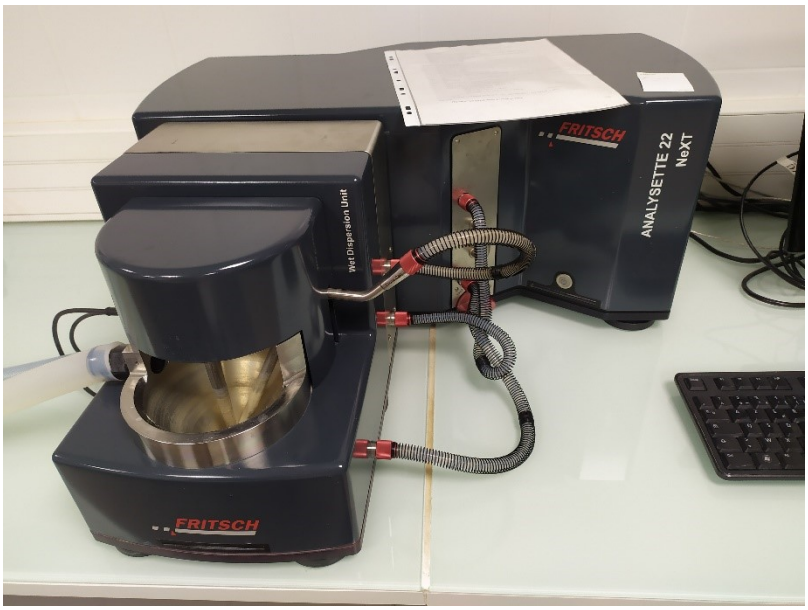

Fig. 8: Fritsch Analysette 22 Next granulometer used for laser granulometric analysis. (Photo: Matteo Pili).

Appendix III – Photos of microplastics

1. Fragments found in fossil cores

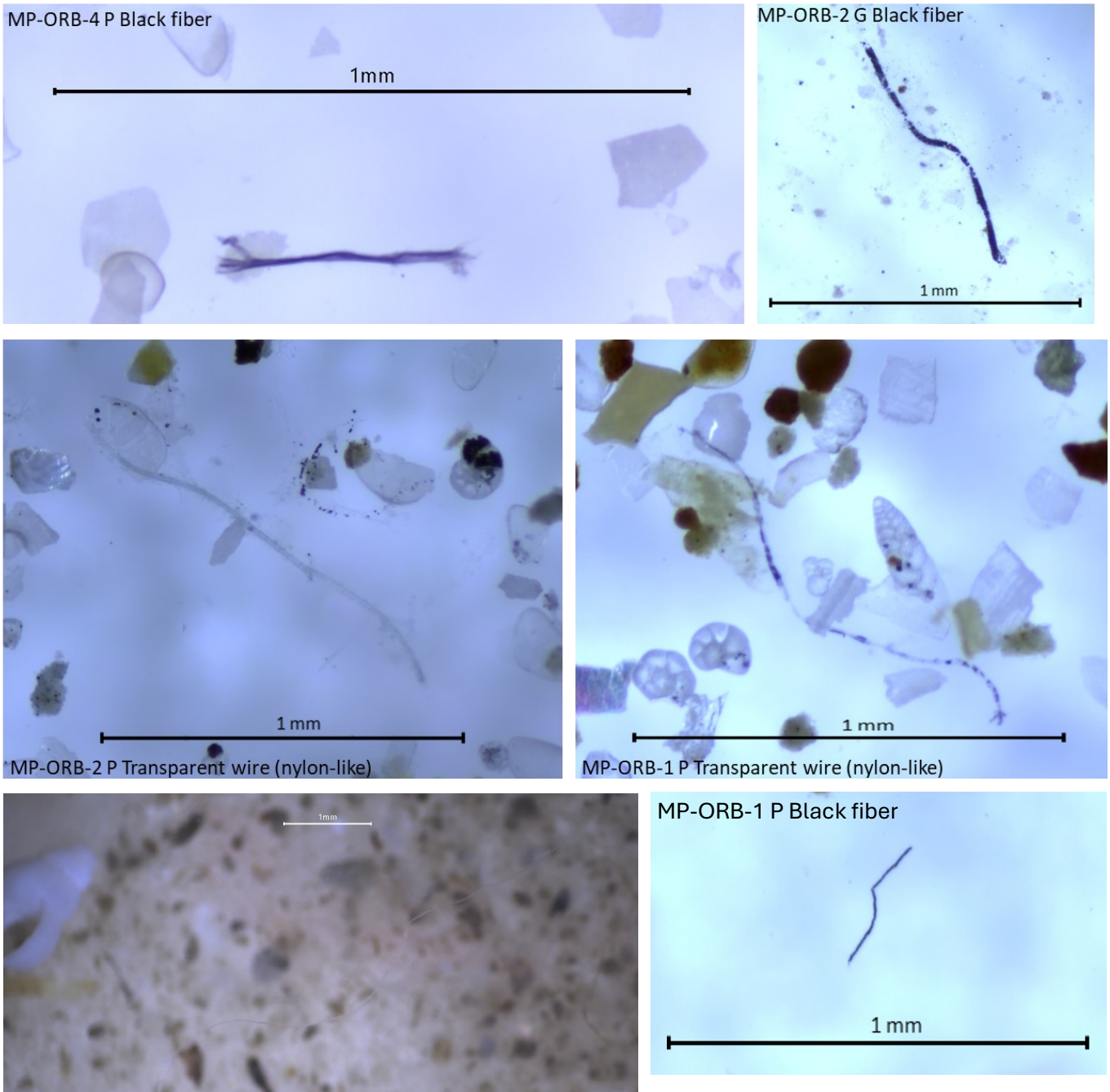

Fig. 1: Black fibers and transparent wires found in various samples (sample code indicated next to each photo) of the LB5B and OLP-11B cores, collected for micro-plastic analysis.

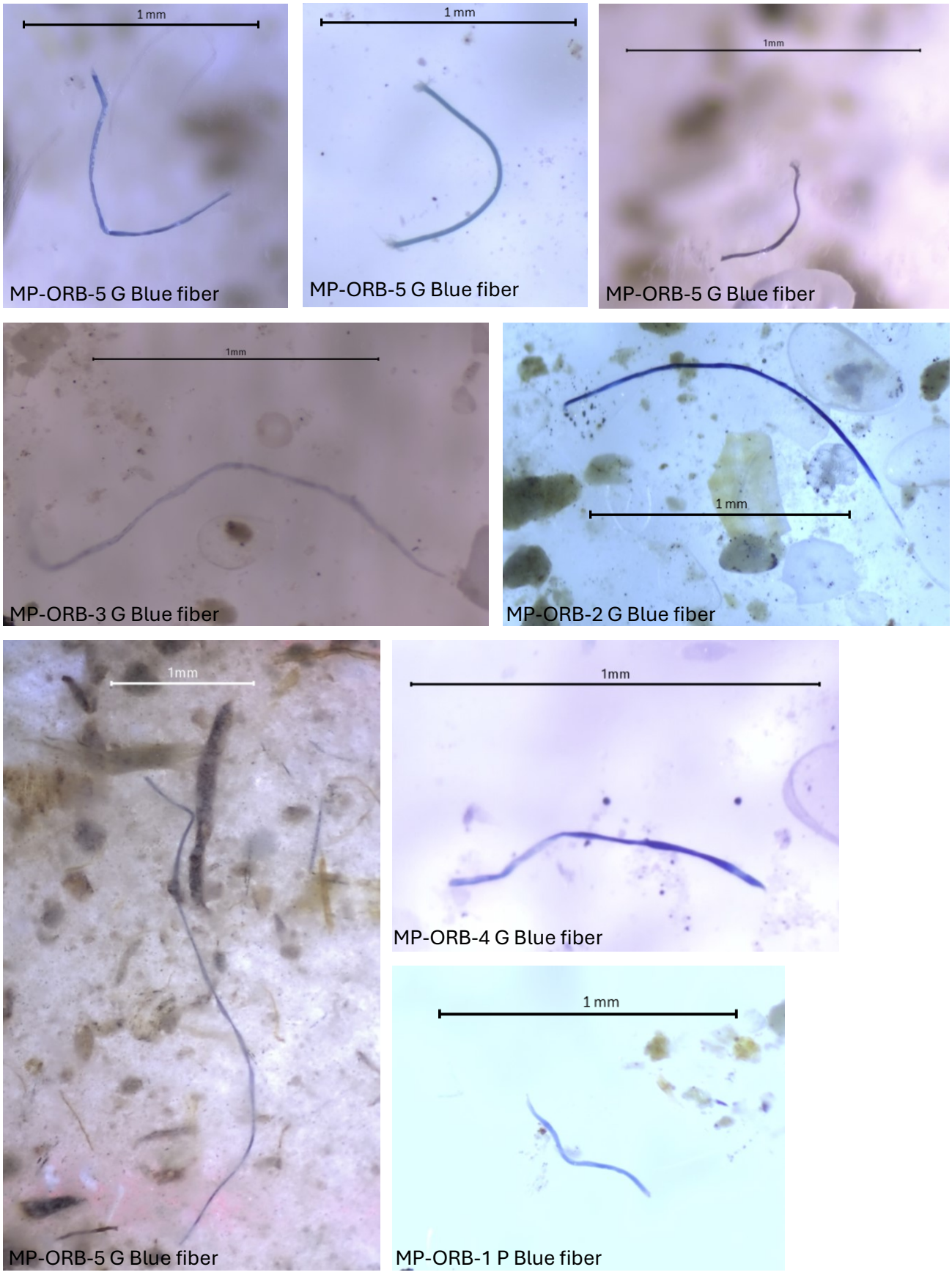

Fig. 2: Blue fibers found in various samples (sample code indicated next to each photo) of the LB5B and OLP-11B cores, collected for microplastic analysis.

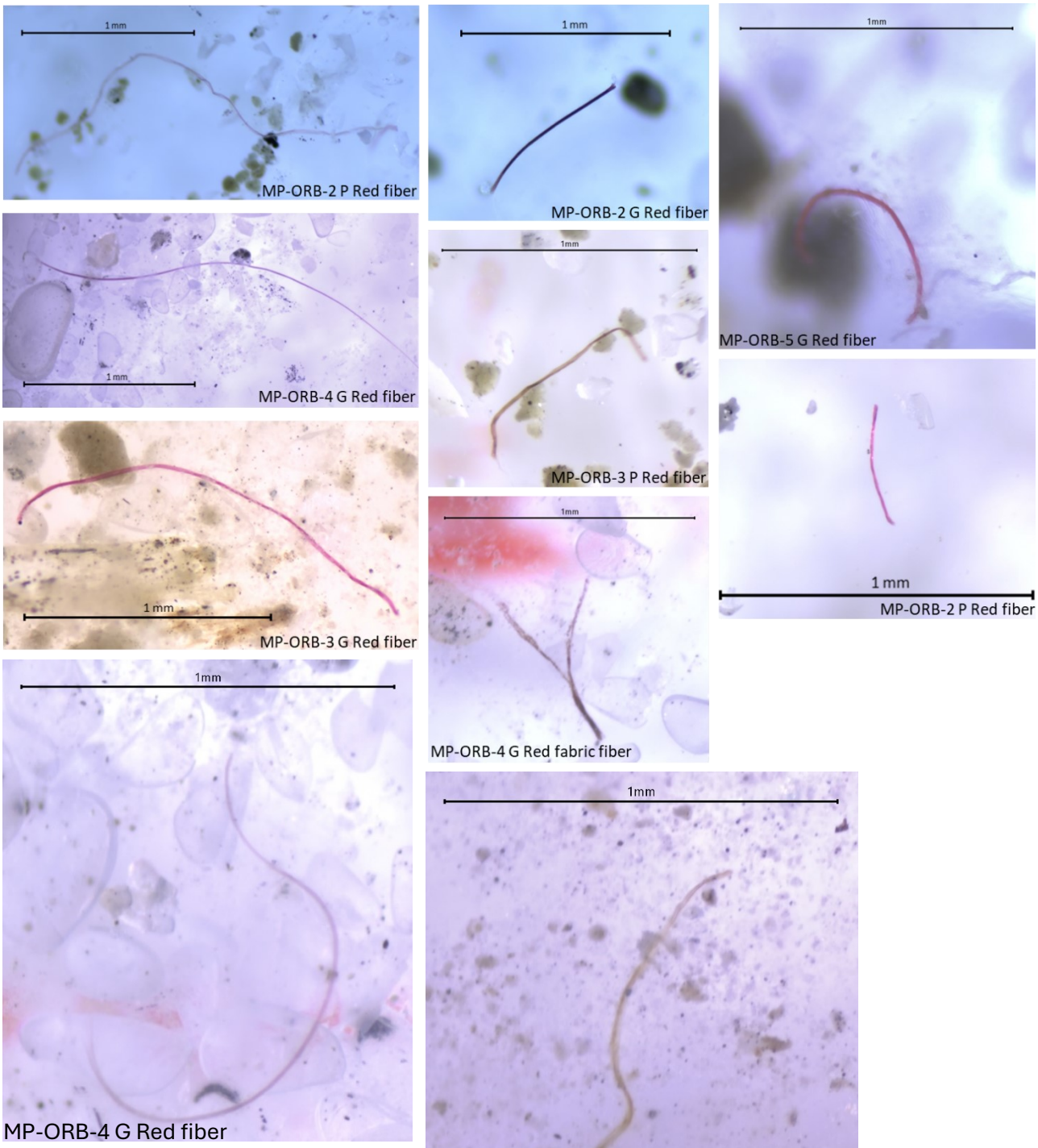

Fig. 3: Red fibers found in various samples (sample code indicated next to each photo) of the LB5B and OLP-11B cores, collected for microplastic analysis.

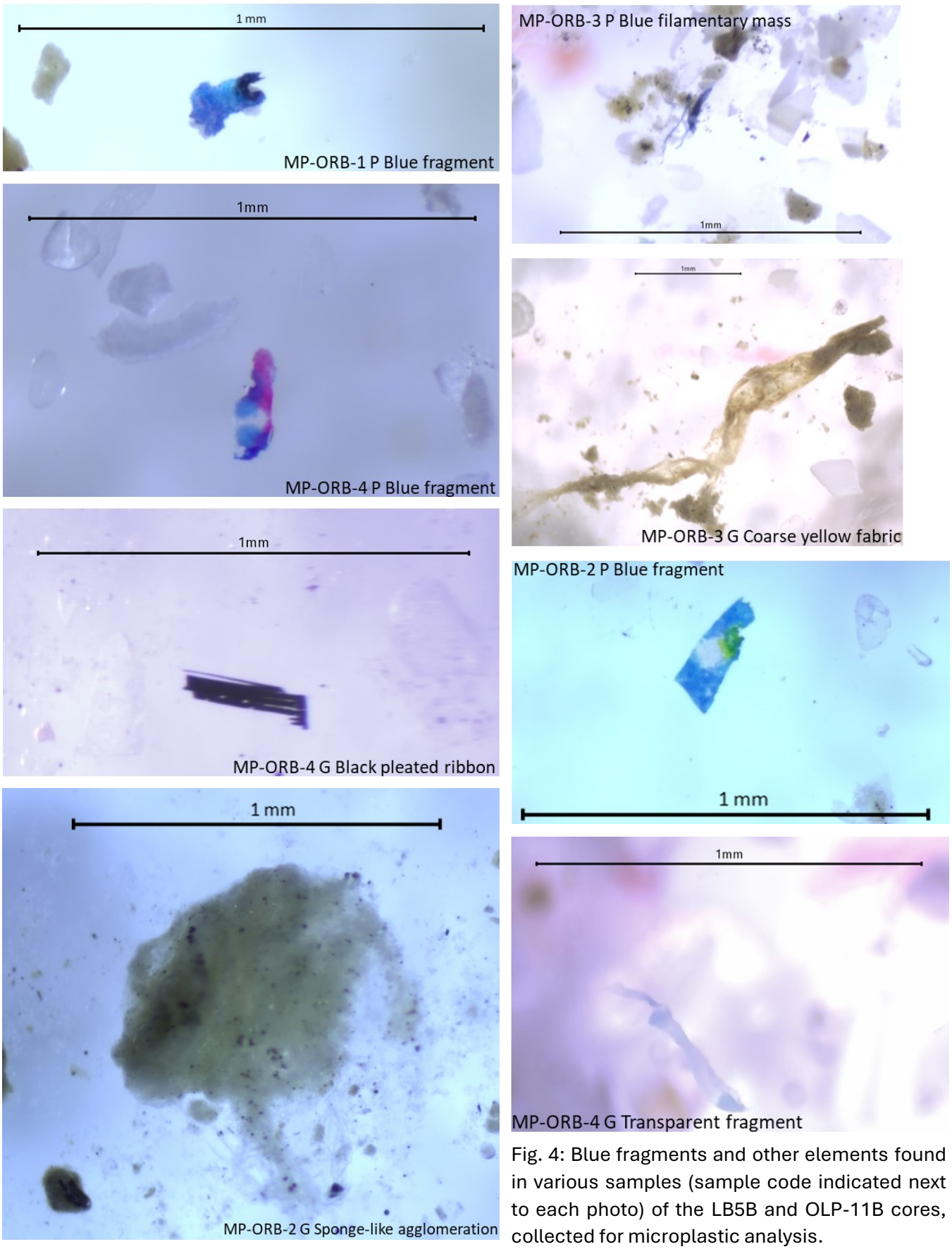

Fig. 4: Blue fragments and other elements found in various samples (sample code indicated next to each photo) of the LB5B and OLP-11B cores, collected for microplastic analysis.

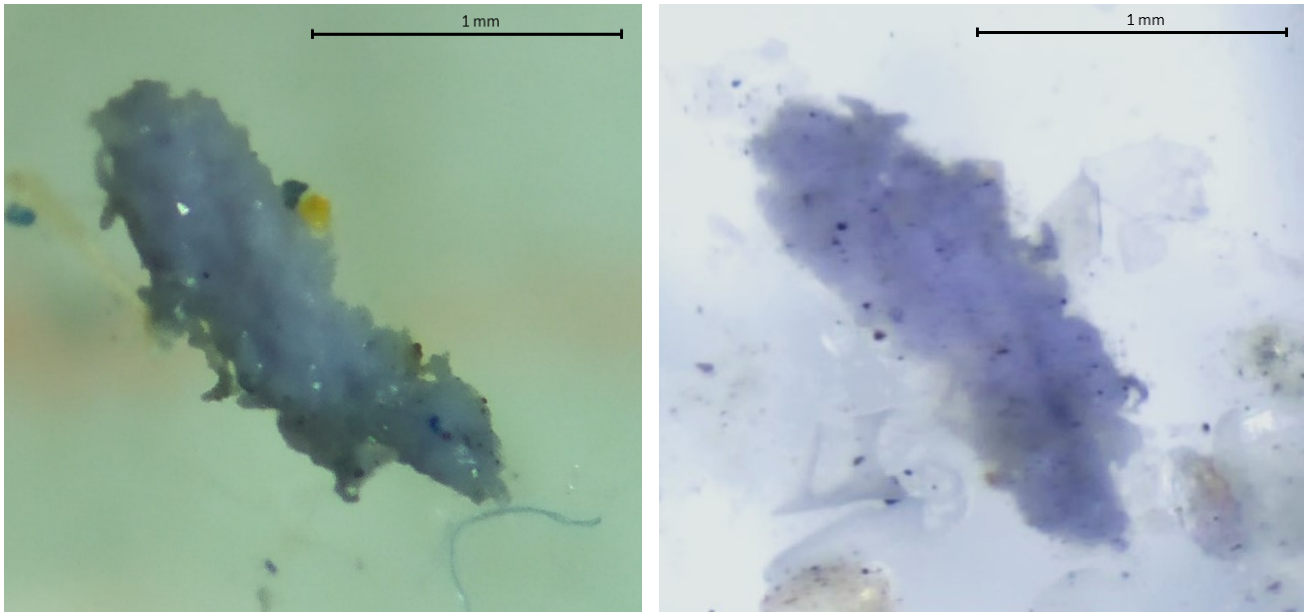

Fig. 5: Blue agglomerate found in sample MP-ORB-4 G of the core OLP-11B (two views).

2. Control blanks

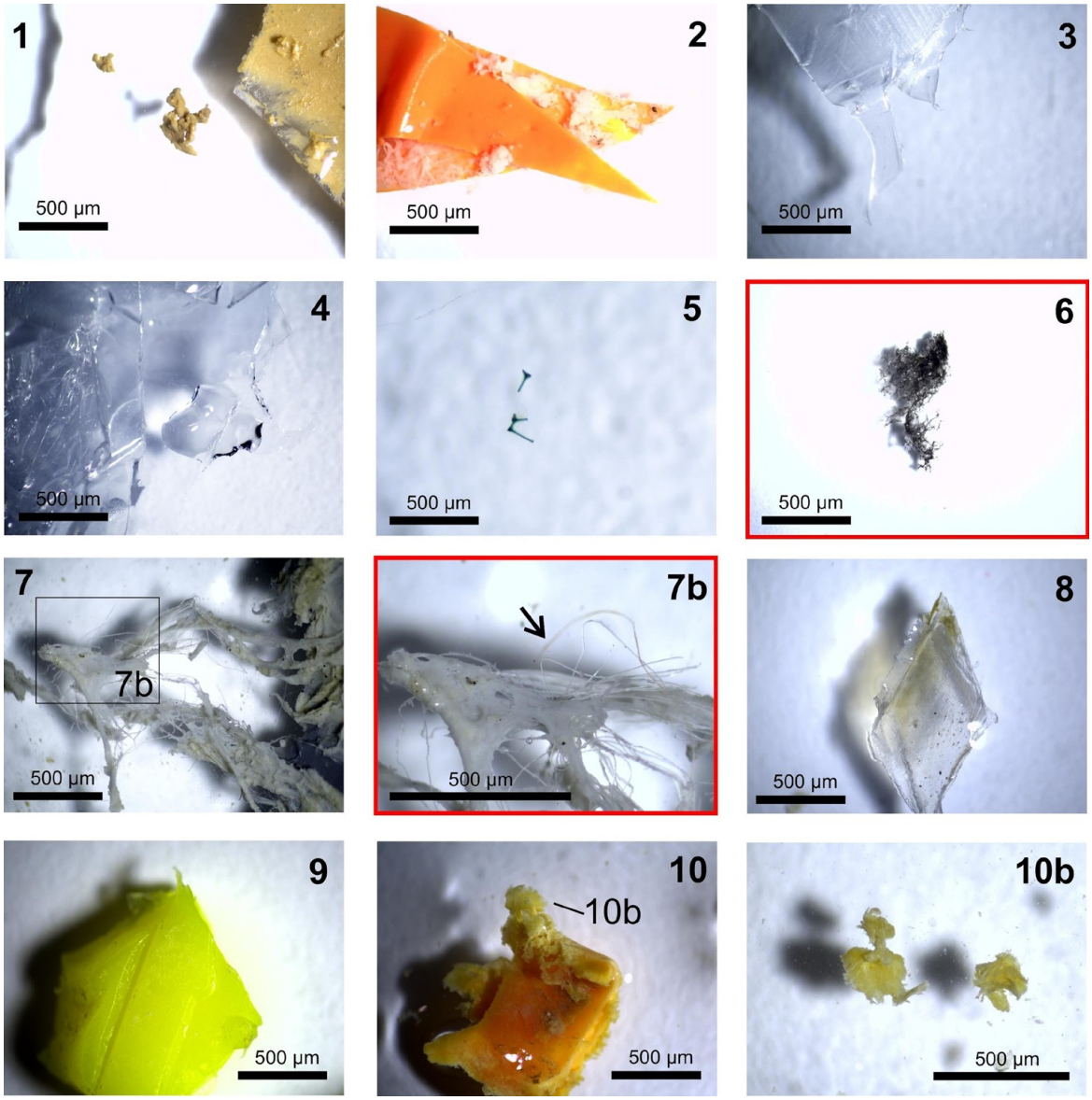

Fig. 6: Plastic samples collected from the casing material of cores and surface samples. 1, 2, 7, 7b: fragments of adhesive tape; 3, 4: fragments of plastic film; 5, 6: fragments of foam rubber; 8, 10, 10b: fragment of plastic tube (gray and orange) for storing the cores; 9: fragment of plastic closure of the tubes.

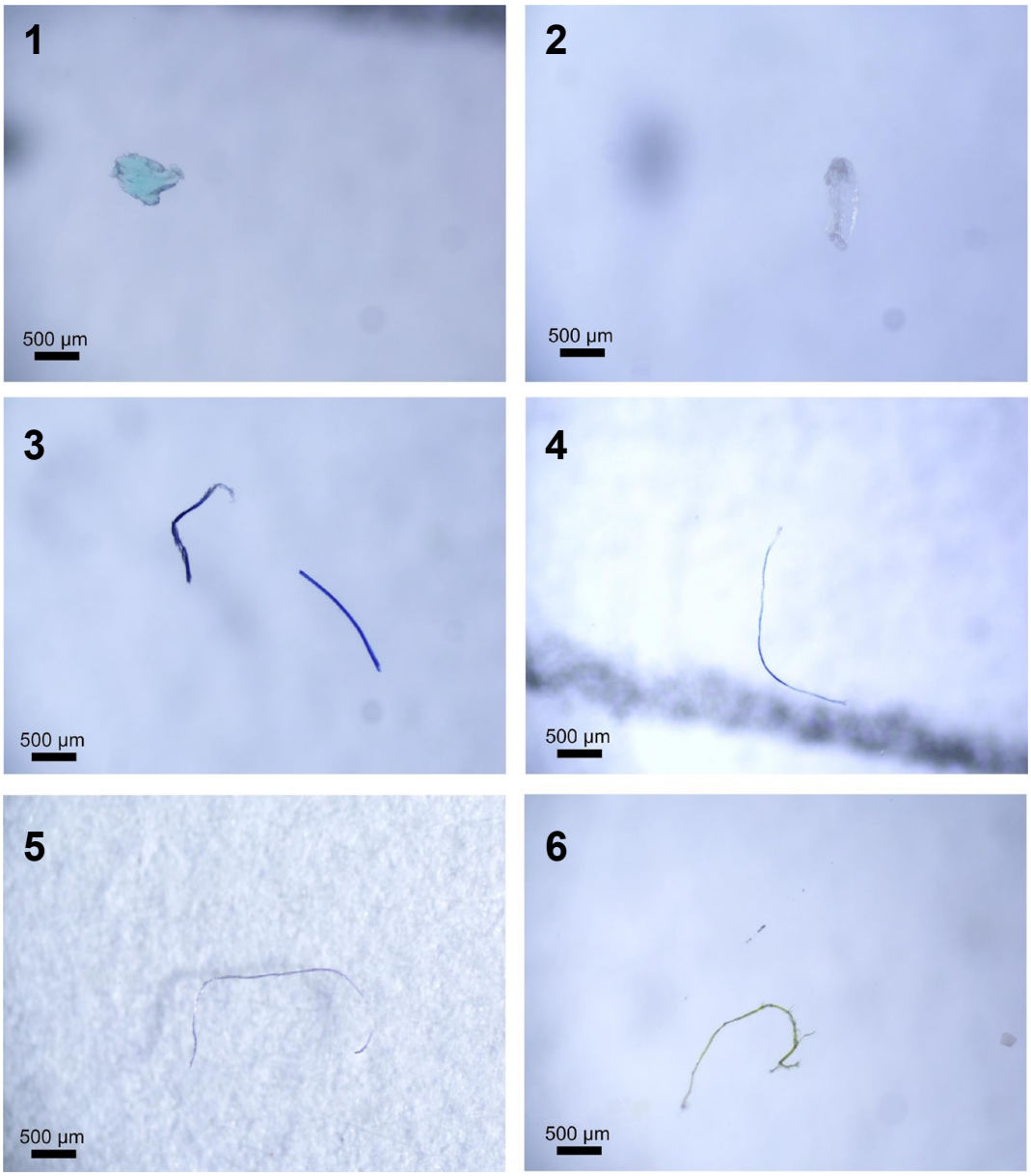

Fig. 7: Fragments and fibers found in the control blanks. 1: blue fragment; 2: transparent fragment; 3, 4: blue fibers; 5: nylon-like transparent wire; 6: red fiber.

	SAMPLE 11	SAMPLE 12	SAMPLE 13	SAMPLE 14	SAMPLE 15	SAMPLE 16	**Max number (+1) found in a blank**
Sample name	SACC PL ROSSO	SACC PL ROSSO	SACC PL ROSSO	SACC PL VERDE	SACC PL VERDE	SACC PL VERDE	i.e. number to subtract from each sample, by type
Blu fiber	4		2	1		3	**5**
Red fiber			1				**2**
Black/dark grey fiber	4	2		2	3	1	**5**
Transparent wire (nylon-like)	9	2	3	8	8	6	**10**
Sponge-like agglomeration							
Coarse yellow fabric							
Red fabric fiber							
Blue fragment							
Black pleated ribbon							
Transparent fragment	2	2	1	7	1	1	**8**
Yellow fiber	1	1			1		**2**
tot	20	7	7	18	13	11	

Tab. 1: Counting of the fragments found in control blanks.